The role of type 2 innate lymphoid cells in the pathogenesis of pancreatitis

University of Cambridge
Gonville & Caius College

Shwethaa Raghunathan
Cancer Research UK Cambridge Institute

This dissertation is submitted for the degree of Doctor of Philosophy, Sep 2021

Declaration

This thesis is the result of my own work and includes nothing which is the outcome of work done in collaboration except as declared in the preface.

It is not substantially the same as any that I have submitted or is being concurrently submitted for a degree or diploma or other qualification at the University of Cambridge or any other University. I further state that no substantial part of my dissertation has already been submitted, or is being concurrently submitted for any such degree, diploma or other qualification at the University of Cambridge or any other University or similar institution.

This work does not exceed the prescribed word limit of 60,000 words excluding the figures, tables and references.

Shwethaa Raghunathan

Summary

The role of type 2 innate lymphoid cells in the pathogenesis of pancreatitis

Shwethaa Raghunathan

Type 2 Innate Lymphoid Cells (ILC2s) are recently discovered tissue resident immune cells, studied more commonly in barrier tissues like the lung and intestine. ILC2s are critical mediators of early type-2 immune responses and play a crucial role in the clearance of parasites, but also in the development of allergic diseases such as asthma. The function of tissue resident ILC2s in the pancreas has not been well characterised and their role in the pathology of pancreatitis remains unknown.

The inflammatory influx associated with pancreatitis has been shown to have several type 2 immune features, including eosinophilia, and considering ILC2s are potent inflammatory mediators, this project addresses the role of ILC2s in epithelial damage and organ remodelling in both acute and chronic pancreatitis.

We identified pancreatic ILC2s and characterised their physiological stimuli in the pancreas. In the caerulein mouse model of AP we found that ILC2s were activated very early, followed by a significant and persistent increase in eosinophils. Using ILC2-deficient mice we found that acute pancreatitis induced inflammation and pancreatic epithelial necrosis were significantly reduced, while immune-profiling indicated that eosinophilia was impaired. This impairment in eosinophilia was observed in ILC2-deficient mice with chronic pancreatitis as well. In acute pancreatitis, we further found that ILC2-dependent eosinophilia was also stromal cell, IL-33 and IL-5 dependent. Mouse models lacking eosinophils revealed that ILC2 dependent eosinophilia however did not regulate epithelial damage in acute pancreatitis. Thus, ILC2-driven damage was likely mediated in an eosinophil independent manner. We investigated other immune cell interactions downstream of ILC2 activation. We used genetically or therapeutically targeted depletion of neutrophils, monocytes, NK cells, T and B cells and did not find a clear mechanism. We found that ILC2 deficient mice that had chronic pancreatitis showed significantly reduced fibrosis and ADM compared to control animals during the recovery phase. However, ILC2 dependent eosinophilia did not seem to play a role in organ remodelling during the recovery phase of chronic pancreatitis either. At the recovery stage, acinar to ductal metaplasia and fibrosis were not regulated by eosinophils.

Altogether, data from this project suggests that ILC2s regulate epithelial damage and oedema in acute pancreatitis, mediate eosinophilia in acute and chronic pancreatitis and also regulate tissue remodelling in chronic pancreatitis. However, eosinophils do not play a role in regulating epithelial damage or organ remodelling during acute or chronic pancreatitis.

Acknowledgements

I'd like to thank Dr. Tim Halim, my supervisor for his balanced and supportive supervision over the last 4 years. Tim has always been available whether for technical questions or patiently listening to new ideas. I'd like to thank Tim for training me when I first started in his lab and teaching me laboratory techniques in immunology and animal work. For helping me learn how to answer my scientific questions, for providing a lab setting with ample resources and for meeting regularly to follow up on the progress of the project and teaching me to see big picture perspectives in science, thank you so much, Tim. I absolutely could not have asked for a better lab to do a PhD in.

I'd like to thank Dr. Julie Stockis, senior post-doc in the Halim lab for her diligent guidance and considerate partnership. I share the larger pancreatitis project with Julie, and this was a challenging project to work on for both of us (considering the tedious pancreatitis model), but with Julie's partnership, this journey felt much more enjoyable. Thank you, Julie, for offering very detailed and diligent feedback on my thesis, I've learnt a lot from your feedback. Julie's rigour in setting up experiments, documenting data, traceability of experimental details, scientific reasoning are all lessons for life I take with me as I pursue a career in science.

This memorable PhD experience would not have been the same if not for my wonderful teammates. I'd like to thank Celine Garcia, our lab manager for consistent support, kind words, hugs, and cheers throughout this period. I'd like to thank her for training me initially and always providing constructive input for all the data that I've shared. I'd like to thank all the students from our lab, Shaun, Sheng, Thomas, Liang, and Stela for being a support group. I'd like to thank Thomas for reading through my methods section meticulously. I'd like to thank Martijn, Silvain and Julia - you are all what makes this lab a joy to be in.

I'd like to thank several cores and operations staff at the CRUK Cambridge Institute. First and foremost, the biological resource unit (BRU) for taking care of our numerous mice. Angela especially for diligently maintaining our mouse colonies and the conventional team consisting of Gemma, Ryan, Rob, Toby, Charlotte and Dani for always being approachable and supportive. I'd like to thank the histology core for blocking, embedding, sectioning, and staining all my histology samples. I'd like to thank Julia Jones from the histopathology core especially for helping me with setting up the classifier tool for analysing necrosis and oedema in H&E sections. I would also like to thank the RICS, genomics and bioinformatics cores for their support. I would like to thank the flow cytometry core, for their advice and technical support.

I would like to specially mention the operations staff at the CRUK CI whose support we benefit immensely from. I would like to thank the media kitchen, glass wash, property services, lab management and security teams who keep the building functioning, laboratory well supplied, stocked, maintained thoroughly, and running smoothly. We are indeed very spoiled by all of you.

I would also like to thank the scientific administration team and especially Ann Kaminski. Thank you, Ann, for always being available for answering numerous questions and providing much needed pastoral care, without your support the challenging times would have been difficult to handle.

For friendships, I am very grateful. Erica, for hanging out with me, always listening, and empathising over several plates of food. Shaun, for providing a listening ear to all my rants over several cups of coffee. For all my loving friends from Eden, who always prayed for me and my strange worries about mice and experiments. For friends at the Institute, the ones I could pop by and ask for advice, the ones I could stop on the corridor and ask quick questions, the ones who make the CRUK CI a warm place to be.

I'd like to thank Amma and Appa (Revathi and Raghunathan) for supporting me through prayers, love, and strength though 1000s of miles away. I did not choose the career they'd like me to have chosen, but they've always supported me, nevertheless. I'd like to thank my parents in law (Rachel and Daniel Barnabas) for their love, kindness, prayers and always being proud of me. Anuj and Raveena, thank you for your joy, love, prayers, and support. Deepak, my husband, who has travelled with me from the first moment I fell in love with biology at 17, for always encouraging me, laughing with me, for his jokes which I find very funny, for love, for picking me up during low times and always being proud of me, thank you. For 14 years of companionship and joy, thank you.

Above all, *Soli Deo Gloria*.

List of abbreviations

Term	Expansion
ADCC	antibody-dependent cell-mediated cytotoxicity
ADM	acinar to ductal metaplasia
APL	acute promyelocytic leukaemia
aSMA	alpha smooth muscle actin
BAL	broncheoalveolar lavage
CAF	cancer associated fibroblasts
CD	cluster of differentiation
CLP	common lymphoid progenitor
DAMP	danger associated molecular patters
DC	dendritc cells
DSS	dextran sulphate sodium
ECM	extracellular matrix
FALC	fat associated lymphoid clusters
Fc	fragment of IgE
IFN-ɣ	interferon ɣ
Ig	immunoglobulin
IL	interleukin
ILC	innate lymphoid cell/cells
ILC2P	innate lymphoid cell progenitor
LMPP	lymphoid-primed multipotent progenitors
LTi cells	lymphoid tissue inducer cells
MDSC	myeloid derived supressor cells
MFI	mean fluorescent intensity
MHC	major histocompatibility complex
MLN	mesenteric lymph node
MSC	multipotent stromal cell
NCR	natural cytotoxicity receptor
NK	natural killer
NSAID	non-steroidal anti-inflammatory drugs
NSG	NOD scid gamma

Term	Expansion
PanIN	pancreatic intraepithelial neoplasia
PDAC	pancreatic ductal adenocarcinoma
PI	PMA/Ionomycin
pLN	pancreatic lymph node
PMA	Phorbol 12-myristate 13-acetate
PSC	pancreatic stellate cells
Rag	recombination activating gene 1
SCF	stem cell factor
TCR	T cell receptor
TGF	transforming growth factor
T_h	T helper
TLR	toll-like receptor
TNF	tumour necrosis factor
Tregs	regulatory T cells
TSLP	thymic stromal lymphopoietin
VAT	visceral adipose tissue
WAT	white adipose tissue
WT	wildtype

Declaration of shared data

Due to the tedious nature of the animal experiments involved in the pancreatitis experiments and due to shared ownership of the pancreatitis project the data shown in figures 25,26,27,28,32,34,35,37,38 is shared with Dr.Julie Stockis, Senior Post-Doc, Halim lab. We have shared equally the tasks of animal injections, dissections, flow cytometry and associated analysis between us in the above-mentioned experiments. Additionally, figure 14 was made by Dr.Silvain Pinaud, Post-Doc, Halim lab, while curation of the gene list was done by me. The image analysis shown in fig S23 was done by Daniel Heraghty, BSc project student, Halim lab under my technical supervision as a part of his BSc project.

TABLE OF CONTENTS

Introduction

The discovery of ILC2s

A report of innate cells capable of producing type 2 cytokines came out in 2002 from the Coffman lab (Hurst et al., 2002). Notably, the first description of T_h1 and T_h2 cells had come from the Coffman lab as well in 1986 (Mosmann et al., 1986). In the 2002 report, the lab set out to characterise IL-17F and IL-25, which had not yet been characterised *in vivo*. In this report, eosinophilia induced by IL-25 was found to be independent of T and B cells, NK cells, mast cells and basophils. The cellular source of eosinophilia inducing IL-5 in IL-25 treated mice was identified in *Rag2*$^{-/-}$ mice as c-kit-, Ly6G-, Ly49-, CD3-, CD4-, B220-, γδTCR- and showing low to negative expression of Thy-1 (Hurst et al., 2002).

Two back-to-back reports from the Artis lab and the McKenzie lab in 2006, demonstrated the role of IL-25 in type 2 inflammation (Fallon et al., 2006; Owyang et al., 2006). Both these reports demonstrated that *Il25*$^{-/-}$ mice showed impaired T_h2 response and pathogen clearance in parasite infections (*Nippostrongylus brasiliensis* and *Trichuris*)(Fallon et al., 2006; Owyang et al., 2006). Additionally, the McKenzie lab report showed that infection with *N. brasiliensis* induced a novel immune population that were non-B non-T cells (NBNT) cells in the lungs. Flow cytometry analysis of this population in the mesenteric lymph node (MLN), revealed them to be CD4-, CD8-, c-kit+, FcεR1- and NBNT. Upon *N. brasiliensis* infection, these cells were found to increase in wildtype (WT) mice MLN. This increase was not seen in MLN of *Il25*$^{-/-}$ mice, thus demonstrating that these cells were regulated by IL-25 in this setting (Fallon et al., 2006).

In 2010 these same cells were identified in fat associated lymphoid clusters (FALC) in the mouse mesentery (Moro et al., 2010). These cells were termed natural helper cells and were identified as Lin- (CD3ε, CD8α, TCR$\alpha\beta$, TCRδ, CD5, B220, NK1.1, Ter119, Ly6g, Mac-1, CD11c and FCεRIα), c-Kit+, Sca-1+, IL-7R+ and IL-33R+. *In vitro*, SCF and IL-7 supported their survival. Natural helper cells were found to proliferate in response to IL-2 and their culture supernatants were found to contain large amounts IL-2, IL-4, IL-5, IL-6 and GM-CSF (Moro et al., 2010). Notably, exposure to the alarmin IL-33, induced production of high levels of IL-5 and IL-13 by these cells *in vitro*. These natural helper cells were found to produce IL-13 during helminth infection which was found to be critical for helminth expulsion from the gut (Moro et al., 2010).

These innate immune sources of type 2 cytokines were christened nuocytes in another report in the same year (Neill et al., 2010). This report explored the activation and function of these cells. Nuocytes were found to be the primary early source of IL-13 in *N. brasiliensis* infection. These cells were found to be Lin-, ICOS+, T1/ST2+, IL-17BR+ and IL-7Ra+. Helminth

expulsion was found to be compromised in *Il17br*$^{-/-}$, hence pointing to a role for IL-25 signalling in nuocyte regulation. This helminth expulsion defect was rescued through adoptive transfer of WT nuocytes to *Il17br*$^{-/-}$ mice. Both, *in vitro* and *in vivo*, IL-25 and IL-33 were found to induce expansion of nuocytes (Neill et al., 2010).

Several of these findings from the McKenzie lab including innate IL-13 production in *N. brasiliensis* infection were corroborated by a subsequent report in the same year from the Locksley lab (Price et al., 2010). They christened these innate sources of type 2 cytokines as innate type 2 helper cells (Ih2 cells). Their report identified these cells in various organs including MLN, spleen, liver, bone marrow, lung and peritoneum. This study also showed that Ih2 cells had a distinctly different transcriptome compared to basophils and T_h2 cells (Price et al., 2010).

These cells, variously called natural helper cells, nuocytes and Ih2 cells by different labs would later in 2013 be given a uniform nomenclature. These cells were called Group 2 innate lymphoid cells (ILC2) and grouped with other innate cells that mirrored T cells in their function (Spits et al., 2013). This classification of innate lymphoid cells (ILCs) laid ground for a brand-new field in immunology exploring the previously unappreciated functions of these cells in various pathological conditions and physiological programs.

This new classification divided ILCs into group 1, group 2 and group 3 (fig 1). Group 1 ILCs were defined as those innate immune cells capable of producing Interferon ɣ (IFN-ɣ) but not T_h2 or T_h17 cytokines. By this definition, group 1 ILCs now included an old discovery, NK cells, mirroring CD8T cells on the adaptive immune side. Another cell type ILC1s, identified as IFN-ɣ producing non-NK, non-cytotoxic innate cells, were also added to Group 1 (Spits et al., 2013).

Group 2 was classified as cells requiring IL-7Rα for their development, GATA-3 transcription factor expressing (mirroring T_h2 cells) and producing T_h2 cytokines like IL-5 and IL-13 (Spits et al., 2013). This group is solely occupied by ILC2s whose discovery has been described above.

Group 3 ILCs were defined as those lineage negative innate immune cells capable of producing IL-17a and/or IL-22. These cells are RorɣT dependent thus mirroring T_h17 cells on the adaptive immune side (Spits et al., 2013). This group consisted of another known cell type, LTi cells (Lymphoid tissue inducer) and a recently described immune cell type called ILC3s. ILC3s depend of RorɣT for development. They come in two further flavours, NCR+ and NCR. NCR- ILC3s produce IL-17, IL-22 and IFN-γ, but NCR+ ILC3s only produce IL-22. The

development of group 3 ILCs also depends on IL-7Rα similar to group 2 ILCs. The activation and functional differences in ILCs have been summarised in fig 1.

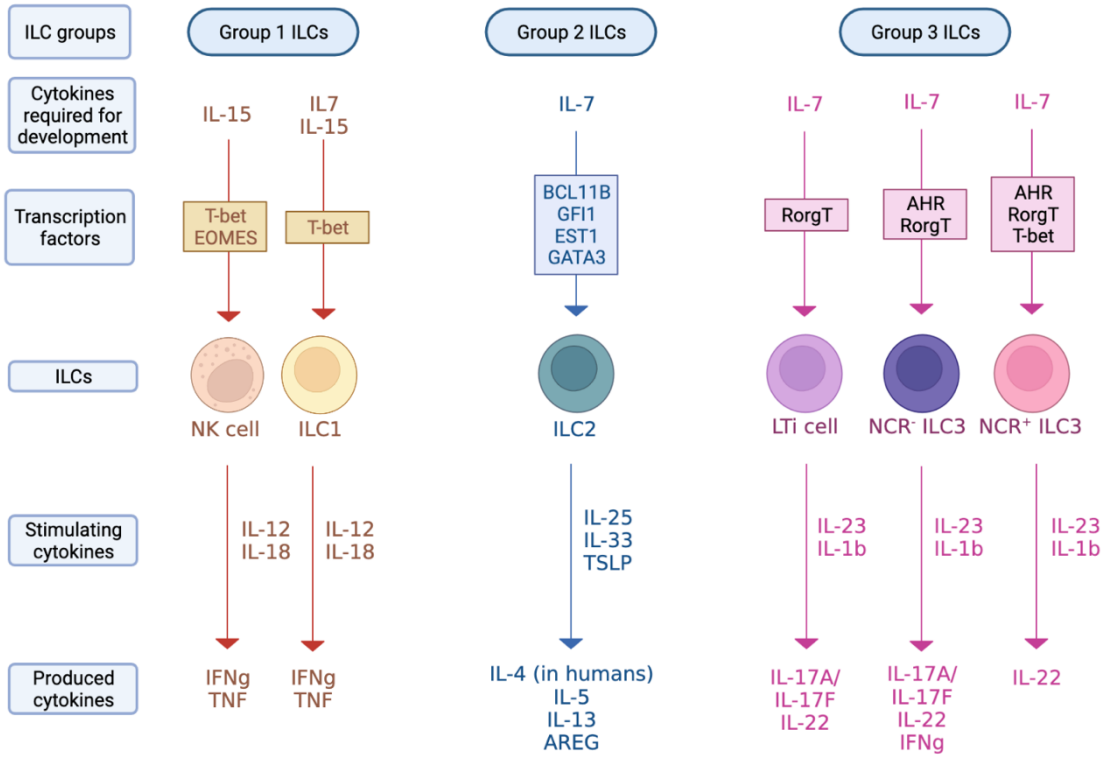

Fig 1 - Innate lymphoid cells have been classified into 3 groups based on their development, key transcription factors and cytokine profile. Group 1 ILCs contain NK cells and ILC1s. Group 1 ILCs are stimulated by IL-12 and IL-18 and produce IFNɣ and TNF. NK cells express the transcription factors T-bet and Eomes. ILC1s only express T-bet. Group 2 ILCs contain only one cell type, ILC2s. ILC2s can be stimulated by IL-25, IL-33 and TSLP to produce the cytokines IL-4, IL-5, IL-13 and AREG. ILC2s express the transcription factor GATA3. Group 3 ILCs are made up of LTi cells and ILC3s. LTi cells express the transcription factor RORɣt, are stimulated by IL-23 and IL-1β and release IL-17A/IL-17F and IL-22 upon activation. ILC3s are further subdivided based on their expression of NCR. ILC3s are stimulated by IL-23 and IL-1β and produce IL-22. NCR- ILC3s additionally produce IL-17A/IL-17F. NCR3- ILC3s express the transcription factors AHR and RORɣt and NCR+ ILC3s express T-bet along with AHR and RORɣt. Fig from *Ebbo et al, 2017*. This figure was made by the student using biorender.com.

The story of the other ILCs

The distinct pathological roles of ILC1 and ILC3s and their apparent plasticity are very interesting. In an effort to capture this section of literature, the discovery of Group 1 and Group 3 ILCs has been briefly outlined and summarised below.

Group 1 ILCs

The first characterisation of ILC1s came from the Spits lab in 2013 (Bernink et al., 2013) in concurrence with the then new classification of ILCs (Spits et al., 2013). This report identified two distinct human non-ILC2 non-ILC3 ILC populations that were c-Kit+ NKp44- and c-Kit-

NKp44-. Of these two populations, the c-Kit- NKp44- ILCs were shown to resemble T_h1 cells. *Ex vivo*, these c-Kit- NKp44- cells, showed high expression of *Ifnγ* transcripts. They also expressed *Tbx21* which encodes for the transcription factor T-bet. When stimulated with a combination of IL-12 and IL-18, these cells also produced IFN-γ in levels comparable to NK cells. Based on T_h1 cell-like T-bet expression and IFN-γ production, these cells were called ILC1 (Bernink et al., 2013).

Ifnγ expressing ILC1s were also found to be the most frequent ILC subset in Crohn's disease patients. This was also observed in mouse models of colitis, where IFN-γ producing ILCs were found accumulating in mice with dextran sulphate sodium (DSS) induced colitis (Bernink et al., 2013). This report also sought to understand the role of the c-Kit+ NKp44- population observed in human tonsils. Interestingly, these cells were found to give rise to NKp44+ ILC3s when cultured with IL-2, IL-1b and IL-23. Alternatively, c-Kit+ NKp44- cells could also give rise to ILC1s if they were cultured with IL-2 and IL-12 (Bernink et al., 2013).

A fraction of these c-Kit+ NKp44- cells were found to express RorγT. These c-Kit+ NKp44- RorγT+ cells had low expression levels of T-bet and were producing IL-22, thus identifying them as ILC3s. Under IL-12 containing culture conditions, these cells then differentiated into RorγT- Tbet+ IFN-γ producing ILC subset, i.e., ILC1. This observation showed that ILC1s could be derived from ILC3s under polarising conditions (Bernink et al., 2013). This particular observation concurred with a previous paper from the same lab in 2010, that RorγT+ ILC3s in mice, lose RorγT expression and start producing IFN-γ instead (Vonarbourg et al., 2010). Both these reports captured the plasticity between ILC1 and ILC3s. This interestingly enough, mirrored a similar plasticity between T_h17 and T_h1 cells in the adaptive immune compartment (Bending et al., 2009).

To complete the set, group 1 ILCs also consist of an older discovery, NK cells. NK cells were the first innate lymphoid cells to be discovered in the 1970s. They are known for their cytotoxic effector functions mediated through the release of perforin and Granzyme B (Vivier et al., 2011). Apart from their role in bringing about cell death of transformed or stressed cells, NK cells are also effective cytokine sources in inflammation. NK cells are known to secrete IFN-γ, TNFα, IL-10 and GM-CSF. NK cells are regulated through a host of activating and inhibitory receptors that work to either stimulate or dampen NK cell activity. Their development, maturation and survival is dependent on IL-15. NK cells can also bring about ADCC (antibody-dependent cell cytotoxicity) mediated cell death of antibody-coated cells through their binding to CD16 on NK cell surface (Vivier et al., 2011).

Group 3 ILCs

LTi cells which were discovered in 1997 were later grouped with ILC3s under group 3 ILCs due to their ability to produce IL-17 and IL-22 (Mebius et al., 1997) (Spits et al., 2013). LTi cells as their name suggests, are critical for the development of Peyer's patches and lymph nodes during foetal development. These cells express lymphotoxin (LT) α1β2 on their cell surface through which they activate LTβR expressing local stromal cells. Once activated these stromal cells recruit more lymphocytes to the milieu which can then be organised for lymphoid structure development. LTi cells, just like ILC3s, depend on RorgT for development (Sawa et al., 2010).

Group 3 ILCs also include ILC3s (Spits et al., 2013). One of the early descriptions of ILC3s came in 2008 from the Di Santo lab (Satoh-Takayama et al., 2008). This report described and characterised a new, reportedly NK cell subset in the intestine. This subset was described as Lin- NKp46+, CD127+ and RorγT+. Functionally these cells were shown to produce IL-22. These cells were also shown to have a potential role in clearance and mucosal immunity against colitis causing *Citrobacter rodentium* infection in mice. The development of these cells was found to be RorγT dependent but not IL-15 unlike NK cells (Satoh-Takayama et al., 2008).

These findings were corroborated in 2009 in a report from the Colonna lab (Cella et al., 2009). This report described these cells as a subset of NKp44+ NK cells and called them NK-22 cells. They identified these NK-22 cells in human tonsils, Peyer's patches and appendix. These cells were activated by IL-23 and were found to secrete IL-22 upon activation. NK-22 were also found to induce proliferation signals and suppress apoptotic signals of epithelial cells and bring about IL-10 secretion from epithelial cells as well (Cella et al., 2009). In *Citrobacter rodentium* infected mice, NK-22 cells were found to be a principal source of IL-22, which was then required for mucosal immunity and survival of the mice from the infection. Their developmental pathway seemed similar to that of T_h17 cells, with NK-22 cells showing expression of aryl hydrocarbon receptor (*Ahr*), *Rora*, *Rorg* and *Irf4*. However, cord blood or peripheral blood NK cells did not turn into NK-22 cells under T_h17 polarising conditions. Thus, alluding to the possibility of NK-22 cells developing from a local progenitor (Cella et al., 2009).

In the same year, a report from the Spits lab identified cells that were Lin- CD127+ and *Rorc* expressing cells in the human mesentery in the 1st trimester and developing lymph nodes in the 2nd trimester. These cells were labelled LTi-like cells as they behaved similarly to LTi cells. These cells could induce I-CAM1 and VCAM expression on mesenchymal stromal cells, just like LTi cells do in lymph node development. These cells could also give rise to CD56+ CD127+ NK cells when cultured with IL-15 (Cupedo et al., 2009). In a subsequent report from

the same lab, these human CD127+ LTi-like cells were described as having a similar phenotype to NK-22 cells reported the previous year (Cella et al., 2009) (Crellin et al., 2010).

NKp44 and NKp46 are coded by a family of genes called Natural Cytotoxicity Receptor (NCR) genes. Both the above reports identified IL-22 producing NCR expressing innate lymphoid cells. Buanocore et al, 2010 reported NCR- (NKp46-) ILCs in the mouse gut that produced both IFN-ɣ and IL-17. In a *H. hepatitis* induced colitis model, neutralising IFN-ɣ or IL-17 led to decreased severity of colitis. When these NCR- innate lymphoid cells were depleted using Thy1.1 antibody in a CD-40 agonist-mediated colitis model, this led to a reduction in Colitis severity as well. In-vitro these cells produced IL-17, IL-22 and IFN-ɣ (Buonocore et al., 2010).

Along with the NCR expression in play, ILC3s got further re-classified based on their expression of NCRs into NCR+ and NCR- ILC3s (Spits et al., 2013). Although, ILC3s express typically NK cell markers like NKp46 and NKp44, the choice to place them in group 3 was due to their production of Th17 like cytokines i.e., IL-17 and IL-22 (Spits et al., 2013).

ILC2s in health and disease

The role of ILC2s in the pathology of barrier sites like lungs and the intestine has been characterised in several reports. The following section is a summary of some of the literature identifying ILC2s as potent inflammatory mediators driving type 2 immune responses.

Airway inflammation

The pathogenesis of allergic asthma is mediated by type 2 cytokines, namely IL-4, IL-5 and IL-13. IL-4 regulates IgE production by B cells, IL-5 drives the characteristic eosinophilia and IL-13 mediates mucus hyperproduction and airway remodelling in the effector phase. T_h2 cells were thought to be the source of these cytokines (Cohn et al., 2004). However, in a mouse model of allergic asthma, induced by intranasal administration of the allergen papain, ILC2s were shown to be an important early source of type 2 cytokines (Halim, Krauss, et al., 2012). In the *Rag2*$^{-/-}$ mouse model, which lacks T and B cells, papain was still able to induce allergic asthma indicating an adaptive immune system independent source of type 2 cytokines. However, papain failed to induce the classic signs of allergic asthma-like lung eosinophilia, increase in IL-5 and IL-13 in the BAL and mucus hypersecretion in *Rag2*$^{-/-}$ *IL2rɣ*$^{-/-}$ mice. *Rag2*$^{-/-}$ *IL2rɣ*$^{-/-}$ unlike *Rag2*$^{-/-}$ mice lack ILC2s. A similar inability to induce allergic asthma by papain was also seen when ILC2s were depleted in *Rag2*$^{-/-}$ mice (Halim, Krauss, et al., 2012). In a subsequent report from the same lab, *Rora*$^{-/-}$ mice exposed to papain were shown to be unable to develop allergic asthma. Notably, *Rora*$^{-/-}$ lacked detectable ILC2s in the lungs, thus

strengthening the evidence for the role of ILC2s in allergic asthma (Halim, MacLaren, et al., 2012).

In concurrence with the above observations, ILC2s were identified as the source of IL-13 in another report using the mouse model of allergen induced asthma. When IL-33 or IL-25 was administered intranasally IL-13 producing ILC2s were seen in the BAL of these mice (Barlow et al., 2012). Additionally, transfer of WT nuocytes into IL-25 administered *Il13*$^{-/-}$ mice led to restoration of airway hyper reactivity (AHR), eosinophilia and inflammation which was typically absent in *Il13*$^{-/-}$ mice. AHR however was not restored in *Il13*$^{-/-}$ mice with adoptive transfer of *Il13*$^{-/-}$ ILC2s. In summary, this report identified that ILC2s produce IL-13 in the lungs during AHR but also that these cells alone were sufficient to induce AHR (Barlow et al., 2012). ILC2s and not T_h2 cells were found to be regulating inflammation in H3N1 subtype influenza A virus induced AHR as well (Y.-J. Chang et al., 2011). Chronic rhinosinusitis is characterised by eosinophilia that is IL-5 dependent. Interestingly, chronically inflamed nasal polyps from patients with chronic rhinosinusitis showed increased number of ILC2s compared to uninflamed nasal tissue from healthy and non-allergic donors (Mjösberg et al., 2011). This suggests that ILC2s are the likely source of IL-5 that drives eosinophilia in chronic rhinosinusitis.

Allergen exposure is known to induce T_h2 cell differentiation in the effector phase of allergic asthma pathogenesis. In a 2014 report, this T_h2 differentiation in allergen exposure was shown to be ILC2 dependent (Halim et al., 2014). In papain administered mice, while the early source of type 2 cytokines are ILC2s, the source of these cytokines by about day 21 are T_h2 cells. In this report, an ILC2 deficient mouse model was generated by bone marrow transplantation of *Rora*$^{-/-}$ cells into WT sublethally irradiated mice. These ILC2 deficient mice, when primed and re-challenged with papain, failed to induce the T_h2 dependent second wave of allergic responses like exacerbated eosinophilia (Halim et al., 2014).

This defect in T_h2 dependent response in ILC2 deficient mice was found to be mediated through DCs. IL-13 released by ILC2s in papain exposed mice was shown to induce IL-13R expressing CD40+ DCs to migrate to the lymph nodes. Post migration, DCs were shown to be important for T_h2 cell differentiation. This ILC2 activation and downstream function was shown to be IL-33 dependent. Thus, ILC2s were shown to regulate the T_h2 dependent allergen pathology phase, via DCs (Halim et al., 2014). Further, a report in the same year showed that ILC2s can also interact with T_h2 cells in an antigen dependent manner in *N brasiliensis* infection. IL-13 expressing ILC2s were found incapable of inducing *N brasiliensis* expulsion in *MhcII*$^{-/-}$ mice (Oliphant et al., 2014). ILC2s were later shown to induce T_h2 chemoattractant,

CCL17 production from IRF4+ CD11b+ CD103- DCs. This CCL17 production was shown to be critical to induce T_h2 memory response in allergen exposed mice (Halim et al., 2016).

ILC2s have been shown to regulate further aspects of adaptive type 2 responses as well. ILC2s activated by IL-33 were shown to express OX40L on their cell surface (Halim et al., 2018). ILC2s were found to induce proliferation of GATA3+ Tregs in lungs, through the interaction of OX40L and its receptor OX40 expressed on Tregs. In a mouse model of OX40L deletion on ILC2s (*IL7ra*$^{cre/+}$ *Tnfs4*$^{fl/fl}$), impaired Treg expansion was noted in allergen exposure and *N brasiliensis* models of type 2 inflammation (Halim et al., 2018). This interaction of ILC2s with T cells via the OX40/OX40L axis had been demonstrated *in vitro* earlier. OX40 expression on the CD4T cells and OX40L on ILC2s was detected by flow-cytometry after co-culture. When anti-OX40L antibody was used to block OX40L expression in a ILC2/CD4T cell co-culture, IL-4 and IL-13 production from the co-culture was significantly inhibited (L. Y. Drake et al., 2014).

In summary, we understand that ILC2s mediate inflammation and associated pathology via several methods like antigen dependent signalling through MHCII, via signalling axes like OX40/OX40L and via cytokines like IL-5 and IL-13. This broad range of effector functions and upstream activation mechanisms make ILC2s a very interesting cell type to study in the context of any type 2 inflammation.

ILC2 development

ILCs similar to T cells develop from common lymphoid progenitors (CLP). The multipotent progenitor CLP gives rise to the unipotent ILC2 progenitor (ILC2P). The *in vivo* development of ILC2s required *Id1* and *Notch2* signalling (Zook & Kee, 2016).

The potential of different BM resident progenitor populations to develop into ILC2s was investigated in a report from the Takei lab (Halim, MacLaren, et al., 2012). They tested Lin- Sca-1+ c-Kit- CD127+ CD25+ ST2+ cells christened iNH cells by this report (immature natural helper, as this paper, came out before publication of the uniform nomenclature), common lymphoid progenitor (CLP) cells identified as Lin- CD127+ Sca-1^{lo} c-Kit^{lo} cells and lymphoid primed multipotent progenitor cells (LMPPs) identified as Lin- Sca-1+ c-Kit^{hi} Flt3+ cells. CLPs, LMPPs and iNH cells were purified and injected into *Nod-Scid IL2rγ*$^{-/-}$ (NSG) mice. Immune compartment analysis revealed that the number of ILC2s reconstituted from CLPs was very low, with reconstitution from LMPPs being slightly higher. Reconstitution from iNH cells, however, was significantly higher than that from both CLPs and LMPPs (Halim, MacLaren, et al., 2012). These Lin- Sca-1+ c-Kit- CD127+ CD25+ ST2+ iNH cells would later be identified as the unipotent ILC2s progenitors.

A report from the Diefenbach lab confirmed that ILC2Ps indeed develop into ILC2s and that GATA3 is needed for ILC2 fate decisions (Hoyler et al., 2012). *Rag2*$^{-/-}$*Il2rg*$^{-/-}$ mice lacking ILC2s are typically unable to manage helminth clearance during *N. brasiliensis* infection. This phenotype can be rescued through adoptive transfer of WT ILC2s. When ILC2Ps instead of ILC2s were adoptively transferred to *Rag2*$^{-/-}$*Il2rg*$^{-/-}$ with *N. brasiliensis* infection as well, helminth clearance was restored. In summary, ILC2Ps could give rise to ILC2s. This paper also used Gata-3$^{i\Delta ILC,T}$ mice (conditional deletion of GATA-3 expression in ILCs and T cells) to show that conditional deletion of GATA-3 expression leads to complete loss of ILC2s (Hoyler et al., 2012). *Yu et al, 2016* identified that high expression of PD-1 and IL-25R marked a committed ILC progenitor population. *Bcl11b* expression was also found to be essential for ILC2 development, the loss of which led to loss of PD-1hi IL-25R+ ILC2s and peripheral ILC2s (Y. Yu et al., 2016).

The role of Rorα in ILC2 development was reported concurrently from the Takei and McKenzie labs in 2012. Microarray analysis of ILC2s had shown that they expressed Rorα transcripts which was also confirmed by qPCR (Halim, Krauss, et al., 2012). In a subsequent report from the same lab, it was shown that ILC2s were almost undetectable in the lung, small intestine and large intestine of *Rora*$^{-/-}$ (Halim, MacLaren, et al., 2012). In this report, WT or *Rora*$^{-/-}$ bone marrow (BM) was injected into sublethally irradiated *Rag2*$^{-/-}$ *IL2rγ*$^{-/-}$ mice which lack ILCs. Sublethally irradiated *Rag2*$^{-/-}$ *IL2rγ*$^{-/-}$ mice that received WT BM transplantation showed ILC2 reconstitution in the lungs, small intestine and large intestine 8-16 weeks after irradiation. However, sublethally irradiated *Rag2*$^{-/-}$ *IL2rγ*$^{-/-}$ that received bone marrow from *Rora*$^{-/-}$ mice showed very low numbers of ILC2s in these tissues. Thus, demonstrating a role for Rorα in the development of ILC2s (Halim, MacLaren, et al., 2012). The findings about the role of Rorα in ILC2 development were corroborated using *Rora*$^{sg/sg}$ mice (gives rise to a Rorα deficiency) in a simultaneous report from the McKenzie lab (Wong et al., 2012). *Rora*$^{sg/sg}$ mice challenged with IL-25 did not lead to ILC2 expansion. This was also associated with lack of goblet cell hyperplasia and eosinophilia which are typically ILC2 dependent in this model. Following sublethal irradiation, bone marrow was reconstituted with a 1:1 mix ofCD45.1+ WT mice and CD45.2+ *Rora*$^{sg/sg}$ mice was administered. 6-8 weeks after reconstitution, ILC2s were shown to develop only from the CD45.1+ WT mice (Wong et al., 2012). Both these reports established the role for Rorα in ILC2 development.

Homeostasis

The role of IL-33 and ILC2s in pathological conditions has been explored in considerable depth for a cell type whose history is roughly a decade long. Less is known about their role in homeostasis, however. In a study looking at the role of ILC2s in lung homeostasis, IL-33 expression was shown to be induced during postnatal lung inflation in mice (Saluzzo et al., 2017). ILC2s were found to be recruited upon this IL-33 spike. ILC2 derived IL-13 was found to be essential to polarise post-natal M1-like alveolar macrophages into an M2-like state. This M2 phenotype of lung resident alveolar macrophages was shown to be critical for maintaining a quiescent immune environment in the lungs. Interestingly, this state of quiescence brought about by M2 macrophages was shown to lead to a delayed response to *Streptococcus pneumoniae* Infection (Saluzzo et al., 2017). ILC2s were shown to accumulate in the lungs after infection with influenza virus and deleting ILC2s after the infection led to diminished lung function and impaired lung remodelling. When amphiregulin a cytokine produced typically by ILC2s was administered, the lung function and airway epithelial integrity was restored (Monticelli et al., 2011). In the small intestine as well, organ remodelling after epithelial injury induced by *Tritrichomonas* spp. Infection was moderated through the tuft cell-ILC2 axis. Tuft cells were shown to produce IL-25 which activated ILC2s. Activation of ILC2s was associated with tuft cell hyperplasia and significant increase in the length of the intestine (Schneider et al., 2018). Taken together, not only do ILC2s play a role in mediating inflammation but are also responsible for restoring homeostasis after epithelial damage.

Skin inflammation

ILC2s being tissue resident immune cells have been characterised in the pathology of various tissues. The next two sections discuss their role in a selection of different tissues. Dermal ILC2s (dILC2s) were identified in mouse skin as CD45+, CD3-, CD2-, CD90hi cells that constituted 5-10% of all CD45+ cells that were isolated (Roediger et al., 2013). dILC2s were shown to produce IL-13 but not IL-4 in the naïve state, however, they produced IL-4 when exposed to inflammatory stimulus. IL-2 was able to activate dILC2s and these cells in turn promoted cutaneous inflammation. This dILC2 driven inflammation was shown to be partly through IL-5 production by ILC2s and associated eosinophilia (Roediger et al., 2013). In an ovalbumin-based model of allergic skin inflammation, ILC2s and T_h2 cells were found to be major sources of IL-13 in an acute and chronic setting respectively. IL-13 was found to be important for the increased transepidermal water loss (TEWL) in this allergic skin inflammation setting. ILC2 activation was also found to be essential for recruiting T_h2 cells in chronic skin inflammation. In the absence of ILC2 activation by IL-25 in chronic allergic skin inflammation, T_h2 infiltration and *Il13* expression in the tissue were significantly reduced (Leyva-Castillo et al., 2020). In both these reports, dILC2s were shown to regulating inflammation in the skin.

In a spontaneous model of atopic dermatitis (AD) in Filaggrin-mutant mice however, the inflammation was found to be independent of ILC2s. While ILC2 numbers were found to increase in adult mice with atopic dermatitis, 3 different models of ILC2 deficiency failed to show a reduction in dermatitis severity (Schwartz et al., 2019). On the contrary, in an allergic contact dermatitis model, induced using 2,4,5-trinitrochlorobenzene (TNCB), lack of ILC2s leads to exaggerated inflammation and ear swelling (Rafei-Shamsabadi et al., 2018). In another report examining the Filaggrin-mutant mice with atopic dermatitis, AD was found to be associated with IL-5 producing ILC2 expansion. This was also corroborated by increased ILC2 infiltration in skin of patients with Filaggrin mutation associated AD (Saunders et al., 2016). Taken together ILC2s mediate inflammation in different models of dermatitis.

ILC2s as inflammatory mediators in other tissues

ILC2s are both able to regulate adiposity and are also sustained by signals from adipose tissue associated cells. Lack of eosinophils has been shown to induce adiposity and increased insulin resistance in experimental mice. IL-5 deficiency was shown to impair eosinophil accumulation in visceral adipose tissue (VAT). This was associated with increased insulin resistance and adiposity in mice on a high fat diet. ILC2s were identified as a major source of IL-5 and deletion of ILC2s led to decreased VAT eosinophils (Molofsky et al., 2013). ILC2s are tissue-resident cells requiring local sources of sustenance signals. *Rana et al, 2019* show that in white adipose tissue (WAT), this sustenance signal for ILC2s is IL-33 and this is provided by WAT - multipotent stromal cells (WAT - MSCs). It was also shown that IL-13 and IL-4 released by ILC2s acted on MSCs to induce eotaxin (CCL11) secretion and resulting eosinophilia (Rana et al., 2019).

ILC2s have been shown to be critical for parasite expulsion in *N brasiliensis* infection in several reports (Neill et al., 2010; Oliphant et al., 2014; Price et al., 2010). Their role in viral infections however is not as straightforward and is context specific. In a study looking at the infection of the H1N1 CA04 virus in *Ifnγ*$^{-/-}$ mice, increased resistance to the infection was observed in these mice compared to controls. Subsequently, IFN-ɣ neutralisation was found to be beneficial for mice infected with CA04. However, IFN-ɣ neutralisation made no difference in ILC2 deficient mice which already showed higher susceptibility to infection compared to WT control mice. IFN-ɣ was hypothesised to be regulating ILC2 production of IL-5 and subsequent downstream eosinophilia via IFN-ɣR2 on ILC2 surface. ILC2s have a protective role in influenza infection which is negated by infection induced IFN-ɣ production (Califano et al., 2018). ILC2s have also been shown to have a detrimental role in infection. In influenza A virus infection associated pathology, ILC2s were found to be essential for the AHR and

inflammation in this mouse model (Y.-J. Chang et al., 2011). Thus, the role of ILC2s in viral infections is context specific.

ILC2s have been studied in several inflammatory models, a few of which are outlined here. In an antigen-induced self-resolving model of arthritis, IL-9 was found to activate ILC2s. Downstream of this activation, ILC2s were found to induce Treg cell activation in a GITR-GITRL and ICOS-ICOSL dependent manner. This IL-9 mediated pathway leads to resolution of inflammation in this model of arthritis and subsequent prevention of overt tissue damage such as cartilage and bone loss. This role of ILC2s in the resolution of inflammation is demonstrated by the lack of resolution of inflammation in antigen-induced arthritis in IL-9-/- mice (Rauber et al., 2017). ILC2s were found to be present in para-aortic adipose tissue and were found to be central to atheroprotection through their production of IL-5 and IL-13. ILC2KO mice were found to show increased atherosclerosis in the aortic arch. Increased atherosclerosis was also observed in ILC2 deficient mice (*Staggerer/Rora*^{flox} *Cd127*^{cre}) that had received IL-5-/- or IL-13-/- BM. This paper demonstrated that type 2 cytokine production by ILC2s was atheroprotective in nature (Newland et al., 2017). Acute graft-versus-host disease (aGVHD) is a complication that arises for people undergoing allogeneic stem cell transplantation (allo-SCT). aGVHD is the cause of mortality for 15-30% of allo-SCT recipients. The higher grades (III-IV) of aGVHD involve the gut in their pathophysiology and is an important cause of mortality associated with aGVHD. Donor-derived T cells are known to drive the pathophysiology of grade III-IV aGVHD. Recently, ILC2s have been shown to be poorly reconstituted in alloSCT. When this was corrected in pre-clinical models through transplantation of ILC2s, it led to improved survival of aGVHD pre-clinical models. ILC2 sourced IL-13 was found to be critical for recruiting MDSCs, which then brought about immunosuppression of the aforementioned donor T cells (Bruce et al., 2017). These reports from various organs and pathologies covered in this section point to the broad repertoire of roles ILC2s can play in an inflammatory setting, thus making the question of what ILC2s maybe doing in the pancreatic pathology context very interesting. Their role would be dependent on the nature of activation and the activation products produced by ILC2s in that setting.

Pancreatitis

Pancreatitis is defined as inflammation of the pancreas. Acute pancreatitis occurs in 15-42 cases out of every 100,000 people every year in the UK and this incidence is rising by 2.7% every year (Goodchild et al., 2019). Of this number approximately 50% of cases tend to be caused by gallstones, 25% by excessive alcohol intake and another 25% by other factors

(*Context* | *Pancreatitis* | *Guidance* | *NICE*, n.d.). 1/4th of all acute pancreatitis patients develop severe disease which requires critical care and prolonged hospitalisation. Severe acute pancreatitis is often characterised by kidney failure, respiratory failure or ascites. The mortality rate from acute pancreatitis is 5% and the mortality rate in patients with severe acute pancreatitis is 25% (*Context* | *Pancreatitis* | *Guidance* | *NICE*, n.d.). Acute pancreatitis is diagnosed based on 2 out of 3 of the following features: elevated serum amylase and lipase levels, acute abdominal pain and CT or MRI showing features of acute pancreatitis (Forsmark et al., 2016). Pancreatic or peripancreatic fluid collections are also common features of acute pancreatitis. Interstitial oedema containing homogenous liquid content may be seen in the first 4 weeks of disease onset and typically is self-limiting. Fluid collections associated with necrotising pancreatitis may also be seen containing varying amounts of fluid and necrotic debris (Boxhoorn et al., 2020).

Early management of pancreatitis involves aggressive fluid resuscitation in the first 24 hours of onset of symptoms and this has been reported to reduce mortality and morbidity (Forsmark et al., 2016). Based on the severity of disease, patients may be fed a regular low-fat diet or artificial enteral feed. Patients with acute pancreatitis may develop necrosis in their pancreas and if the necrosis is associated with infection, then the patients may be started on broad spectrum antibiotics. 33-50% of patients with acute pancreatitis go on to develop chronic pancreatitis (Forsmark et al., 2016).

Chronic pancreatitis is a fibro-inflammatory syndrome that results from prolonged and continuous occurrences of acute pancreatitis (Kleeff et al., 2017). 5 new cases of chronic pancreatitis are diagnosed per 100,000 people every year in western europe. 70-80% of all chronic pancreatitis cases are caused due to excessive alcohol intake and cigarette smoking has also been shown to have an association (*Context* | *Pancreatitis* | *Guidance* | *NICE*, n.d.). Chronic pancreatitis is associated with several complications such as biliary obstruction, pancreatic duct obstruction, haemorrhage, ascites or pleural effusion. Both endocrine and exocrine functions of the pancreas are compromised in chronic pancreatitis. Diabetes (endocrine insufficiency), maldigestion and steatorrhoea (due to exocrine insufficiency) are common consequences of chronic pancreatitis (Kleeff et al., 2017). Some symptoms of pancreatitis like recurring abdominal pain, diabetes mellitus and steatorrhoea are not pancreas specific which leads to delay in diagnosis of chronic pancreatitis (Kleeff et al., 2017). Risk of developing pancreatic cancer is 70 times higher in patients with hereditary pancreatitis. In the first report identifying pancreatitis as a risk factor for pancreatitis cancer, the relative risk of developing pancreatic cancer in patients with pancreatitis in a 5 year follow up has been estimated to be 14.4 (95% CI of 8.5-22.8) (Lowenfels et al., 1993). However, considering the

low incidence of chronic pancreatitis and the lower incidence of chronic pancreatitis patients developing pancreatic cancer, chronic pancreatitis is a rare cause of pancreatic cancer (Yadav & Lowenfels, 2013).

Pathogenesis of the epithelial damage stage of acute and chronic pancreatitis

Alcohol consumption is thought to increase viscosity of pancreatic secretions thus leading to formation of protein plugs that block small ducts (Klochkov et al., 2021). This obstruction can further lead to calculi formation and the pathophysiology of how duct obstruction is associated with epithelial damage is explained through two hypotheses. Claude Bernard discovered in 1856 that bile injected into the pancreatic duct could cause pancreatitis in laboratory animals. In 1901 Ernest Olpie suggested two hypotheses for the pathogenesis of pancreatitis: the 'duct obstruction theory' and the 'common channel' hypothesis. The duct obstruction hypothesis suggested that duct obstruction leading to blockage in outflow of pancreatic juices caused pancreatitis. The common channel hypothesis suggests that when a gallstone is impacted at the papilla of Vater, it causes a channel to be formed between the bile duct and pancreatic duct. This common channel leads to bile flowing through the pancreatic duct and thus causing pancreatitis (Lerch & Aghdassi, 2010).

Pathogenesis of pancreatitis leads to 3 hallmarks of the epithelial damage phase in acute pancreatitis - oedema, acinar cell injury and inflammation (fig 2). A block in digestive enzyme secretion either by gallstones or supramaximal stimulation of the secretagogue cholecystokinin, leads to co-localisation of zymogens and lysosomes. This is followed by activation of zymogens like trypsinogen by Cathepsin B, a lysosomal component. This premature activation of trypsin in the pancreas leads to acinar cell injury followed by the 3 hallmarks of acute pancreatitis (Saluja et al., 2007).

Pathophysiology of recovery in acute and chronic pancreatitis

One of the key features of the pathophysiology of chronic pancreatitis is fibrosis that follows extensive destruction of the acinar cell compartment. Pancreatic stellate cells (PSCs) are a subset of fibroblasts that are reported to drive the fibrogenesis in the pancreas by formation of the extracellular matrix (ECM) in regions of acinar cell injury and other interstitial spaces (Brock et al., 2013). Epithelial injury is associated with activation of stromal cells which involves increased expression of α-smooth muscle actin (αSMA) by PSCs, increases proliferation of PSCs and secretion of collagen and other ECM components that cement fibrosis. This fibrotic modification of the pancreas is irreversible and it eventually compromises both the endocrine and exocrine function of the pancreas (Apte et al., 1999) (Shek et al.,

2002). PSCs have been shown to produce collagen and other matrix components when stimulated by TGFβ (Apte et al., 1999). FK565 is a NOD1 agonist which when administered with low-dose caerulein induces pancreatitis (Tsuji et al., 2012). In a FK565+Caerulein model of chronic pancreatitis, IL-13 signalling that is downstream of IL-33 signalling was shown to be able to activate PSCs. Neutralisation of IL-13 signalling limited the development of inflammation and fibrosis in chronic pancreatitis. This report however identified T cells as the major source of IL-13 (Watanabe et al., 2016). ILC2s as a source of IL-13 is yet to be investigated in chronic pancreatitis.

Acinar cells are highly plastic and can dedifferentiate and transdifferentiate into a ductal marker expressing embryonic progenitor phenotype through a process called acinar to ductal metaplasia (ADM, fig 2). In pancreatitis ADM is common and reversible and it is through ADM that the acini are thought to regenerate (Storz, 2017). RANTES, TNFα, TGFβ has been shown to induce ADM (Liou et al., 2013) and TGFβ also facilitates the induction of PanINs from ADM (Chuvin et al., 2017). In the pancreas, *Sox9* and *Ck19* are expressed by ductal cell progenitors and mature ducts, *Mist1, Ptf1a, Cpa1* and *Ela1* are expressed by acinar cell progenitors and NGN3 is expressed by endocrine cell progenitors. *Ptf1a* is a marker for pancreatic progenitor cells but later on in development becomes acinar cell specific. When undergoing ADM, acinar cells downregulate acinar specific markers like CPA1 and upregulate ductal lineage markers like CK19 (Chuvin et al., 2017).

While ADM is reversible, if cells undergoing ADM also acquire an aberrant and persistent growth factor signalling *Kras* mutation the transformation could become irreversible. Mouse model experiments have demonstrated that oncogenic signalling prevents redifferentiation and pushes progression of transformed cells. This irreversible ADM can then transform into pancreatic intraepithelial neoplasia (PanINs) which are precursor lesions for pancreatic ductal adenocarcinoma (PDAC) (Shi et al., 2013). Histological representation of PanINs and PDAC has been shown in fig 3.

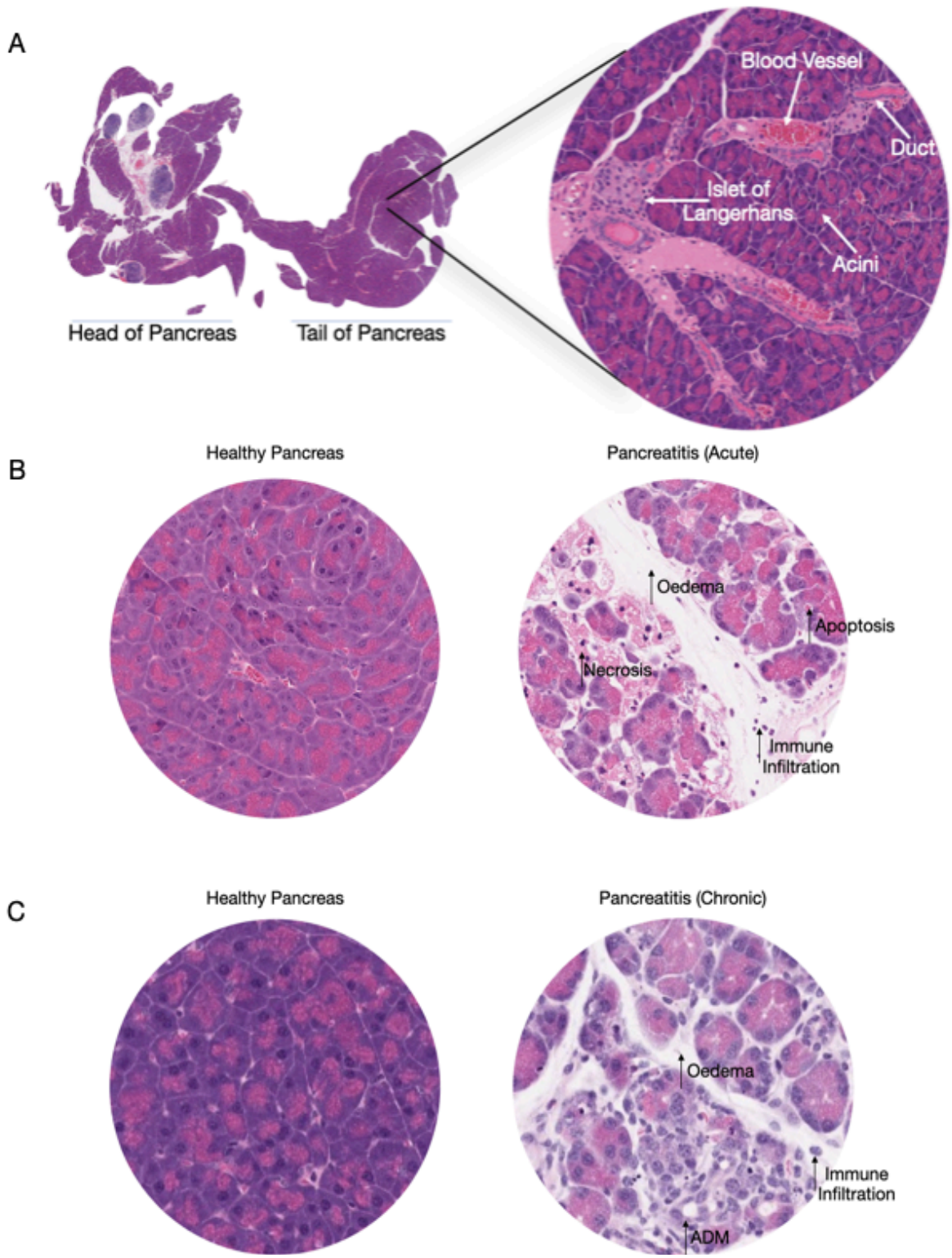

Fig 2 - A, Anatomy of the pancreas. The pancreas is made up of endocrine and exocrine components. Endocrine function of the pancreas is performed by the islet of Langerhans that contains β cells which produce insulin to regulate blood sugar levels. The exocrine function in the pancreas is performed by acinar cells and ductal cells. Acinar cells produce digestive enzymes such as amylase and lipase which are carried by ducts formed by ductal cells to the duodenum. B, Excessive alcohol intake and gall stones lead to acute pancreatitis which shows features such as cell death by necrosis, oedema and immune infiltration during the epithelial damage phase. C, The remodelling phase of pancreatitis is characterised by immune infiltration, oedema, acinar to ductal metaplasia (ADM) and fibrosis. Fibrosis is more exaggerated in chronic pancreatitis.

Immunopathogenesis of acute and chronic pancreatitis.

Inflammatory response in the epithelial damage phase of acute pancreatitis is thought to be initiated by the release of damage associated molecular patterns (DAMPs) from dying pancreatic acinar cells. DAMPs then interact with pattern recognition receptors on innate immune cells to kick off the inflammation during the epithelial damage phase of acute pancreatitis. High-mobility group box protein 1 (HMGB1), adenosine triphosphate, self-DNA and the nuclear cytokine IL-33 are some of the DAMPs that have been reported to be pancreatitis associated (Watanabe et al., 2017). HMGB1 levels in the serum are considerably elevated in acute pancreatitis and this correlates with severity of the disease (Yasuda et al., 2006). Mouse models lacking HMGB1 expression in the pancreas have been shown to develop more severe acute pancreatitis compared to control mice treated with L-arginine or caerulein. Intracellular HMGB1 seemed to be blocking nucleosome release and subsequent inflammation and thus limiting disease severity. Extracellular HMGB1 which is released from the cell however had the opposite effect and it was shown to exacerbate disease severity by promoting inflammatory response (Kang et al., 2014). Self-DNA, another DAMP typically signals via TLR9 and the downstream signalling induces inflammasome formation and subsequent inflammation. Inflammasome formation was found to be mediated by TLR9 and $P2X_7$ after activation by DAMPs. Neutrophil accumulation in acute pancreatitis which follows epithelial damage marks the first of the inflammatory influx, and this neutrophil influx was found to be TLR9 dependent (Hoque et al., 2011). IL-33, another DAMP molecule that is known to regulate type 2 immune responses, was shown to regulate inflammation in chronic pancreatitis. In a model involving repeated administration of low-dose caerulein and the NOD1 ligand, FK565, blocking IL-33 signalling led to prevention in development of chronic pancreatitis (Watanabe et al., 2016). In this model, IL-33 was shown to be expressed in peri-acinar spaces and did not localise with the PSC marker αSMA. (Watanabe et al., 2016).

Patients with acute pancreatitis show increased serum levels of several pro-inflammatory cytokines like TNFα, IL1β and IL-6 and chemokines like MCP-1, IL-8 and macrophage migration inhibitory factor. These cytokines and chemokines are presumably released by various cells in the pancreas that are activated downstream of DAMP release from damaged acinar cells (Watanabe et al., 2017). The roles of various immune cells in the pathogenesis of acute and chronic pancreatitis have been specifically discussed along with results from experiments investigating the role of individual immune cells.

Pancreatic Cancer

Epidemiology and clinical presentation

With around 10,300 cases of pancreatic cancer diagnosed every year, it is the 10th most common cancer in the UK and it accounts for 3% of all new cancer cases. A dismal 25% of the people diagnosed with pancreatic cancer survive the disease for more than a year. About 5% of those diagnosed with pancreatic cancer survive for more than 10 years after diagnosis. This dismal statistic is largely because of the challenges in diagnosing pancreatic cancer, which often leads to diagnosis in very late stages of the disease (*Pancreatic cancer statistics*, 2015).

This late diagnosis of pancreatic cancer is due to nonspecific and sometimes no symptoms, lack of tumour specific blood makers and challenges in imaging early-stage tumours due to anatomical location of the organ. Pancreatic cancer is marked by vascular local growth and early metastasis to distant organs that are not conducive to surgical removal in most patients. One of the biggest challenges in translational medicine with respect to pancreatic cancer is the disease's extreme resistance to any form of treatment - chemotherapy, radiotherapy or targeted therapy. Additionally, pancreatic cancer’s dense stromal microenvironment makes drug delivery very challenging (Kleeff et al., 2016).

In terms of treatment, 10% of pancreatic cancer patients undergo surgery for tumour removal, 28% undergo chemotherapy which may be curative or palliative and 5% of patients undergo radiotherapy. Smoking, obesity and excessive alcohol intake are the most common risk factors for pancreatic cancer. Pancreatic cancer risk is 2.2 times higher in current smokers compared to non-smokers and 22% of all pancreatic cancer cases in the UK are associated with smoking (*Pancreatic cancer statistics*, 2015). In the UK, 12% of all pancreatic cancer cases are associated with being overweight and obesity. In those who consume more than 3 units of alcohol per day, the risk of developing pancreatic cancer is 15-19% higher compared to non-consumers or occasional drinkers. Risk of developing pancreatic cancer is 62-75% higher in first-degree relatives of those diagnosed with the disease (*Pancreatic cancer statistics*, 2015).

Inflammation has been well explored for its capability to accelerate the development of pre-neoplasms into full-blown cancers. Inflammation and the cellular components of inflammation are thought to be an enabling characteristic that can push neoplasms to acquire core cancer hallmarks (Hanahan & Weinberg, 2011). Pancreatitis as well has been shown to experimentally accelerate pancreatic cancer development. While embryonic induction of *K*-

Ras^{G12V} mutation in cells of acinar/centroacinar lineage led to development of PanINs and invasive PDAC, adult mice with *K-Ras*^{G12V} mutation were resistant to developing PDAC. However, if the adult mice were challenged with chronic pancreatitis after induction of the *K-Ras*^{G12V} mutation, they developed PanINs and invasive PDAC (Guerra et al., 2007). It was also shown that pancreatic acinar cells did not undergo tumorigenic transformation with several oncogenic insults including expression of K-Ras oncogenes and loss of tumour suppressors like *p16Ink4a/P19Ark* and *Trp53*. However, when these oncogenic insults were combined with bouts of pancreatitis, PanIN and PDAC development were seen. It was shown that low grade PanINs don't progress due to senescence and that pancreatitis helps abrogate this senescence barrier. Correlating with human data, patients on anti-inflammatory drugs showed senescent PanINs. Extending from this observation, mice that had been treated with a nonsteroidal anti-inflammatory drug (NSAID) and bearing a *K-Ras*^{G12V} mutation did not develop the accelerated PanIN lesions and PDAC. Administration of anti-inflammatory agents in people diagnosed with pancreatitis was suggested as a measure that may reduce risk of developing PDAC (Guerra et al., 2011). Similar findings were seen in another report where *K-ras*^{G12D} mutation bearing mice, in early stages of PanINs showed rapid tumour progression and development of higher grade PanINs after just two brief instances of acute pancreatitis (Carrière et al., 2009). Taken together, while pancreatitis might be a rare cause of pancreatic cancer, in the case of pre-existing oncogenic insults, pancreatitis is capable of accelerating tumour progression.

Molecular pathology of pancreatic cancer

Roughly 75-80% of all pancreatic cancers are adenocarcinomas leading to the term 'pancreatic ductal adenocarcinoma' (PDAC) being used interchangeably with 'pancreatic cancer'. PDAC is characterised by dense stroma and neoplastic ducts arising from the precursor lesions PanINs (fig 3). About 15-20% of all pancreatic cancers are neuroendocrine tumours which display a nested growth pattern and express neuroendocrine markers such as synaptophysin and chromogranin (Kleeff et al., 2016). Colloid carcinomas are characterised by formulation of mucin pools in the stroma are about 2% of all pancreatic cancer cases. Solid-pseudopapillary tumours make up another 2% of pancreatic cancers and are characterised by poorly cohesive cells. Acinar cell carcinomas characterised by single prominent nuclei and granular cytoplasm form about 1% of all pancreatic cancers. Pancreatoblastomas have squamoid nests and neoplastic cells that show acinar differentiation and are about 0.5% of all pancreatic cancers (Kleeff et al., 2016).

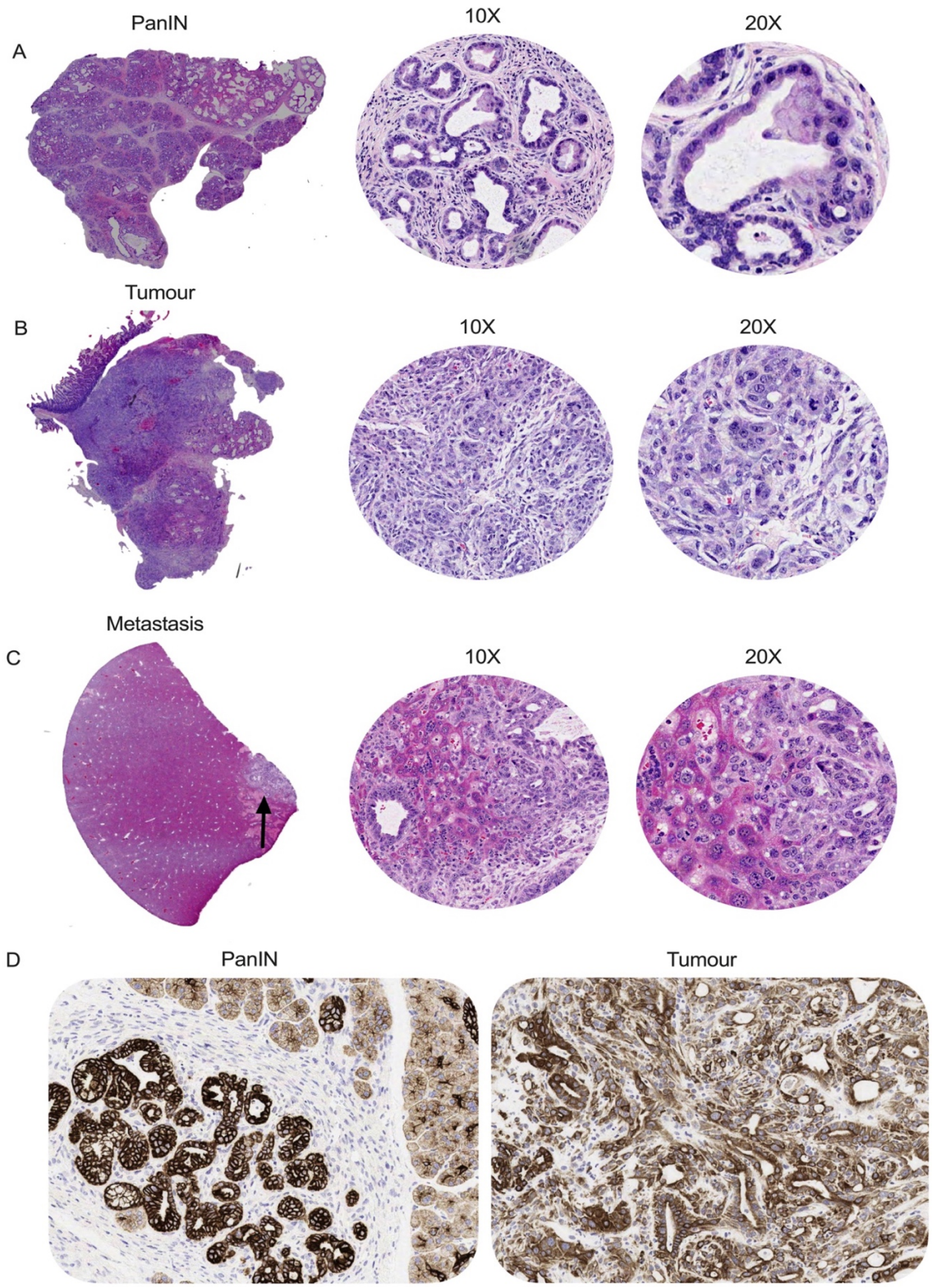

Fig 3 - Histological representations of different stages of PDAC development. Mouse PanIN, PDAC and liver metastasis tissue have been shown here. A, Pancreas with PanINs show several duct like structures in what would typically be acinar cell regions surrounded by intense fibrosis. Acinar cell frequency is heavily reduced and replaced by ductal cells. B, PDAC tissue does now show the distinct duct like arrangement seen in PanINs. Cells are disordered and embedded in fibrotic extracellular matrix. C, PDAC metastasis to the liver is shown here. Distinction between host liver tissue and invading metastatic tissue can be seen at both magnifications. D, Immunohistochemical staining for cytokeratin 19 a ductal cell marker. CK19 staining shows organised ductal like structured in PanINs while this arrangement of ductal cells is disordered in tumour tissue.

As mentioned earlier, PanINs are the preneoplastic lesions that give rise to PDAC. A small proportion of PDAC can also arise from mucinous cystic neoplasms or intraductal papillary mucinous neoplasms which tend to be larger precursor lesions (Hezel et al., 2006). Over 90% of all PDAC tumours present with an activating *KRAS* mutation. 50-80% of PDAC have inactivating mutations of *TP53, SMAD4* and *CDK2NA.* Genes like *ARID1A, TGFBR2 and MLL3* are mutated in 10% of all PDAC tumours (Kleeff et al., 2016).

Tumour microenvironment in PDAC

Histology sections of PDAC have characteristic dense stroma resulting from a fibrotic reaction called desmoplasia, where fibroblasts deposit ECM that occupies a large part of the tumour. An excessive deposition of Collagen type I, III and IV is seen in PDAC (Hosein et al., 2020). This excessive production of ECM proteins by the stromal cells is triggered by PDAC cells in a paracrine manner (Bachem et al., 2005). Fibroblasts are of mesenchymal origin and form the supportive framework of most structural organs. In homeostasis they support organ function through secreted soluble factors and secreting ECM. Their expression profile is specific to the organ they are present in and local tissue requirements (Hosein et al., 2020).

Cancer associated fibroblasts (CAFs) are fibroblasts found in the tumour microenvironment and these have been shown to actively promote tumorigenesis. This makes CAFs an attractive therapeutic target, however CAFs are a heterogeneous population and an understanding of the biology of each subtype is required for efficient targeting. Pancreatic stellate cells (PSCs) are a subset of fibroblasts that are present in periductal, periacinar and perivascular spaces in normal pancreas (Hosein et al., 2020). When co-cultured with organoids derived from mouse PDAC, PSCs showed increased expression of α-smooth muscle actin (αSMA) and displayed a myofibroblast like gene expression profile. These cells with a myofibroblast gene expression profile have been named myCAFs. However, when PSCs and mouse tumour derived organoids were co-cultured without direct contact, the PSCs expressed IL-6 and other inflammatory cytokines (and chemokines like CXCL12) and did not upregulate αSMA. This subtype has been referred to as inflammatory CAFS (iCAFs). In mouse and human PDAC tissue, myCAFs were shown to be proximal to the tumour while the iCAFs were more distal to the tumour edge (Öhlund et al., 2017). Single cell RNAseq of human and mouse model PDAC tissues revealed an additional fibroblast population with high expression of MHC II family members. These fibroblasts have been termed antigen presenting CAFs (apCAFS) (Elyada et al., 2019).

Among mouse models of pancreatic cancer, the KPC model (*LSL-Kras*$^{G12D/+}$*;LSL-Trp53*$^{R172H/+}$*;Pdx-1-Cre*) and the KC model (*LSL-Kras*$^{G12D/+}$*;Ptf1a-Cre*) are most commonly

used. Although KPC mice tumours showed CD8 T cell infiltration similar to human PDAC tissues, they did not respond to immune checkpoint inhibitors like aCTLA-4 or aPD-1. CAFs seemed to be regulating this immune evasion and when CAFs were depleted using a fibroblast depletion mouse model, aCTLA4 and aPD-1 therapies became effective in bringing about tumour control. CAFs were found to be secreting CXCL12 which coated tumour cells and mediated immune evasion. When the mice were treated with AMD3100, a drug that targets CXCR4 (the receptor through which CXCL12 signals), tumour control was regained (Feig et al., 2013). These CAFs are now retrospectively identified as iCAFs and this subset of fibroblasts has been shown to influence tumour growth and survival (Hosein et al., 2020). In summary, CAFs form an integral part of PDAC's survival kit.

The tumour microenvironment PDAC is also marked with extensive inflammation and some of these inflammatory and immune changes have been reviewed below. Based on the various tumour-host immune system interactions, PDAC tumours are classified as Immune-escape phenotype, Immune-rich phenotype or Immune-exhausted subtypes (Karamitopoulou, 2019). Tumours of the immune-escape phenotype tend to be rich in Tregs and M2 macrophages which are immune suppressive and pro-tumorigenic in function. In a mouse PDAC study, the suppression of dendritic cell function was found to be regulated by Tregs. DCs are required in the tumour microenvironment to process and present tumour antigens to CD8 T cells, which can then bring about targeted killing of tumour cells (Jang et al., 2017). Tregs present in the PDAC tumour microenvironment were found to induce a tolerogenic phenotype in DCs. Namely, Tregs induced low expression of co-stimulatory molecules, reduced the ability of DCs to process antigen and lowered their production of proinflammatory cytokines (Jang et al., 2017), thus, affecting the anti-tumorigenic function of dendritic cells. In the context of inflammation induced due to acinar to ductal metaplasia (ADM), tuft cells in the pancreas were found to release IL-13 (Liou et al., 2017). This IL-13 was found to convert inflammatory M1 macrophages to Ym1+ M2 macrophages which are pro-tumorigenic in function. These M2 Macrophages then release IL-1ra and CCL2 which drive pancreatic fibrosis and tumorigenesis (Liou et al., 2017). PDAC tumours of the immune-escape subtype tend to be poor in CD3+, CD4+ and CD8+ T cells, CD20+ B cells and M1 macrophages which have anti-tumorigenic roles. Most PDAC tumours belong to this subtype (Karamitopoulou, 2019).

Immune-rich PDAC tumours are the exact opposite of the immune-escape subtype in immune composition. This subtype is associated with favourable clinical and pathological features with prolonged survival. These tumours tend to have fewer Tregs and M2 macrophages and tend to be rich in CD3+, CD4+ and CD8+ T cells, CD20+ B cells and M1 macrophages (Karamitopoulou, 2019). These tumours typically present with tertiary lymphoid structures

which are associated with an anti-tumorigenic response. These tumours tend to be rich in immunogenic characteristics like high mutational frequency in genes associated with DNA damage response, high neoantigen load, upregulation of antigen presentation and interferon signalling (Karamitopoulou, 2019). This immune phenotype is associated with the classical tumour stroma phenotype described by Moffit et al, 2015 which was computationally stratified based on PDAC gene expression microarray data. Patients with this sub-type of tumour showed significantly higher survival compared to other groups (Moffitt et al., 2015).

The immune exhausted phenotype shows high PD-L1 expression on tumour cells, either activated by inflammatory cytokines or oncogenic signalling (Zheng, 2017). PD-L1 expressed on tumour cells inhibits T cell activation followed by targeted tumour killing. Blocking PD-L1 and thereby improving T cells activation and tumour cells killing is a highly favoured therapeutic strategy (Wang et al., 2020). The clinicopathological outcome of this subtype of PDAC is poor. As mentioned earlier, aPD-1 (PD-L1's receptor) therapy has been shown to be less effective in PDAC due it's highly desmoplastic microenvironment.

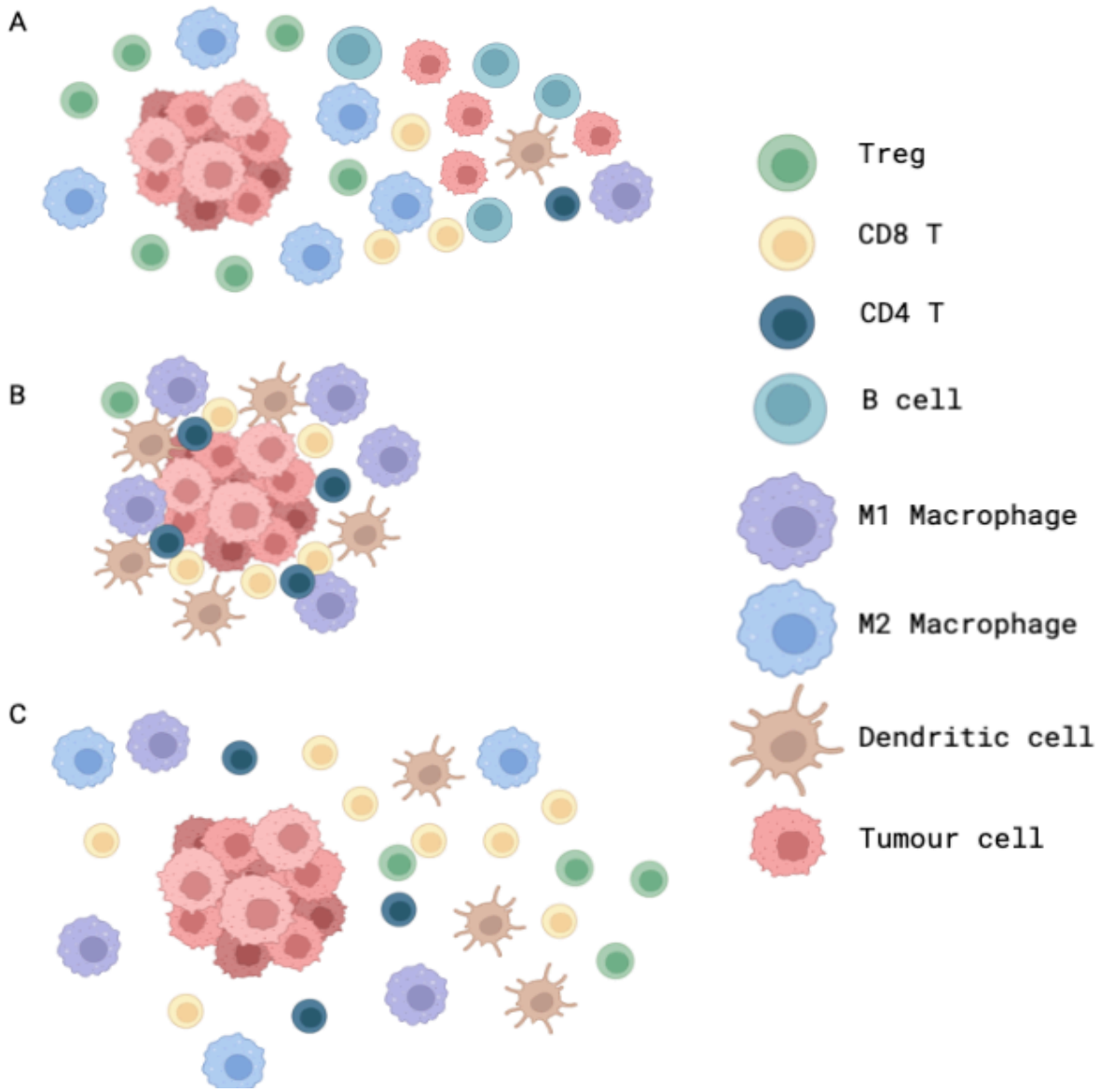

Fig 4 - Classification of PDAC based on the immune microenvironment. A, Immune escape subtype of PDAC are rich in Tregs and M2 macrophages. B, Immune rich subtype of PDAC are infiltrated with high numbers of DCs and CD8 T cells. C, Immune exhausted subtype of PDAC show high PD-L1 expression on tumour cells, which signals via PD-1 on CD8 T cells to bring about immune exhaustion thus preventing tumour killing. Figure from *Karamitopoulou et al, 2019.* Figure made by the student using biorender.com.

ILCs in cancer

The role of each ILC in cancer is dependent on both the tumour type and the kind of cytokine produced by the ILC in that context (Bruchard & Ghiringhelli, 2019).

Group 1 ILCs in cancer

NK cells, which are now recognised as a subset of ILC1s, are well known to play an important role in anti-tumour immunity. NK cells can distinguish stressed cells such as infected cells, tumour cells and other cell types that have had physical or chemical injuries (Vivier et al., 2012). In non-small cell lung carcinoma, NK cell infiltration in the tumour has been associated

with better prognosis. NK cells can bring about direct cell death of stressed cells through cytotoxic mediators. NK cell released IFNg can also shape adaptive immune response in a tumour micro-environment (Vivier et al., 2012). In mouse models, NK cells have been shown to have an antimetastatic function (Nakamura & Smyth, 2020). ILC2s were shown to supress NK cell anti-metastatic function through IL-5 mediated eosinophilia (Schuijs et al., 2020). In a study looking at a cohort of acute myeloid leukaemia patients, cytokine production by ILCs was found to be impaired. Interestingly an increase in ILC1 and a corresponding decrease in ILC3s was also seen in these patients, pointing to a possible plasticity in response to the microenvironment (Trabanelli et al., 2015). In MMTV-PyMT mice (breast tumour models), with constitutive IL-15 overexpression, ILC1s were found to expand. This expansion was associated with an inhibition of tumour growth. In MMTV-PyMT mice lacking IL-15 expression however, were found to be ILC1 deficient and showing accelerated tumour growth (Dadi et al., 2016). The role of ILC1s in tumour development is definitely context specific as based on the cytokine they produce, ILC1s could be pro or anti-tumorigenic in function (Bruchard & Ghiringhelli, 2019).

Group 3 ILCs in cancer

ILC3s have been shown to be present in tumour tissues and play a role in cancer development (Goc et al., 2016). In a mouse model of colon cancer, NCR- ILC3s derived IL22 was found to be important for tumour maintenance (Kirchberger et al., 2013). Human and mouse colorectal carcinoma (CRC) tissues showed a reduction in ILC3s compared to adjacent normal tissues. The interaction of MHCII+ ILC3s with T cells was shown to be disrupted in CRC and selectively depleting MHCII expression in ILC3s led to more aggressive CRC and resistance to anti-PD1 immunotherapy. Taken together this report projects a protective role for ILC3s in cancer (Goc et al., 2021). Further work looking at the specific role of ILC3s in cancer are needed to establish the role of ILC3s in each tumour context.

Group 2 ILCs in cancer

ILC2s have been found to have tissue dependent role in cancer development as well. In liver cancer, inflammation and fibrosis triggered by disruption of the epithelial lining of the bile duct was shown to become cholangiocarcinoma through malignant transformation. IL-33 was found to be increased in human and murine biliary atresia. Based on this observation, it was further shown that IL-33 induced proliferation of ILC2s in the liver. IL-33 activated ILC2s then released IL-13 which in turn induced proliferation of cholangiocytes. Also, IL-33 administration in mice genetically susceptible to cholangiocarcinoma, accelerated biliary tract carcinogenesis thus establishing a pro-tumorigenic role for ILC2s in this context (Li et al., 2014). Relatedly, IL-33 levels were found to be increased in clinical studies of patients with liver cirrhosis. The same

observation was recorded in mouse models of hepatic fibrosis as well. In this mouse model of hepatic fibrosis, stressed hepatic stellate cells were found to secrete IL-33, which then led to expansion and activation of ILC2s. These activated ILC2s secreted IL-13, which through hepatic stellate cells helped with progression of fibrosis (McHedlidze et al., 2013). In gastric cancers, T_h2 phenotype was found to correlate with poor prognosis in cancer patients. Also, the frequency of circulating ILC2s was found to be high in gastric cancer patients (W.-J. Chang et al., 2014).

Moreover, in a mouse model of lung metastatic melanoma, rIL-33 administration was found to induce ILC2s in the lung to produce IL-5. Through IL-5 secretion ILC2s were found to recruit eosinophils, which then induced tumour cell death and prevented tumour metastasis (Ikutani et al., 2012). Though this paper argues for an anti-tumorigenic role for ILC2s, an opposite role (that is metastasis/tumour promoting) was described for ILC2s in the lung metastasis of melanoma mouse model. ILC2 mediated eosinophilia was also found to regulate IFN-ɣ production by NK cells in this model. Several mouse models of ILC2 activation were used to show that activated ILC2s were suppressing NK cell production of IFN-ɣ and subsequent control of melanoma metastasis spread in the lung (Schuijs et al., 2020).

ILCs were found to play a role in tumour progression in the 4T1 syngeneic mouse model of human triple negative breast cancer. In this model, tumour cells produced IL-33, which was associated with increased Tregs, ILC2s and TGF-β producing Myeloid derived suppressor cells (MDSCs). This paper suggests that IL-13 released by ILC2s in this tumour model, helps MDSCs to express nitric oxide synthase and arginase. This then contributes to maintaining an immunosuppressive environment (Jovanovic et al., 2014).

In acute promyelocytic leukaemia (APL), ILC2s have been shown to be at the centre of a tumour immunosuppressive axis. ILC2s numbers were found to be increased in the circulation of patients with APL. Through the engagement of NKp30 on ILC2s and B7H6 on APL blasts, ILC2s were shown to be activated to produce IL-13. Prostaglandin D2 (PGD2) produced by APL blasts was also found to activate ILC2s through their binding to the CRTH2 receptor on ILC2. ILC2 sourced IL-13 was also shown to be critical for the expansion of monocytic-myeloid derived suppressor cells (m-MDSCs). In mouse models of APL, blocking components of this tumour immunosuppressive axes like NKp30, IL-13 or PGR1 lead to increased survival of APL affected mice compared to controls (Trabanelli et al., 2017). Taken together, ILC2s do play a context specific role in tumour development, which does skew more toward anti-tumorigenic based on literature.

Indirect evidence for the role of ILC2s in PDAC have also been discussed in literature, like IL-13 playing a role in skewing M1 to pro-tumorigenic M2 macrophages in PDAC. This supporting evidence suggests a potential role for ILC2s in PDAC and pancreatic inflammation (Liou et al., 2017).

The only report on ILC2s in PDAC, prescribed ILC2s as playing an anti-cancer role in the PDAC microenvironment. IL-33 was used to activate ILC2s and CD8 T cells in mouse orthotopic models of PDAC and these activated ILC2s expressed the immune checkpoint receptor PD-1. When PD-1 was blocked using a neutralising antibody, blockade of IL-33 activated ILC2 expansion (cell intrinsic) was relieved and subsequently enhanced tumour control was also achieved (Moral et al., 2020). While this report did propose an anti-tumour role for ILC2s, the model of excessive pre-exposure to IL-33 to bring about ILC2 activation differs from ILC2 activation in the PDAC microenvironment in humans. The role of ILC2s in the development of PDAC, in tumour promoting inflammation in PDAC and PDAC microenvironment needs to be extensively investigated.

Aims and hypothesis

ILC2s have been shown to be potent inflammatory mediators in barrier tissues like the lungs and the intestine. The role of ILC2s in the pathology of the exocrine pancreas is however unknown. ILC2s have been shown to play a predominantly pro-tumorigenic in other tumour settings but an anti-tumorigenic role in PDAC. Based on this background, the following are the aims of this thesis.

1. Identify and characterise activation of ILC2s in the pancreas
2. Characterise the role of ILC2s in the development of PDAC using autochthonous PDAC mouse models
3. Characterise the role of ILC2s in the inflammation associated with acute and chronic pancreatitis
4. Characterise the role of ILC2s in the pathology of acute and chronic pancreatitis – namely epithelial damage and tissue remodelling

Materials & methods

In vivo animal studies

C57BL/6 (B6) mice were purchased from Charles River Laboratories, Inc., and maintained in the Cancer Research UK Cambridge Institute (CRUK CI) for all *in vivo* experiments under specific pathogen free conditions. *Il7ra*$^{cre/+}$*Rora*$^{loxP/loxP}$, *Il7ra*$^{cre/+}$, *Kras*^{G12D}*Ptf1a*^{cre}, *Il33*$^{cit/cit}$, *Il33*$^{cit/+}$, Tg-FAP-DTR, *ΔdblGATA,* μ*MT*$^{KO/KO}$, *Rag1*$^{-/-}$,*Il13*$^{tom/+}$ and *Il13*$^{tom/tom}$ mice were bred in-house and maintained in the CRUK CI animal facility. Animals were age and sex matched for all experiments. All mice used for inflammation experiments were 6-12 weeks of age (except KC mice). All experiments were conducted according to the UK Home Office guidelines under PPL TH. PD7484FB9. After experiments, mice were sacrificed using a Schedule I method, and organs collected in appropriate collection buffers.

In vivo experiments

Alarmin treatment

For ILC2 activation experiments performed in the first chapter, mice were given 200ng recombinant IL-33 (BioLegend, 12022-09) or 200ng IL-25 (BioLegend, 587306) or 200ng TSLP (eBioscience, 34-8498-82) in 200µl endotoxin free sterile sterile PBS intraperitoneally.

Pancreatitis model

Mice were given 50µg/kg or 75µg/kg caerulein (Sigma, C9026) intraperitoneally in 200µl sterile PBS. To study epithelial damage in acute pancreatitis mice were injected with caerulein 6 times at hourly intervals and sacrificed 24 hours after the first injection. To study tissue remodelling, mice were injected with caerulein 6 times at hourly intervals for two consecutive days and sacrificed 3 days after start of caerulein administration. To study tissue remodelling during chronic pancreatitis, mice were injected with caerulein 6 times at hourly intervals for two consecutive days and this set was repeated over 3 consecutive weeks. The mice were sacrificed 16 days after administration of the first caerulein injection. Pain was managed with 50ng/g buprenorphine using subcutaneous injections.

Reagent administration

Mice were injected with 10mg/kg IL-33RFc (AstraZeneca), Cetirizine (500µg, Sigma, C3618-50MG), 10ng/g diphtheria toxin (Sigma, D0564), monoclonal antibody to anti-Ly6G (200µg, clone 1A8, Bio X Cell, BE0075-1), anti-Gr-1 (200µg, clone RB6-8C5, Bio X cell, BE 0075), anti-CD4 (100µg, clone GK1.5, Bio X cell, BE0003-1), anti-CD8 (200µg, clone 53.6.7, Biolegend, 100764), anti-NK1.1 (50µg, clone PK136, Bio X cell, BE0036), anti-CCR2 (20µg, clone MC-21, provided by M.Mack (Mack et al., 2001)), anti-IL-5 (100µg, clone TRFK5, Bio X cell, BE0198) and Rat IgG1 2a (200µg, BioXcell, BE0089). All reagents were prepared in sterile endotoxin free PBS.

Tissue collection

Pancreas was collected in PBS plus 10%FCS containing 0.1mg/ml Soybean trypsin inhibitor (Sigma, T6522) and cOmplete™ protease inhibitor cocktail and pancreatic lymph nodes (pLN) were collected in 500µl HBSS (Life Technologies, 24020091).

Single-cell preparation

Pancreas and pLN were digested in HBSS (Life Technologies, 24020091) with 375U/ml Collagenase type I (Life Technologies, 17100-017), 0.15mg/ml DNAse I (Sigma, DN25-1G) and 0.05mg/ml Soybean trypsin inhibitor (Sigma, T6522). Pancreas and pLN were digested for 30 minutes and 45 minutes respectively at 37℃ with constant shaking. Digested pancreas was broken down further using a 21G needle and passed through a 70µ cell strainer. The strainer was further washed with DMEM plus 10% FCS. Cells were spun down, treated with red blood cell lysis buffer (1ml, 3 minutes, RT), washed, and re-suspended in DMEM plus 10% FCS. pLN were broken down using a 21G needle after digestion and washed with PBS+2%FCS. The cell pellet was resuspended in PBS+2%FCS.

Antibody staining and flow cytometry

In order to detect intracellular cytokines, cells were treated with 1X cell stimulation cocktail with protein transport inhibitor (eBioscience, 00-4975-03) and control samples were treated with protein transport inhibitor cocktail (eBioscience, 00-4980-93) alone at 37℃ for 2 hours. Pancreas and pLN cells were stained with lymphoid, myeloid, stromal and cytokine panel antibodies (Tables 1-4) along with CD16/32 (BioLegend, 101320) to block Fc Receptors. Intra-nuclear staining was done using Foxp3 / Transcription Factor Staining Buffer kit (eBioscience, 00-5523-00) for the lymphoid and stromal panels according to manufacturer's instructions. Intracellular staining for the cytokine and myeloid panels was done using Cytofix/Cytoperm™ fixation/permeabilization kit (BD, 554714) according to manufacturer's instructions. Stained cells were analysed using the BD LSRFortessa™ or the BD FACSymohony™ flow cytometers and analysis of FACS data was done using FlowJo software.

Flow cytometry analysis

FlowJo software was used for analysis of flow cytometry data. The gating strategy for the lymphoid panel, myeloid panel and non-immune cell panel has been shown in figures 5-7. Cell numbers were extracted from FlowJo, post-processed on MS Excel and plotted on GraphPad prism.

Surface stain					
Fluorophore	**Protein**	**Clone**	**Manufacturer**	**Catalogue#**	**Dilution**
PerCP eF710	CD8	53-6.7	ThermoFisher	46-0081-82	1:500
eF450	CD5	53-7.3	ThermoFisher	48-0051-82	1:2000
eF450	CD11b	M1/70	ThermoFisher	48-0112-82	1:2000
eF450	CD11c	N418	ThermoFisher	48-0114-82	1:2000
eF450	Gr-1	RB6-8C5	ThermoFisher	48-5931-82	1:2000
eF450	Ter119	TER-119	ThermoFisher	48-5921-82	1:2000
eF450	CD19	eBio1D3 (1D3)	ThermoFisher	48-0199-42	1:2000
eF450	F4/80	BM8	ThermoFisher	48-4801-82	1:2000
eF450	FcERa	MAR-1	ThermoFisher	13-5898-82	1:2000
BV510	CD45	30-F11	BioLegend	103138	1:500
BV786	OX40	OX-86	BD	740945	1:100
BUV 395	NK1.1	PK136 (RUO)	BD	564144	1:500
UV 455	Live/Dead (Fixable)		ThermoFisher	65-0868-14	1:500
AF700	CD4	RM4-5	BioLegend	300526	1:500
APC eF780	B220	A3-6B2	ThermoFisher	47-0452-82	1:500
PE	OX40L	RM134L	ThermoFisher	12-5905-82	1:250
PE CF 594	CD127	SB/199 (RUO)	BD	562419	1:250
PE Cy7	CD3e	145-2C11	ThermoFisher	25-0031-82	1:250
N/A	CD16/32		BioLegend	101320	1:500
Intracellular stain					
AF488	FoxP3	FJK-16S	ThermoFisher	53-5773-80	1:250
BV650	RorgT	Q31 378	BD	563424	1:250
eF660	Gata3	TWAJ	ThermoFisher	50-9966-42	1:250

Table 1 - Antibodies used in the lymphoid panel

Surface stain					
Fluorophore	**Protein**	**Clone**	**Manufacturer**	**Catalogue#**	**Dilution**
AF488	CD172a	P84	BioLegend	144024	1:500
eF450	CD5	53-7.3	ThermoFisher	48-0051-82	1:2000
	CD19	eBio1D3 (1D3)	ThermoFisher	48-0199-42	1:2000
	NK1.1	PK136	ThermoFisher	48-5941-82	1:2000
	CD3e	145-2C11	ThermoFisher	48-0031-82	1:2000
	B220	RA3-6B2	ThermoFisher	48-0452-82	1:2000
BV510	CD45	30-F11	BioLegend	30-F11	1:500
SB600	Siglec F/CD170	1RNM44N	ThermoFisher	63-1702-82	1:250
BV650	XCR1	ZET	BioLegend	148220	1:500
BV711	CD64/FcgRI	X54-5/7.1	BioLegend	139311	1:250
BV786	CD11b	M1/70	BioLegend	101243	1:500
BUV 395	MHCII (I-A/I-E)	CI2G9	BD	743876	1:2000
UV 455	Live/Dead (Fixable)		ThermoFisher	65-0868-14	1:500
AF700	CD11c	N418	BioLegend	337219	1:500
APC-ef780	F4/80	BM8	ThermoFisher	47-4801-82	1:500
PE-Efl610	Ly-6G	1A8-Ly6g	ThermoFisher	61-9668-82	1:1000
PE-Cy7	Ly-6C	HK1.4	ThermoFisher	25-5932-82	1:2000
N/A	CD16/32		BioLegend	101320	1:500
Intracellular stain					
APC	RELM alpha	DS8RELM	ThermoFisher	17-5441-82	1:500

Table 2 - Antibodies used in the myeloid panel

Surface stain					
Fluorophore	**Protein**	**Clone**	**Manufacturer**	**Catalogue#**	**Dilution**
PerCP eF710	CD8	53-6.7	ThermoFisher	46-0081-82	1:500
eF450	CD5	53-7.3	ThermoFisher	48-0051-82	1:2000
	CD11b	M1/70	ThermoFisher	48-0112-82	1:2000
	CD11c	N418	ThermoFisher	48-0114-82	1:2000
	Gr-1	RB6-8C5	ThermoFisher	48-5931-82	1:2000
	Ter119	TER-119	ThermoFisher	48-5921-82	1:2000
	CD19	eBio1D3 (1D3)	ThermoFisher	48-0199-42	1:2000
	F4/80	BM8	ThermoFisher	48-4801-82	1:2000
	FcERa	MAR-1	ThermoFisher	13-5898-82	1:2000
BV510	CD45	30-F11	BioLegend	103138	1:500
BUV 395	NK1.1	PK136 (RUO)	BD	564144	1:500
UV 455	Live/Dead		ThermoFisher	65-0868-14	1:500
AF700	CD4	RM4-5	BioLegend	300526	1:500
APC eF780	B220	A3-6B2	ThermoFisher	47-0452-82	1:500
PE CF 594	CD127	SB/199 (RUO)	BD	562419	1:250
PE Cy7	CD3e	145-2C11	ThermoFisher	25-0031-82	1:250
N/A	CD16/32		BioLegend	101320	1:500
Intra-cellular stain					
BV786	Ifn-g	XMG1.2	BioLegend	505838	1:250
APC	IL-5	TRFK5	BD	554396	1:250
PE	IL-13	eBio13A	eBioscience	12-7133-82	1:250

Table 3 - Antibodies used in the cytokine panel

Surface stain					
Fluorophore	**Protein**	**Clone**	**Manufacturer**	**Catalogue#**	**Dilution**
BV421	CD133	315-2C11	BioLegend	141213	1:500
BV510	CD45	30-F11	BioLegend	103138	1:500
BV605	CD31	390	BioLegend	102427	1:500
BV711	EpCAM	G8.8	BioLegend	118233	1:500
AF700	DRAQ5		ThermoFisher	62-254	1:2000
eF780	Live/Dead		Scientific	65-0865-18	1:4000
PE cy7	Podoplanin	8.1.1	BioLegend	127412	1:500
N/A	CD16/32		BioLegend	101320	1:500
Intracellular stain					
AF700	Ki67	SolA15	BD	563756	1:500

Table 4 - Antibodies used in the non-immune cell panel

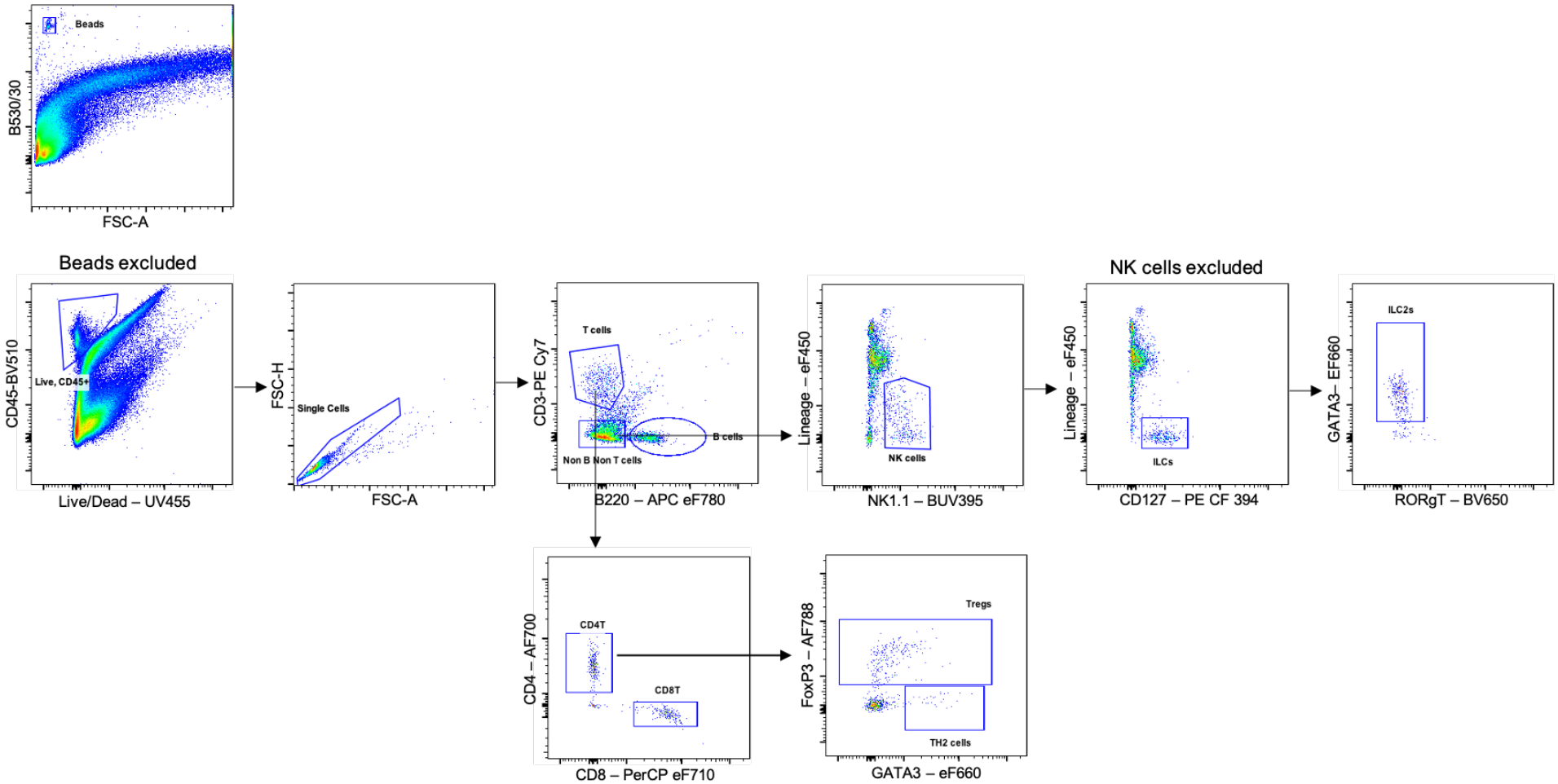

Figure 5 - Lymphoid panel gating strategy. Lymphoid cells are gated on CD45+ Live cells. CD3+ T cells and B220+ B cells are then identified from this population. Cells double negative for CD3 and B220 are gated for Lineage negative, NK1.1+ NK cells. NK cells are excluded and ILCs are identified as Lineage negative and CD127+. Within this population, ILC2s are identified as GATA3+. Within the CD3+ T cell gate, CD4 and CD8 T cells are gated for. Within the CD4 T cells gate, Tregs are identified based on FoxP3 expression and T_h2 cells are identified based on GATA3 expression.

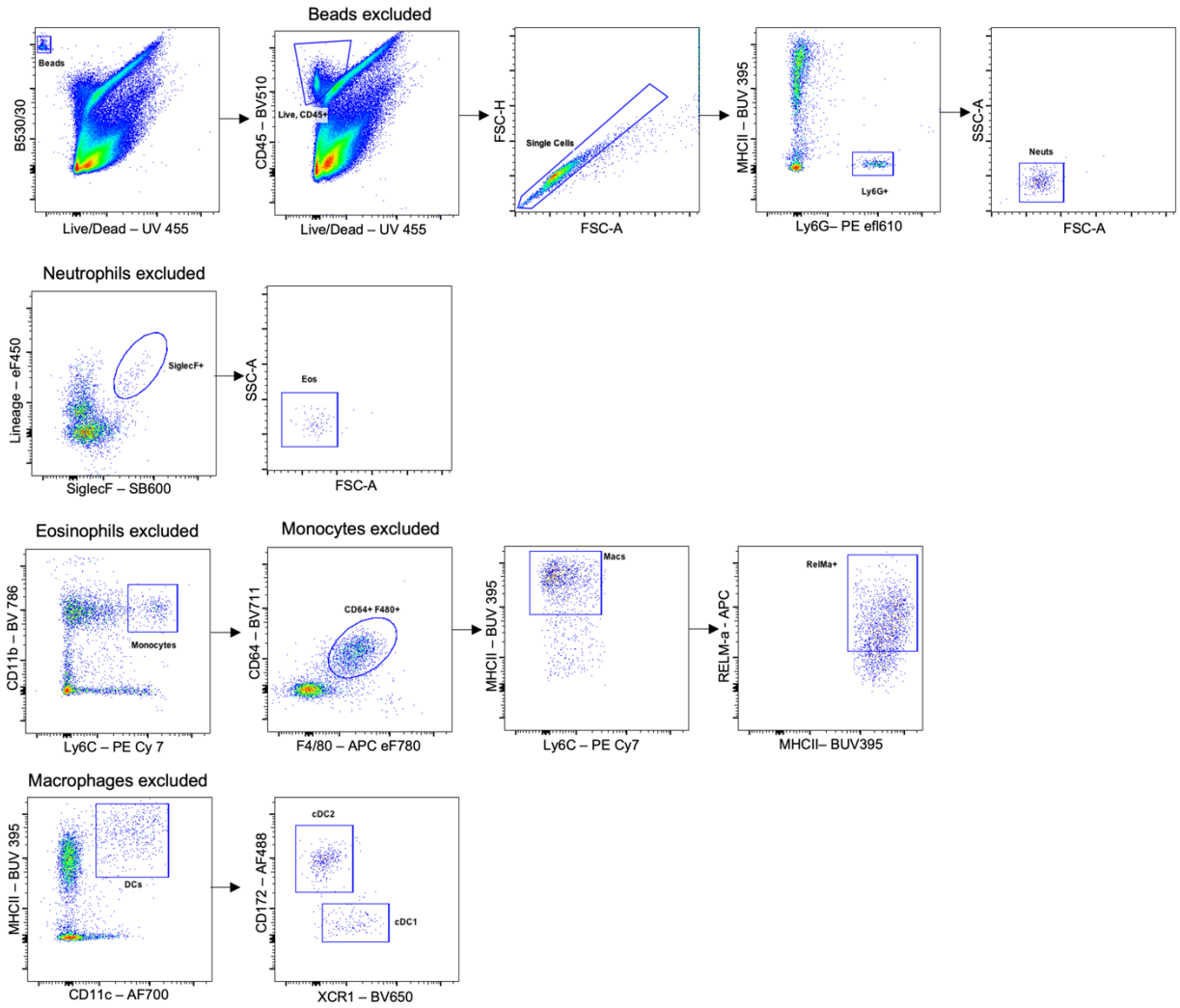

Figure 6 - Myeloid gating strategy. Myeloid cells are identified within the CD45+ live compartment. Neutrophils are identified based on their Ly6G expression and further selected based on size and granularity. Once Ly6G+ cells are excluded, Eosinophils are identified based on CD11b and SiglecF expression and further selected based on size and granularity. Once SiglecF+ cells are excluded, monocytes are identified as Ly6C+ and CD11b+. Once monocytes are excluded, CD64 and F4/80 double positive population is identified. MHCII+ cells are gated within this population and are identified as macrophages. Once macrophages are excluded, DCs are identified based on their expression of CD11c and MHCII. DCs are further subdivided into cDC1 and cDC2 based on their expression of XCR1 and SirpA respectively.

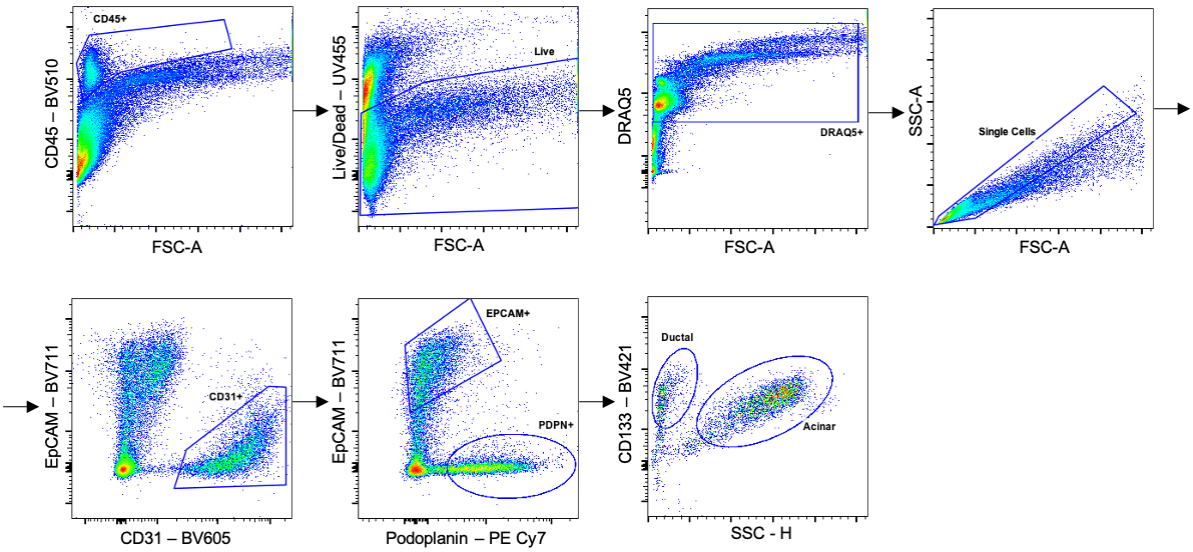

Figure 7 - Non-immune cell panel gating strategy. Non immune cells are identified within the CD45 negative and live cell population. Epithelial cells are identified based on EpCAM expression and endothelial cells based on CD31 expression. EpCAM and CD31 double negative cells are used to gate for stromal cells using podoplanin expression. Cycling of cells within the stromal compartment is identified using Ki67 staining. Epithelial cells are further subdivided into ductal and acinar cells based on their expression of CD133 and granularity respectively.

Histology and Image analysis

Pancreas tissues were fixed in 10% neutral buffered formalin for 24 hours, transferred to 70% ethanol for an hour and then embedded in paraffin. 4µm sections were cut, deparaffinised and stained with haematoxylin & eosin or modified Masson's trichrome histological stains. Immunohistochemistry for CK19 was also performed. Stained slides were scanned with the Aperio AT2 scanner. Tissue embedding, sectioning, staining and scanning were performed by the CRUK CI histology core. Images were analysed using the image analysis software Halo (Indica labs) by the author.

RNA extraction

Sorted ILC2s were spun down and the pellet was resuspended in Trireagent (Thermo Fisher, AM9738) and frozen in a -80 freezer. RNA was extracted using the RNeasy mini kit (Qiagen, 74104) and DNAse was eliminated using the Turbo DNase kit according to manufacturer's instructions (ThemoFisher, AM1907). The RNA was then concentrated using the RNeasy micro kit (Qiagen, 74004). RNA quality and quantity were analysed using the Agilent RNA 6000 pico kit (Agilent Technologies, 5067-1513) on the Agilent 2100 Bioanalyser instrument according to manufacturer's instructions.

Imaging flow cytometry for neutrophil extracellular trap formation

Pancreas from caerulein and PBS treated animals were digested as mentioned earlier in this section and the suspensions were stained with a fixable live/dead stain and Ly6G (clone 1A80Ky6g) for 30 minutes at 4C. The cells were then washed with PBS. The stained cells were then fixed with 0.4% PFA for 15 minutes at room temperature. The cells were washed twice with PBS. The cells were then incubated with 4ug/ml Hoechst 33342 in PBS/2%FCS for 2 minutes on ice. The cells were then washed with PBS/2%FCS and finally re-suspended in 100µl PBS/2%FCS and acquired on the Amnis®Imagestream® according to previously described acquisition protocol (Zhao et al., 2015).

Library preparation for bulk RNAseq

Library preparation was done by the CRUK CI genomics core using the NEBNext® Single Cell/Low Input RNA Library Prep Kit for Illumina®(New England Biolabs). Library quantification and quality check of the libraries were done using the Bioanalyser DNA 1000 kit (Agilent Technologies, 5067-1505) and the KAPA library quantification kit for Illumina (KAPA Biosystems, KK4828) respectively. The libraries were then pooled and sequenced on 2 lanes of the HiSeq 4000 system (single end 50).

Bioinformatics analysis

Bioinformatics analysis was done by the bioinformatics core at the CRUK Cambridge Institute as follows. Reads were aligned to the mouse genome version GRCm38 using hisat2. Read counts were obtained using feature Counts function in Subread and read counts were normalised and tested for differential gene expression using the DESeq2. Multiple testing correction was applied using the Benjamini–Hochberg method. Exploratory analysis of the DESeq gene lists were done by the PhD student. Heatmaps shown in Fig 14 were done by Silvain Pinaud, Post-doc in the Halim lab.

Statistics

Statistical significance for experiments with more than 2 groups was calculated using one-way ANOVA. For grouped data with more than 2 groups, statistical significance was calculated using two-way ANOVA. For experiments with 2 groups, statistical significance was calculated using Student's t-test. All statistical analysis was done on GraphPad prism. Significance was ranked as ns=non significant. *= $P \leq 0.05$, **= $P \leq 0.01$, ***= $P \leq 0.001$, ****=$P \leq 0.0001$.

Results & Discussion

Chapter 1

Characterisation of pancreatic ILC2s

Pancreatic ILC2 activation and characterisation.

First, we identified ILC2s in the pancreas using flow cytometry. Pancreas single cell suspension was stained with the lymphoid antibody panel described in the methods section (Table 1). Live, single cell and CD45+ populations were identified and gated on using FlowJo software. Non-B and Non-T cell population was further identified based on their non-expression of CD3 and B220. NK cells were identified and gated out using the Boolean gate function based on the cells' expression of NK 1.1. ILCs were identified within the NK cell excluded population as lineage negative and CD127+ cells. Among the live, singe cells, CD45+, non-B, non-T, non-NK, lineage negative, CD127+ population, ILC2s were identified as GATA3 expressing. Going forward, ILCs are defined as live, single cells, CD45+, Lineage – (lineage = CD5, CD11b, CD11c, Gr-1, Ter119, CD19, F4/80, FcERα), CD3-, CD127+ cells and ILC2s are identified as GATA3+ ILCs (fig 8).

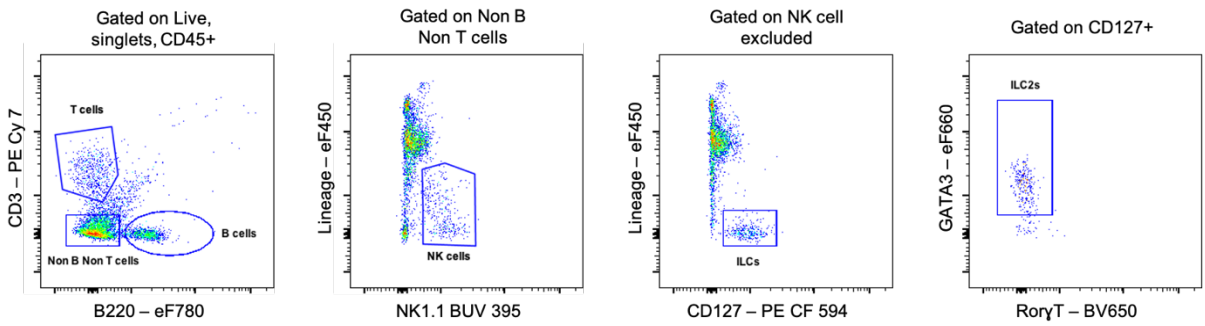

Fig 8 - Identifying ILC2s in the pancreas. Naïve mice pancreas was digested and the single cell suspension was staining with the lymphoid antibody panel described in the methods section. ILCs were identified as Live, single cells, CD45+, Lineage – (lineage = CD5, CD11b, CD11c, Gr-1, Ter119, CD19, F4/80, FcERa), CD3-, CD127+ and ILC2s are identified as GATA3+ ILCs.

As discussed earlier, ILC2s can be activated by various alarmins such as IL-25, TSLP and IL-33. Upon activation ILC2s produce type 2 cytokines like IL-5, IL-13, IL-4 and Amphiregulin (Areg) (Vivier et al., 2018). When activated with the alarmin IL-33 and other immunostimulatory agents like papain in the lung, ILC2s have been shown to express the co-stimulatory molecule, OX40L (Halim et al., 2018).

Very little is known about ILC2s in the pancreas, their activation and functional characterisation. In one of the few reports on ILC2s in the pancreas, mesenchymal cells in the islet of Langerhans were reported to be a source of IL-33 and ILC2s activated by IL-33 in the pancreas showed increased expression of *Il13* message (Dalmas et al., 2017). We sought to

identify alarmins that could activate ILC2s in the pancreas and functionally characterise pancreatic ILC2s in depth.

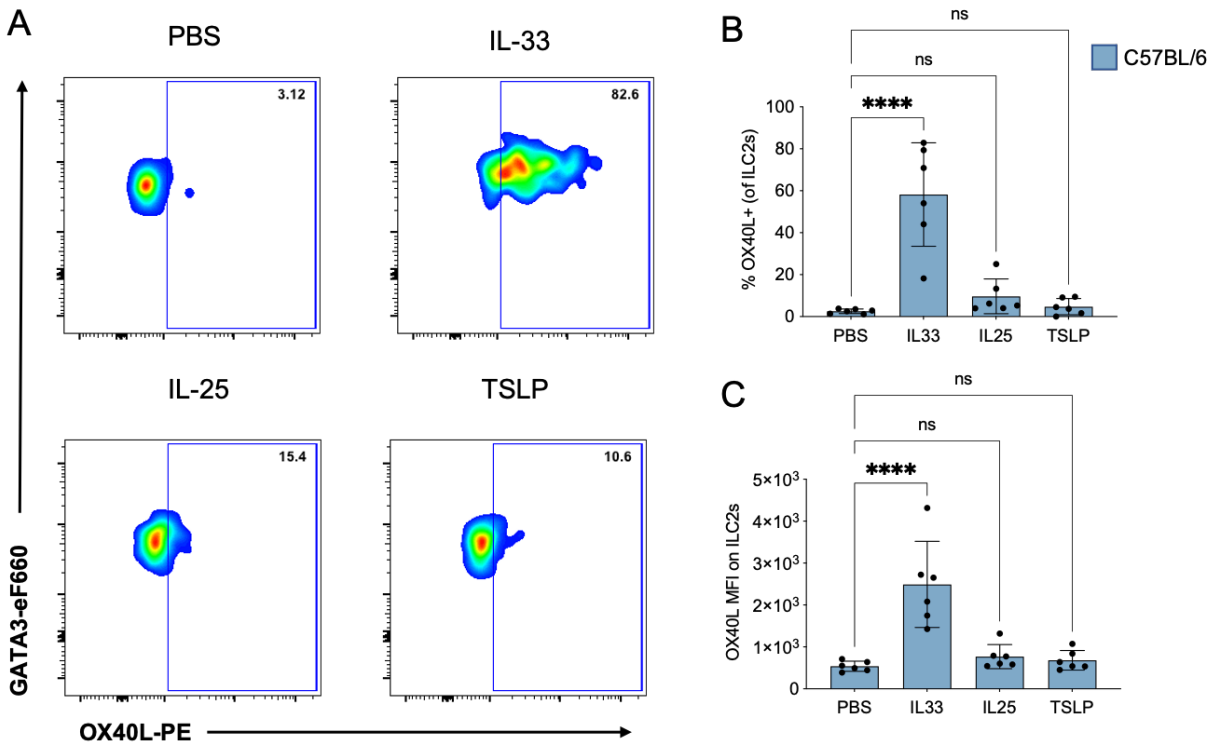

Figure 9 – IL-33 induces ILC2 activation in the pancreas. C57BL/6 mice were treated with 200ng recombinant IL-33, IL-25 or TSLP intraperitoneally on days 0 and 1 and were sacrificed on day 3. Single cell suspension prepared from the pancreas were analysed using flow cytometry. A, Representative gating for OX40L expression on ILC2s in the pancreas. B, Quantification of OX40L+ pancreatic ILC2s (n=6). C, Mean fluorescence intensity (MFI) of OX40L-PE on ILC2s (n=6). B,C, Bar graphs indicate the mean (± s.e.m.) and show combined data from two independent experiments. Statistical significance was calculated using one-way ANOVA. ns=non-significant, ****=P≤0.0001.

To this end, C57BL/6 mice were treated with 200ng of recombinant mouse IL-33, IL-25 or TSLP, and OX40L expression on ILC2s, cytokine production and immune cell numbers in the pancreas were analysed using flow cytometry. ILC2s from IL-33 injected mice showed high expression of OX40L but not ILC2s from IL-25 or TSLP treated mice when compared to control animals (fig 9A, B). ILC2s from IL-33 treated mice also showed significantly increased OX40L-PE Mean fluorescence intensity (MFI) compared to PBS treated mice (fig 9C) which was not observed with IL-25 or TSLP.

ILCs from IL-33 treated mice also showed high expression of IL-5 (fig 10A, B) and IL-13 (fig 11A,B) at rest or 2 hours after restimulation with phorbal 12-myrisate 13-acetate (PMA) and Ionomycin (PI) when compared to PBS treated mice whether in percentage or MFI (fig 10B,C and fig11B,C). This was however not the case for IL-25 or TSLP treated mice.

Taken together, increased expression of OX40L on ILC2s and an increase in IL-5 and IL-13 expression on ILCs indicates that ILC2s are activated by IL-33 in the pancreas. IL-25 and TSLP though able to activate ILC2s in other organs are unable to do so in the pancreas.

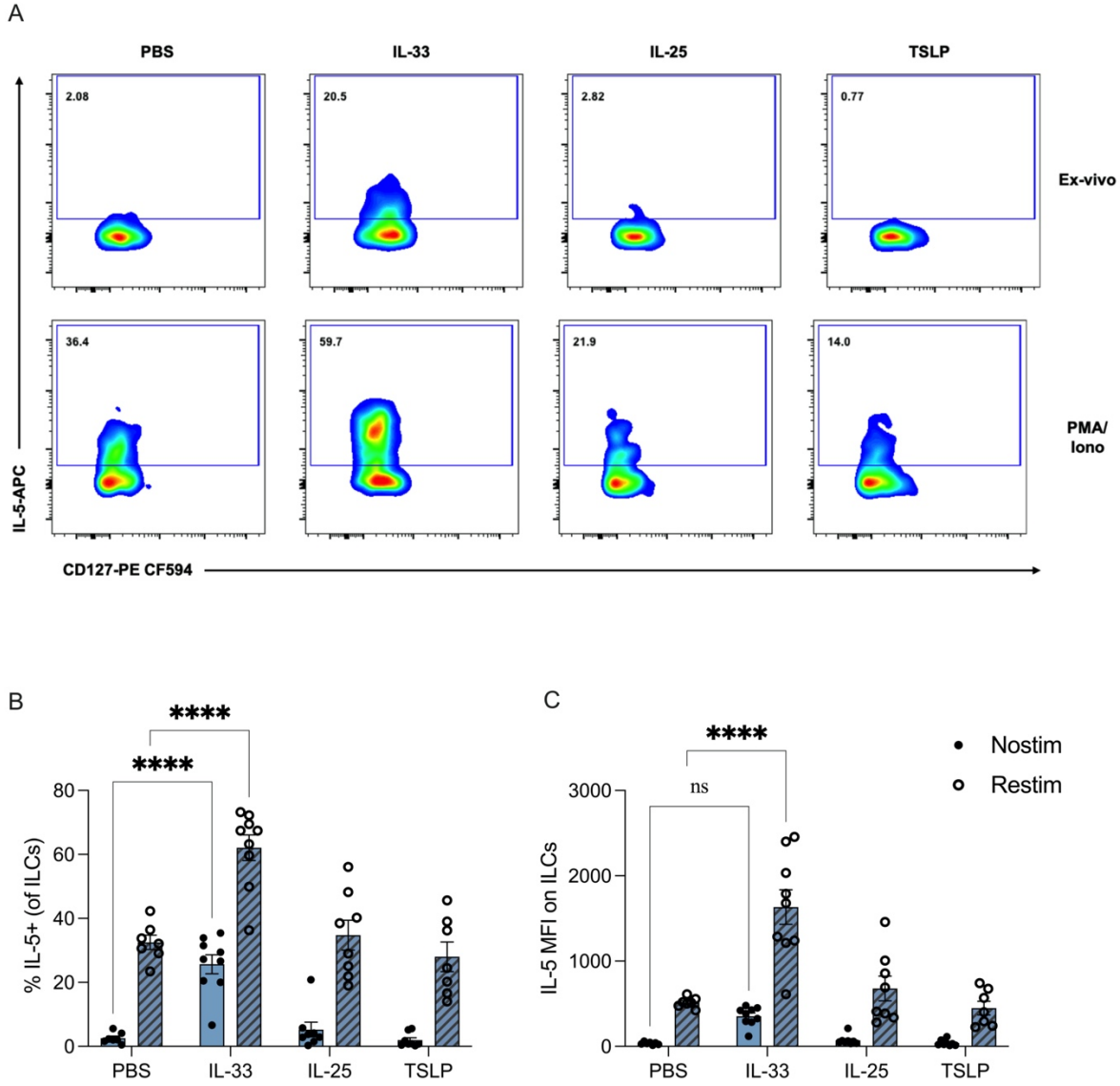

Figure 10 – IL-33 induces IL-5 expression by ILC2s in the pancreas. C57BL/6 mice were treated with 200ng recombinant IL-33, IL-25 or TSLP intraperitoneally on days 0 and 1 and were sacrificed on day 3. Single cell suspension prepared from the pancreas were analysed using flow cytometry (n=7,9,8,8). A, Representative gating for IL-5 expression on ILCs in the pancreas with and without PI stimulation. B, Quantification of IL-5+ pancreatic ILCs C, MFI of IL-5-APC on ILCs. B,C, Bar graphs indicate the mean (± s.e.m.) and show combined data from two independent experiments. Statistical significance was calculated using two-way ANOVA. ns=non-significant, ****=P≤0.0001.

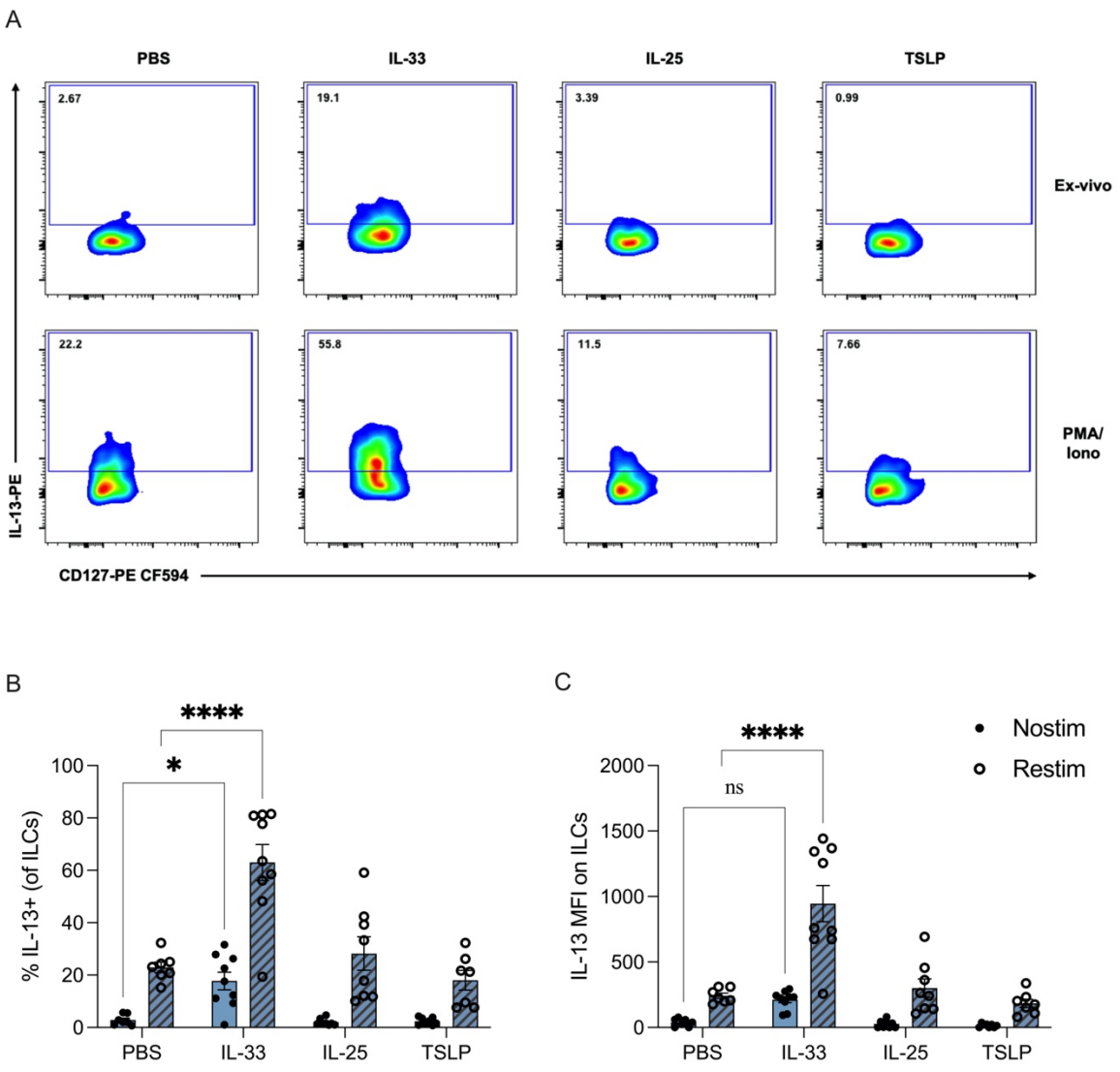

Figure 11 – IL-33 induces IL-13 expression on ILC2s in the pancreas. C57BL/6 mice were treated with 200ng recombinant IL-33, IL-25 or TSLP intraperitoneally on days 0 and 1 and were sacrificed on day 3. Single cell suspension prepared from the pancreas were analysed using flow cytometry (n=7,9,8,8). A, Representative gating for IL-13 expression on ILCs in the pancreas with and without PI stimulation. B, Quantification of IL-13+ pancreatic ILCs C, MFI of IL-13-PE on ILCs. B, C, Bar graphs indicate the mean (± s.e.m.) and show combined data from two independent experiments. Statistical significance was calculated using two-way ANOVA. ns=non-significant, ****=P≤0.0001.

In order to characterise the IL-33 induced immune changes, we looked at changes in the lymphoid immune compartment in mice treated with the alarmins IL-33, IL-25 and TSLP. IL-33 treated mice showed a significant increase in total number immune cells numbers (CD45+ cells), ILC2s and Tregs compared to PBS treated mice (fig 12A, E, I, fig S33). This increase was not seen in IL-25 and TSLP treated mice however (fig 12A, E, I, fig S33). IL-33, IL-25 and TSLP treated mice did not show any difference in number of B cells, NK cells, T cells, CD4 T cells, T_h2 cells or CD8 T cells in the pancreas (fig 12). These alarmins did not induce any changes in the composition of the lymphoid immune compartment in pancreatic lymph nodes (pLN) either as shown in Fig S2.

We also looked at type 2 cytokine production by CD4 T cells in the pancreas when stimulated by alarmins. Contrary to ILCs, CD4 T cells show limited expression of IL-5 or IL-13 in the pancreas in either IL-33, IL-25 or TSLP treated mice (fig S1). Thus, these results suggest that ILC2s are the most prominent source of IL-5 and IL-13 in IL-33 treated mice.

Finally, we analysed myeloid immune cells in IL-33 treated mice and several changes were seen including significant increase in number of eosinophils, dendritic cells (DCs), macrophages and monocytes (fig 13C-F, fig S34). A significant decrease in proportion of cDC1 and significant increase in proportion of cDC2s was seen in IL-33 treated mice compared to PBS treated mice (fig 13G, H). IL-33 treated mice also showed a significant increase in the proportion of RelMα+ macrophages (M2 macrophages) compared to PBS treated mice (fig 13I, fig S34). IL-33 did not induce any changes in the myeloid immune compartment in pLN however (fig S3).

Similar to the lungs (Li Yin Drake & Kita, 2017) and the intestine (Hodzic et al., 2017), our results demonstrate that IL-33 induces a type 2 inflammatory environment in the pancreas as well and that pancreatic ILC2s can be activated by IL-33 but not IL-25 or TSLP as measured by increased expression of OX40L and production of the type 2 cytokines IL-5 and IL-13.

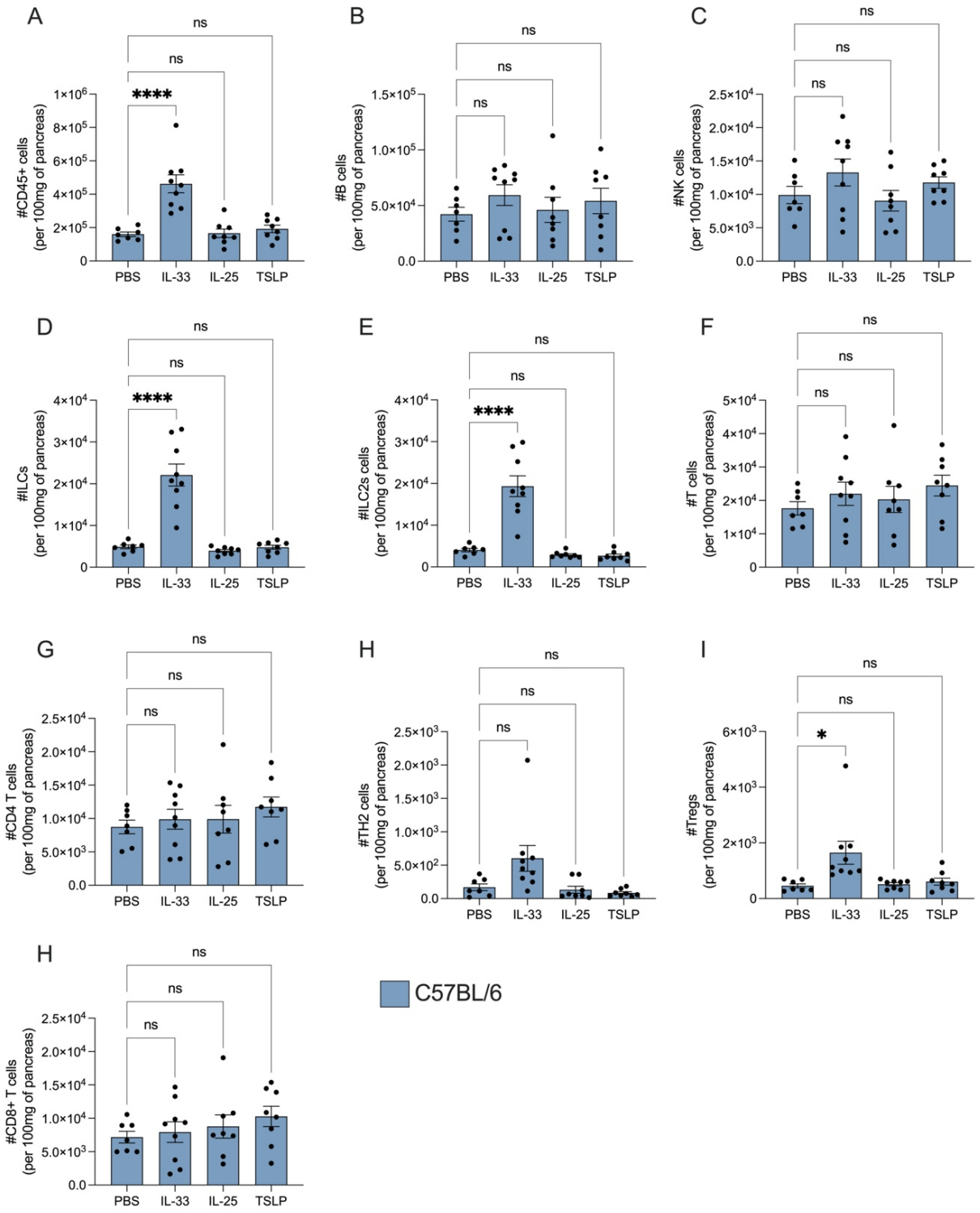

Figure 12 – IL-33 induces ILC2 and Treg expansion in the pancreas C57BL/6 mice were treated with 200ng recombinant IL-33, IL-25 or TSLP intraperitoneally on days 0 and 1 and were sacrificed on day 3. Single cell suspension prepared from the pancreas were analysed using flow cytometry (n=7,9,8,8). A-H, Quantification of CD45+, B cells, NK cells, ILCs, ILC2s, T cells, CD4 T cells, TH2 cells, Tregs and CD8 T cells in the pancreas using flow cytometry. A-H, Bar graphs indicate the mean (± s.e.m.) and show combined data from two independent experiments. Statistical significance was calculated using two-way ANOVA. ns=non-significant, ****=P≤0.0001.

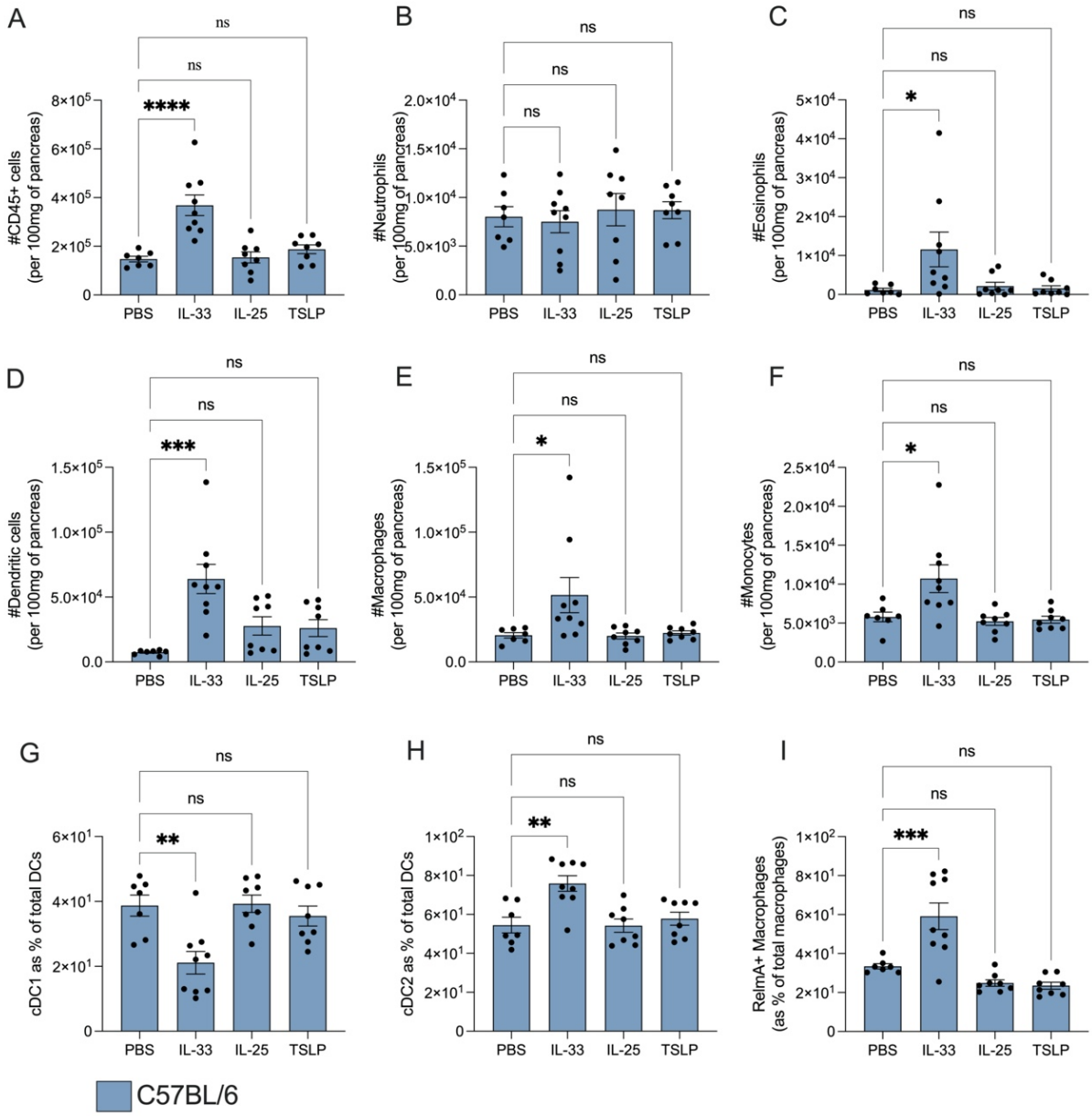

Figure 13 – IL-33 induces myeloid cell expansion in the pancreas. C57BL/6 mice were treated with 200ng recombinant IL-33, IL-25 or TSLP intraperitoneally on days 0 and 1 and were sacrificed on day 3. Single cell suspension prepared from the pancreas were analysed using flow cytometry (n=7,9,8,8). A-F – Quantification of CD45+ immune cells, neutrophils, eosinophils, dendritic cells (DCs), macrophages and monocytes. G,H – Proportion of cDC1 and cDC2 as a proportion of total DCs. I, Proportion of RelMa+ M2 macrophages as a proportion of total macrophages. A-H, Bar graphs indicate the mean (± s.e.m.) and show combined data from two independent experiments. Statistical significance was calculated using two-way ANOVA. ns=non-significant, ****=P≤0.0001.

As IL-33 emerged as an ILC2 activating alarmin in the pancreas, we characterised IL-33 activated ILC2s using bulk RNAseq. ILC2s were sorted from naïve and IL-33 treated C57BL/6 mice pancreas as shown in fig S14. ILC2s from naïve C57Bl/6 mice showed expression of genes that defined ILC2s in other organs (Ricardo-Gonzalez et al., 2018) including genes associated with chemokine signalling (*Ccr8, Ccrl2* and *Ccr2)*, the gene encoding the lineage marking transcription factor *Gata3* and genes encoding key factors for ILC development (*Il2ra* and *Il7r)* (fig 14A). Pancreatic ILC2s also expressed other genes such as *Il1rl1, Klrg1, Ar,*

Ltbr4r1, Il10ra and *Icos* (fig 14A) and genes encoding secreted factors such as *Il5, Lif, Il13* and *Il4* whose expression has been observed in other organs (Ricardo-Gonzalez et al., 2018) such as lungs and intestine (fig 14B).

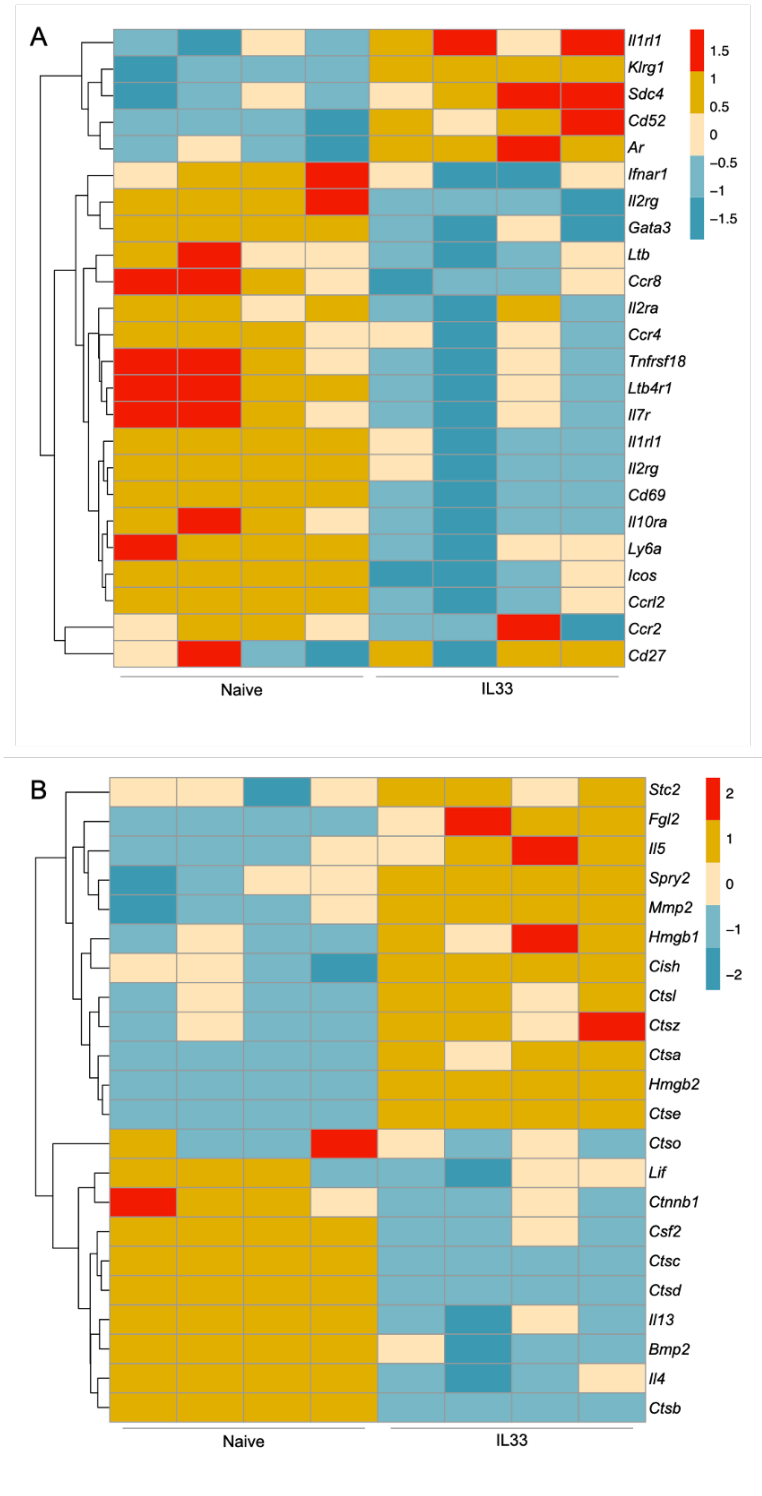

Figure 14 – Bulk RNAseq of pancreatic ILC2s. C57BL/6 mice were treated with 200ng recombinant IL-33 intraperitoneally on days 0 and 1 and were sacrificed on day 3 followed by sorting of ILC2s for RNA. A, Z-scaled expression values for genes that are commonly expressed by ILC2s. B, Z-scaled expression values for genes for secreted proteins expressed by pancreatic ILC2s. Each block represents the expression value obtained by one replicate for a given gene at a given time point.

ILC2s regulate Type 2 immunity and Treg expansion in the pancreas

Having observed a highly type 2 skewed immune environment upon IL-33 treatment in the pancreas, we asked if this response would be exaggerated upon repeated stimulation with IL-33. Indeed, mice that received repeated stimulation with IL-33 (re-stim) showed a significant increase in the number of CD45+ cells, ILC2s, Tregs and TH2 cells (fig 15A-D, figS35). These mice showed a significant increase in OX40L expression on ILC2s and OX40 expression on Tregs (Fig 15E,F, fig S35), confirming the ability of IL-33 to induce the expression of the co-stimulatory axis similar to what was observed in the lungs. Re-stim with IL-33 also led to expansion of ILCs, NK cells, T cells and CD4 T cells, but not B cells (fig S4). Similarly, in the pLN, repeated IL-33 stimulation led to expansion of ILCs, ILC2s and Tregs (fig S5B,C,J). An increase in OX40 expression on Tregs was also observed (fig S5K).

In the myeloid immune compartment an increase in number of neutrophils, eosinophils, total DCs, cDC1s and cDC2s were observed in mice that received repeated stimulation with IL-33 (fig S6A,C,D,E,F). No other changes were observed in the lymphoid (fig S4) and myeloid (fig S6) immune compartment of mice that received repeated IL-33 stimulation.

To further understand if the IL-33 induced type 2 inflammatory changes in the pancreas were sustained long-term, we studied immune changes 2 and 3 months after IL-33 treatment. While increase in the number of CD45+ cells, B cells in the pLN, ILCs and ILC2s in the pancreas was sustained long term (fig 16B,C, fig S7A), it was not the case for Tregs (fig 16E). Other immune changes in the lymphoid compartment were also not sustained (fig 16, S7).

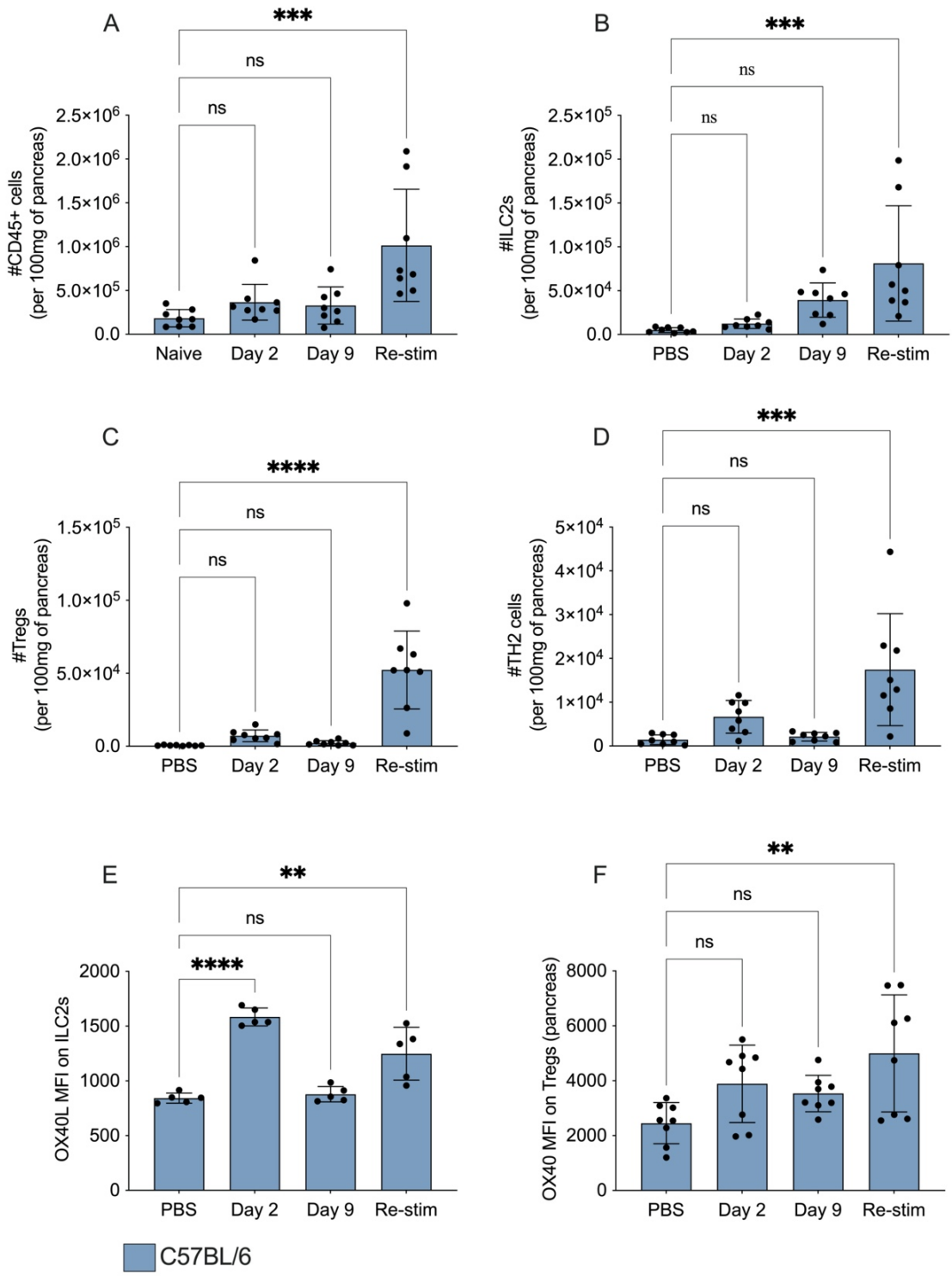

Figure 15 - Re-stimulation with IL-33 leads to enhanced ILC2 and Treg expansion. C57BL/6 mice were treated with 200ng recombinant IL-33 intraperitoneally either on 0 and 1 and sacrificed on day 2 and day 9, or on day 0,1,7 and 8 and were killed on day 9 (re-stim). This was followed by quantification of lymphoid cells, OX40L MFI on ILC2s and OX40 MFI on Tregs in the pancreas by flow cytometry (n=7,8,8,8). A-D – Quantification of number of CD45+ immune cells, ILC2s, Tregs and TH2 cells respectively in the pancreas. E, MFI of OX40L-PE on ILC2s in the pancreas. F, MFI OX40-BV786 on Tregs in the pancreas. A-F, Bar graphs indicate the mean (± s.e.m.) and show combined results from two experiments. Statistical significance was calculated using one-way ANOVA. ns=non-significant. *= P≤0.05, **= P≤0.01, ***= P≤0.001, ****=P≤0.0001.

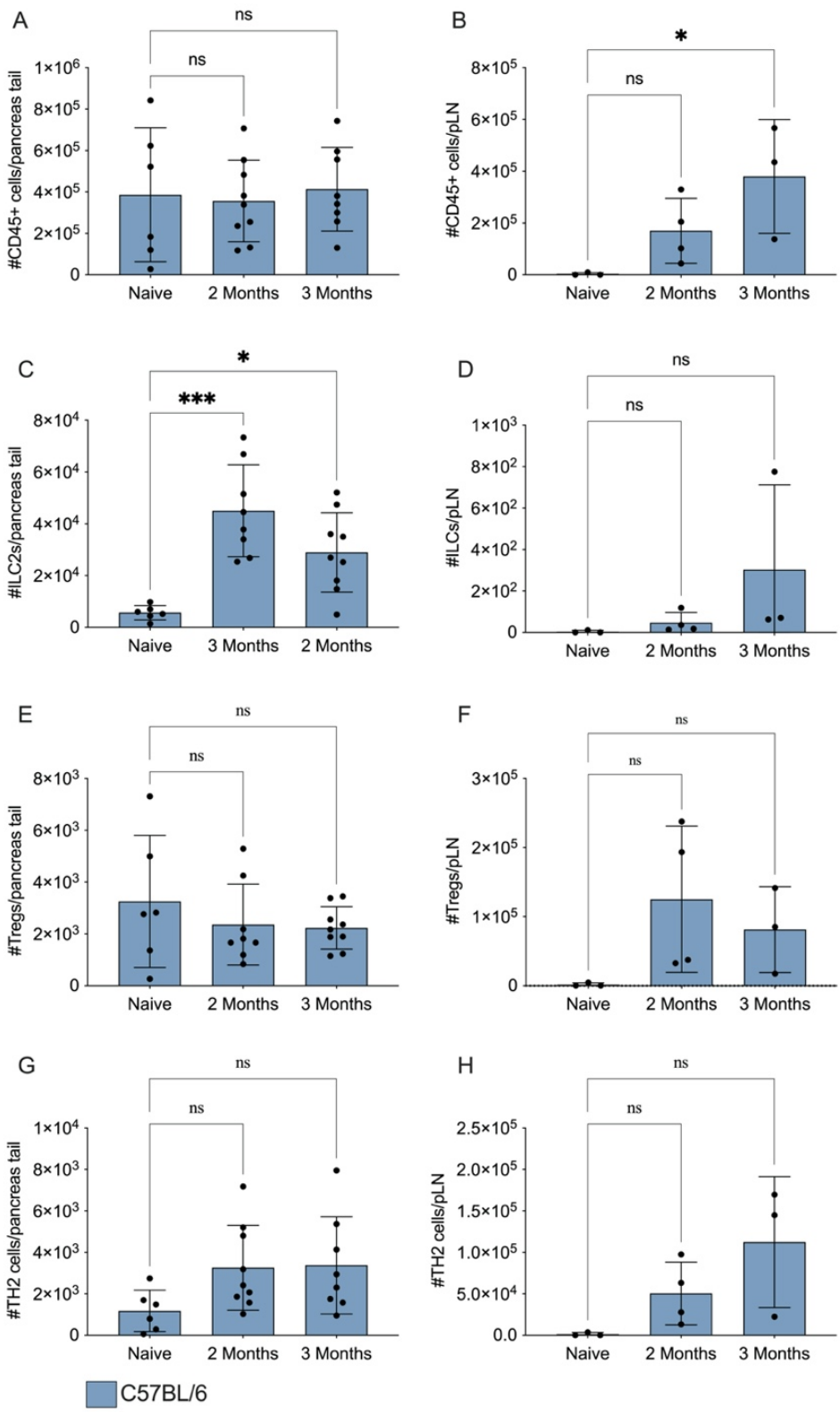

Figure 16 – IL-33 induced ILC2 expansion in the pancreas is sustained long term. C57BL/6 mice were treated with 200ng recombinant IL-33 intraperitoneally on day 0 and 1 and sacrificed 2 or 3 months after. This was followed by quantification of lymphoid cells in the pancreas (n=6,9,8) and pLN (n=3). A,C,E,G – Quantification of number of CD45+ immune cells, ILC2s, Tregs and TH2 cells in the pancreas by flow cytometry. B,D,F,H, Quantification of CD45+ immune cells, ILC2s, Tregs and TH2 cells in the pLN. A,C,E,G, Bar graphs indicate the mean (± s.e.m.) and show combined results from two independent experiments. B,D,F,H, Bar graphs indicate the mean (± s.e.m.) and is representative of one experiment. Statistical significance was calculated using one—way ANOVA. ns=non-significant. *= P≤0.05, **= P≤0.01, ***= P≤0.001, ****=P≤0.0001.

ILC2s have been shown to modulate adaptive type 2 immunity via expansion of TH2 cells and Tregs in the lungs (Halim et al., 2018). From earlier results, we see that ILC2s show an IL-33 induced expression of the co-stimulatory molecule, OX40L and Tregs express the associated receptor OX40. This observation coupled with the increase in Treg numbers in IL-33 treated mice, led us to ask if Treg expansion was ILC2 and OX40L dependent similar to what has been observed in the lungs (Halim et al., 2018).

To address this we used *Il7ra*$^{cre/+}$*Rora*$^{loxP/loxP}$(ILC2 deficient mice) and *Il7ra*$^{cre/+}$*Tnfsf4*$^{loxP/loxP}$(wherein IL7Rα expressing cells, including ILC2s lack OX40L expression) mice. Reduction in OX40l expression on ILC2s in the *Il7ra*$^{cre/+}$*Tnfsf4*$^{loxP/loxP}$ mouse model has been fig S5A of *Halim et al, 2018* where the model was also first reported. Both *Il7ra*$^{cre/+}$*Rora*$^{loxP/loxP}$ and *Il7ra*$^{cre/+}$*Tnfsf4*$^{loxP/loxP}$ showed significant reduction in Treg and T_h2 cell numbers when treated with IL-33 compared to control mice (fig 17C,D). This was however not the case in the pLN (fig 17F). Lack of ILC2s in *Il7ra*$^{cre/+}$*Rora*$^{loxP/loxP}$ mice has been captured in Fig 17B,E. It is to be noted here that, *Il7ra*$^{cre/+}$*Tnfsf4*$^{loxP/loxP}$ mice show reduced ILC2 numbers but not a complete lack of them. Both *Il7ra*$^{cre/+}$*Rora*$^{loxP/loxP}$ and *Il7ra*$^{cre/+}$*Tnfsf4*$^{loxP/loxP}$ do not mount the same level of inflammation as the control mice that received IL-33 (fig 17A). This demonstrates the key role that ILC2s play in mediating IL-33 driven inflammation.

A significant reduction in number of B cells was observed in pLN of IL-33 treated *Il7ra*$^{cre/+}$*Rora*$^{loxP/loxP}$and *Il7ra*$^{cre/+}$*Tnfsf4*$^{loxP/loxP}$ mice (fig S8I). A reduction of CD45+ cells in the pLN of IL-33 treated *Il7ra*$^{cre/+}$*Rora*$^{loxP/loxP}$ and *Il7ra*$^{cre/+}$*Tnfsf4*$^{loxP/loxP}$ mice (fig S8F) and a reduction in CD4 T cell numbers in *Il7ra*$^{cre/+}$*Tnfsf4*$^{loxP/loxP}$ (fig S8E) was observed. No other changes were found in the lymphoid immune compartment of the pancreas or the pLN (fig S8).

Among other type 2 immune changes, eosinophilia in both the pancreas and the pLN was found to be ILC2 dependent but not OX40L dependent (fig S9A,G). Although other type 2 immune changes were observed in C57BL/6 mice treated with IL-33 like increase in DCs and macrophages, these trends were not seen in Il7ra$^{cre/+}$ control mice, and neither were these changes found to be ILC2 dependent (fig S9).

In summary, our results show that ILC2s regulate the adaptive immune changes i.e., T_h2 and Treg expansion in the pancreas upon IL-33 induced activation in a OX40L dependent manner. In addition, we also found that ILC2s regulate eosinophilia in the pancreas in upon IL-33 stimulation.

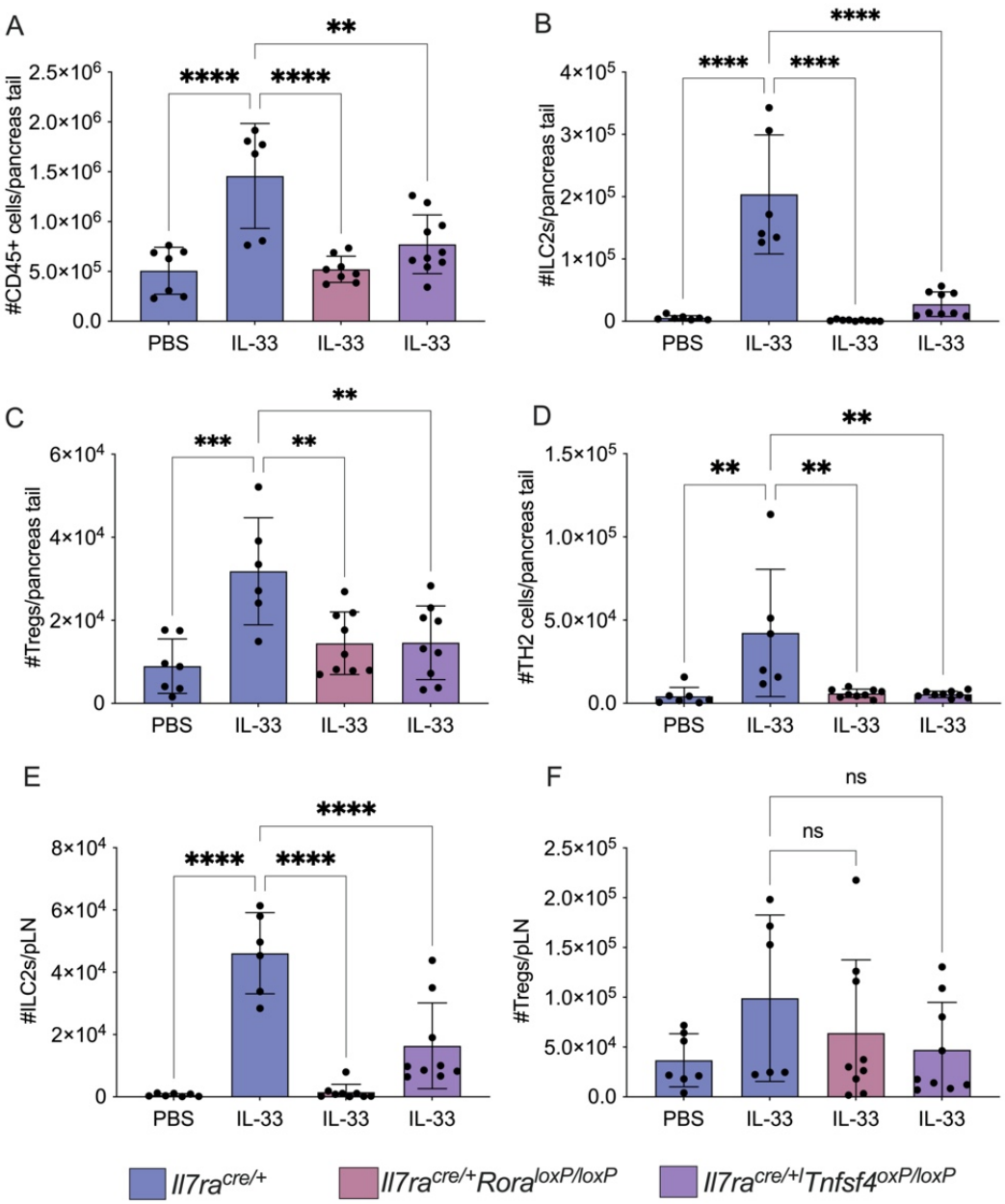

Figure 17 – IL-33 induced expansion of Tregs in the pancreas is ILC2 and OX40L dependent. *IL7Ra$^{cre/+}$, IL7ra$^{cre/+}$Rora$^{loxP/loxP}$ and IL7Ra$^{cre/+}$ Tnfsf4$^{loxP/loxP}$* mice were treated with 200ng recombinant IL-33 on days 0 and 1 and were sacrificed on day 5. This was followed by quantification of lymphoid cell numbers in the pancreas and pancreas lymph node by flow cytometry (n=6,6,9,8). A-D, Quantification of the number CD45+ immune cells, ILC2s, Tregs and TH2 cells in the pancreas respectively. E,F, Quantification of the number of ILC2s and Tregs in the pancreatic lymph nodes respectively. A-F, Bar graphs indicate the mean (± s.e.m.) and show combined results from two experiments. Statistical significance was calculated using one-way ANOVA. ns=non-significant. *= P≤0.05, **= P≤0.01, ***= P≤0.001, ****=P≤0.0001.

Characterising ILC2s in Pancreatic Ductal Adenocarcinoma (PDAC) development

Several reports have described features of a type 2 immune environment during PDAC development. The type 2 cytokine, IL-13 has been shown to skew macrophages to a more M2 phenotype in PDAC. These M2 macrophages in turn have been shown to drive fibrogenesis and tumorigenesis in PDAC through IL-1ra and CCL2 (Liou et al., 2017). Tregs, shown to be regulated by ILC2s in the pancreas earlier in this chapter, have been shown to induce tolerance against tumour associated antigens and have been shown to restrain DC expansion in PDAC (Jang et al., 2017).

As discussed in the introduction, ILC2s have been implicated in regulating type 2 immunity in several tumour models. A type 2 cytokine, IL-5 has been shown to mediate eosinophil recruitment in lung tumour and metastasis models. These recruited eosinophils were shown to be essential for tumour rejection and reduced metastasis formation in the lung. The source of IL-5 in the model were identified to be CD3- c-kit+ cells (Ikutani et al., 2012). In the pancreas, PD-1 expressing ILC2s were found to be infiltrating tumours. IL-33 induced activation and expansion of these ILC2s led to enhanced control of tumour and improved survival of tumour bearing mice (Moral et al., 2020).

Considering our observation of ILC2 mediated regulation of a type 2 immune environment and Treg expansion in the healthy pancreas, we asked if ILC2s may be playing a similar role in PDAC development. To this end, we used *Kras*^{G12D} *Ptf1a*$^{cre/+}$(KC) mice which develop PDAC over a period of one year (Hingorani et al., 2003) to study the role of ILC2s in PDAC development.

KC mice of different ages and hence different stages of PanIN development were studied. Total number of ILC2s, Tregs and TH2s but not total CD45+ cell numbers were found to be higher in KC mice compared to controls at 4 months of age (fig 18, fig S36). A trend toward higher number of ILC2s in KC mice pancreas at 6 months of age was also seen (fig 18D, fig S36).

Total number of ILCs, T cells and CD4 T cells were also found to be significantly higher in pancreas from KC mice at 4 months of age (fig S10a,C,E). B cell, NK cell and CD8 T cell numbers were however unaffected in pancreas from KC mice (fig S10B,D,F). In the pLN however, the most difference was seen in 2-month-old KC mice. Total number of ILCs, ILC2s, T cells, B cells, CD8 T cells, NK cells and CD4 T cells were higher in pLN from KC mice

compared to controls (fig S11A-G). Thus, suggesting an earlier disruption of immune homeostasis in the pLN during early panIN development followed dynamically by a similar disruption in the pancreas as panINs progress. Type 2 immune changes were also captured in the myeloid compartment in KC mice of different age groups. Total number of eosinophils, macrophages, neutrophils, DCs and cDC2s were found to be higher in the pancreas of 4-month-old KC mice (fig S12A-F). Total number of neutrophils was found to be higher in younger KC mice at 2 months of age as well (fig S12C). Total number of DCs and cDC2s were found to be increased in pLN of KC mice at 2 months of age but not later ages (fig S12G,I) but no change was found in number of cDC1s (fig S12H).

Altogether, our immune analysis of KC mice at early stages of PanIN development reveals a type 2 skewed immune environment characterised by increased eosinophils, cDC2s, ILC2s, T_h2s and Tregs.

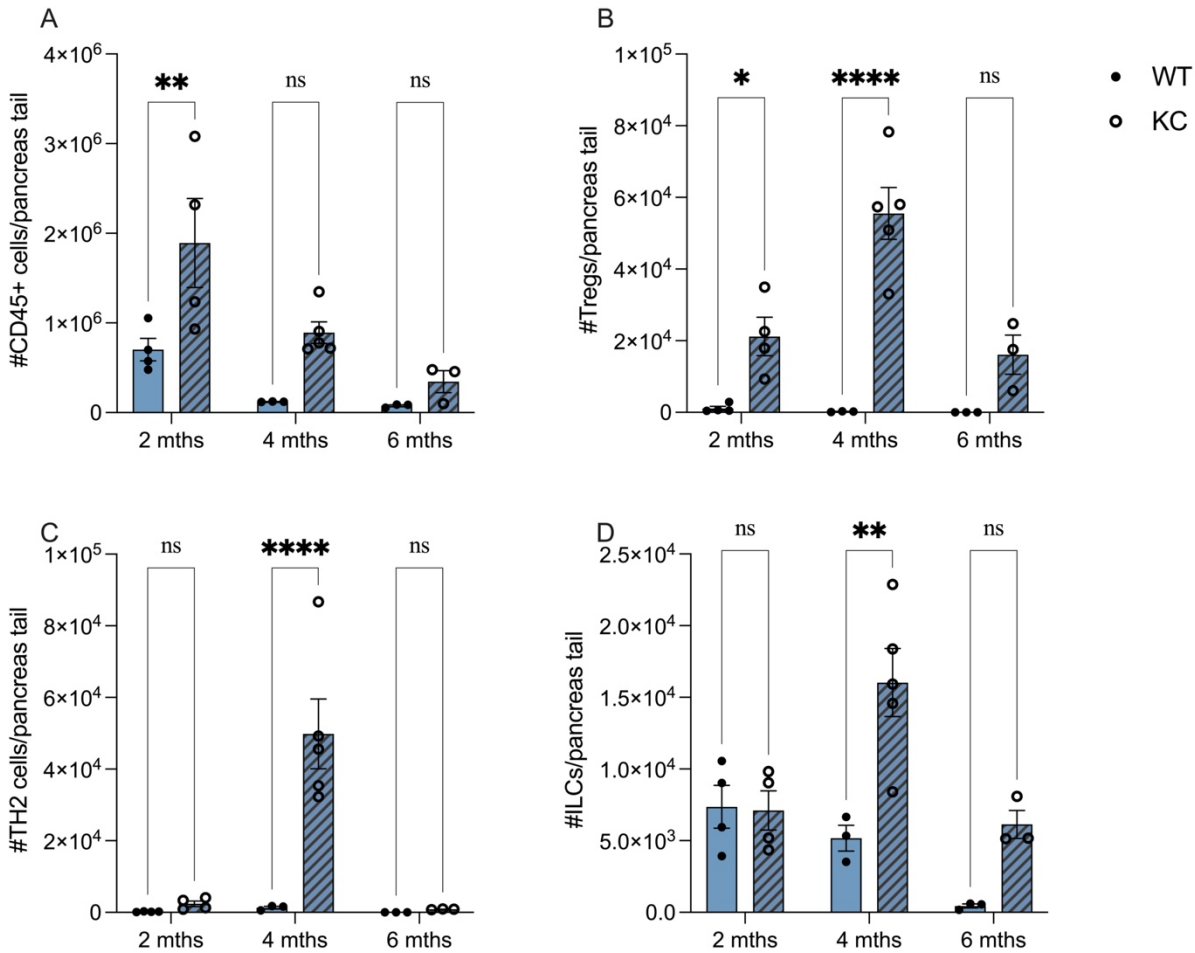

Figure 18 – ILC2 and Treg numbers are increased in pancreatic intraepithelial neoplasia (panIN). Pancreas from KC mice were collected at 2, 4 and 6 months of age and lymphoid immune cells were quantified by flow cytometry (n=4,4,3,5,3,3). A-D, Quantification of CD45+ immune cells, Tregs, TH2 cells and ILC2s in the pancreas. A,B,C, Bar graphs indicate the mean (± s.e.m.) and show results of 3 individual experiments. Statistical significance was calculated using two-way ANOVA. ns=non-significant. *= P≤0.05, **= P≤0.01, ***= P≤0.001, ****=P≤0.0001.

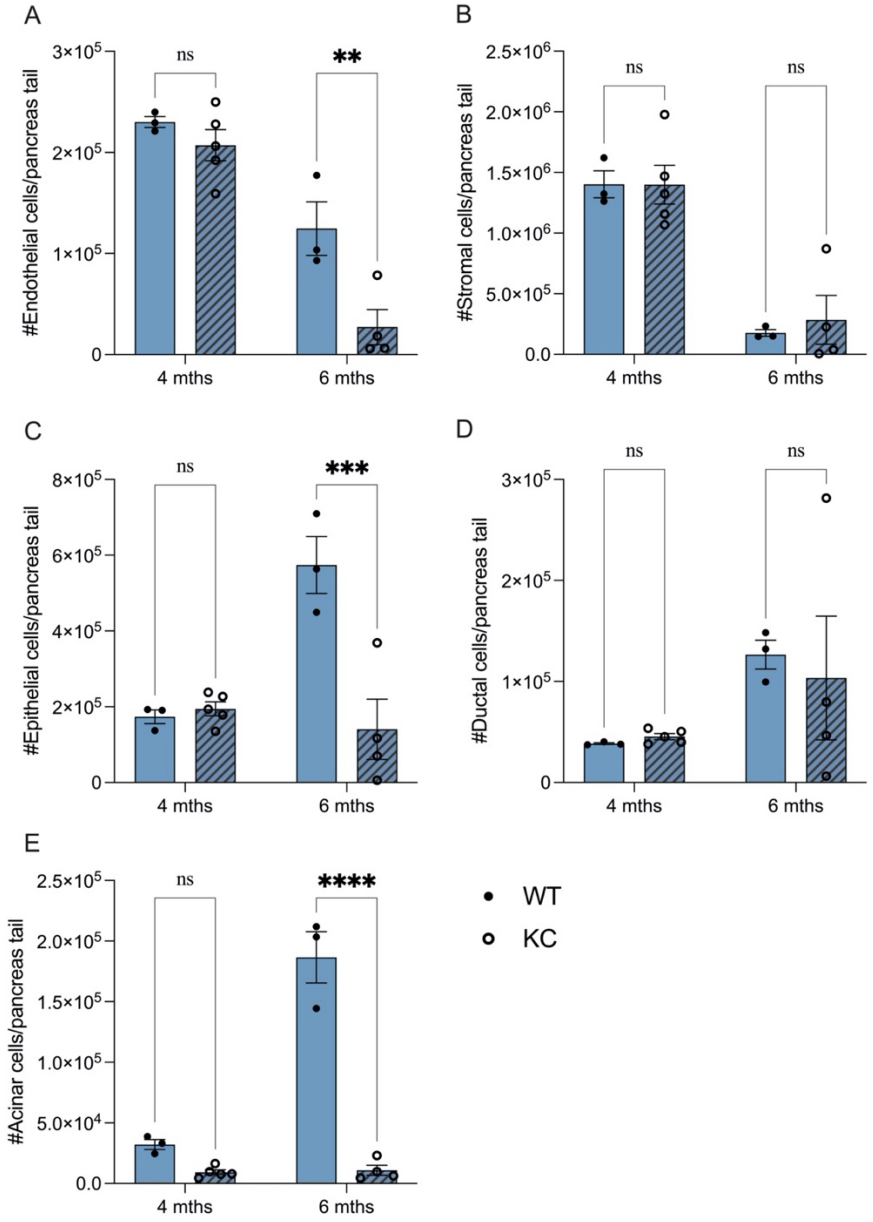

Figure 19 – Non-immune cell changes in PanINs captured by flow cytometry. Pancreas from *Kras^{G12D}, Ptf1a$^{cre/+}$ or Kras^{G12D} Ptf1a$^{cre/+}$ mice* were collected at 4 and 6 months of age and non-immune cells were quantified by flow cytometry (n=3,5,3,3). A-E, Quantification of endothelial cells, stromal cells, epithelial cells, ductal cells and acinar cells in the pancreas. A-E, Bar graphs indicate the mean (± s.e.m.) and show results 2 individual experiments. Statistical significance was calculated using two-way ANOVA. ns=non-significant. *= P≤0.05, **= P≤0.01, ***= P≤0.001, ****=P≤0.0001.

In order to analyse the non-immune compartment in the pancreas, we developed a flow cytometry panel and it has been described in the methods section. We identified epithelial cells with EpCAM (Trzpis et al., 2007), endothelial cells with CD31 (L. Liu & Shi, 2012), stromal cells using podoplanin (Eckert et al., 2016) and ductal cells using CD133 (Jin et al., 2016). Peanut agglutinin (PNA) a lectin has high affinity to acinar cells (Xiao et al., 2016) and PNA

tagged to PE was used to identify acinar cells. The gating strategy for this panel has been shared in the methods section (fig 7).
Using this non-immune cell flow cytometry panel, we observed that 6-month-old KC mice showed a reduction in total number of acinar cells (fig 13E) possibly capturing the permanent acinar to ductal metaplasia (ADM) leading to PanIN formation. A reduction in epithelial cell and endothelial cells was also seen in KC mice pancreas from 6 month old mice compared to controls (fig 19A,C). However, the increase in ductal cells due to PanINs was not captured (fig 19 B), indicating a possible need to for a more robust ductal cell marker. No change was seen in stromal cell numbers in pancreas from KC mice (fig 19B) although fibrosis is a key feature of PDAC development (Hingorani et al., 2003).

We previously showed that IL-33 is a potent regulator of type 2 immunity in the pancreas. As several type 2 immune changes were captured in KC mice, we asked if these changes could be regulated by IL-33. To this end, we used KC mice lacking expression of IL-33 (KC *Il33*$^{cit/+}$ of KC *Il33*$^{cit/cit}$). KC *Il33*$^{cit/+}$ mice are reporters for the *Il33* gene and retain *Il33* expression while KC *Il33*$^{cit/cit}$ lacked expression of *Il33*.

Total number of CD45+ cells, ILC2s, TH2 cells, eosinophils, DCs, cDC1s or cDC2s were not different between 3 month old KC *Il33*$^{cit/+}$ and KC *Il33*$^{cit/cit}$ mice (fig 20 A,B,D-H). Total number of Tregs however was significantly higher in 3 months old KC *Il33*$^{cit/cit}$ mice compared to KC *Il33*$^{cit/+}$ mice (fig 20C). This observation is at odds given our previous observations: while recombinant IL-33 was able to induce Treg expansion in the healthy pancreas, the absence of IL-33 in the KC *Il33*$^{cit/cit}$ seems to increase Treg numbers. This suggests the presence of a compensatory mechanism in KC *Il33*$^{cit/cit}$ mice and during Treg expansion.

We also noted no change in the number of B cells, T cells, CD8 T cells, NK cells, ILCs, neutrophils, CD4 T cells and macrophages between 3-month-old KC *Il33*$^{cit/+}$ and KC *Il33*$^{cit/cit}$ mice (fig S13). While several of the type 2 immune signatures like increase in ILC2s and cDC2s were still captured in both KC *Il33*$^{cit/+}$ and KC *Il33*$^{cit/cit}$ mice, the lack of difference between these two genotypes, indicates that these signatures are not regulated by IL-33. Alternatively, similar to the Treg observation, a compensatory mechanism could be active in regulating the type 2 immune environment in KC *Il33*$^{cit/cit}$ mice.

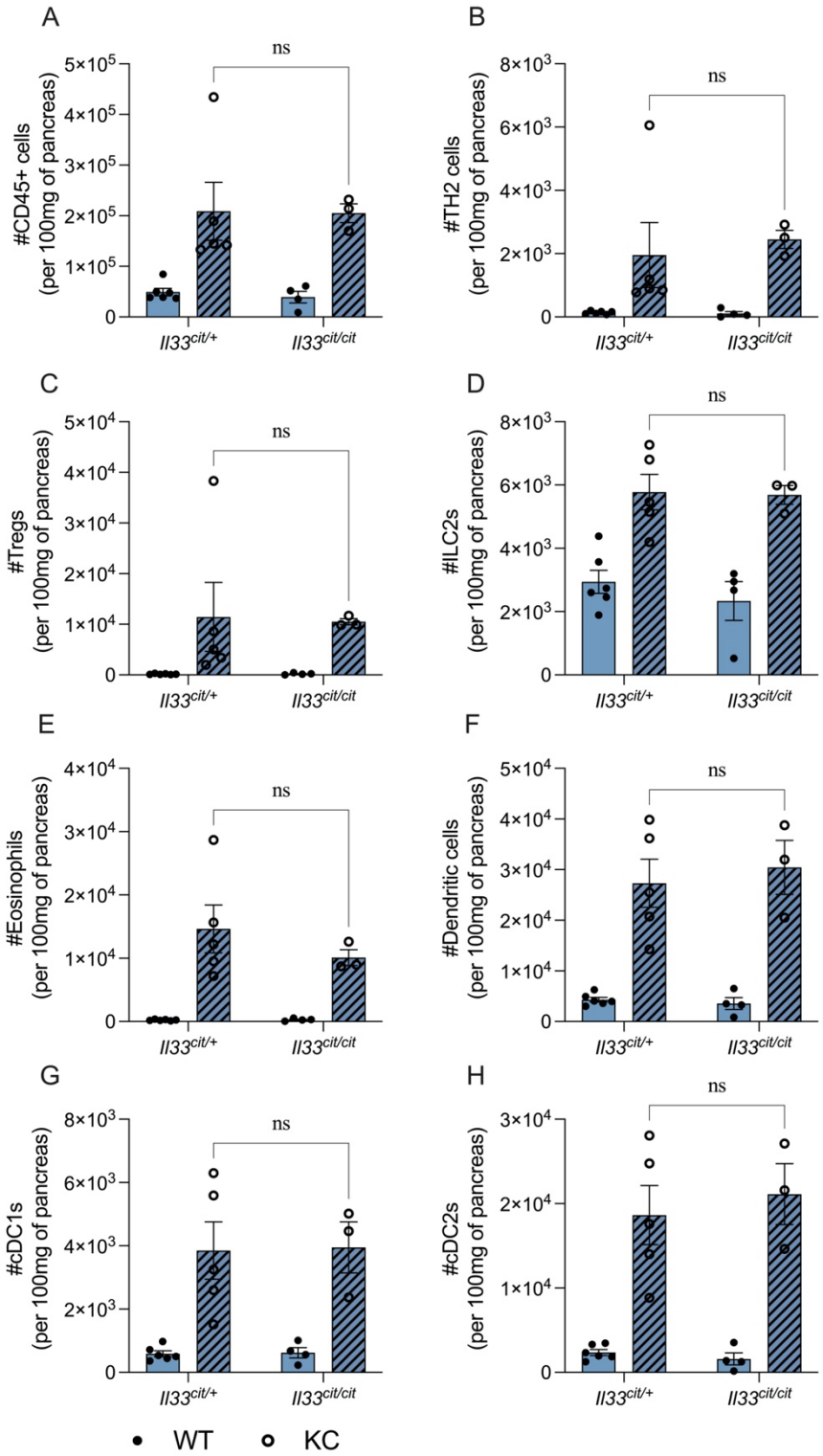

Figure 20 – Type 2 immune environment in PanINs is not IL-33 dependent. Pancreas from KC mice with or without IL-33 expression (IL-33$^{cit/+}$ or IL-33$^{cit/cit}$) were collected at 3 months of age and immune cells were quantified by flow cytometry (n=4,3,6,5). A-H, Quantification of CD45+ immune cells, ILC2s, Tregs, TH2 cells, eosinophils, DCs, cDC1s and cDC2s in the pancreas. A-H, Bar graphs indicate the mean (± s.e.m.) and show results of 1 experiment. Statistical significance was calculated using two-way ANOVA. ns=non-significant. *= P≤0.05, **= P≤0.01, ***= P≤0.001, ****=P≤0.0001.

Finally, we asked if the lack of IL-33 expression might affect the survival of KC *Il33*$^{cit/cit}$ mice compared to either KC or KC *Il33*$^{cit/+}$ mice. A survival study showed no significant difference in probability of survival between KC, KC *Il33*$^{cit/+}$ and KC *Il33*$^{cit/cit}$ mice (fig 21).

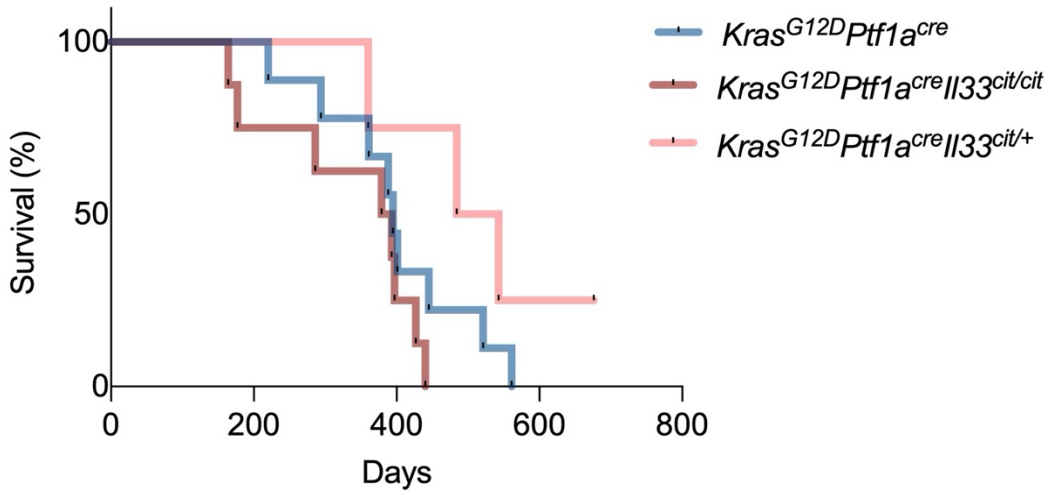

Figure 21 – IL-33 does not influence survival of tumour bearing KC mice. Survival analysis of *Kras*^{G12D} *Ptf1a*$^{cre/+}$, in *Kras*^{G12D}*Ptf1a*$^{cre/+}$ *Il33*$^{cit/+}$ and *Kras*^{G12D}*Ptf1a*$^{cre/+}$ *Il33*$^{cit/cit}$ mice (n=9,8,4). Statistical analyses were calculated using log-rank (Mantel–Cox) test and the difference was found to be non-significant.

Summarising this chapter, we have identified that ILC2s in the pancreas can be activated by IL-33. When activated by IL-33, ILC2s show strong expression of OX40L and produce type 2 cytokines such as IL-5 and IL-13. ILC2s have also been found to regulate Treg expansion after IL-33 treatment in a OX40L dependent manner. Increased numbers of ILC2s can be seen in PanINs. However, neither ILC2 numbers or other type 2 immune features seen in PanINs seem to be regulated by IL-33. Survival of KC mice was also not altered by the absence of IL-33.

Chapter 2

The role of ILC2s in epithelial damage in acute pancreatitis

Mouse models of pancreatitis

Acute pancreatitis clinically shows a varying degree of severity in presentation ranging from mild disease that is self-limiting to multiple organ dysfunction syndrome (MODS) associated severe disease (Hines & Pandol, 2019). Studying pancreatitis in humans is limited by the anatomical position of the pancreas (deep seated) which leads to challenges in getting tissues from individuals with pancreatitis (Hyun & Lee, 2014). Due to these challenges, studying pancreatitis requires use of animal models that capture the histopathological changes seen in human pancreatitis. A range of animal models of pancreatitis are available to use with varying degrees of disease severity, a few of these models have been discussed below.

Biliary reflux in the pancreas due to gall bladder obstruction by gall stones is thought to be the most common clinical reason for acute pancreatitis (Lerch & Aghdassi, 2010) and this model is the best at replicating the clinical setting during onset of acute pancreatitis. Introduction of sodium taurocholate, a bile salt into the duct of rats was shown to induce severe haemorrhagic pancreatitis and necrosis in rats (Aho et al., 1980). To induce pancreatitis, a canula is inserted into the duodenum and the bile salt sodium taurocholate is infused in retrograde fashion. Severe haemorrhagic necrosis of the pancreas can be observed 6-12 hours after the infusion has been performed (Serra et al., 2021). The mechanism by which sodium taurocholate induces severe acute pancreatitis is not clearly understood. This model is limited in scalability that is required for large immunology experiments. Abdominal incision and special technical expertise is required to insert a cannula for infusion of sodium taurocholate (Hyun & Lee, 2014).

Pancreatic duct ligation model attempts to recreate the ‘common channel’ mechanism for induction of pancreatitis (Yang et al., 2020). This model is meant to mimic ampullary orifice obstruction by gallstones, thus causing bile reflux into the pancreatic duct which eventually leads to acute pancreatitis. All common features of acute pancreatitis like oedema, increased amylase secretion and immune cell influx can be captured in this model. If the duct ligation persists, acute pancreatitis gives way to chronic pancreatitis with features like fibrosis and acinar to ductal metaplasia (Yang et al., 2020). With this model as well, scalability is the main limitation due to the invasive nature of the procedure that needs to be performed (Hyun & Lee, 2014).

The choline-deficient, ethionine-supplemented (CDE) diet pancreatitis model is a non-invasive model of pancreatitis. To induce pancreatitis, 4–6-week-old female mice weighing around 10-14g are freely fed on the CDE diet (Hyun & Lee, 2014). These mice develop acute

haemorrhagic pancreatitis in roughly 5 days and this model exhibits a high mortality rate of up to 100%. The high mortality rate makes this model a poor representation of acute pancreatitis in humans (as acute pancreatitis in humans is most often self-limiting). Additionally, this model's efficacy is maximised only in young female mice (Hyun & Lee, 2014).

Among other non-invasive models, L-arginine, an essential amino acid, is often used to induce severe necrotising acute pancreatitis in rats. Excessive L-arginine administration (500mg/100g body weight of rat) leads to development of acute necrotising pancreatitis which resolves completely by 14 days (Hyun & Lee, 2014). Necrosis of pancreatic acini and immune cell influx are common features of this model. The mechanism by which L-arginine and other basic amino acids like L-ornithine and L-lysine induce pancreatitis is not well understood. This model is preferentially used in rats and is not adapted for use in mice (Hyun & Lee, 2014).

Caerulein induced pancreatitis is the most widely used model of pancreatitis owing to its reproducibility and scalability, making it the model of choice to use in several genetically modified mouse models (Lerch & Gorelick, 2013). Caerulein is an analogue of the hormone cholecystokinin (CCK). CCK binds to two receptors on acinar cells – high affinity CCK receptor and low affinity CCK receptor (CCKR). When CCK binds to the high affinity CCKR, proenzyme containing granules or zymogen granules are released from the cell by exocytosis. This leads to increased secretion of digestive enzymes. The low affinity CCKR is only bound by CCK when the high affinity CCKR has been saturated. When CCK binds low affinity CCKR, this leads to inhibition of the secretion of the digestive enzyme, thus balancing any excessive enzyme secretion that might occur (Hyun & Lee, 2014). When acinar cells are stimulated with excessive CCK or their analogue caerulein, an accumulation of zymogen granules containing digestive proenzymes occur. As the low affinity CCKR are also bound, the release of these zymogen granules by exocytosis is inhibited. Following this accumulation, the mechanism by which these proenzymes get activated in the pancreas and thereby induce pancreatitis is unclear (Hyun & Lee, 2014). Caerulein induced pancreatitis causes increased pancreatic amylase and lipase secretions, oedema and necrosis which are all resolved within a day. ADM can be seen after resolution of oedema and necrosis (Yang et al., 2020).

Low dose caerulein is sometimes combined with other compounds to induce pancreatitis. NOD1 an intracellular sensor that plays a role in host-defence against a variety of pathogens was shown to play a role in regulating non-infectious pancreatitis. Further, FK156 a NOD1 ligand was administered along with low doses of caerulein. While low dose caerulein does not induce pancreatitis in itself, when combined with FK156, pancreatitis was induced with classic features of pancreatic oedema, necrosis and immune influx (Tsuji et al., 2012). Typically, in

the caerulein model, pancreatitis is induced by injecting 50-100μg/Kg caerulein several times in hourly intervals in a day. Our study uses 50 or 75μg/Kg caerulein i.p., 6 times a day in hourly intervals. Mice are also given buprenorphine for analgesia, before start of caerulein injections.

Characterising caerulein induced pancreatitis

Histological features which mark the severity of caerulein induced pancreatitis and the dynamics of these changes vary based on mouse model, injection schedule and dose of caerulein used. In order to characterise the dynamics of caerulein indued pancreatitis in our model and setting, a time course experiment was set up looking at histology of the pancreas 6,12,18, 24, 30, 36, 42 and 48 hours after induction of pancreatitis. On H&E-stained pancreas sections, oedema (yellow arrow) was seen at 6, 12,18 and 24h timepoints (fig 22). Necrosis (red arrow) was seen at 18 and 24h time points and ADM (red arrow) at 42 and 48h timepoints (fig 22).

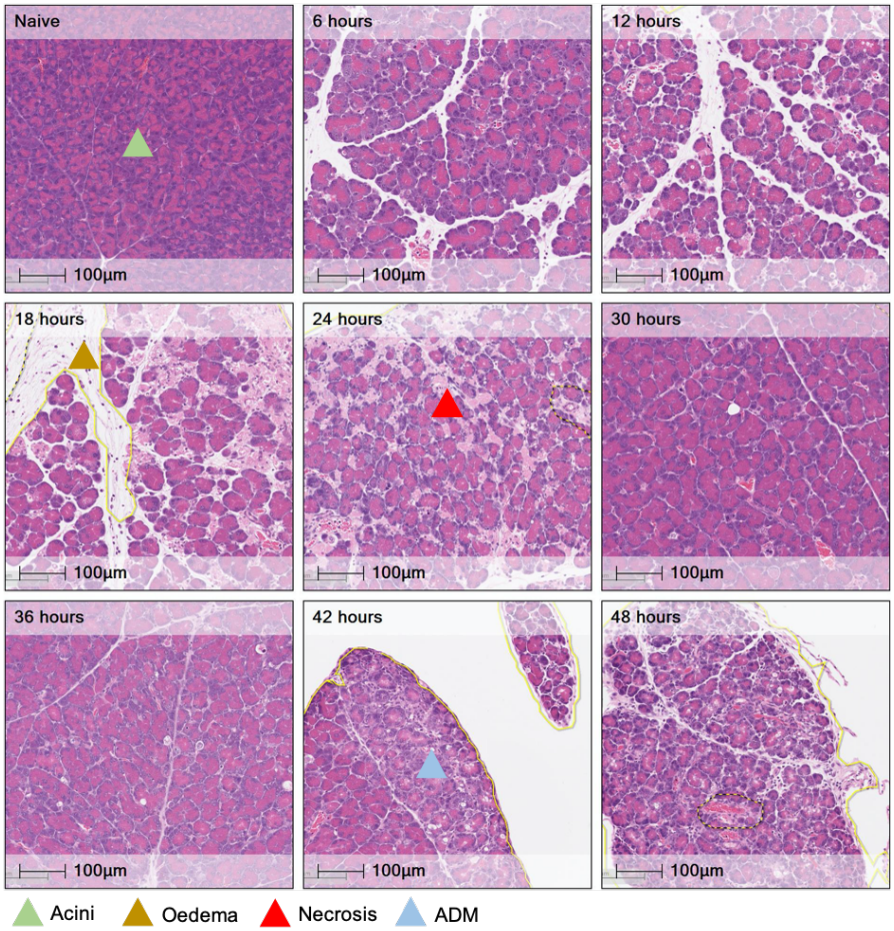

Figure 22 – Histological features of acute pancreatitis are dynamic. C57BL/6 mice were treated with 75ug/Kg caerulein once every hour for 6 hours and sacrificed at different time points after the first caerulein injection. Figure shows H&E staining of pancreas. Normal acini have been marked with a green arrow. Oedema (yellow arrow) seen at 6,12,18 and 24 hours. Necrosis (red arrow) was seen at 18 and 24 hours. Acinar to ductal metaplasia (ADM) identified with a blue arrow seen at 42 and 48 hours.

In order to quantify the extent of necrosis, oedema and ADM, a classifier tool on the image analysis software Halo was trained to identify these features. Representative images of the

performance of the trained classifier and its identification of acini (green), necrosis (red), oedema (yellow) and ADM (blue) have been shown in fig 23.

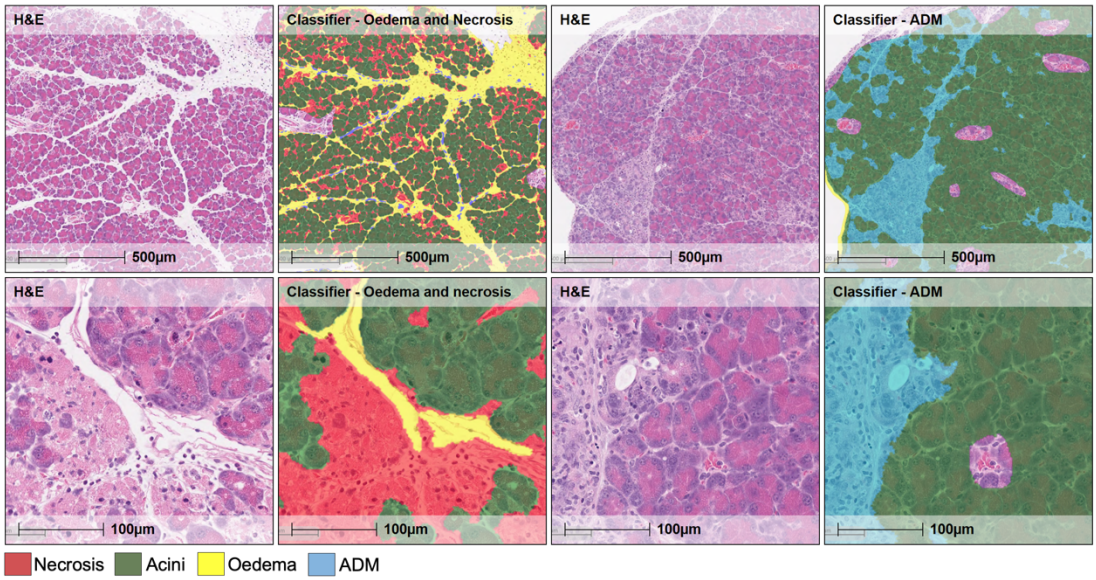

Figure 23 – Quantification of oedema, necrosis and ADM from H&E sections. Classifier function of the image analysis software Halo was trained to identify normal acini (green), oedema (yellow), necrosis (necrosis) and ADM (blue) on images of H&E-stained histological sections.

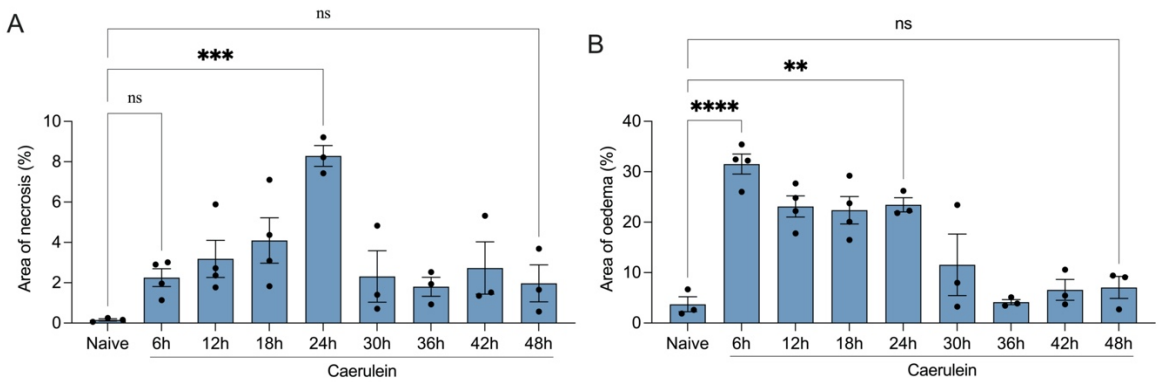

Figure 24 – Oedema and necrosis in acute pancreatitis peak at 24 hours. C57BL/6 mice were treated with 75ug/Kg caerulein and sacrificed at different timepoints following the first caerulein injection. A,B, Quantification of area of necrosis and oedema respectively from images of H&E stained histological sections using the classifier function on the image analysis software, Halo. Bar graphs indicate the mean (± s.e.m.) and show data from one experiment. Statistical significance was calculated using one-way ANOVA. ns=non significant. *= P≤0.05, **= P≤0.01, ***= P≤0.001, ****=P≤0.0001.

Using such a trained classifier on the whole pancreas sections of our time-course experiment, we found that necrosis peaked at 24h whilst oedema increased at 6h and plateaued until the 24h timepoint (fig 24A,B). The 24h timepoint was found to be the only timepoint at which a significant increase in necrosis and oedema could be seen compared to naïve mice pancreas (fig 24A,B). As the 24h timepoint was found to be ideal for capturing necrosis and oedema,

this timepoint has been used for experiments investigating epithelial damage in acute pancreatitis.

ILC2s regulate disease severity in acute pancreatitis

Several type 2 immune features have been reported in association with the immunopathogenesis of pancreatitis. Pancreatic lysates from C57BL/6 mice with FK565-caerulein induced pancreatitis showed an increase in IL-33 and IL-13 expression (Watanabe et al., 2016). An increase in serum IL-33 levels was also seen in mice with chronic pancreatitis (Watanabe et al., 2016). In this paper, IL-33 was shown to be expressed by necrosing acinar cells. Additionally, the authors report that the depletion of IL-33 using anti-ST2 Ab led to decrease in pancreatitis severity (Watanabe et al., 2016). Earlier in this report, we showed that IL-33 can activate pancreatic ILC2s and induce their production of IL-13 (fig 18).

CD11c.DTR mice in which CD11c expressing cells (DCs) can be depleted using diphtheria toxin was shown to develop severe acinar necrosis and consequent death following caerulein induced pancreatitis. DCs have been suggested to protect the pancreas from cellular stress (Bedrosian et al., 2011). Earlier in this report, we demonstrated that IL-33 was shown to induce significant increase in total DC numbers (fig 13D) and the number of Cd11b- DCs or type 1 DCs was found to be ILC2 dependent (fig S9F).

Considering evidence of type 2 immune features that could potentially be regulated by ILC2s, we looked at whether ILC2s could play a role in regulating inflammation and disease severity associated with pancreatitis. To this end, we first looked at histological features of disease severity, namely necrosis and oedema in ILC2 deficient ($Il7ra^{cre/+}Rora^{loxP/loxP}$) compared to control mice ($Il7ra^{cre/+}$) over several time points following induction of pancreatitis (fig 25A). Strikingly, ILC2 deficient mice showed a significant reduction in oedema at the 24h timepoint compared to controls. (Fig 25B,C).

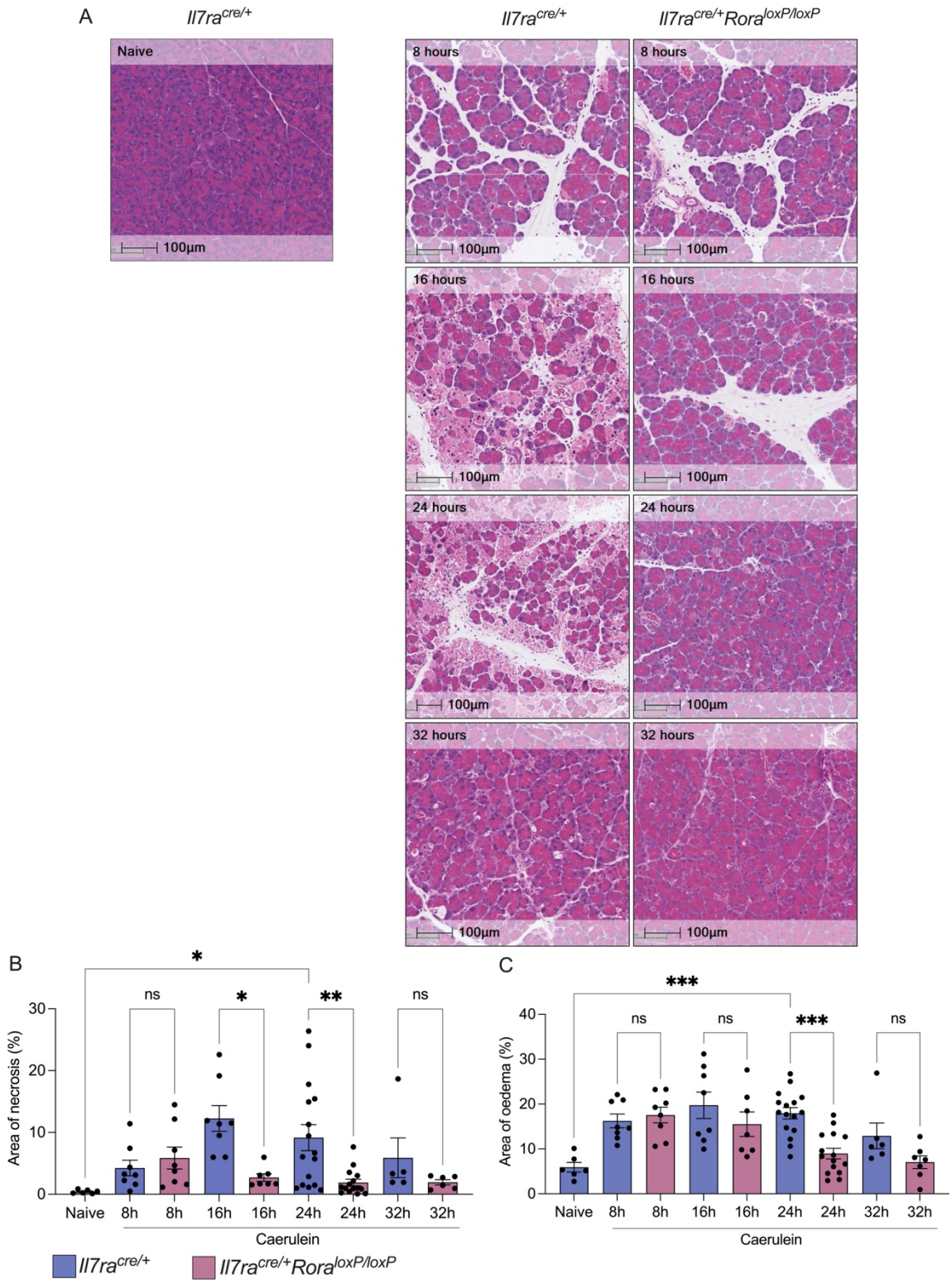

Figure 25– ILC2 deficient mice are protected from acute pancreatitis. *Il7ra*$^{cre/+}$ or *Il7ra*$^{cre/+}$ *Rora*$^{loxP/loxP}$ mice were injected with 50 or 75ug of caerulein and the mice were sacrificed at the indicated timepoints after the first caerulein injection. A, Figure shows representative images from H&E staining of pancreas. B,C, Quantification of area of necrosis (B) and oedema (C) from images of H&E stained histological sections using the classifier function on the image analysis software Halo. B,C, Bar graphs indicate the mean (± s.e.m.) and show data from two to four independent experiments.. B,C, Statistical significance was calculated using one-way ANOVA. ns=non-significant. *= P≤0.05, **= P≤0.01, ***= P≤0.001, ****=P≤0.0001.

Serum amylase and lipase levels increase in patients and mice with pancreatitis (Boxhoorn et al., 2020) and are a standard measure of disease severity. We therefore measured these biomarkers in ILC2 deficient mice compared to controls. We found that ILC2 deficient mice exhibit a significant reduction in both serum amylase and lipase levels compared to controls (fig 26 A,B). Altogether the histological and serum analysis, revealed that ILC2 deficient mice are protected from acute pancreatitis. Thus, our data suggests that ILC2s play a role in regulating epithelial damage and associated disease severity in acute pancreatitis.

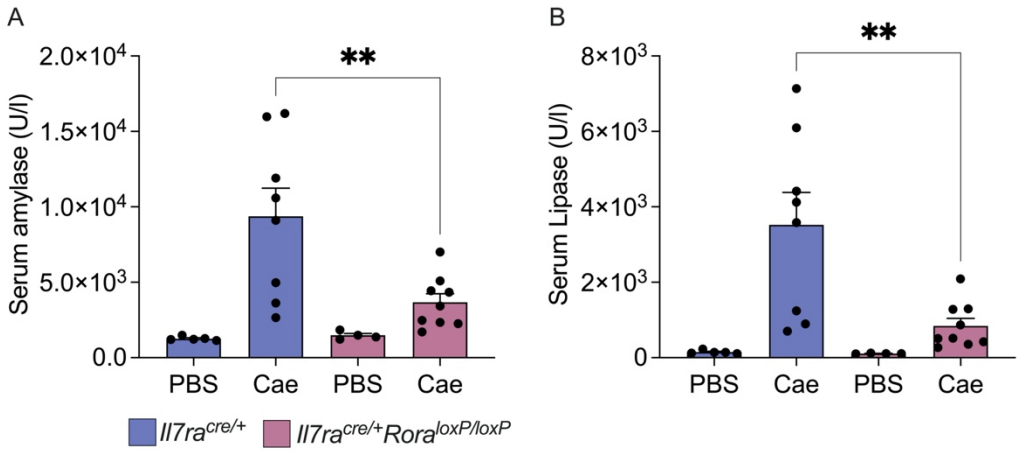

Figure 26 – ILC2 deficient mice are protected from acute pancreatitis. *Il7ra*$^{cre/+}$ or *Il7ra*$^{cre/+}$ *Rora*$^{loxP/loxP}$ mice were injected with PBS or 50ug/Kg of caerulein and sacrificed at 24 hours after the first caerulein injection. A,B, Quantification of serum amylase and lipase levels. Bar graphs indicate the mean (± s.e.m.) and show data from two independent experiments. Statistical significance was calculated using one-way ANOVA. ns=non significant. *= P≤0.05, **= P≤0.01, ***= P≤0.001, ****=P≤0.0001.

As noted, influx of leukocytes is also often used as a marker of disease severity. We further characterised the pancreas of ILC2-deficient animals during pancreatitis by performing deep immunophenotyping by flow cytometry. We found that ILC2 deficient mice show a reduction in total CD45+ at the 24h and 3-day timepoints compared to control animals, in line with the aforementioned disease protection (fig 27A, S16A, S37A). Lack of ILC2s in the pancreas of *Il7ra*$^{cre/+}$*Rora*$^{loxP/loxP}$ mice was confirmed by such analysis (fig 27B and S16C). At the 24h timepoint no difference was seen in number of B cells, CD4 T cells, Tregs, CD8 T cells and NK cells between ILC2-deficient and sufficient animals (fig 27B-G).

We analysed the epithelial (including ductal and acinar) populations in the pancreas using the non-immune flow cytometry panel described chapter 1 of results. Although we observed acinar cell necrosis histologically, the same was not captured using flow cytometry. While a reduction in acinar cell numbers was seen in both control and ILC2 deficient with pancreatitis, there was no significant difference in acinar cells numbers between the two genotypes (fig S15C). This difference in observation between what was captured using histology and flow-cytometry could be due to change in expression of acinar cell surface markers (used for flow-cytometry)

owing to cellular stress. No difference in endothelial, total epithelial, ductal, stromal or percentage of cycling stromal cells was seen between control and ILC2 deficient mice at the 24h timepoint either (S15A,B,D,E,F).

We also characterised the immune compartment using deep immunophenotyping by flow cytometry at the 6 hour and day 3 timepoint after pancreatitis in ILC2 deficient mice and controls. Similar to the ILC2 dependent Treg expansion in the recombinant IL-33 model earlier (fig 12I), Treg expansion was seen to be ILC2 dependent (fig S16F) 3 days after pancreatitis induction. Number of B cells, CD4 T cells and CD8 T cells were also found to be ILC2 dependent (fig S16A,B,C,D,G). We also analysed eosinophilia which has been shown to be ILC2 dependent in literature (Nussbaum et al., 2013) in other conditions and also earlier in this report (S9A). In acute pancreatitis as well, eosinophilia was observed in at the 6h, 24h and 3-day timepoints and this was found to be ILC2 dependent (S20B, fig 28D, S17B, S37C).

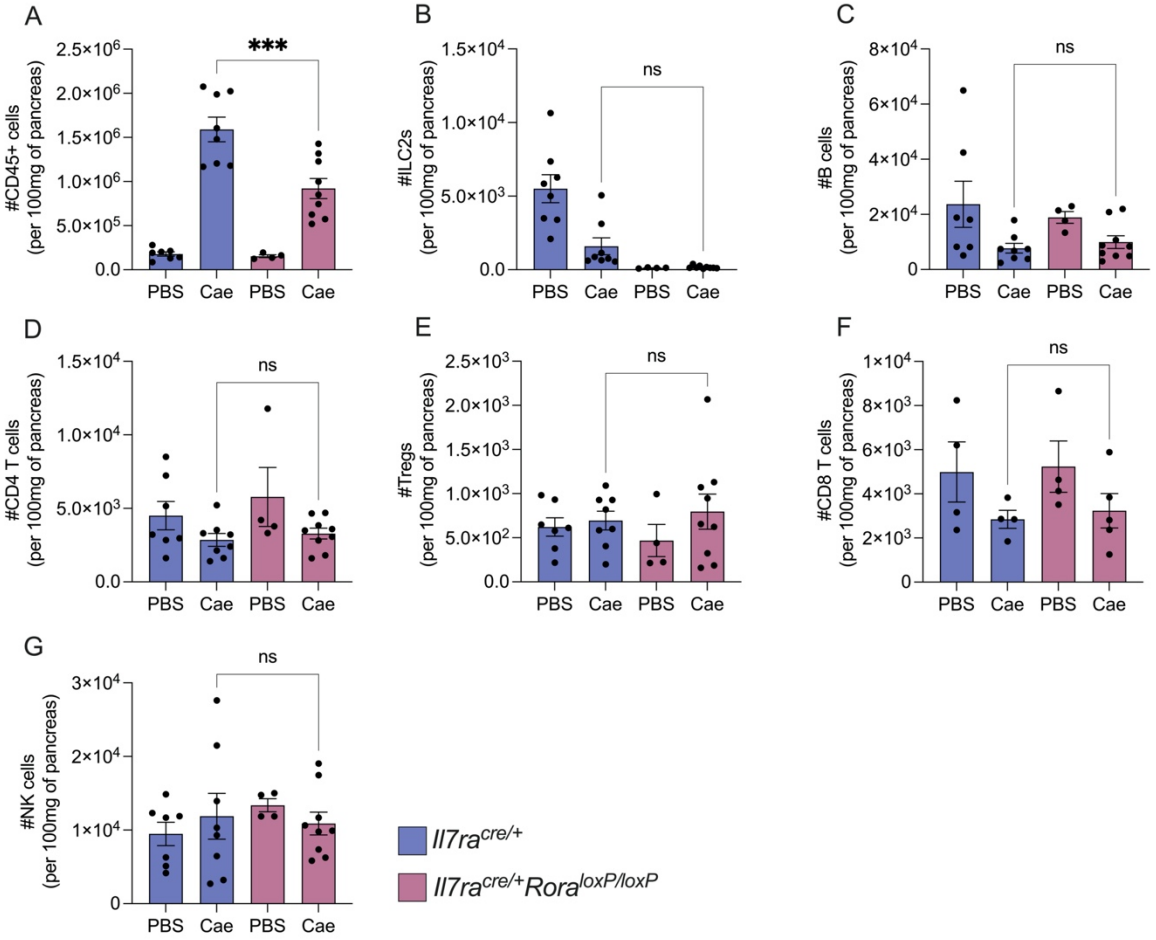

Figure 27 – ILC2 deficient mice show reduced inflammation during acute pancreatitis. *Il7ra*$^{cre/+}$ or *Il7ra*$^{cre/+}$ *Rora*$^{loxP/loxP}$ mice were injected with PBS or 50ug/Kg of caerulein and the mice were sacrificed at 24 hours after the first caerulein injection. This was followed by quantification of lymphoid immune cells in the pancreas by flow cytometry. A-H, Bar graphs indicate the mean (± s.e.m.) and show data from two independent experiments. A-H, Statistical significance was calculated using one-way ANOVA. ns=non-significant. *= P≤0.05, **= P≤0.01, ***= P≤0.001, ****=P≤0.0001.

In the myeloid compartment, an increase in monocytes and cDC2s at the 24h timepoint was found to be ILC2 dependent (fig 28A,F). Changes in number of macrophages, neutrophils, DCs and cDC1s were not found to be ILC2 dependent at the 24h timepoint (fig 28B,C,E,F S37). Increase in cDC2 numbers was found to be ILC2 dependent at the 3-day timepoint as well (fig S17G). Changes in number of neutrophils, monocytes, macrophages, total DCs and cDC1s were not found to be ILC2 dependent during pancreatitis recovery at the 3-day timepoint. At the 6h timepoint, no difference was seen in number of neutrophils, monocytes, macrophages, total DCs, cDC1 and cDC2s between *Il7ra*$^{cre/+}$*Rora*$^{loxP/loxP}$ and control mice (fig S20A,C-G).

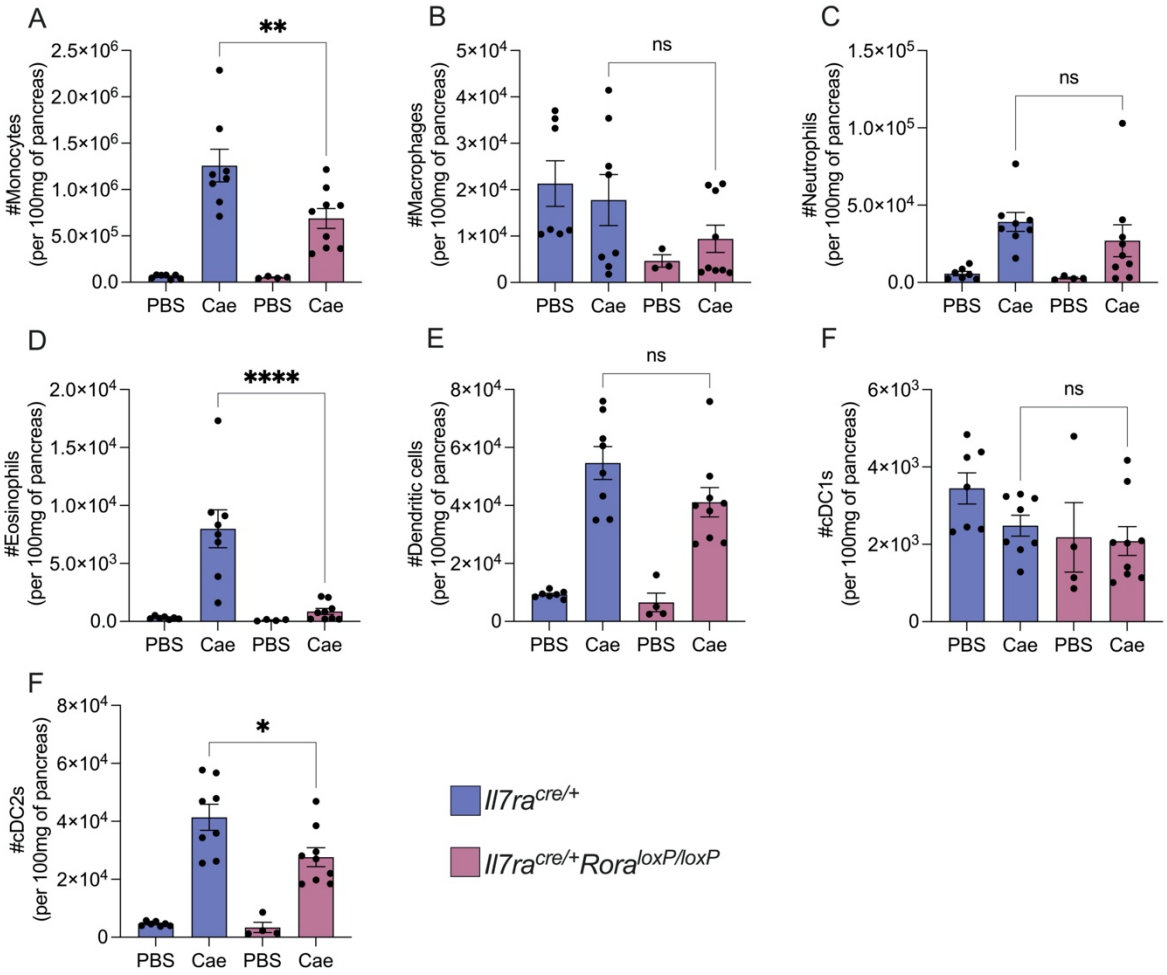

Figure 28 – ILC2 deficient mice show reduction in eosinophil and monocyte infiltration in acute pancreatitis. *Il7ra*$^{cre/+}$ (control) or *Il7ra*$^{cre/+}$ *Rora*$^{loxP/loxP}$ (ILC2 deficient) mice were injected with PBS or 50ug/Kg of caerulein and the mice were sacrificed at 24 hours after first caerulein injection. This was followed by quantification of myeloid immune cells in the pancreas by flow cytometry. A-F, Bar graphs indicate the mean (± s.e.m.) and show data from two repeats. A-F, Statistical significance was calculated using one-way ANOVA. ns=non-significant. *= P≤0.05, **= P≤0.01, ***= P≤0.001, ****=P≤0.0001.

In the non-immune compartment, a significant reduction in cycling stromal cells (Ki67+ stromal cells) was seen at the 3-day timepoint in ILC2 deficient mice compared to controls (fig S18G). However, no difference was seen in number of stromal cells at this timepoint (fig S18E). No

ILC2 dependent change was seen in number of endothelial cells, epithelial cells, acinar cells or ductal cells during pancreatitis recovery at the 3-day timepoint (fig S18A-D). No ILC2 dependent change was seen in percentage of cycling ductal cells at this timepoint either (fig S18F). A significant reduction was see in number of endothelial cells, acinar cells and stromal cells at the 6h timepoint, however this was not ILC2 dependent (fig S19A,B,D).

In summary, disease severity in acute pancreatitis as assessed by histological features (necrosis and oedema), serum markers (amylase and lipase) and immune influx (total CD45+ cell numbers by flow cytometry) was found to be ILC2 dependent. Apart from disease severity in acute pancreatitis, several of the ILC2 dependent type 2 inflammatory changes like eosinophilia and Treg expansion which were found to be ILC2 dependent in the recombinant IL-33 model in the previous chapter, were also found to be ILC2 dependent in acute pancreatitis. The next few sections of this chapter will explore the mechanistic relationship between these ILC2 dependent immune cell changes and the pathogenesis of acute pancreatitis.

ILC2 are activated in acute pancreatitis

As ILC2 dependent features like eosinophilia were seen in acute pancreatitis (S20B, fig 28D, S17B), we hypothesised that ILC2s could be activated in an IL-33 dependent manner in acute pancreatitis. Similar to our approach in recombinant IL-33 treated animals (fig 3), we looked at IL-5 expression at by ILCs in C57BL/6 and *Il33*$^{cit/cit}$ (IL-33 KO) 6 hours after the induction of acute pancreatitis (fig 29 A). The lack of IL-33 protein in the *Il33*$^{cit/cit}$ mouse model has been confirmed using western blot in fig S40. We observed that both ex-vivo and with PI stimulation, ILCs from pancreatitis affected mice showed increased expression of IL-5 compared to controls (fig 29 A,B). Furthermore, this increased production of IL-5 was found to be IL-33 dependent (fig 29 A,B).

We also looked at other immune cells that could produce IL-5 to understand if ILCs were the only source of IL-5 in acute pancreatitis. TH2 cells a subset of CD4 T cells has been shown to be source of IL-5 in allergic conditions in the lungs (Hogan et al., 1998). We looked at IL-5 expression in the CD4 T cell compartment ex-vivo and with PI stimulation (fig S38). No increase in IL-5-APC MFI or percentage of IL-5 producing CD4 T cells was seen (fig 29C,D). As shown in the first chapter of results, recombinant IL-33 induced IL-13 expression in ILC2s (fig 11). As this is another measure of ILC2 activation, we also looked at IL-13 production by ILC2s in acute pancreatitis (fig 30, S39). Similar to the recombinant IL-33 model, ILCs also showed an increase in IL-13 production during pancreatitis (fig 30B, S39). This increase in IL-13 production by ILCs in acute pancreatitis was also IL-33 dependent (fig 30C). We also

looked at IL-13 production by CD4 T cells (fig S39) as CD4 T cells are also known to produce IL-13. Similar to what was observed with IL-5, CD4 T cells did not show an increase in IL-13 production with or without PI stimulation (fig 30C,D). Thus, ILCs emerged as the only source of IL-5 and IL-13 in the early stage following onset of acute pancreatitis, and this production depends on the present of the alarmin IL-33.

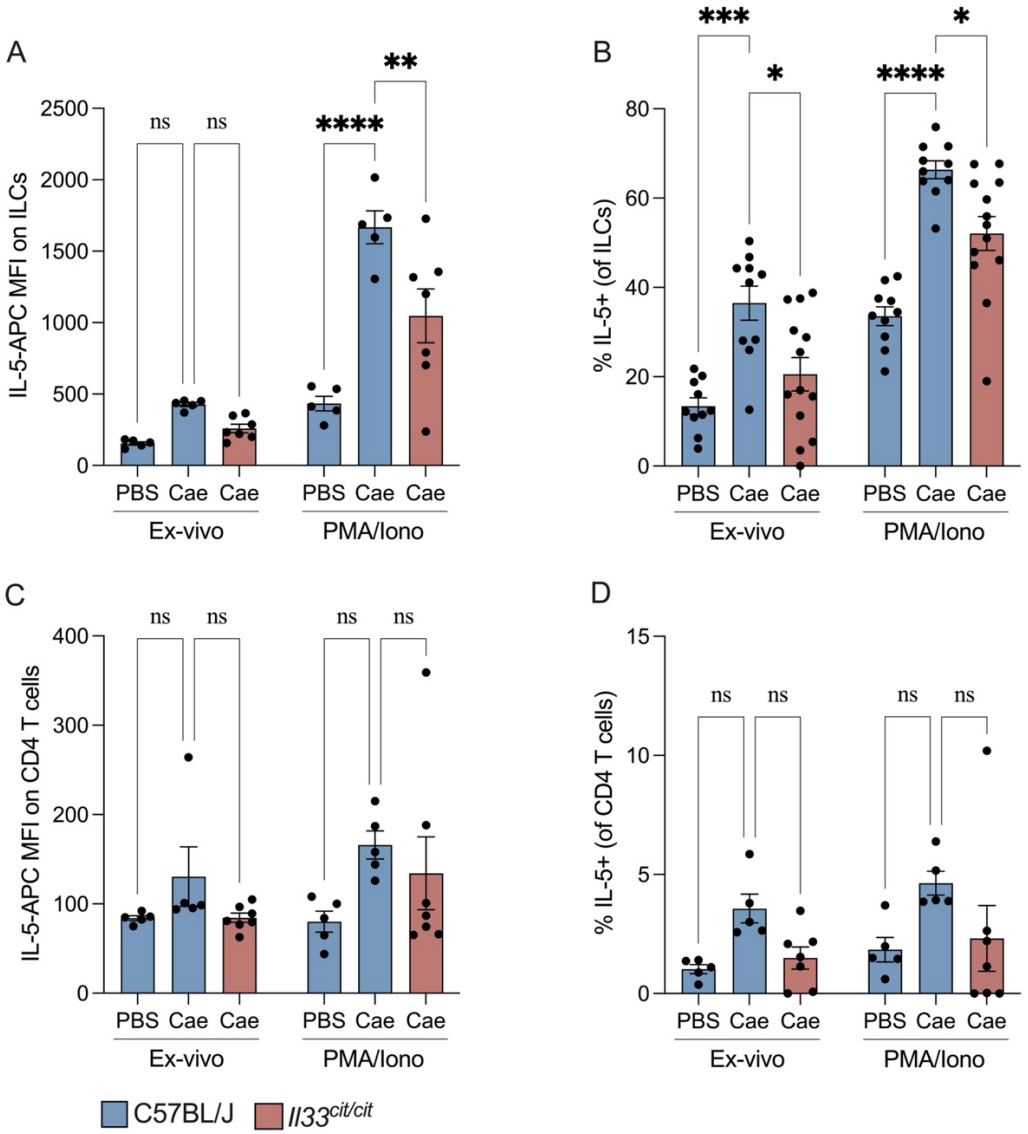

Figure 29 – ILC2s are activated in acute pancreatitis. C57BL/6 mice, Il33$^{cit/+}$ or Il33$^{cit/cit}$ were injected with 50ug/Kg of caerulein and sacrificed 6 hours after the first caerulein injection. Single cell suspension prepared from the pancreas were analysed using flow cytometry A, MFI of IL-5-APC on ILCs B, Quantification of IL-5+ pancreatic ILCs C, MFI IL-5-APC on CD4 T cells D, Quantification of IL-5+ CD4 T cells. Bar graphs indicate the mean (± s.e.m.) and show combined data from 1-2 independent experiments. Statistical significance was calculated using two-way ANOVA. ns=non-significant. *= P≤0.05, **= P≤0.01, ***= P≤0.001, ****=P≤0.0001.

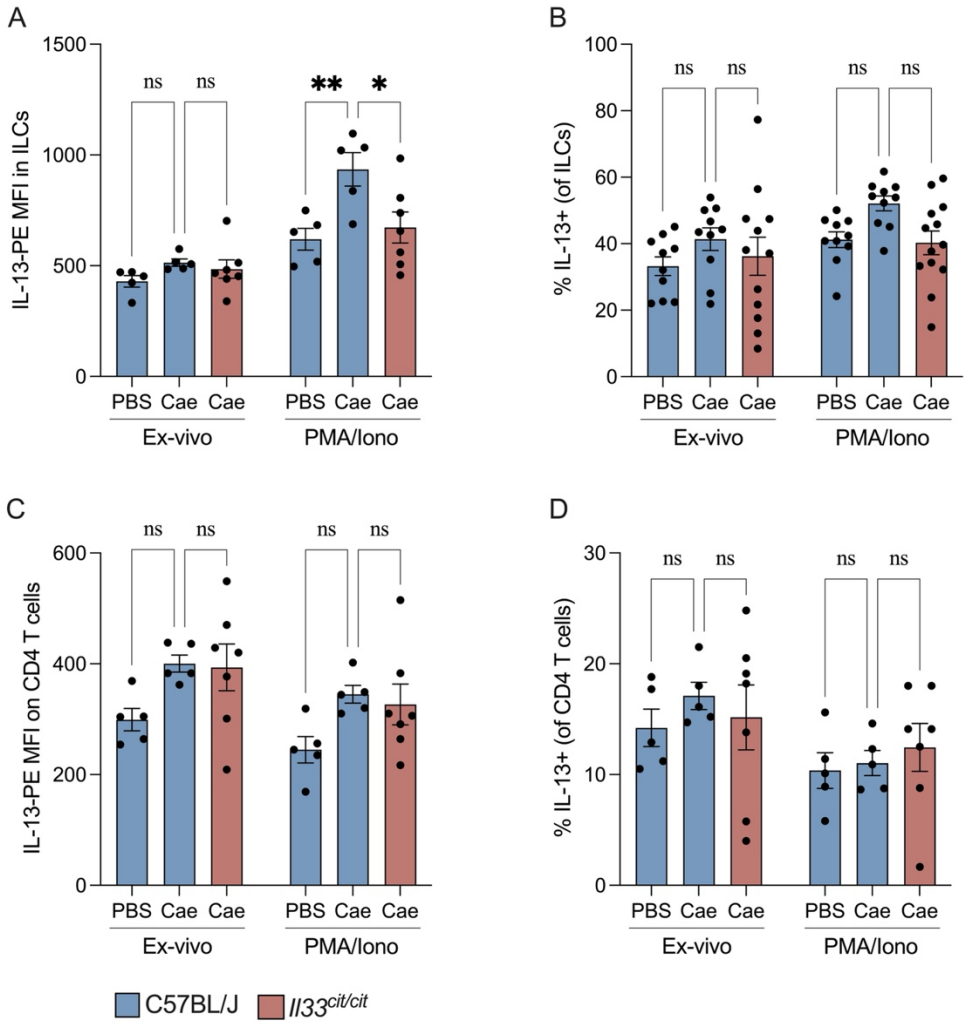

Figure 30 – IL-13 production by ILC2s in acute pancreatitis is IL-33 dependent. C57BL/6 mice, *Il33*$^{cit/+}$ *or Il33*$^{cit/cit}$ were injected with 50ug/Kg of caerulein and sacrificed 6 hours after the first caerulein injection. Single cell suspension prepared from the pancreas were analysed using flow cytometry. A, MFI of IL-13-PE on ILCs B, Quantification of IL-13+ pancreatic ILCs C, MFI IL-13-PE on CD4 T cells D, Quantification of IL-13+ CD4 T cells. Bar graphs indicate the mean (± s.e.m.) and show combined data from 1-2 independent experiments. Statistical significance was calculated using two-way ANOVA. ns=non-significant. *= P≤0.05, **= P≤0.01, ***= P≤0.001, ****=P≤0.0001.

Neutrophils may be involved in IL-33 processing

IL-33 is a nuclear cytokine that is chromatin associated. The nuclear version of IL-33 is a 270 amino acid (AA) long isoform (Lefrançais et al., 2012). Typically, upon cell death by necrosis, nuclear IL-33 is cleaved by proteases into smaller mature forms which can be up to 30 times more potent in activity compared to the full length (FL) version of IL-33 (Scott et al., 2018). FL IL-33 can be cleaved by neutrophil cathepsin G and elastase into the biologically active mature forms (Lefrançais et al., 2012). A massive influx of neutrophils is seen in acute pancreatitis at the 6h timepoint (fig 24A). Although this influx was not found to be ILC2 dependent (fig S20A) we asked if neutrophils (through cathepsin G and elastases) could be responsible for IL-33 processing into its highly potent mature forms.

To answer this question, we measured IL-5 and IL-13 production by ILCs as a proxy for IL-33 activity in in mice whose neutrophils were depleted using an anti-Ly6G antibody. Efficient neutrophil depletion using aLy6G antibody was confirmed in treated animals (figS21B). While an increase in IL-5 expression can be seen in control mice with pancreatitis as expected, no significant difference was seen in neutrophil depleted mice (fig 31A). However, IL-13 expression is significantly reduced in neutrophil depleted mice (fig 31B). This difference in phenotype between two cytokines produced by ILC2s at the same timepoint in acute pancreatitis could be attributed to a slight offset in peak of IL-5 and IL-13 production. A time course of IL-5 production in neutrophil depleted mice (4-8h timepoints) may be best suited for capturing neutrophil dependent IL-5 production by ILC2s. We looked at total CD45+ cell and eosinophil numbers which have been shown to be ILC2 dependent earlier in this chapter. No change was seen in neutrophil depleted mice with respect to total CD45+ and eosinophil numbers either (fig S21 A,C).

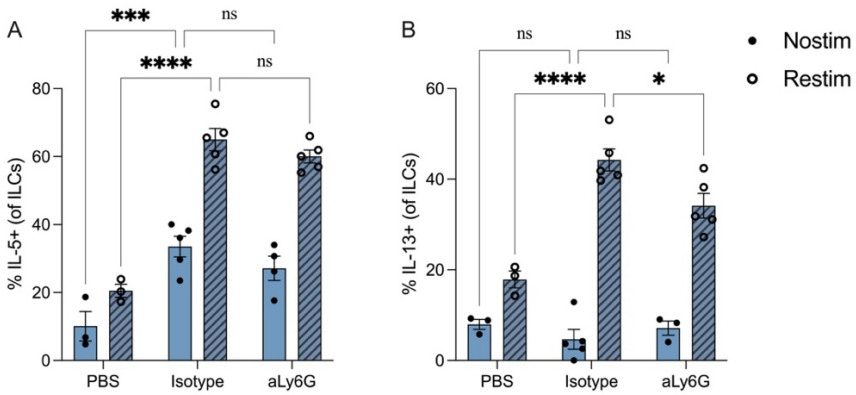

Figure 31 – Neutrophils possibly influence ILC2 activation in pancreatitis. C57BL/6 mice were treated with aLy6G (200ug) on day -1 and day 0. These mice were treated with 75ug/Kg Caerulein on day 0 and were sacrificed 24h after the first caerulein injection and ILC activation was quantified by flow cytometry. A, Quantification of IL-5+ pancreatitis ILCs B, Quantification of IL-13+ pancreatic ILCs. A,B, Bar graphs indicate the mean (± s.e.m.) and show data from one experiment. Statistical significance was calculated using one-way ANOVA. ns=non significant. *= P≤0.05, **= P≤0.01, ***= P≤0.001, ****=P≤0.0001.

These results suggest that neutrophils could be processing FL IL-33 into its highly bio-active form during pancreatitis. However, additional experiments are needed to confirm this observation. Western blots for IL-33 in neutrophil depleted mice compared to control mice would be helpful to understand the ratio of full length versus cleaved IL-33 in the presence and absence of neutrophils.

Eosinophilia in acute pancreatitis is IL-33 dependent

ILC2s are producing the eosinophil recruiting cytokine IL-5 in an IL-33 dependent and the eosinophilia in acute pancreatitis is ILC2 dependent (fig S20B, 28D, S17B). Considering these, we next asked if the eosinophilia we see in acute pancreatitis could be IL-33 dependent. We looked at eosinophilia in *Il33*$^{cit/cit}$ mice compared to C57BL/6 mice with pancreatitis. The

eosinophilia in acute pancreatitis was found to be IL-33 dependent 3 days after induction of pancreatitis (fig 32E). Interestingly, Treg expansion which was found to be ILC2 dependent in both the recombinant IL-33 model and pancreatitis was also found to be IL-33 dependent as well (fig 32C). Number of TH2 cells at this timepoint was also found to be IL-33 dependent (fig 32D). Total number of CD45+ cells, ILC2s and stromal cells however were not found to be IL-33 dependent (fig 32A,B,F). No difference was seen in number of CD4 T cells, CD8T cells, NK cells, B cells, neutrophils, macrophages, cDC1s, cDC2s, endothelial cells, acinar cells and ductal cells between C57BL/6 and *Il33*$^{cit/cit}$ mice with pancreatitis (fig S22). Although eosinophilia and Treg expansion were both IL-33 and ILC2 dependent, the same trend was not seen for necrosis and oedema in acute pancreatitis. In summary, the eosinophilia observed in acute pancreatitis is IL-33 dependent. Considering the IL-33 dependent production of the eosinophil recruiting cytokine IL-5 by ILC2s, this observation alludes to IL-33 activating ILC2s, followed by production of IL-5 and subsequent eosinophilia.

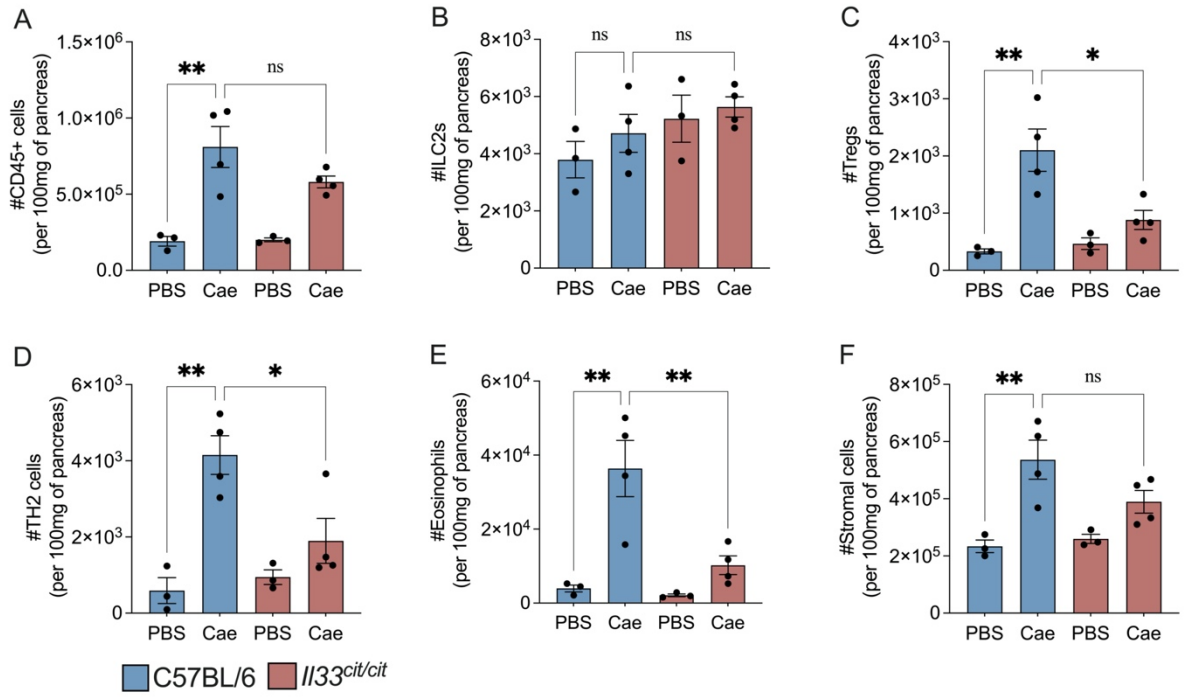

Figure 32 – Eosinophilia in acute pancreatitis recovery is IL-33 dependent. C57BL/6 mice or *Il33*$^{cit/cit}$ mice were injected with 50ug/Kg of caerulein on day 0 and day 1 and the mice were sacrificed 3 days after induction of pancreatitis. This was followed by quantification of immune cell numbers by flow cytometry. A-F, Bar graphs indicate the mean (± s.e.m.) and show data from one experiment. Statistical significance was calculated using one-way ANOVA. ns=non-significant. *= P≤0.05, **= P≤0.01, ***= P≤0.001, ****=P≤0.0001.

Stromal cells are the cellular source of IL-33

We next sought to identify the cellular source of IL-33 in acute pancreatitis. Acinar cells had previously been reported as the source of IL-33 in acute pancreatitis using immunohistochemistry (Watanabe et al., 2016). A recently published report indicates that adventitial stromal cells are major source of IL-33 in the lungs (Dahlgren et al., 2019). Myeloid

cells and particularly monocytes have also been described as a source of IL-33 (Nile et al., 2010). In order, to ascertain the source of IL-33 in the pancreas and during pancreatitis we used *Il33*$^{cit/+}$ mice which are reporters for IL-33 expression (Hardman et al., 2013). C57BL/6 mice were used as controls to set gate for citrine expression, and the expression of IL-33 was assessed in the endothelial, epithelial, immune and stromal compartments (fig 33A).

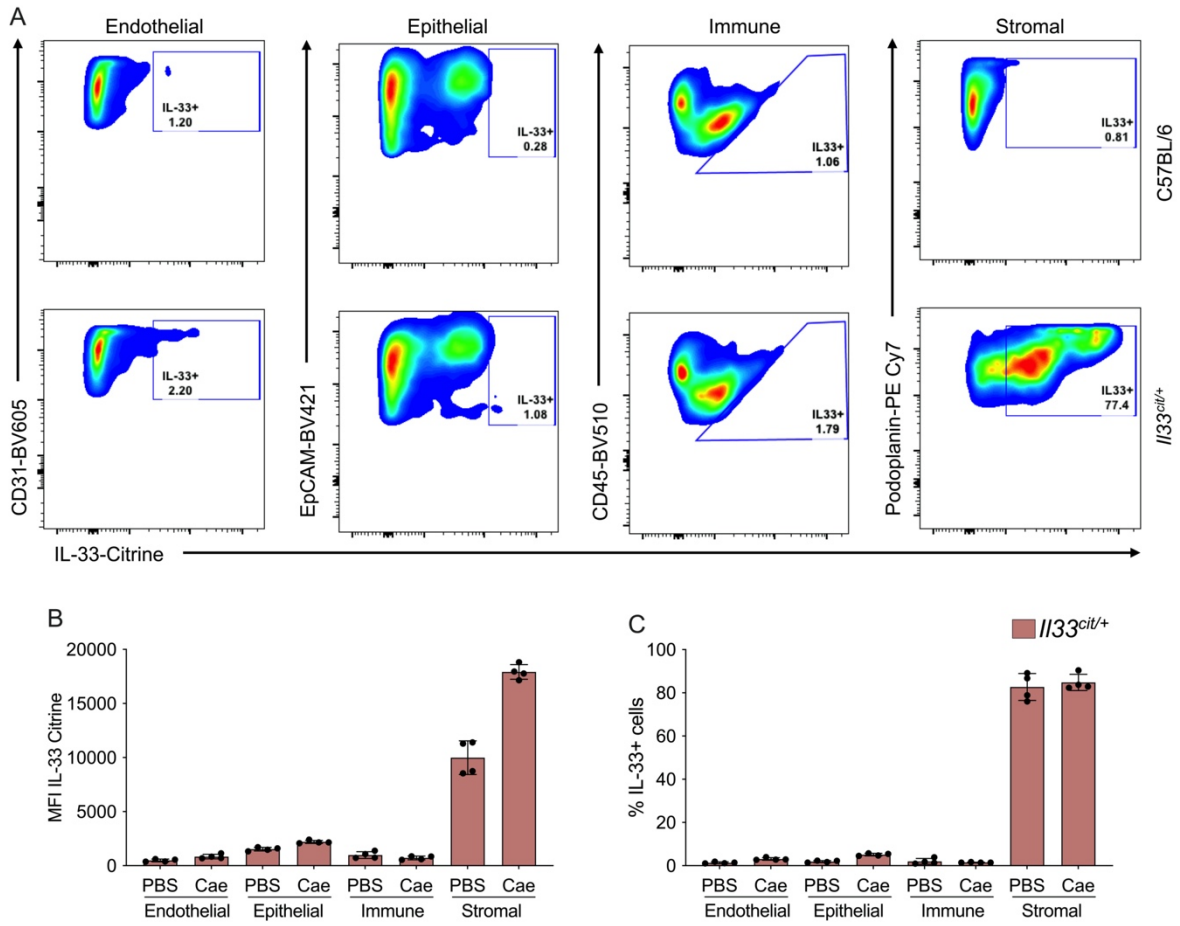

Figure 33 – Stromal cells are the largest IL-33 expressing population in the pancreas. *Il33*$^{cit/+}$ (IL-3reporter) mice were injected with PBS or 50ug/Kg of caerulein and sacrificed at 6h after the first caerulein injection. This was followed by quantification of IL-33-citrine expression in different cellular compartments by flow cytometry. A, Representative gating for IL-33-citrine expression on endothelial cells, stromal cells, epithelial cells and immune cells in C57BL/6 and *Il33*$^{cit/+}$ mice. B, C, Quantification of IL-33-citrine MFI (B) or % of IL-33+ cells (C) in endothelial, epithelial, immune and stromal compartments respectively with and either injected with PBS or caerulein. B,C, Bar graphs indicate the mean (± s.e.m.) and show data from one experiment.

The non-immune flow cytometry panel described in chapter 1 of the results section was used for this experiment. IL-33-citrine MFI and percentage of IL-33 expressing cells were found to be highest in stromal cells (fig 33B,D) in naïve animals and during pancreatitis. Expression of IL-33 was negligible in the endothelial, epithelial and immune compartments. As previously discussed, stromal cells decrease in number at the 6h timepoint in pancreatitis (fig S19D). As

this timepoint also coincides with IL-33 dependent activation of ILC2s, this alludes to necrosing stromal cells to be a likely source for released IL-33 in pancreatitis.

In summary, stromal cells were identified as the most likely source of IL-33 in the pancreas and during pancreatitis. This differs from earlier observations in the field that acinar cells are the cellular source of IL-33.

Eosinophilia in acute pancreatitis is stromal cell dependent

Having established stromal cells as a source of IL-33, we next asked if the IL-33 and ILC2 dependent eosinophilia, described earlier, could be stromal cell dependent. To address this question we used a stromal cell depleting mouse model from the Fearon lab (Roberts et al., 2013). Fibroblast activation protein (FAP) is a stromal cell marker. The Tg-FAP-DTR mice can be used to image FAP+ cells based on mCherry expression and also deplete FAP expressing cells using diphtheria toxin (DT) (Roberts et al., 2013). Stromal cell depletion was confirmed using flow cytometry (fig 34H). Stromal cell depletion is more prominent in the pancreatitis affected mice, compared to mice without pancreatitis. This could likely be due to increase in FAP expression on stromal cells in pancreatitis. Using this model, we found that eosinophilia was indeed stromal cell dependent as shown in fig 34E. A reduction in total immune cells (CD45+), monocytes, macrophages, CD4 T cells, NK cells and DCs was also seen in Tg-FAP-DTR mice compared to control mice (fig 34 A,F,G, fig S25 C,E,G). Number of ILC2s, Tregs, TH2 cells, B cells, neutrophils and cDC2 were however unchanged (fig 34 B,C,D, fig S25 F,I), whilst cDC1 numbers showed a significant increase in Tg-FAP-DTR mice compared to controls (fig S25H). No difference was seen in number of endothelial cells, epithelial cells and ductal cells between Tg-FAP-DTR mice and controls (fig S25J,KL) Interestingly, Tg-FAP-DTR mice showed a significant decrease in acinar cell numbers compared to control mice with pancreatitis, indicating greater depletion of acinar cells and hence greater damage (fig 34I).

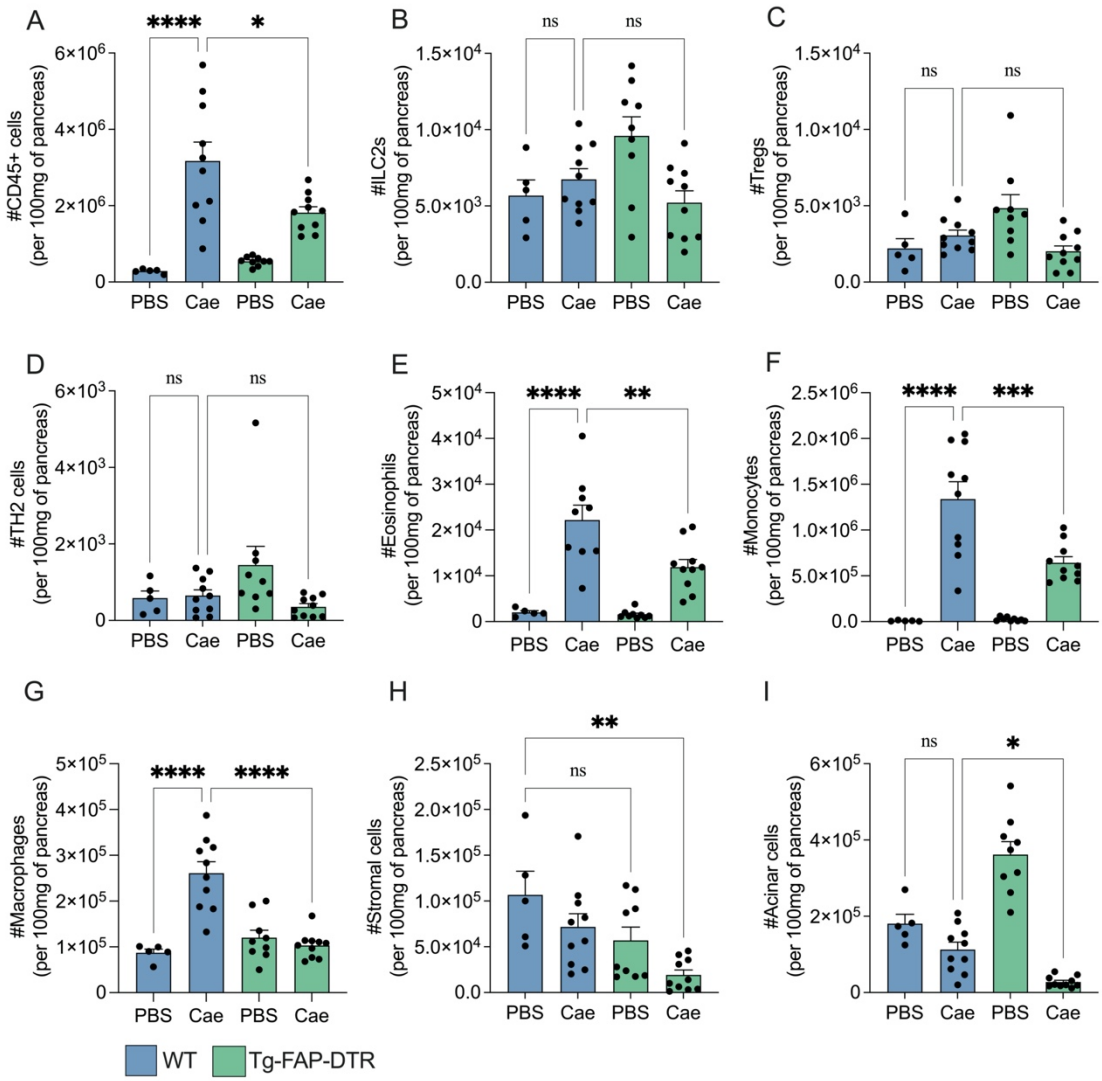

Figure 34 – Eosinophilia in acute pancreatitis is stromal cell dependent. Tg-FAP-DTR (stromal cell KO) mice were injected with 50ug/Kg of caerulein and sacrificed at 24h after first caerulein injection. This was followed by quantification of immune and stromal/epithelial cells in the pancreas by flow cytometry. A-I, Bar graphs indicate the mean (± s.e.m.) and show pooled data from two independent experiments. Statistical significance was calculated using one-way ANOVA. ns=non significant. *= P≤0.05, **= P≤0.01, ***= P≤0.001, ****=P≤0.0001.

In summary, using the Tg-FAP-DTR model we found the eosinophilia in acute pancreatitis is stromal cell dependent in acute pancreatitis. Stromal cells are a source of the monocyte recruiting cytokine CCL2 (Whelan et al., 2020) and this could explain the reduction in monocytes and macrophages observed in Tg-FAP-DTR mice.

Eosinophilia in acute pancreatitis is IL-5 dependent

Having established that eosinophilia in pancreatitis is ILC2, IL-33 and stromal cell dependent, and that ILC2s produce IL-5 in an IL-33 dependent fashion, we asked whether eosinophilia in acute pancreatitis is IL-5 dependent. We depleted IL-5 using a depleting antibody over a period of 9 days and looked at eosinophilia in pancreatitis in these mice. Similar to what has been described in literature in other tissues (Nussbaum et al., 2013), eosinophilia during

pancreatitis was found to be IL-5 dependent (fig 35D). IL-5 depleted mice also showed a significant increase in number CD45+ cells, monocytes, DCs and cDC2s compared to controls (fig 35 A,B,F,H). No difference was seen in number of neutrophils, macrophages and cDC1s (fig 35C, E,G).

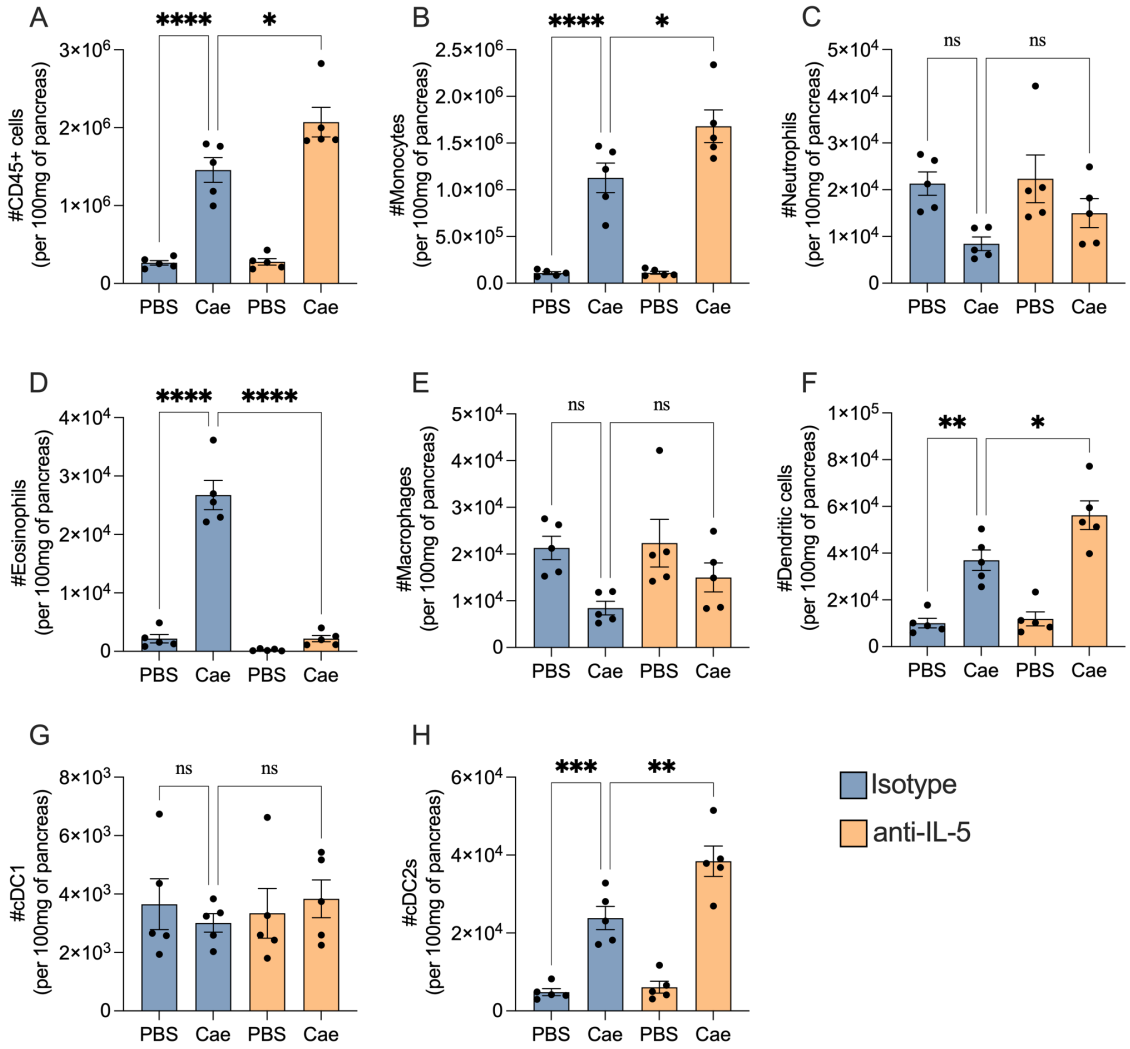

Figure 35 – Eosinophilia in acute pancreatitis is IL-5 dependent. C57BL/6 mice were treated with 100µg aIL-5 on day-9, day-4, day-1 and treated with 75ug/kg caerulein on day 0. Mice were sacrificed 24 hours after the first caerulein injection and immune cells numbers was quantified using flow cytometry. A-H, Bar graphs indicate the mean (± s.e.m.) and show pooled data from two independent experiments. A-H, Statistical significance was calculated using one-way ANOVA. ns=non-significant. *= P≤0.05, **= P≤0.01, ***= P≤0.001, ****=P≤0.0001.

In summary, we found that eosinophilia is ILC2, IL-33, stromal cells and IL-5 dependent in acute pancreatitis. The pathway we discovered so far has been illustrated in fig 36. In the following sections, we asked whether this eosinophilia could be regulating epithelial damage in acute pancreatitis. In the process we also asked whether other components of this eosinophilia pathway, namely IL-33, stromal cells and IL-5 could be regulating epithelial damage in acute pancreatitis.

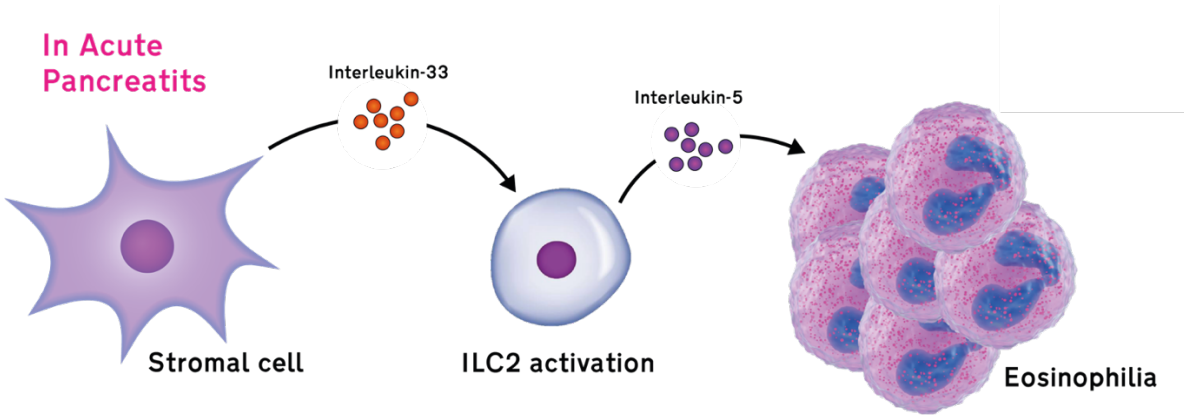

Figure 36 – Eosinophilia in acute pancreatitis is stromal cells, IL-33, ILC2 and IL-5 dependent. Through a series of experiments using genetically engineered and antibody-based depletion mouse models, we discovered a ILC2 dependent eosinophilia pathway active in acute pancreatitis. Stromal cells release IL-33 which activates ILC2s and promotes their production of IL-5. This IL-5 then recruits eosinophils in acute pancreatitis.

Eosinophils do not regulate epithelial damage in acute pancreatitis

The role of eosinophils in airway epithelial damage in allergic disease and asthma has been well documented. Eosinophils are capable of releasing highly charged basic proteins that are cytotoxic (McBrien & Menzies-Gow, 2017). Major basic protein (MBP), a granule component of eosinophils, has been shown to be cytotoxic to airway epithelial cells *in-vitro*. Post-mortem analysis of lung tissues from patients who have died from asthma has shown that MBP in associated with damaged epithelium (McBrien & Menzies-Gow, 2017). Eosinophil degranulation has been associated with epithelial injury in eosinophilic oesophagitis as well (Cheng et al., 2012). Considering the role that eosinophils have played in epithelial damage in other organs, we hypothesised that eosinophils could play a role in epithelial cell (acinar cell) damage in acute pancreatitis.

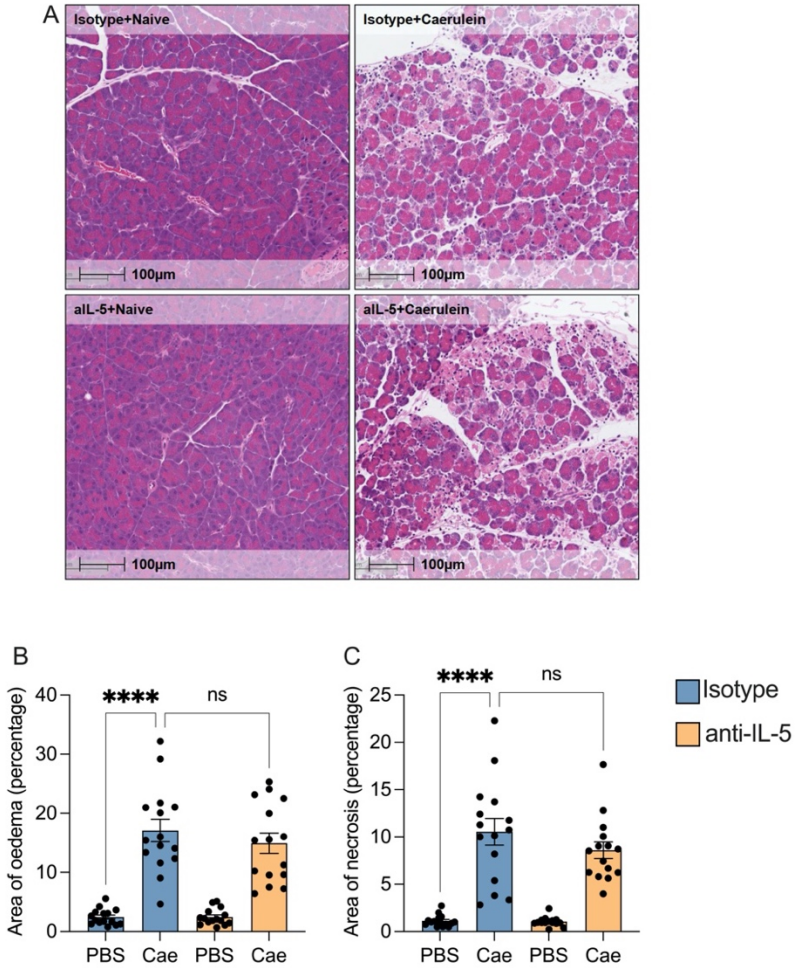

Figure 37 – Necrosis and oedema in acute pancreatitis is not IL-5 dependent. C57BL/6 mice were treated with 100µg aIL-5 on day-9, day-4, day-1 and treated with 75ug/kg caerulein on day 0. Mice were sacrificed 24 hours after the first caerulein injection. A, Pancreas was fixed, embedded, sectioned and stained with H&E and scanned images at 10X magnification are shown. B,C, Quantification of area of necrosis (B) and oedema (B) from images of H&E stained histological sections using the classifier function on the image analysis software Halo. Bar graphs indicate the mean (± s.e.m.) and show data from one experiment. Statistical significance was calculated using one-way ANOVA. ns=non-significant. *= P≤0.05, **= P≤0.01, ***= P≤0.001, ****=P≤0.0001.

As IL-5 blockade brings about near-complete depletion of eosinophils (fig 35D), this model as well as IL-5KO mice have often been used as a proxy for eosinophil depletion (Renninger et al., 2010). We looked at necrosis and oedema following pancreatitis in mice treated with anti-IL-5 (fig 37A). Surprisingly, we observed no difference in area of necrosis and oedema in anti-IL-5 treated mice compared to control animals (fig 37B,C). This suggests that eosinophils do not contribute to epithelial damage in acute pancreatitis.

To confirm this observation we used ΔdblGATA mice in which deletion of a high-affinity GATA-binding site (mediates auto-regulation of GATA-1 expression) in the GATA-1 promoter leads to selective loss of the eosinophil lineage (C. Yu et al., 2002). Lack of eosinophils was confirmed by flow cytometry (fig S26C). We further looked at oedema and necrosis in these mice (fig 38A) and observed no significant difference following pancreatitis in area of necrosis and oedema compared to controls (fig 38B,C).

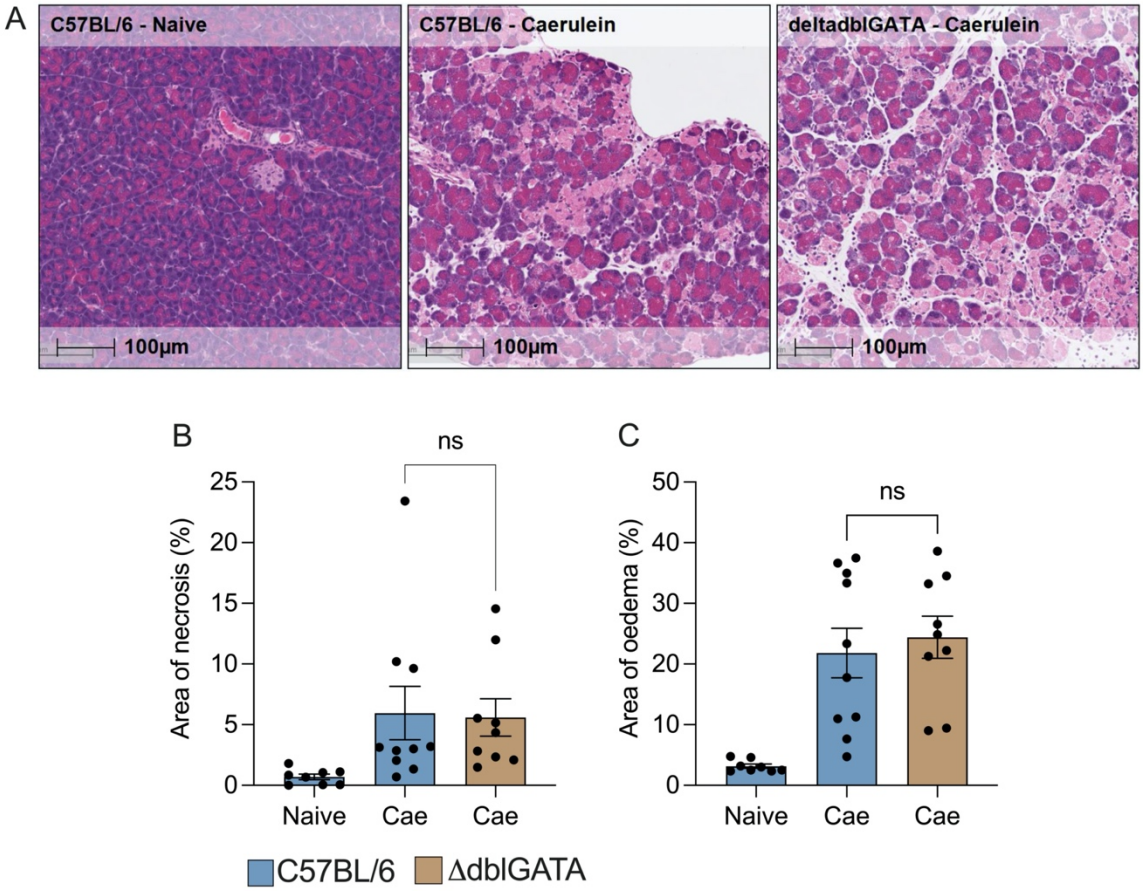

Figure 38 – Necrosis and oedema in acute pancreatitis are not eosinophil dependent. C57BL/6 mice or ΔdblGATA mice were injected with 75ug/Kg Caerulein and sacrificed 24 hours after the first caerulein injection. A, Pancreas was fixed, embedded, sectioned and stained with H&E and scanned images at 10X magnification have been shown B,C, Quantification of area of necrosis (B) and oedema (C) from images of H&E stained histological sections using the classifier function on the image analysis software, Halo. B,C, Bar graphs indicate the mean (± s.e.m.) and show pooled data from two experiments. B,C, Statistical significance was calculated using one-way ANOVA. ns=non-significant. *= P≤0.05, **= P≤0.01, ***= P≤0.001, ****=P≤0.0001.

In summary, using both the IL-5 blockade and ΔdblGATA mouse models of eosinophil depletion we confirmed that eosinophils do not play a role in regulating epithelial damage in acute pancreatitis. We additionally found that necrosis in acute pancreatitis is not IL-33 or stromal cell dependent either (fig S23 and S24). Although an ILC2 dependent eosinophilia pathway is active in acute pancreatitis, this pathway does not regulate epithelial damage in acute pancreatitis. We investigated further mechanisms by which ILC2s could be regulating epithelial damage in acute pancreatitis.

Neutrophils do not regulate epithelial damage in acute pancreatitis

We immunophenotyped the ΔdblGATA mice and a significant decrease in neutrophils was seen in ΔdblGATA mice compared to controls. Reduction in neutrophils in ΔdblGATA mice has been reported previously (Vieira et al., 2009), however as neutrophils are not completely ablated in this model, it is not possible to attribute any phenotype or lack thereof to neutrophils. The role that neutrophils could potentially have in acute pancreatitis has been explored later in this chapter. We additionally looked at immune changes in this model. We additionally confirmed that no change was seen in other myeloid immune cells in this model (fig S26A,D-H).

In order to address the role of granule compounds released by granulocytes particularly neutrophils, we attempted to block degranulation using a second generation, antihistamine, cetirizine (H. Zhang & Verkman, 2013). Anti-histamines are known to block degranulation by both neutrophils and eosinophils. To tease out the effect of cetirizine on each cell type individually, cetirizine was given at two different time points – 0h and 12h. As discussed earlier, neutrophils peak at the 6h timepoint and eosinophilia becomes prominent at the 24h timepoint. Accordingly, we hypothesised that the administration of cetirizine at the 0h timepoint would block both neutrophil and eosinophil degranulation while administration of cetirizine at the 12h timepoint would block only eosinophil degranulation, assuming neutrophils had already degranulated by then.

Interestingly, while no change was seen in oedema in cetirizine treated mice compared to controls (fig 39A,C), we observed a significant reduction in necrosis in mice that received cetirizine at the 0h timepoint (fig 39A,B). This effect however was not seen in mice that received cetirizine at the 12h timepoint (fig 39A,B). Although there is difference in phenotypes based on duration of cetirizine administration, granulocytes do seem to be playing a role in regulating epithelial damage in acute pancreatitis. According to our earlier hypothesis,

administration of cetirizine at the 0h timepoint should likely be able to block both neutrophil and eosinophil degranulation. However, as we have ruled out the role of eosinophils in regulating epithelial damage using two different mouse models already, we hypothesised that ILC2s could be regulating epithelial damage in acute pancreatitis by moderating neutrophil function

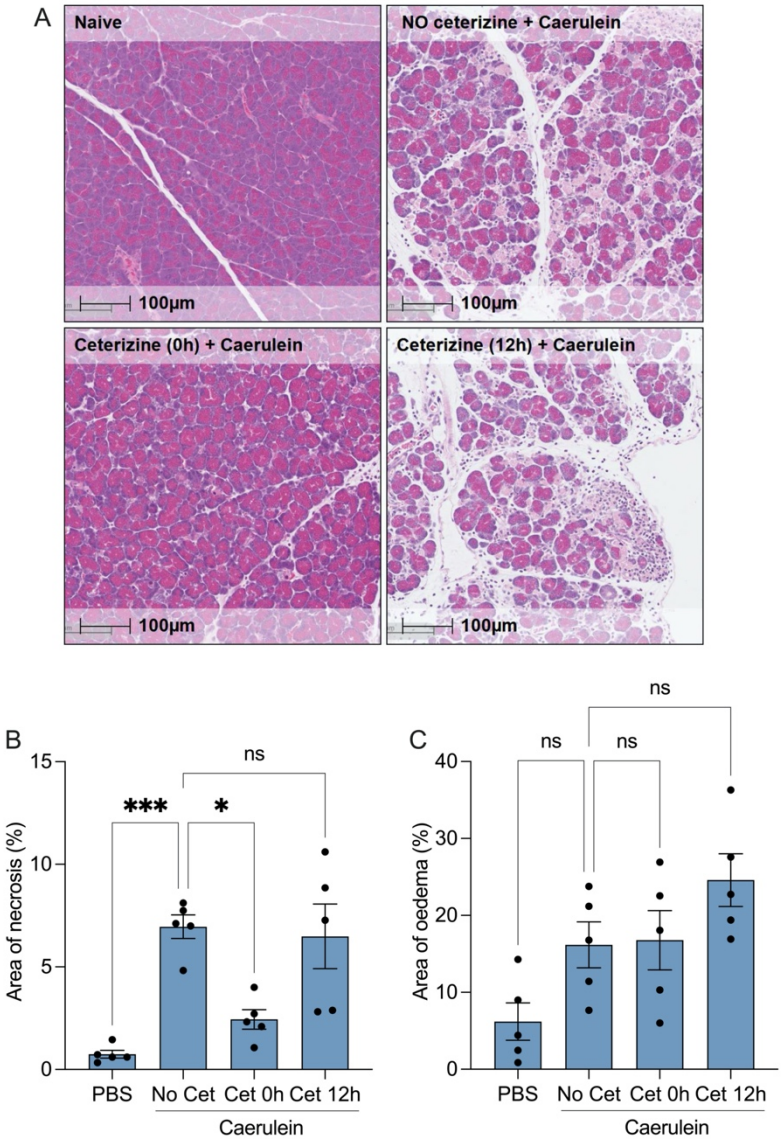

Figure 39 – Blocking degranulation leads to reduced necrosis during acute pancreatitis. C57BL/6 mice were treated with 25mg/Kg cetirizine to block degranulation at 0h and 12h timepoint. These mice were also treated with 75ug/Kg caerulein and sacrificed at 24h after the first caerulein injection. A, Pancreas was fixed, embedded, sectioned and stained with H&E and scanned images at 10X magnification are shown B,C, Quantification of area of necrosis (B) and oedema (C) from images of H&E stained histological sections using the classifier function on the image analysis software Halo. Bar graphs indicate the mean (± s.e.m.) and show data from one experiment. Statistical significance was calculated using one-way ANOVA. ns=non-significant. *= P≤0.05, **= P≤0.01, ***= P≤0.001, ****=P≤0.0001.

As reported earlier in this chapter, neutrophil numbers were not affected in mice lacking ILC2s (fig 20A). Thus, we asked if ILC2s could be regulating neutrophil function whilst not affecting

their numbers. Neutrophil extracellular trap (NET) formation is a function of neutrophils capable of causing tissue damage (Papayannopoulos, 2018). NETs are cytosolic and granular protein containing web of decondensed chromatin released by neutrophils. Typically, NETs are used to trap parasite, bacteria, viruses and fungi and neutralise them. NET associated lung injury has been well documented (Papayannopoulos, 2018).

The role of NETs in tissue damage has also been described in acute pancreatitis. Significant NET deposits were found in inflamed pancreas using the Taurocholate model of acute pancreatitis at 6 and 24 hours. Both administration of DNAse I and depletion of neutrophils using anti-Ly6G antibody led to reduction in NETs in this model. Interestingly, inhibition of NET formation coincided with reduced oedema and inflammation (Merza et al., 2015). It was also shown that incubation of acinar cells *in vitro* with NETs increased trypsin activation by these acinar cells (Merza et al., 2015). In order to study if ILC2s could be regulating NET formation in acute pancreatitis, we quantified Net formation using a imaging flow cytometer (Zhao et al., 2015).

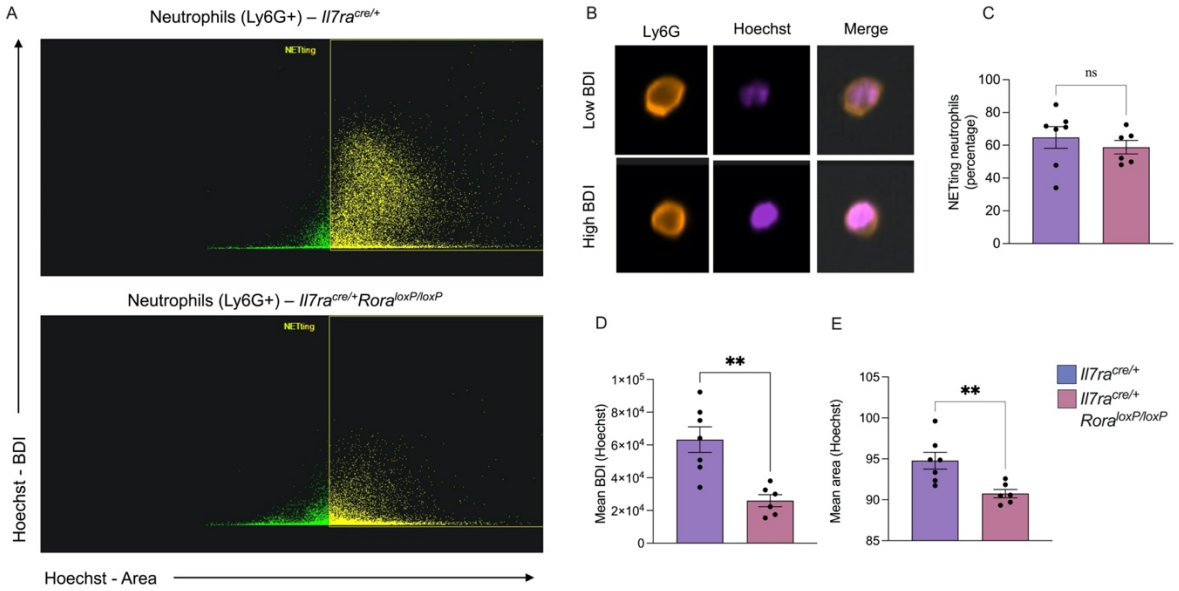

Figure 40 – Neutrophils from ILC2KO mice with pancreatitis show changes in NETting. *Il7ra*$^{cre/+}$ (control) or *Il7ra*$^{cre/+}$ *Rora*$^{loxP/loxP}$ (ILC2KO) mice were injected with PBS or 75ug/Kg of caerulein and sacrificed 6 hours after the first caerulein injection A, Representative gating on the Image stream and NETting neutrophils were identified based on images of NETing cells on larger nuclear area as shown in (B). B, Representative images of neutrophils with low and high hoechst-BDI. C, Quantification of percentage of NETting neutrophils. D,E, Quantification of mean Hoechst-BDI and Hoechst area. C-E, Bar graphs indicate the mean (± s.e.m.) and shows data from one experiment. C-E, Statistical significance was calculated using unpaired T-test. ns=non significant. *= P≤0.05, **= P≤0.01, ***= P≤0.001, ****=P≤0.0001.

Neutrophils were gated based on their expression of Ly6G, and Hoechst staining was used to identify nuclear content. Nuclear area (based on the area of Hoechst staining) and the bright detail intensity (BDI) feature were used to capture the extent of NET formation by neutrophils.

BDI is a feature available on the Image stream software IDEAS that can calculate the intensity of localised bright spots (Barbu et al., 2021). The BDI_R7 feature identifies normal nuclei as having bright high intensity spots of 7 pixels in size or less (Zhao et al., 2015). These bright high intensity spots are a result of condensed chromatin. In NETting neutrophils, these spots become less intense, more spread out, and an increase in area of the nuclear content can also be seen. Typically, NETting nuclei show reduction in BDI and increase in nuclear area (Zhao et al., 2015).

As the influx of neutrophils is highest at the 6h timepoint, we looked at NETting potential of neutrophils in control (*Il7ra*$^{cre/+}$) and ILC2 deficient mice (*Il7ra*$^{cre/+}$*Rora*$^{loxP/loxP}$). The gating for NETting neutrophils has been shown in fig 39A. While NETting neutrophils in literature have been identified as having low BDI, in this experiment, we noticed that neutrophils with high Hoechst BDI and high Hoechst area could be seen NETting (fig 39B). Although BDI did not follow the same trend as seen in literature, NETting neutrophils were gated for based on images and high Hoechst area. No difference in percentage of NETting neutrophils was seen between ILC2 deficient mice and control animals (fig 39C). However, neutrophils from ILC2 deficient mice showed significantly lower Hoechst BDI and Hoechst area compared to control animals (fig 39D,E). While we observed no difference in quantity of NETing neutrophils, we found a difference in quality of NETting between ILC2 deficient mice and control animals. Whether neutrophils could regulate epithelial damage in this experimental setup, timepoint and model needed to be validated using a neutrophil depletion model. We also observed that whilst NETting neutrophils in literature showed a reduction in BDI and increase in nuclear area compared to controls (Zhao et al., 2015), in our experiments NETting neutrophils show increased BDI and increased nuclear area. Our gating of NETting neutrophils has been setup based on individual images of cells on the scatter plots in fig 39A. This difference in BDI of NETting neutrophils in literature compared to our experimental setup requires technical expertise to interpret.

We next assessed the role of neutrophils in epithelial damage and pancreatitis severity using a neutrophils depletion model. Neutrophil depletion using aLy6G and aGR1 has been confirmed in fig S27B. Neutrophils depletion did not affect severity of pancreatitis in our setting at the 24h timepoint (fig 42A) and no difference could be seen in area of oedema and necrosis between neutrophil depleted mice and isotype treated control mice (fig 42B,C). Thus, although a difference in quality of NETting neutrophils was evidenced in ILC2 deficient mice, neutrophil depletion did not produce the protection that should have been seen if neutrophils were indeed regulating epithelial damage in acute pancreatitis. The discrepancy in the outcome of neutrophil depletion experiments between the literature and the experiments conducted in our

setting could be due to difference in pancreatitis models. While pancreatic duct ligation (Merza et al., 2015) and L-arginine (Murthy et al., 2019) have been used in literature when looking at neutrophils in acute pancreatitis, our setting uses caerulein induced pancreatitis. This observation confirmed that neutrophils were not regulating epithelial damage in acute pancreatitis.

The adaptive immune compartment may play a role in regulating epithelial damage in acute pancreatitis

Having eliminated eosinophils and neutrophils as the downstream mechanism through which ILC2s could be regulating epithelial damage in acute pancreatitis, we conducted a series of experiments to tease out this elusive mechanism. In nude mice lacking thymus and hence unable to generate mature T cells, caerulein-induced pancreatitis severity was found to be reduced and this severity could be restored by adoptive transfer of T-lymphocytes (Demols et al., 2000). Another report using *Rag1*$^{-/-}$ mice lacking T and B cells, showed that regeneration following pancreatitis was impaired and persistent and unresolved ADM was seen (Folias et al., 2014).

We thus asked if the adaptive immune compartment could be playing a role in regulating epithelial damage in acute pancreatitis in experimental setting. To this end we used *Rag1*$^{-/-}$ mice lacking T and B cells, *μMT*$^{KO/KO}$ mice lacking mature B cells and *Rag1*$^{-/-}$ *Il7ra*$^{cre/+}$*Rora*$^{loxP/loxP}$ lacking T cells, B cells and ILCs (fig 41A). Following pancreatitis, we found that *Rag1*$^{-/-}$, *μMT*$^{KO/KO}$ and *Rag1*$^{-/-}$ *Il7ra*$^{cre/+}$*Rora*$^{loxP/loxP}$ mice showed a reduction in area of necrosis compared to control mice (fig 41B). A reduction in area of oedema was seen in *Rag1*$^{-/-}$ and *Rag1*$^{-/-}$ *Il7ra*$^{cre/+}$*Rora*$^{loxP/loxP}$ mice compared to controls whilst it was not the case in *μMT*$^{KO/KO}$ mice (fig 41C). Taken together these data demonstrate that the adaptive immune compartment promotes epithelial injury in acute pancreatitis.

We further performed depletion of selected immune populations in wild-type mice using well established depletion antibodies. CD4 and CD8 T cells were depleted using anti-CD4 and anti-CD8 depleting antibodies (depletion confirmed in fig 42A). We saw no difference in area of oedema or necrosis (fig 42B,C) in treated mice compared to isotype treated control animals.

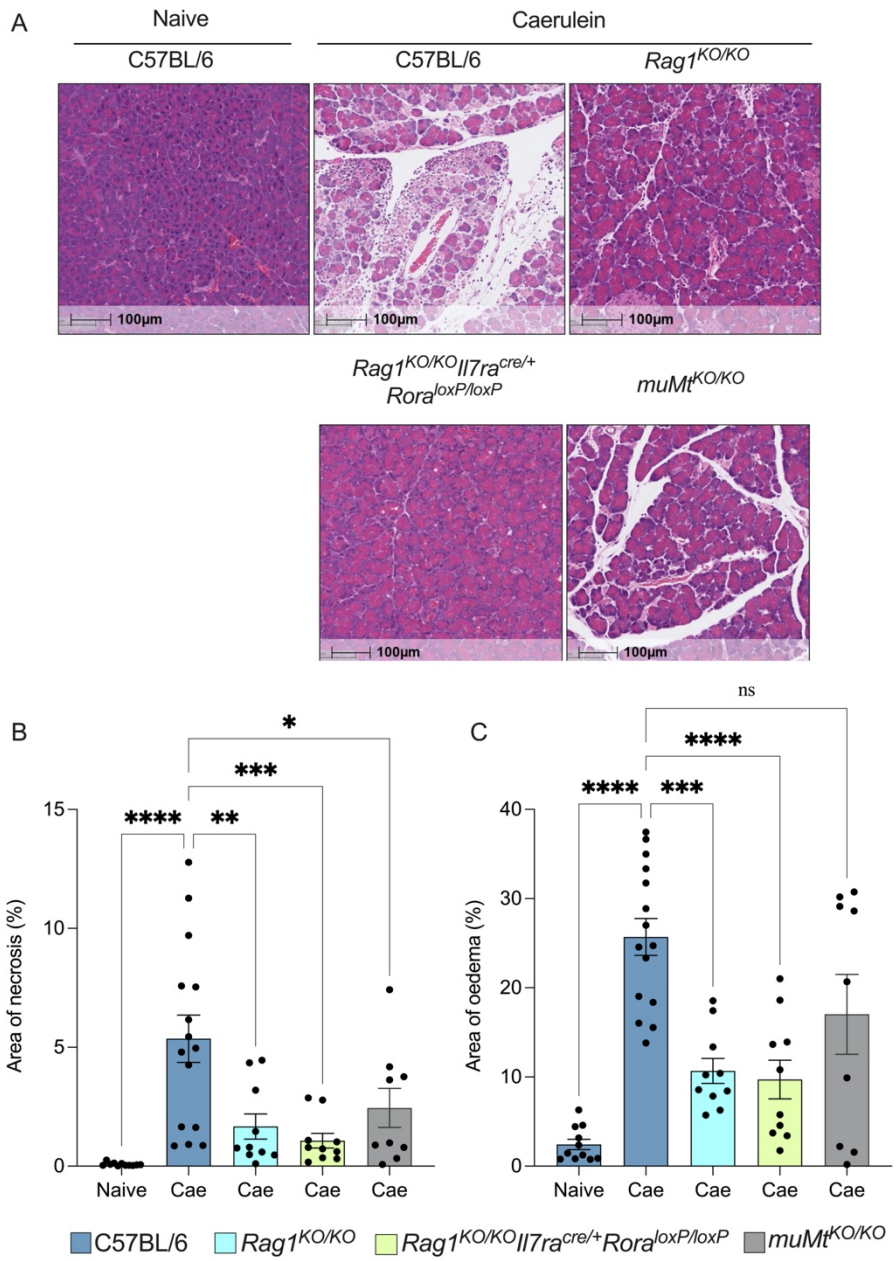

Figure 41 – The adaptive immune compartment plays a role in acute pancreatitis. C57Bl/6 mice, *Rag1*$^{Ko/KO}$, *Rag1*$^{Ko/KO}$*Il7ra*$^{cre/+}$*Rora*$^{loxP/loxP}$ *or muMT*$^{KO/KO}$ mice were injected with 75ug/Kg caerulein and sacrificed 24h after the first caerulein injection. A, Pancreas was fixed, embedded, sectioned and stained with H&E and scanned images at 10X magnification are shown B,C, Quantification of area of necrosis (B) and oedema (C) respectively from images of H&E stained histological sections using the classifier function on the image analysis software Halo. Bar graphs indicate the mean (± s.e.m.) and shows data pooled from two independent experiments. Statistical significance was calculated using one-way ANOVA. ns=non-significant. *= P≤0.05, **= P≤0.01, ***= P≤0.001, ****=P≤0.0001.

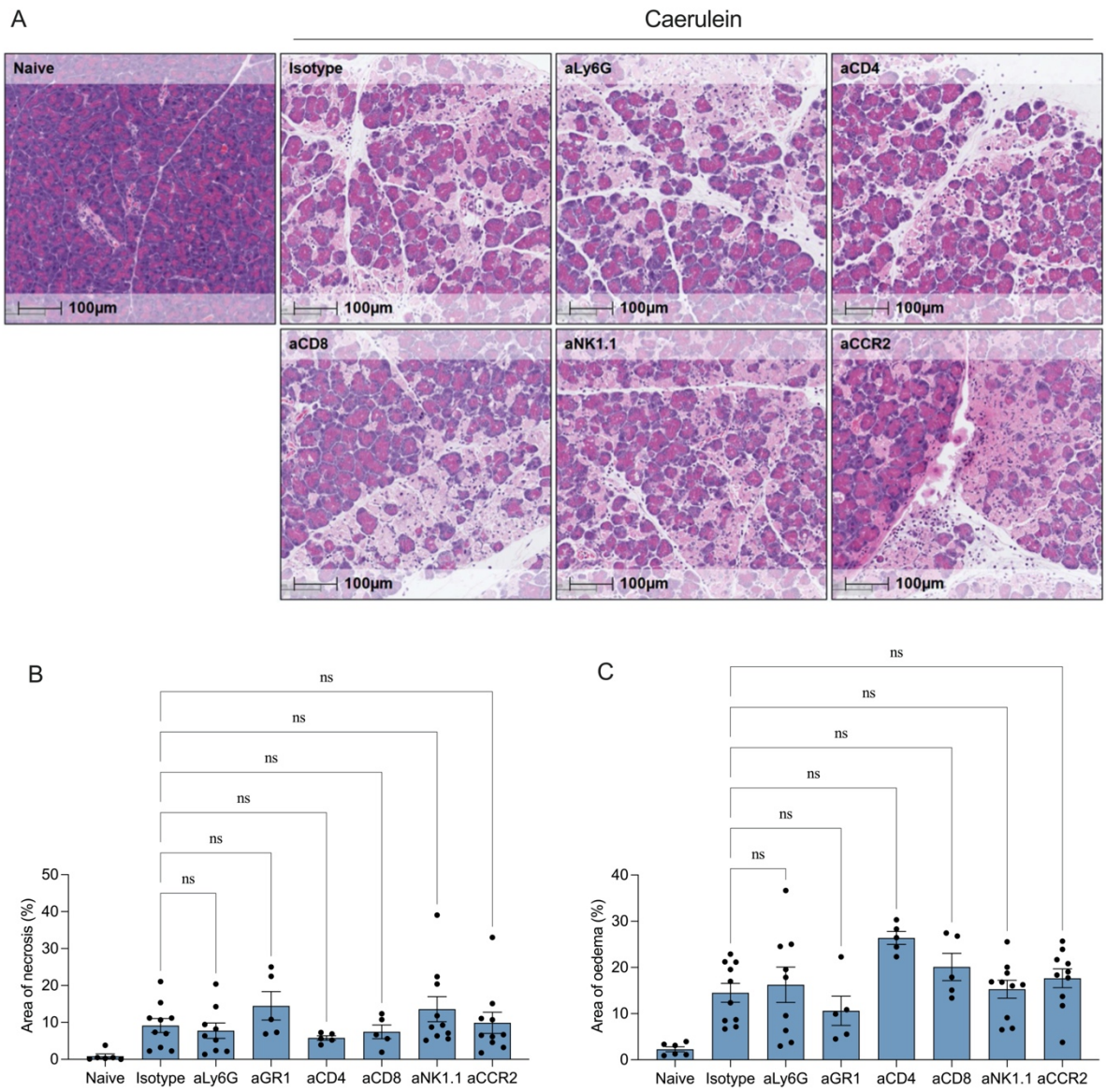

Figure 42 – NK cells, monocytes, neutrophils, CD4 T cells and CD8 T cells don't play a role in acute pancreatitis. C57BL/6 mice were treated i.p. with aNK1.1 (50ug), aCCR2 (20ug), aGR1 (200ug), aLy6G (200ug), aCD4 (100ug) or aCD8 (200ug) on day -1 and day 0, and further received 75ug/Kg Caerulein on day 0. Mice were sacrificed 24h after the first caerulein injection. A, Pancreas was fixed, embedded, sectioned and stained with H&E and scanned images at 10X magnification are shown B,C, Quantification of area of necrosis (B) and oedema (C) from images of H&E stained histological sections using the classifier function on the image analysis software Halo. Bar graphs indicate the mean (± s.e.m.). Naïve, Isotype, aNK1.1, aCCR2 and aLy6G groups show data pooled from two experiments. aGR1, aCD4 and aCD8 groups show data from one experiment. Statistical significance was calculated using one-way ANOVA. ns=non-significant. *= P≤0.05, **= P≤0.01, ***= P≤0.001, ****=P≤0.0001.

Thus, the phenotype seen in *Rag*$^{-/-}$ mice could not be attributed to CD4 or CD8 T cells. Therefore, considering the similarity between the phenotype of *Rag*$^{-/-}$ mice and μMT$^{KO/KO}$ mice, it appears that B cells could be responsible for promoting epithelial damage in acute pancreatitis. B cell production of IgA (through which clearance of H. pylori infection was mediated in the stomach) was found to be regulated by ILC2s through IL-5 (Satoh-Takayama et al., 2020). However, as IL-5 depletion has not shown protection in acute pancreatitis earlier in this chapter (fig 37), it is unlikely that ILC2s are regulating B cell function via IL-5. In

summary, the mechanism by which ILC2s could be regulating B cells and the mechanism by which B cells could be promoting epithelial damage are unknown. It is also worth noting that at the 24h timepoint where we see the disease promotion by ILC2s, B cell numbers are not ILC2 dependent (fig 27C). Thus, whether ILC2s could be regulating B cell function at this timepoint is left to be determined. These questions could unfortunately not be addressed within the remits of this thesis.

NK cells and monocytes do not promote epithelial damage in acute pancreatitis

We also addressed the possibility of NK cells and monocytes regulating epithelial damage in acute pancreatitis in an ILC2 dependent manner. While NK cell numbers were not ILC2 dependent at the 24h timepoint (fig 27G), ILC2s have been shown to regulate NK cell production of IFNγ (Schuijs et al., 2020). Interestingly, monocyte numbers at the 24h timepoint are ILC2 dependent (fig 28A) and *Ccl2*$^{-/-}$ mice lacking monocytes have been shown to display reduced pancreatitis severity (Saeki et al., 2012). To check the involvement of NK cells and monocytes in promoting epithelial damage in acute pancreatitis, we treated mice with aNK1.1 and aCCR2 antibodies followed by pancreatitis induction. Depletion of these cells has been confirmed by flow cytometry in fig S29A and S31. However, NK cell and monocyte depleted mice did not show any difference in area of necrosis or oedema compared to isotype antibody treated control mice (fig 42). Other immune cells that could be affected as collateral for any of the immune cell depletions have been shown in fig S27 and fig S28.

In summary, through a series of immune cell deficient mouse experiment we learnt that NK cells, monocytes, CD4 T cells and CD8 T cells did not promote epithelial damage in caerulein induced pancreatitis. We also found that B cells could be playing a role in promoting necrosis in acute pancreatitis. However, their regulation by ILC2s and the mechanism downstream of B cell induced epithelial damage could not be determined.

IL-13 does not promote epithelial damage in acute pancreatitis

The last mechanism to be considered from the perspective of this thesis with respect to epithelial damage is the role IL-13 produced by ILC2s in acute pancreatitis (fig 30B). IL-13 activated alternatively activated macrophage (AAM) have been shown to play a role in fibrosis in chronic pancreatitis (Xue et al., 2015). In the early pro-inflammatory phases of acute pancreatitis characterised histologically by tissue damage, M1 macrophages were found to be dominant. However, in later stages of regeneration, M2 or AAMs were found to be more

dominant. Depletion of macrophages right after the early inflammatory phase (day 1 and 2) led to reduction of ADM on day 3, suggesting a role for macrophages in promoting of ADM. However, depletion of macrophages later on after ADM formation delayed regeneration of the pancreas (Wu et al., 2020). IL-13 signals via a receptor formed by a heterodimer of IL-13Ra and IL-4Ra. Activation of macrophages to an alternative or more M2 like phenotype was found to be IL-4Ra dependent (Wu et al., 2020). Although the role for IL-13 or IL-13 activated M2 macrophages have been described in pancreatitis recovery, we asked if IL-13 could be playing a role in epithelial damage. To this end we used *Il13*$^{tom/tom}$ mice lacking IL-13 production.

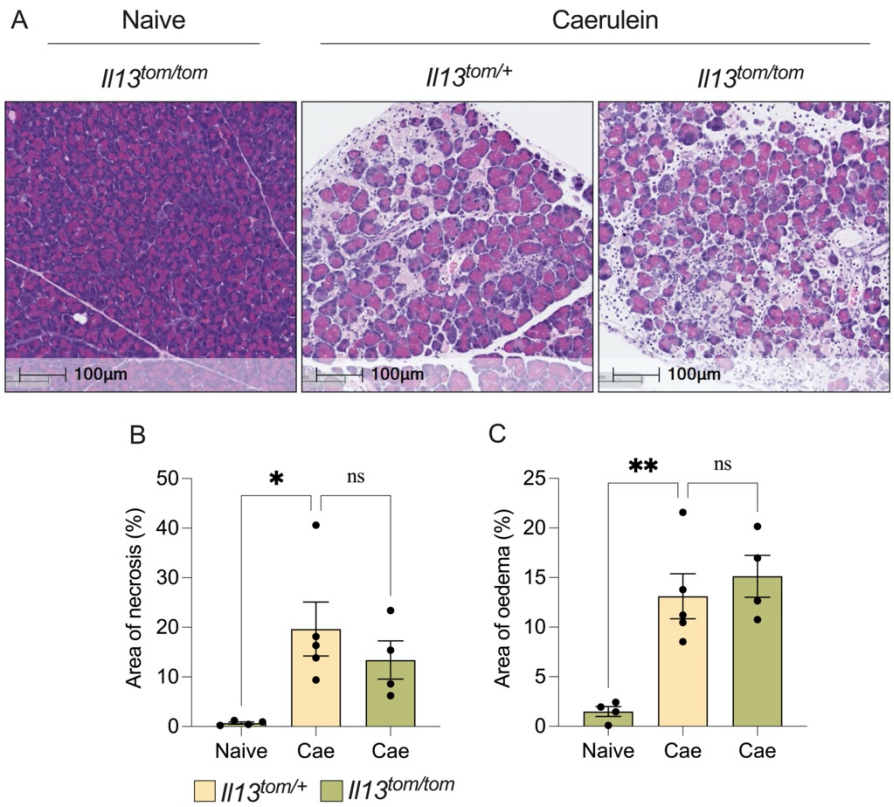

Figure 43 – IL-13 does not affect necrosis and oedema in acute pancreatitis. C57BL/6 or *Il13*$^{tom/tom}$ were injected with 75ug/Kg caerulein and sacrificed 24 hours after the first caerulein injection. A, Pancreas was fixed, embedded, sectioned and stained with H&E and scanned images at 10X magnification are shown. B,C, Quantification of area of necrosis (B) and oedema (C) respectively from images of H&E stained histological sections using the classifier function on the image analysis software Halo. Bar graphs indicate the mean (± s.e.m.) and show data from one experiment. Statistical significance was calculated using one-way ANOVA. ns=non significant. *= P≤0.05, **= P≤0.01, ***= P≤0.001, ****=P≤0.0001.

Our results did not show any significant difference in area of necrosis or oedema compared to controls following pancreatitis in IL-13 deficient animals (fig 43A-C). We also looked at immune influx at the 24h timepoint. Number of NK cells were found to be higher (fig S32B) in IL-13 deficient mice with pancreatitis compared to controls. As NK cells don't express IL-13Ra or IL-4Ra, is likely to be an indirect effect of IL-13 deficiency rather than direct IL-13 mediated regulation of NK cells. No difference was seen in number of CD45+ cells, neutrophils, cDC1s, cDC2s, monocytes and stromal cells. (fig S30 A,C-H). IL-13 has previously been shown to

induce cycling of rat αSMA+ pancreatic stellate cells (Shinozaki et al., 2010). However, we did not observe an IL-13 dependent increase in Ki67+ stromal cells during epithelial damage in-vivo in pancreatitis (fig S30I). IL-13 did not influence any other immune cell changes in the adaptive immune compartment at this timepoint either (fig S31).

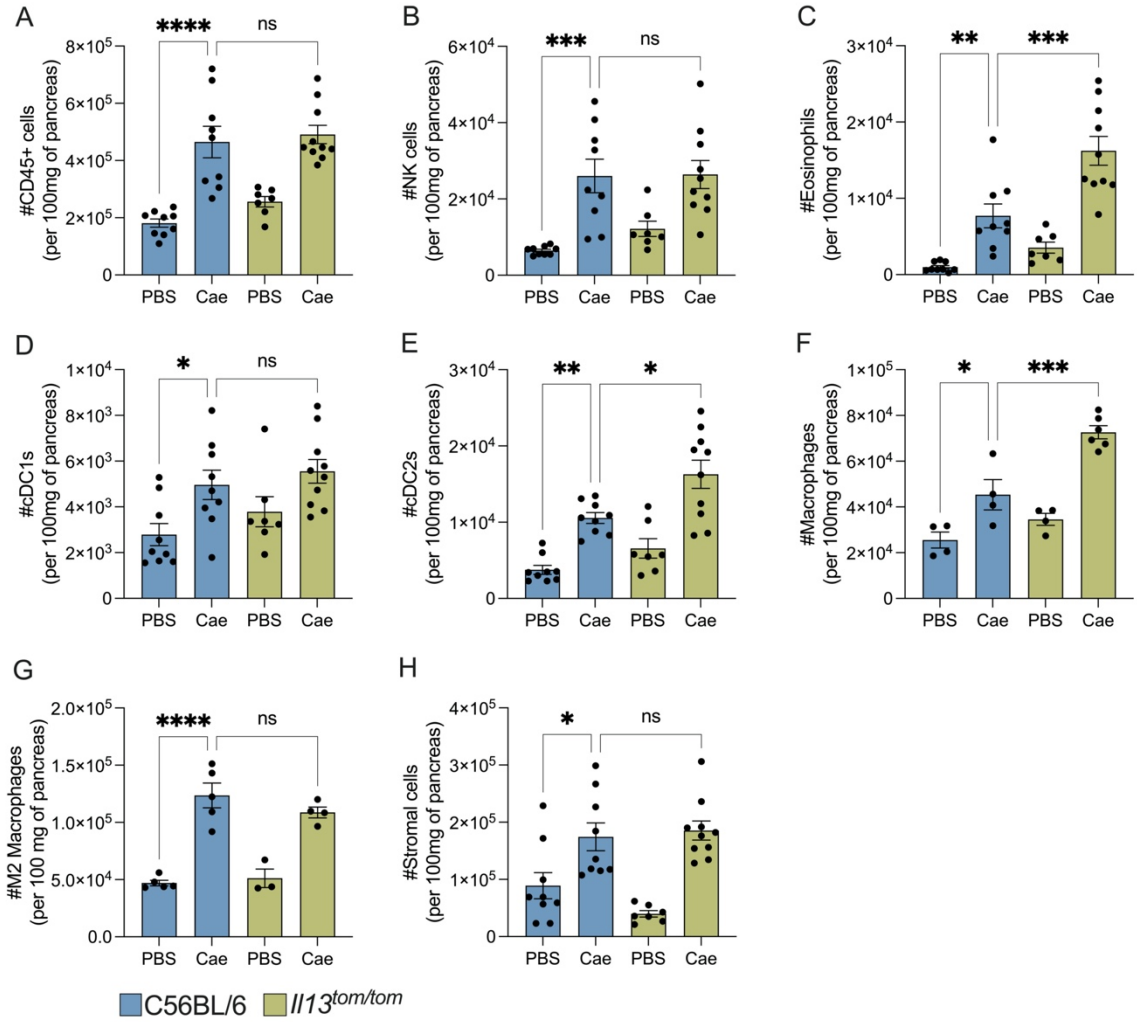

Figure 44 – IL-13 influences eosinophils and dendritic cells in pancreatitis recovery. C57BL/6 or *Il13*$^{tom/tom}$ (IL-13 KO mice) were injected with 50ug/Kg caerulein and mice on day 0 and day 1 then sacrificed day7. This was followed by quantification of immune cells numbers using flow cytometry. A-E,H, Bar graphs indicate the mean (± s.e.m.) and shows data pooled from two independent experiments. F,G, Bar graphs indicate the mean (± s.e.m.) and show data from one experiment. Statistical significance was calculated using one-way ANOVA. ns=non-significant. *= P≤0.05, **= P≤0.01, ***= P≤0.001, ****=P≤0.0001.

In order to look the role of IL-13 in regulating M2 macrophages, we looked at immune change at the 1-week timepoint during pancreatitis recovery. Although IL-13 has been shown to regulate M2 macrophages in acute pancreatitis (Wu et al., 2020), number of M2 macrophages as defined by RelMα expression was not found to be IL-13 dependent in this model (fig 44G). Number of total macrophages was found to be IL-13 dependent however (fig 44F). IL-13 was shown to be regulating number of eosinophils, total DCs and cDC2s (fig 44C,D,E). Interestingly early phases of eosinophilia in acute pancreatitis from 24h to 3 days seem to IL-

5 dependent, but in later stages such as 1 week, IL-13 also seems to be playing a role in regulating eosinophilia. In line with the DC observation, IL-13 has been shown to regulate DC function previously in the lungs as well (Leyva-Castillo et al., 2021). During recovery, IL-13 dependency was not noticed in number of CD45+ cells, NK cells or stromal cells either (fig 44A,B,H). Other immune cells numbers were not found to be IL-13 dependent (fig S32).

In summary, while IL-13 did not play a role in promoting oedema or necrosis in acute pancreatitis, we found that it was exerting some inflammatory changes in acute pancreatitis. Interestingly, those changes that were expected based on literature like number of M2 macrophages or cycling stromal cells were not found to be IL-13 dependent. Other IL-13 dependent inflammatory changes that were noted like NK cell numbers and DC numbers have not been explored further in this thesis.

Summary

In this chapter we characterised the caerulein induced pancreatitis model. We setup image analysis protocols to quantify area oedema and necrosis as markers of epithelial damage and disease severity in acute pancreatitis using H&E-stained histological sections. We discovered that ILC2 deficient mice show reduced oedema, necrosis and immune influx compared to control mice. A reduction in these three parameters in ILC2 deficient mice indicates that ILC2s are promoting epithelial damage and disease severity in acute pancreatitis.

While deep immunophenotyping ILC2 deficient mice with pancreatitis we observed ILC2 dependent eosinophilia in mice with acute pancreatitis. Using various genetically engineered or antibody depletion mouse models, we also discovered that this eosinophilia is stromal cells, IL-33 and IL-5 dependent as well. We discovered that stromal cells are the source of IL-33 and that IL-33 activates ILC2s and induces IL-5 production. IL-5 was found to induce eosinophilia in acute pancreatitis.

We next looked at the role of this ILC2 dependent eosinophilia in promoting acute pancreatitis. Using two different mouse models, we showed that eosinophils did not promote epithelial damage in acute pancreatitis. We performed a series of experiments using genetically modified and antibody depleted mouse models to tease out the downstream mechanism by which ILC2s might be regulating epithelial damage. We found that neutrophils, CD4 T cells, CD8 T cells, NK cells, monocytes and IL-13 did not play a role in promoting epithelial damage in acute pancreatitis.

In summary, we discovered a ILC2 dependent eosinophilia pathway active in acute pancreatitis but it's role in the pathogenesis of acute pancreatitis is not known. We found that ILC2s promote epithelial damage in acute pancreatitis, however the mechanism by which this happens is not known.

Chapter 3

The role of ILC2s in tissue remodelling in chronic pancreatitis

Eosinophilia in chronic pancreatitis is ILC2 dependent

We earlier showed that eosinophilia of the exocrine pancreas, induced either by administration of recombinant IL-33 or through acute pancreatitis, are both ILC2 dependent (S9A, Fig 28D). Human pancreas tissues samples from patients with chronic pancreatitis show increased eosinophil accumulation compared to control pancreas (Manohar et al., 2018). Pancreatitis in humans that show features of eosinophilia are classified as eosinophilic pancreatitis. It has been speculated that eosinophilia in chronic pancreatitis could be more common than currently acknowledged (Manohar et al., 2018), but difficult to assess as pancreatic biopsies are currently performed mainly for the purpose of identifying pancreatic malignancy. Moreover, as this procedure does not leave much tissue for histological analysis, eosinophilia in pancreatitis has not been studied in detail (Manohar et al., 2018).

Having demonstrated earlier that eosinophilia in acute pancreatitis is ILC2 dependent, we asked if the same was true for chronic pancreatitis. In order to induce chronic pancreatitis, we administered caerulein (hourly injections x 6) on days 0, 1, 7, 8, 14 and 15, and sacrificed the mice on 18 days after first caerulein injection. We observed both a significant increase in eosinophilia in CP compared to PBS control, and a reduction in eosinophil numbers in caerulein injected ILC2 deficient mice compared to control animals (fig 45). The number of eosinophils seen in control animals with chronic pancreatitis is comparable to number seen in control animals during acute pancreatitis recovery (fig S17B).

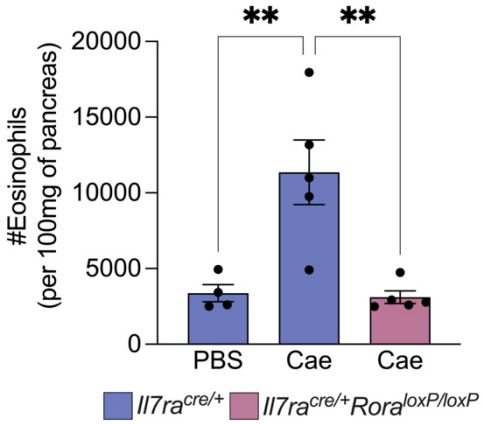

Figure 45 – Eosinophilia is ILC2 dependent in chronic pancreatitis. *Il7ra*$^{cre/+}$ or *Il7ra*$^{cre/+}$ *Rora*$^{loxP/loxP}$ mice were injected with 50ug/Kg of caerulein on day 0, day 1, day 7, day 8, day 14, day 15 and sacrificed on 18 days after the first caerulein injection. This was followed by quantification of myeloid immune cells in the pancreas by flow cytometry. Bar graph indicates the mean (± s.e.m.) and shows data from one experiment. Statistical significance was calculated using one-way ANOVA. ns=non significant. *= P£0.05, **= P£0.01, ***= P£0.001, ****=P£0.0001.

Tissue remodelling after chronic pancreatitis is ILC2 dependent

Tissue remodelling after epithelial injury involves epithelial regeneration and fibrosis. When all ILCs were depleted in Rag$^{-/-}$ mice using CD90.2 antibody in a mouse model of skin wounding, ILC depleted mice showed delayed wound closure and associated reduction in replenishing of epithelial cells after injury (Rak et al., 2016). Systemic fibrosis an autoimmune skin condition involving extensive fibrosis is induced by dermal application of hypochlorous acid (HOCl) in mice. HOCl-treated mice skin showed an increased frequency of ILC2s (Laurent et al., 2021). Similarly, a significant increase in ILC2s was also seen in human systemic sclerosis samples compared to healthy donor skin. This increase in ILC2s also showed a strong correlation with fibrosis (Laurent et al., 2021).

ILC2s have been shown to regulate fibrosis in the lungs. These cells were increased in lung tissues of patients with idiopathic pulmonary fibrosis. RORα deficient mice that lack ILC2s showed a reduction in *Schistosoma mansoni* infection associated lung fibrosis (Hams et al., 2014). This observation was confirmed using *Rag1*$^{-/-}$ mice in which ILC2s were depleted with CD90.1 antibody. In the absence of ILC2s in the latter model as well, *Schistosoma mansoni* infection resulted in reduced collagen deposition (Hams et al., 2014).

In the pancreas acinar cells, undergo dedifferentiation and then transdifferentiation into ductal-like cells in a process called acinar to ductal metaplasia (ADM). ADM after epithelial injury in the pancreas is key to regeneration and repopulation of the pancreas (Storz, 2017). ADM in chronic pancreatitis also presents with extensive fibrosis (Xue et al., 2015). ILC2s have been shown to regulate epithelial regeneration in DSS induced colitis through their production of amphiregulin (AREG) and AREG mediated epithelial proliferation (Monticelli et al., 2015). As ILC2s promote epithelial regeneration and fibrosis in other organs, we asked if ILC2s could be regulating ADM and fibrosis in chronic pancreatitis.

To address this, we looked at ADM and fibrosis in ILC2 deficient mice using the caerulein induced chronic pancreatitis model. To identify ADM we used CK19 which is a ductal cell marker that is upregulated in acinar cells when they undergo ADM (J. Liu et al., 2016). Modified Masson's trichrome (MMT) staining was used to identify fibrosis in the pancreas. ILC2 deficient mice with chronic pancreatitis showed reduced ADM and fibrosis compared to control animals (fig 46A). Positively stained areas for CK19 and fibrosis was quantified using the image analysis software Halo. ILC2 deficient mice showed significantly reduced ADM and fibrosis compared to control animals (fig 46B,C). In summary, ILC2s are regulating ADM and

fibrosis in chronic pancreatitis. Whether this reduction in ADM and fibrosis is due to ILC2s promoting tissue regeneration or a result of reduced epithelial damage to begin with in ILC2 deficient mice (fig 25) remains to be confirmed.

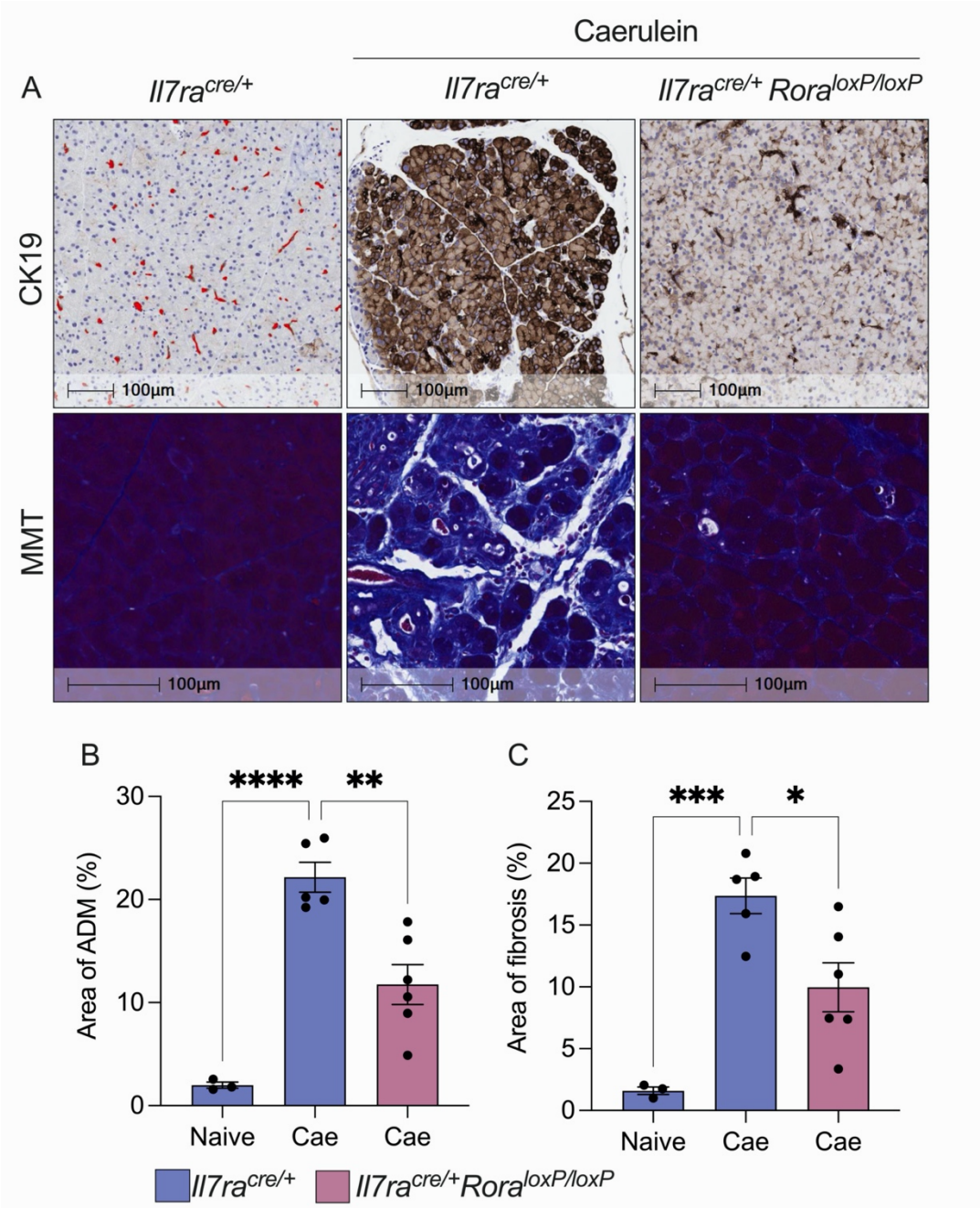

Figure 46 – ADM and fibrosis in chronic pancreatitis is ILC2 dependent. *Il7ra*$^{cre/+}$ or *Il7ra*$^{cre/+}$ *Rora*$^{loxP/loxP}$ mice were injected with 75ug/Kg of caerulein on day 0, day 1, day 7, day 8, day 14, day 15 and sacrificed on 18 days after the first caerulein injection. A, Pancreas was fixed, embedded, sectioned and stained with CK19 IHC (10X) and MMT (20X) are shown. B,C, Quantification of area of ADM by CK19 staining (B) and area of fibrosis by modified Masson's trichrome staining (C) from histological sections on the image analysis software Halo. Bar graph indicates the mean (± s.e.m.) and shows data from one experiment. Statistical significance was calculated using one-way ANOVA. ns=non-significant. *= P£0.05, **= P£0.01, ***= P£0.001, ****=P£0.0001.

ILC2 dependent eosinophilia does not regulate tissue remodelling in chronic pancreatitis

Eosinophils have been shown to moderate tissue remodelling in various models of epithelial injury a few of which have been summarised here. For instance, eosinophilia was observed in a carbon tetrachloride associated mouse model liver injury, while eosinophil lacking ΔdblGATA mice showed reduced proliferation of hepatocytes in this model of liver damage (Goh et al., 2013).This eosinophil mediated liver regeneration was shown to be mediated via IL-4 secreted by eosinophils (Goh et al., 2013). In a cardiotoxin induced mouse model of muscle injury as well eosinophils were shown to be critical for muscle regeneration. ΔdblGATA mice with cardiotoxin induced mouse injury were unable to regenerate their injured muscles (Heredia et al., 2013). When eosinophils were depleted using anti-IL-5 monoclonal antibody (mepolizumab) in consenting participants with atopic asthma, treated patients showed a reduction in expression of extracellular matrix proteins like tenascin, procollagen III and lumican. Eosinophils were shown to mediate extracellular matrix protein secretion via TGFβ1 (Flood-Page et al., 2003). In chronic pancreatitis as well, eosinophil deficient *Il5*$^{-/-}$ and ΔdblGATA mice with chronic pancreatitis showed a significant reduction in collagen thickness and an associated down regulation of fibrosis associated genes like TGFβ, collagen-1 and fibronectin (Manohar et al., 2018).

We had earlier shown that eosinophilia in acute pancreatitis is stromal cell, IL-33, ILC2 and IL-5 dependent. We have also shown that eosinophilia in chronic pancreatitis is ILC2 dependent (fig 38). While eosinophilia did not play a role in regulating epithelial damage in acute pancreatitis (fig 31), we asked if eosinophils and their upstream regulators play a role in tissue remodelling in chronic pancreatitis.

To understand the role of IL-33, IL-5 and eosinophils in tissue remodelling after chronic pancreatitis we used IL-33 deficient *Il33*$^{cit/cit}$, IL-5 deficient Il5$^{tom/tom}$ and eosinophil deficient ΔdblGATA mouse models (fig 47A). *Il33*$^{cit/cit}$, Il5$^{tom/tom}$ and ΔdblGATA mice with chronic pancreatitis did not show a change in ADM or fibrosis compared to control animals (fig 47B,C). Although eosinophilia has been shown to regulate tissue remodelling in literature, eosinophilia in chronic pancreatitis did not play a role in promoting ADM or fibrosis in our hands. These data specifically contradicts a report showing reduction in collagen thickness in Il5$^{-/-}$ and ΔdblGATA mice (Manohar et al., 2018). This could be because the mice used in report are of the BALB/c background which are known to be more skewed toward type 2 immunity in their inflammatory responses.

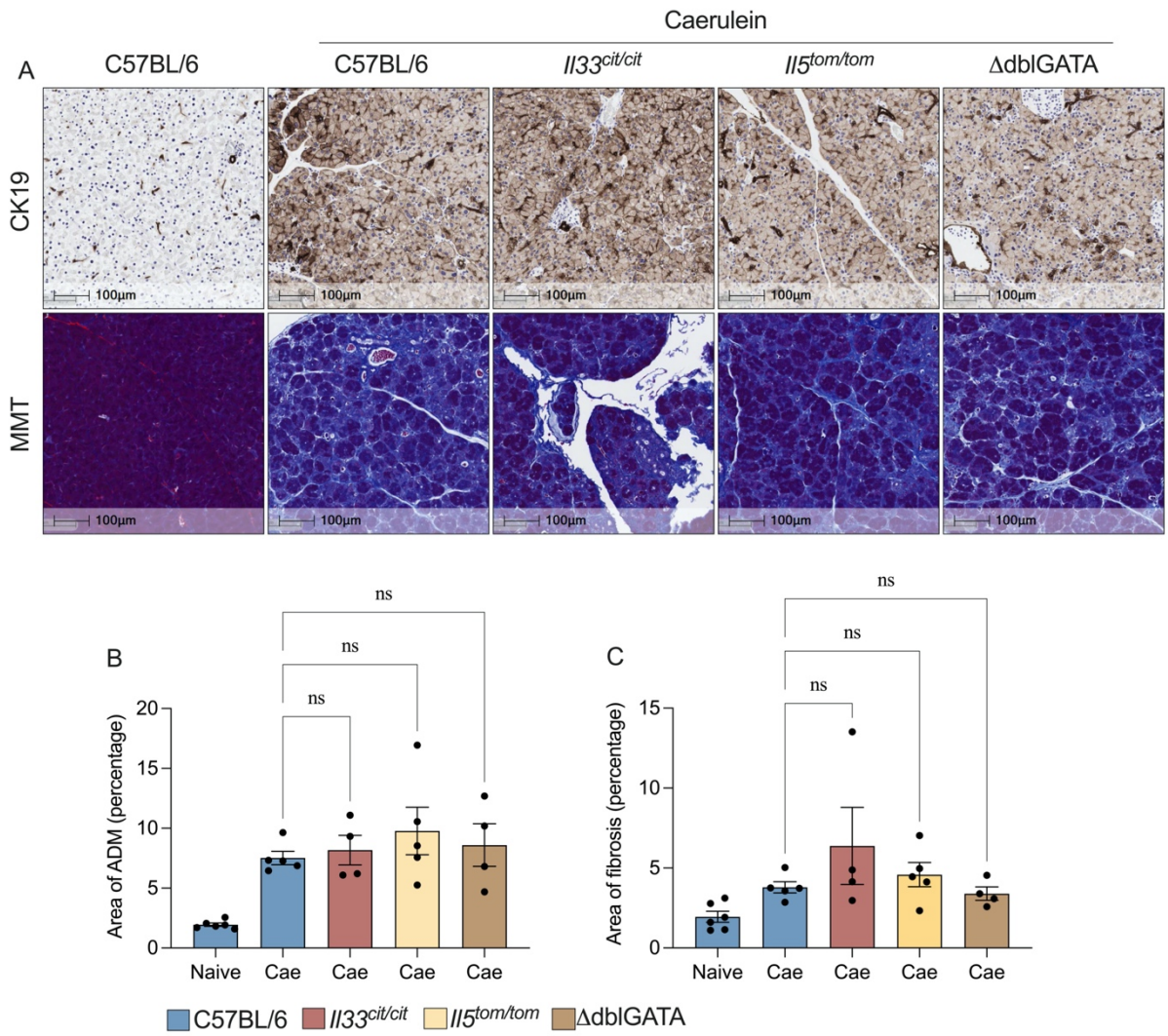

Figure 47 – ILC2 dependent eosinophilia does not regulate ADM and fibrosis in chronic pancreatitis. *Il33$^{cit/cit}$, Il5$^{tom/tom}$ or* DdblGATA mice were injected with 75ug/Kg of caerulein on day 0, day 1, day 7, day 8, day 14, day 15 and sacrificed 18 days after the first caerulein injection. A, Pancreas was fixed, embedded, sectioned and stained with CK19 IHC (10X) and MMT (20X) are shown. B,C, Quantification of area of ADM by CK19 staining (B) and area of fibrosis by modified Masson's trichrome staining (C) from histological sections on the image analysis software Halo. Bar graph indicates the mean (± s.e.m.) and shows data from one experiment. Statistical significance was calculated using one-way ANOVA. ns=non significant. *= P£0.05, **= P£0.01, ***= P£0.001, ****=P£0.0001.

ILC2s are activated in chronic pancreatitis

We had earlier shown that ILC2s are activated in acute pancreatitis (fig 29,30), we asked if this could be the case in chronic pancreatitis as well. We used *Il13$^{tom/+}$* mice which are reporters for IL-13 expression. We found a significant increase in IL-13 production by ILC2s in mice with chronic pancreatitis compared to control animals (fig 48B). This was however not the case for CD4 T cells, which showed no difference in IL-13 production compared to control animals (fig 48C). In summary, we identified that ILC2s were activated in chronic pancreatitis and were actively producing IL-13.

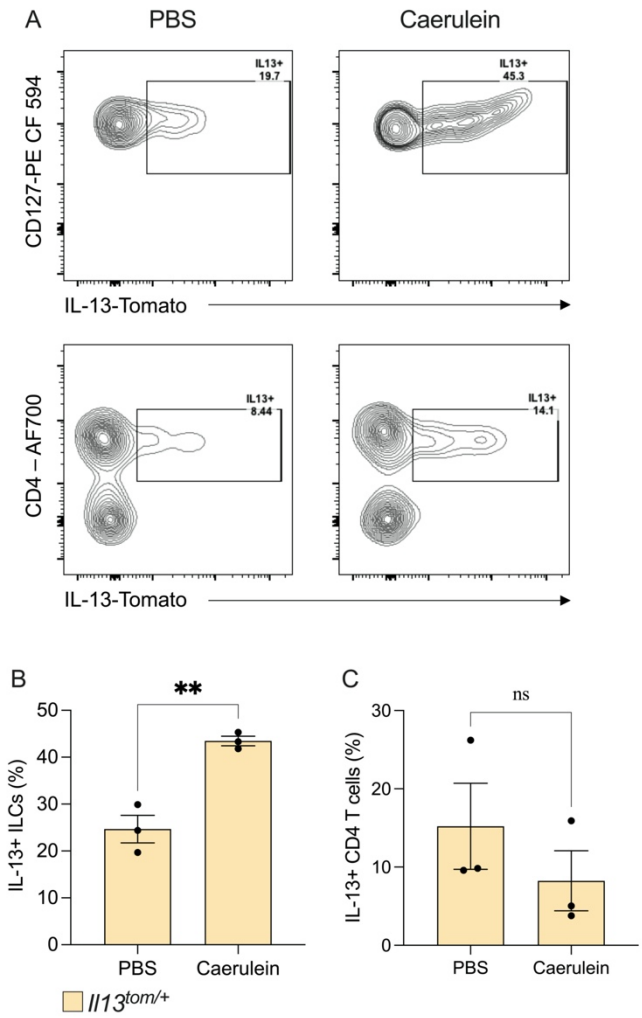

Figure 48 – ILC2s are activated in chronic pancreatitis. *Il13*$^{tom/+}$ were injected with 50ug/Kg of caerulein on day 0, day 1, day 7, day 8, day 14, day 15 and sacrificed after the last caerulein injection. Single cell suspension prepared from the pancreas were analysed using flow cytometry. A, Representative gating for IL-13-tomato expression on ILCs and CD4 T cells in the pancreas. B, Quantification of IL-13+ pancreatic ILCs C, Quantification of IL-13+ CD4 T cells. Bar graphs indicate the mean (± s.e.m.) and show data from one experiment. Statistical significance was calculated using two-way ANOVA. ns=non-significant, ****=P□0.0001.

IL-13 does not regulate tissue remodelling in chronic pancreatitis

IL-13 has been shown to mediate fibrosis and epithelial regeneration in various settings of epithelial injury. IL-13 has been shown to regulate macrophage mediated fibrosis in *Schistosoma mansoni* egg-induced granuloma formation model (Borthwick et al., 2016). In mouse and human chronic pancreatitis, alternatively activated macrophages (AAMs) were found to regulate fibrosis in an IL-13 dependent manner. Here, IL-13 was shown to be produced by pancreatic stellate cells (Xue et al., 2015).

As we found more Il33tom+ ILC2s in chronic pancreatitis, we asked if IL-13 could be playing a role in regulating fibrosis chronic pancreatitis. Interestingly, *Il13*$^{tom/tom}$ mice did not show

difference in area of fibrosis compared to either control mice (fig 49). This model of chronic pancreatitis added a period of 3 weeks after the end of caerulein injections. This could explain the lack of phenotype associated with IL-13 when compared to literature. Earlier timepoints after chronic pancreatitis may be better suited to capture IL-13 mediated regulation of fibrosis.

It remains to be confirmed with repeats and modified experimental setup as to whether ILC2 derived IL-13 plays a role in regulating tissue remodelling in chronic pancreatitis.

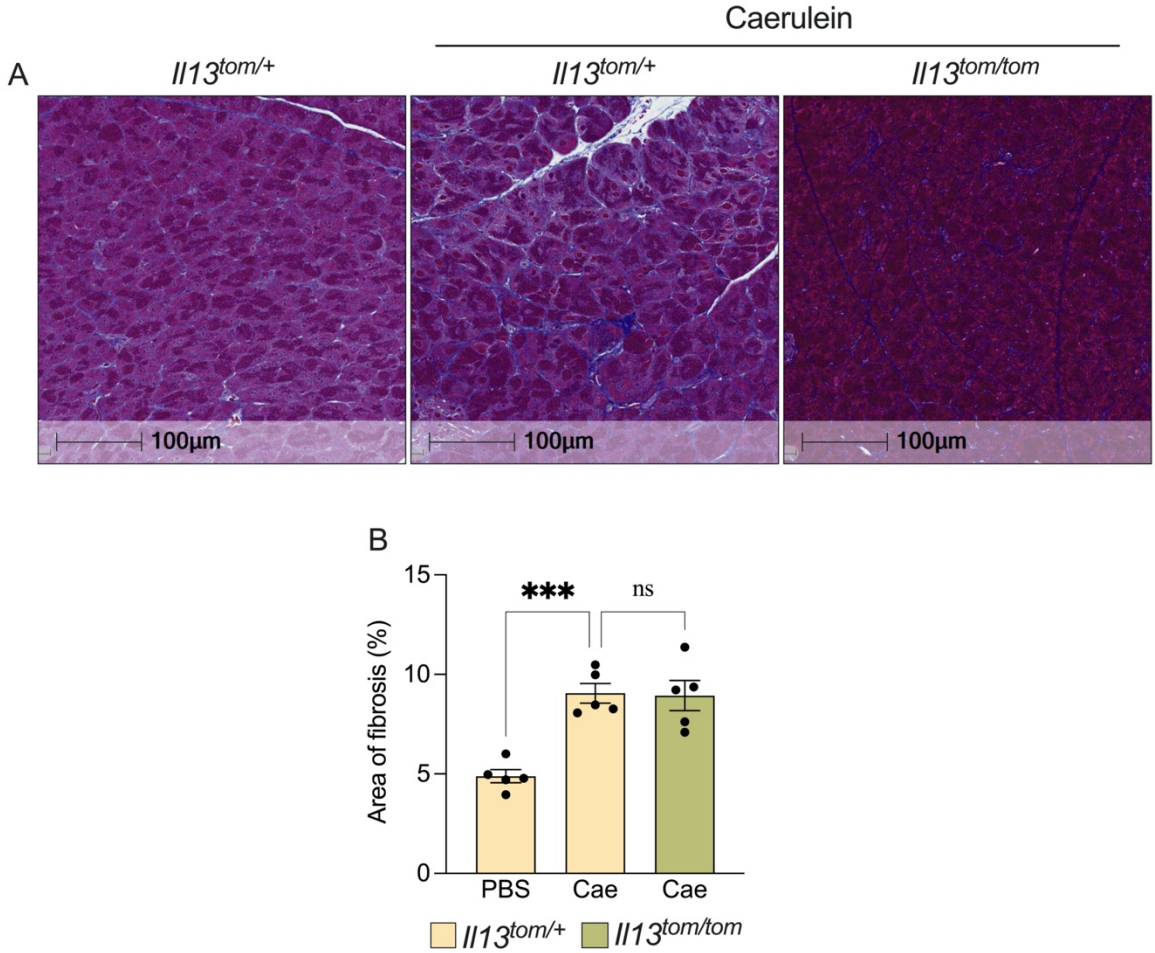

Figure 49 – Fibrosis in chronic pancreatitis is not IL-13 dependent. *Il13tom/tom* mice were injected with 75ug/Kg of caerulein on day 0, day 1, day 7, day 8, day 14, day 15 and sacrificed on 34 days after the first caerulein injection. A, Pancreas was fixed, embedded, sectioned and stained with Masson's trichome (10X) are shown. B, Quantification of area of fibrosis by Masson's trichrome staining from histological sections on the image analysis software Halo. Bar graph indicates the mean (± s.e.m.) and shows data from one experiment. Statistical significance was calculated using one-way ANOVA. ns=non-significant. *= P£0.05, **= P£0.01, ***= P£0.001, ****=P£0.0001.

In summary, we found that similar to acute pancreatitis, in chronic pancreatitis as well, eosinophilia is regulated by ILC2s. ILC2s have been shown to regulate tissue remodelling after epithelial injury in skin and lungs (Hams et al., 2014; Laurent et al., 2021; Rak et al., 2016). We investigated the role of ILC2s in tissue remodelling in chronic pancreatitis, and found ADM and fibrosis were reduced in ILC2-deficient mice. When taking in account our

failure to attribute a role for eosinophils or IL-13 in CP-induced ADM or fibrosis, we hypothesise that the phenotype observed in ILC2-deficient mice is likely due to decreased epithelial damage in response to acute pancreatitis (fig 46, fig25).

Conclusion &

Future directions

Conclusion

ILC2s are tissue resident immune cells that are potent inflammatory meditators and are known to be important in the pathogenesis of asthma and clearance of helminth infections (Ebbo et al., 2017). ILC2s are commonly found at barrier sites and are innate counterparts of T helper 2 cells. ILC2s mediate their inflammatory function via type 2 cytokines like IL-5, IL-13 and amphiregulin (Vivier et al., 2018). Very little is known about pancreatic ILC2s and much less about their function in the pathology of the exocrine pancreas. To the best of our knowledge no report exists exploring the role of ILC2s in the pathology of pancreatitis. Nevertheless, there is ample evidence for the involvement of type-2 immunity in both pancreatitis and pancreatic cancer, hence we sought to identify and characterise ILC2s in the mouse pancreas.

We identified ILC2s as CD45+, CD3-, B220-, Lineage-, NK1.1-, CD127+ and GATA3+ cells, which represent the most prevalent ILC (excluding NK) in the exocrine pancreas (fig 8). ILC2s can be activated by various alarmins like IL-33, IL-25 and TSLP in barrier tissues (Ebbo et al., 2017). Given the tissue-specific regulatory mechanisms of ILC2s (Ricardo-Gonzalez et al., 2018), we sought to define the physiological stimulus of pancreatic ILC2. We administered recombinant IL-33, IL-25 and TSLP to mice and characterised ILC2 activation in the pancreas using flow cytometry. ILC2s have been shown to upregulate OX40L expression (Halim et al., 2018) and produce type 2 cytokines like IL-5 and IL-13 (Schuijs & Halim, 2018) when activated. Pancreatic ILC2s from IL-33 administered mice but not IL-25 or TSLP administered mice showed an increase in OX40L expression, IL-5 and IL-13 production (fig 9-11).

In order to characterise the IL-33 associated type 2 immune environment in the mouse pancreas, we next analysed the immune changes in alarmin administered mice and found that IL-33 administered mice showed an expansion of total immune cells, ILC2s and Tregs in the pancreas (fig 12). We also observed that recombinant IL-33 administration led to an expansion of eosinophils in the pancreas (fig 13). ILC2s have been shown to induce Treg expansion through the OX40-OX40L axis in the lungs (Halim et al., 2018). ILC2s have also been shown to induce eosinophil expansion through their production of IL-5 (Nussbaum et al., 2013). Considering pancreatic ILC2s were activated by IL-33 to upregulate OX40L and produce IL-5, we asked if Treg and eosinophil expansion the pancreas could be ILC2 dependent. ILC2 deficient *Il7ra*$^{cre/+}$*Rora*$^{loxP/loxP}$ mice showed impaired Treg and eosinophil expansion upon IL-33 administration (fig 17). Treg expansion was also impaired in mice lacking OX40L expression on ILCs (*Il7Ra*$^{cre/+}$ *Tnfsf4*$^{loxP/loxP}$). In summary, we found that pancreatic ILC2s regulate Treg expansion via the OX40-OX40L axis in an IL-33 dependent manner.

Additionally, we also found that pancreatic ILC2s regulate IL-33 induced eosinophilia in the pancreas. Interestingly, both Tregs and eosinophils are implicated in serious diseases of the exocrine pancreas, namely PDAC (Manohar, Verma, Venkateshaiah, & Mishra, 2017; Siret et al., 2019) and pancreatitis-induced fibrosis (Manohar et al., 2018).

Having identified and characterised pancreatic ILC2s we looked at these cells in precursors of pancreatic ductal adenocarcinoma (PDAC) called pancreatic intraepithelial neoplasia (PanINs). We used the KC mouse model of PDAC and found that ILC2 and Treg numbers were upregulated in early stages of PanINs (fig 18). However, when we characterised KC *Il33*$^{cit/cit}$ mice lacking IL-33 expression this expansion of Tregs and ILC2s in PanINs was not found to be IL-33 dependent (fig 20). We did a survival analysis of KC mice lacking IL-33 expression to understand the role of IL-33 in PDAC tumour progression. We found no difference in survival between KC mice with and without IL-33 expression (fig 21). These data suggest that IL-33-independent mechanisms contribute to pancreatic ILC2 activation in KC mice, prompting future investigation using my transcriptomic dataset to predict alternative regulatory mechanisms. These data provide an important insight into the role of IL-33 in PDAC development; recent papers provide conflicting views on the role, and cellular source, of IL-33 in PDAC (Moral et al., 2020).

In parallel, having established pancreatic ILC2s as capable of mounting a type 2 immune response, and the known ability of ILC2s to respond to acute tissue damage, we sought to ask what role ILC2s could be playing in pancreatitis. Pancreatitis is an inflammatory condition leading to epithelial damage and oedema affecting the exocrine pancreas (Manohar, Verma, Venkateshaiah, Sanders, et al., 2017). Considering type 2 immune features like eosinophilia and IL-13 associated fibrosis are commonly found in pancreatitis (Manohar et al., 2018; Xue et al., 2015) we sought to investigate the role of ILC2s in pancreatitis. Pancreatitis in mice is commonly induced by a compound called caerulein which is an analogue of the hormone cholecystokinin. Supra-stimulation with caerulein induces pancreatitis with 3 signature features – oedema, necrosis and immune influx.

Histological changes in caerulein induced pancreatitis are very dynamic. We first characterised the histological changes in our acute pancreatitis model over a period of 48 hours at 6-hour intervals and concluded that necrosis and oedema are both easily identifiable at 24 hours after the first caerulein injection (fig 22); this led us to choose this time-point for much of our subsequent analysis. Typically, severity of pancreatitis has been scored on a scale of 0-4 based on level of necrosis, oedema and immune influx. This scoring tool is however subjective, and scoring may vary from user to user. We trained a classifier function

on an image analysis software called Halo to identify oedema and necrosis in H&E-stained pancreas section. We used the trained classifier to quantify oedema and necrosis across images of H&E-stained pancreas sections (fig 24). This is the first report of using image analysis of H&E sections to quantify disease severity in pancreatitis to the best of our knowledge.

We next looked at pancreatitis severity in ILC2 deficient and control mice. We found that ILC2 deficient mice showed a significant reduction in markers of disease severity including area of oedema, necrosis (fig 25), serum amylase, serum lipase (fig 26) and total immune influx (fig 27) in acute pancreatitis. These data suggested that ILC2s regulate epithelial damage and disease severity in acute pancreatitis. Moreover, we characterised the cellular immune changes in ILC2 deficient mice and found that eosinophilia (fig 28) and Treg expansion (fig S16) were ILC2 dependent in acute pancreatitis as well. While ILC2 deficient mice showed attenuated disease severity and immune cell recruitment, we next asked if ILC2s were activated in acute pancreatitis.

We found that ILC2s are activated in early stages of acute pancreatitis and produce IL-5 and IL-13 in an IL-33 dependent manner (fig 29, 30). Irrespective of ILC2 status, we observed an influx of neutrophils in early stages of acute pancreatitis, around the same timepoint as ILC2 activation (fig S20). Neutrophil proteases are known to cleave full length IL-33 into its the biologically active mature form which up to 30 times more potent that full-length IL-33 (Lefrançais et al., 2012). We asked if neutrophils might be processing full-length IL-33 in acute pancreatitis as well, thereby leading to IL-33 activation. We depleted neutrophils and looked at IL-5 production by ILC2s as a proxy for ILC2 activation. Interestingly, neutrophil depleted mice showed a significant reduction in IL-5 production compared to control animals with acute pancreatitis (fig 31). In summary, neutrophils likely play a role in processing of IL-33 into its more bioactive form. In the future, to confirm this observation, IL-33 from whole pancreas lysates of neutrophil depleted and control animals could be analysed by western blotting. If this hypothesis holds true, western blots from neutrophil depleted blots should have significantly lesser cleaved or biologically active IL-33 compared to control animals.

Considering that eosinophilia in acute pancreatitis s ILC2 dependent and that ILC2s produce the eosinophil recruiting cytokine IL-5 in an IL-33 dependent manner, we asked if eosinophilia in acute pancreatitis is IL-33 and IL-5 dependent. Using IL-33 deficient and IL-5 depleted mice we discovered that eosinophilia in acute pancreatitis is indeed IL-33 and IL-5 dependent (fig 32, 35). Using an IL-33 reporter mouse model, we identified podoplanin+ stromal cells as the main IL-33 expressing population in the pancreas in homeostasis and pancreatitis (fig 33).

This is in contradiction with earlier reports that identify acinar cells as the source of IL-33 in pancreatitis (Watanabe et al., 2016). IL-33 is thought to be released upon necrosis (Liew et al., 2016). A significant reduction in number of stromal cells is seen in acute pancreatitis at early stages when ILC2 activation is also observed (fig S19). Stromal cells are found to be cycling at later stages of acute pancreatitis (fig S15 and fig S18) to replenish. In summary, we report for the first time that stromal cells are the largest IL-33 expressing population in pancreatitis and are likely the source of IL-33 in early stages of acute pancreatitis. This IL-33 is likely processed by neutrophil proteases into more bioactive form which then activate ILC2s. We confirmed that stromal cells indeed influence eosinophilia using a stromal cell depleting mouse model. We found a significant reduction in eosinophils in stromal cell depleted mice (fig 34). However, a caveat is that stromal cells are also an important source of CCL11 an eosinophilia modulating chemokine, and depletion of stromal cells may affect this pathway too (Dahlgren et al., 2019; Rana et al., 2019).

In summary, we discovered an eosinophilia axis in acute pancreatitis that involves stromal immune crosstalk. We show that in acute pancreatitis, stromal cells express IL-33 which is likely released upon death of stromal cells in early stages of acute pancreatitis. This IL-33 is processed by neutrophil proteases into more mature bioactive form. This is followed by ILC2 activation by IL-33 and subsequent IL-5 release. We show that IL-5 produced by ILC2s promotes eosinophilia in acute pancreatitis.

Having discovered an ILC2 dependent eosinophilia pathway in acute pancreatitis, we looked at the role of this pathway in the pathology of acute pancreatitis. We used IL-5 depleted and ΔdblGATA mice as models of eosinophil deficiency. However, we found that eosinophil deficiency in both models did not affect epithelial damage in acute pancreatitis (fig 37, fig 38). In the process of addressing the role of eosinophils in acute pancreatitis, we also blocked granulocyte degranulation using cetirizine. Interestingly, degranulation blocking led to a significant reduction in necrosis (fig 39). Considering, our discovery that eosinophils don't play a role in the severity of acute pancreatitis, we hypothesised that this phenotype could be due to other granulocytes whose degranulation cetirizine could be blocking. Although there is an influx of neutrophils in acute pancreatitis this influx is however not ILC2 dependent (fig S20). We asked if ILC2s could be regulating the neutrophil function of NETting through which neutrophils have been shown to promote necrosis in acute pancreatitis. We found although there was no difference in percentage of NETting neutrophils, a difference in quality of NETting was seen in neutrophils from ILC2 deficient mice with pancreatitis compared to control animals. This observation however needs further technical clarity as NETting neutrophils we identified from images showed different scatter profile from literature. Ultimately, we did not

see a difference in necrosis and oedema in neutrophil depleted mice either (fig 42). However, these data are inconsistent previous reports on the role of neutrophils in AP, and further work is required to clarify whether ILC2s regulate neutrophil function. This failure to reproduce However, this enquiry falls outside the scope of this PhD.

Having ruled out eosinophils and neutrophils, we next asked how ILC2s could be regulating epithelial damage in acute pancreatitis. We found a significant reduction in necrosis in *Rag1*$^{-/-}$, *Rag1*$^{-/-}$*Il7ra*$^{cre/+}$*Rora*$^{loxP/loxP}$ and *muMT*$^{KO/KO}$ mice (fig 41) suggesting a role for the adaptive immune system in regulating epithelial damage in acute pancreatitis. It is to be noted additional deletion of ILC2s in the, *Rag1*$^{-/-}$*Il7ra*$^{cre/+}$*Rora*$^{loxP/loxP}$ mouse model did not show any difference from ILC2 sufficient *Rag1*$^{-/-}$ mice. We further attempted to resolve the mechanism by which the adaptive immune system influences epithelial damage in acute pancreatitis. We depleted CD4 and CD8 T cells and found no difference in oedema or necrosis in acute pancreatitis (fig 42). In summary, we understand that although adaptive immune system lacking Rag1$^{KO/KO}$ mice show a reduction in oedema and necrosis, this is not regulated via CD4 or CD8 T cells. While B cell lacking *muMT*$^{KO/KO}$ mice show a reduction in necrosis in acute pancreatitis, investigating the role of B cells in acute pancreatitis is beyond the scope of this PhD. In the future, the mechanism by which B cells might be regulating epithelial damage and ILC2 regulation of B cell function will have to be characterised.

We found that NK cells and monocytes do not regulate epithelial damage in acute pancreatitis either (fig 41). Further, although we show that Treg expansion is ILC2 dependent in the recombinant IL-33 model and acute pancreatitis, the role of Tregs in pancreatitis is an independent project outside the scope of this PhD. In summary, while we discovered that ILC2s promote epithelial damage in acute pancreatitis, but our systematic investigation did not reveal the mechanism by which ILC2s act.

Considering ILC2s have been shown to regulate fibrosis and tissue remodelling in other organs (Laurent et al., 2021; Rak et al., 2016), we next sought to understand the role of ILC2s in tissue remodelling in pancreatitis. For this we chose chronic pancreatitis as the setting and looked at acinar to ductal metaplasia and fibrosis as a measure of tissue remodelling. We discovered that ILC2 deficient mice show reduced ADM and fibrosis after chronic pancreatitis (fig 46), which coincided with our finding that eosinophilia during both acute and chronic pancreatitis is ILC2 dependent. While others report that eosinophils are important for CP-induced fibrosis, our experiments with eosinophil-, IL-33-, or IL-5-deficient mice fail to ascribe a clear role for this immune axis in our mode (fig 47). Moreover, we found that ILC2s were activated in chronic pancreatitis and were producing IL-13 (fig 48). IL-13 has been reported to

regulated fibrosis in other organs (Borthwick et al., 2016), in chronic pancreatitis however, we did not find an IL-13 dependent change in fibrosis (fig 49). It remains to be understood if other fibrotic factors like TGFβ (Meng et al., 2016) could be regulating fibrosis in chronic pancreatitis in an ILC2 dependent manner. Blocking TGFβ has been shown to lead to reduced fibrosis in chronic pancreatitis (Nagashio et al., 2004), future experiments are needed to address the role of ILC2s in this mechanism.

In summary, ADM and fibrosis in chronic pancreatitis was found to be ILC2 dependent and this is likely due to reduced epithelial damage to start with. However, as ILC2 are the primary source of IL-5 during acute pancreatitis and critical for pancreatic eosinophilia, we posited that the ILC2-IL-5-eosinophilia axis underpinned the known role of eosinophils in CP-induced fibrosis. Unexpectedly, we found that targeting individual components, which do not impact acute epithelial damage, did not substantially influence fibrosis.

This report identifies and characterises pancreatic ILC2s. Pancreatic ILC2s promote epithelial damage in acute pancreatitis. We also discover a stromal cell, IL-33, ILC2 and IL-5 dependent eosinophilia pathway in acute pancreatitis. We are unable to identify the downstream mechanism by which ILC2s promote epithelial damage despite systematic analysis of different immune cells. We report that ILC2s regulate tissue remodelling in chronic pancreatitis which is independent to eosinophils, IL-33, IL-5 and IL-13.

Future directions

The mechanism by which ILC2s regulate epithelial damage and remodelling in pancreatitis remains to be identified and established. In this section, I will briefly discuss future experiments to explore mechanisms of epithelial damage and exploiting these findings in the context of pancreatic cancer.

Neutrophils have been shown to regulate epithelial damage in pancreatitis via neutrophils extracellular trap formation (Merza et al., 2015). While neutrophil depletion using aLy6G antibody did not bring about any change in oedema or necrosis, a difference in quality of NET formation was seen in ILC2 deficient mice (fig 40). Experimentally, aLy6G based neutrophil depletion showed protection from pancreatitis in the first repeat and no protection was seen in the second repeat of the same experiment. Pooled data of the two repeats showed no difference in oedema and necrosis between neutrophil depleted and control mice. Whether this difference is due to change in batches of caerulein or aLy6G antibody remains to be determined. A repeat of neutrophil depletion with a fresh batch of aLy6G antibody and

confirmation of neutrophil depletion by flow cytometry with a different antibody clone would be helpful to completely rule out neutrophils. Additionally, alternative methods of NET assessment could be considered to understand if NETs are reduced in ILC2 deficient mice. Immunofluorescence staining for NETs would be an efficient way to use already available paraffin embedded pancreas tissue.

muMT$^{KO/KO}$ with pancreatitis showed reduced oedema and necrosis. Here I would like to discuss some data that was not originally included in the thesis due compensation issues in the flow cytometry data leading to poor data quality. Following the observation of protection from pancreatitis in *muMT*$^{KO/KO}$ mice, B cells were explored using a flow cytometry panel developed by David Posner from the Clatworthy Lab at the MRC-LMB, Cambridge.

This panel looked at IgM, IgD and B1 cells in mice with and without pancreatitis. The only discernible data from this experiment was an increase in B1 cells in mice with pancreatitis which has been shown below in fig 50. B cells were not the original focus of this project as the epithelial damage pancreatitis is acute pathology and it was assumed that adaptive immune cells like B cells would not have a role to play in acute settings where innate immune cells are usually active. However, B1 cells defined as CD11b+ B220/CD19+ cells are known to have features of both the adaptive and innate immune systems (Baumgarth, 2011). B1 cells are commonly found in the pleural and peritoneal cavities and tend to traffic from the peritoneal cavities through the omentum (Baumgarth, 2011). The omentum is found to be in close contact with the pancreas in mice. B1 cells have been shown to accumulate in sites of tissue injury or infection and secrete IgM antibodies. B1 cell activation is not B cell receptor dependent, making them well suited for response in an acute pathological setting. Natural IgM antibodies have been shown to induce or enhance injury induced by ischaemia-reperfusion injury by binding altered tissue antigens and apoptotic cells (M. Zhang et al., 2006). Taken together, the role of B1 cells, their production of IgM and its role in epithelial damage in acute pancreatitis is worth exploring.

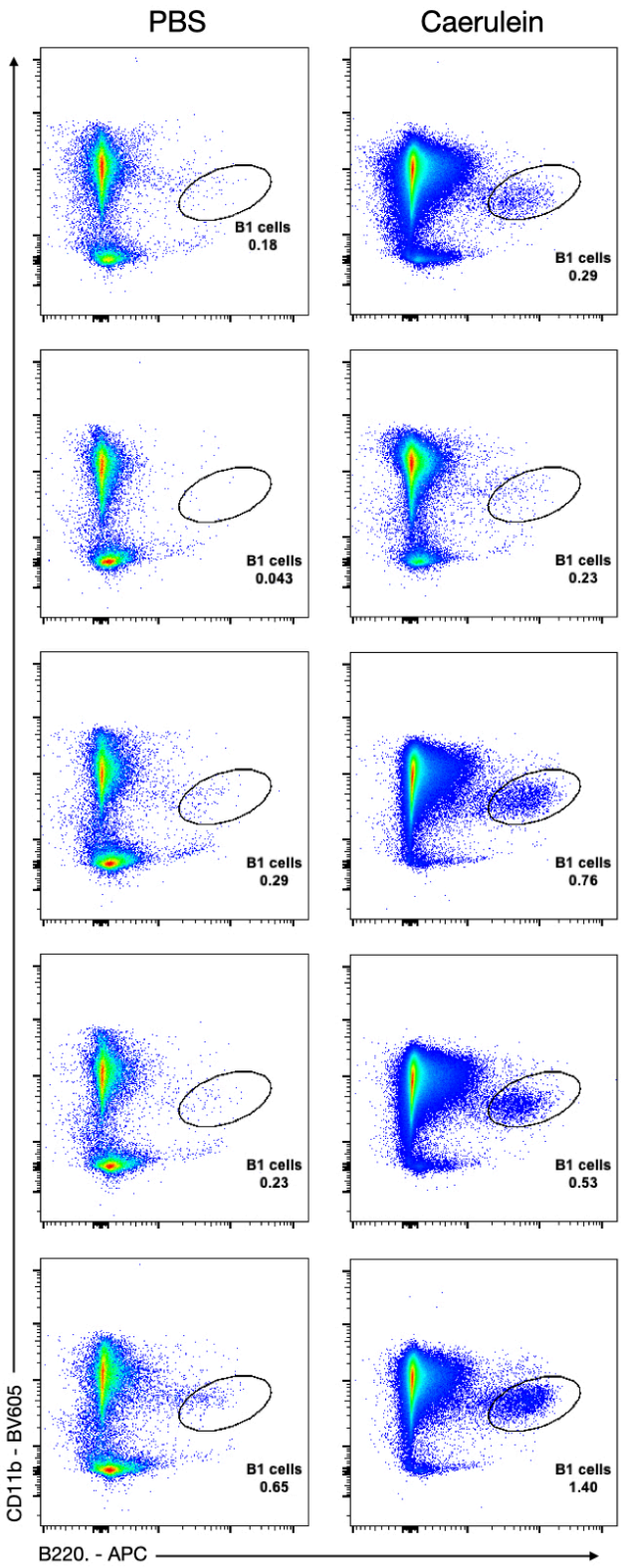

Figure 50 – B1 cells are increased in acute pancreatitis. C57BL/6 mice were injected with PBS or 75ug/Kg of caerulein, and the mice were sacrificed at 24 hours after the first caerulein injection. This was followed by quantification of B cells in the pancreas by flow cytometry. Representative gating for B1 cells in the pancreas has been shown here.

Finally, the role of ILC2s in pancreatitis associated tumour promoting inflammation in PDAC development remains to be explored. The Halim lab has setup a reproducible model of orthotopic transplantation of tumour cells into the pancreas surgically. It has previously been shown that pancreatitis induces PDAC acceleration in mice with *Kras* mutation (Carrière et al., 2009; Guerra et al., 2011, 2007). Orthotopic transplantation of PanIN cells in ILC2 deficient mice followed by induction of pancreatitis would be an interesting experiment to explore the role of ILC2s in inflammation driven acceleration in PanIN to PDAC development.

In summary the role of B1 cells and neutrophils in regulating epithelial damage in acute pancreatitis and how ILC2s might be influencing their function are options left to be explored in an aim to complete the story presented in this thesis.

Supplementary figures

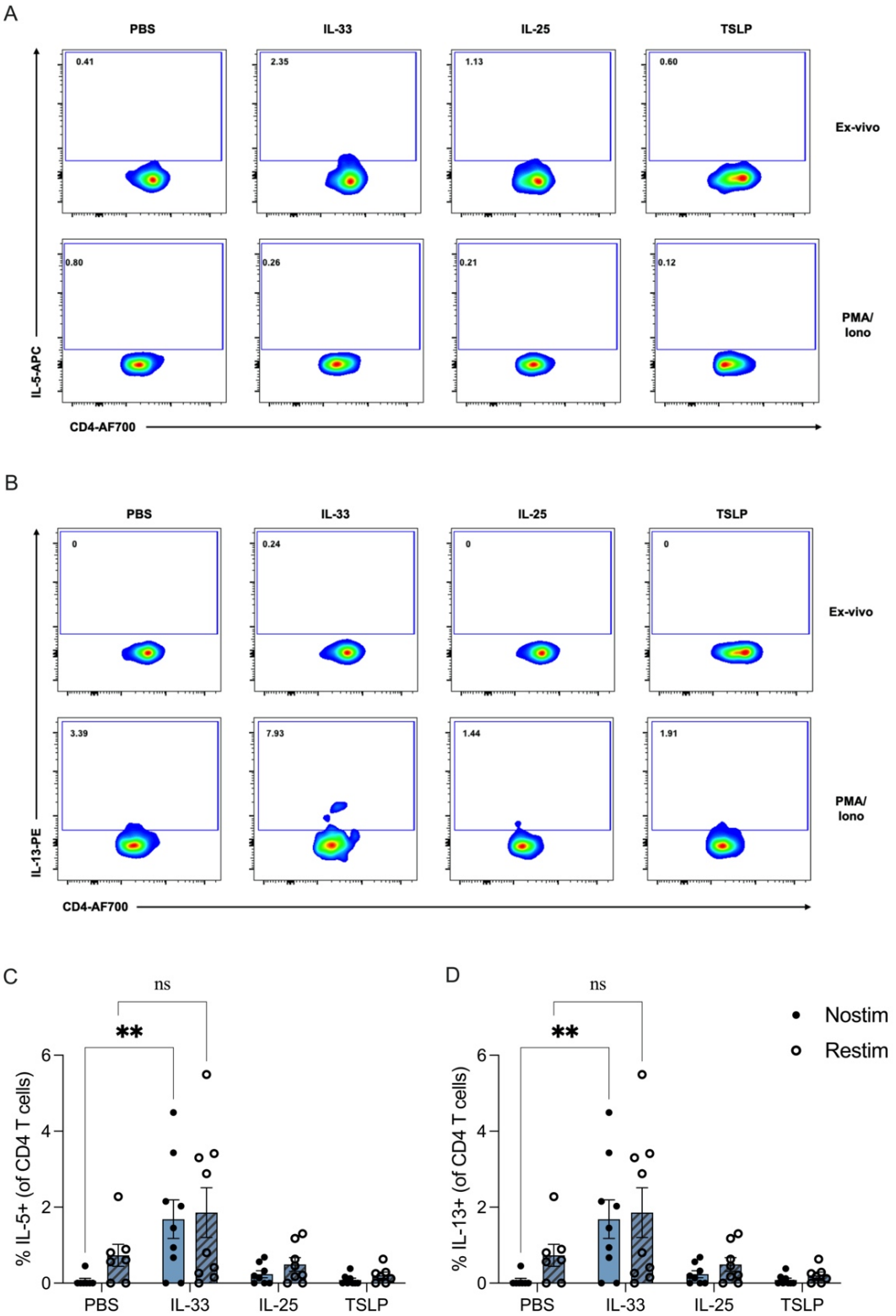

Figure S1 – **IL-33 does not induce IL-5 production by CD4 T cells in the pancreas.** C57BL/6 mice were treated with 200ng recombinant IL-33, IL-25 or TSLP intraperitoneally on days 0 and 1 and were sacrificed on day 3 followed by cytokine quantification using flow cytometery. A, Representative gating for IL-5 expression on CD4 T cells in the pancreas with and without PI stimulation. B, Representative gating for IL-13 expression on CD4 T cells in the pancreas with and without PI stimulation. C,D, Quantification of IL-5+ and IL-13 CD4 T cells (percentage) C,D, Bar graphs indicate the mean (± s.e.m.) and show pooled data from two independent experiments. Statistical significance was calculated using two-way ANOVA. ns=non significant, ****=P≤0.0001.

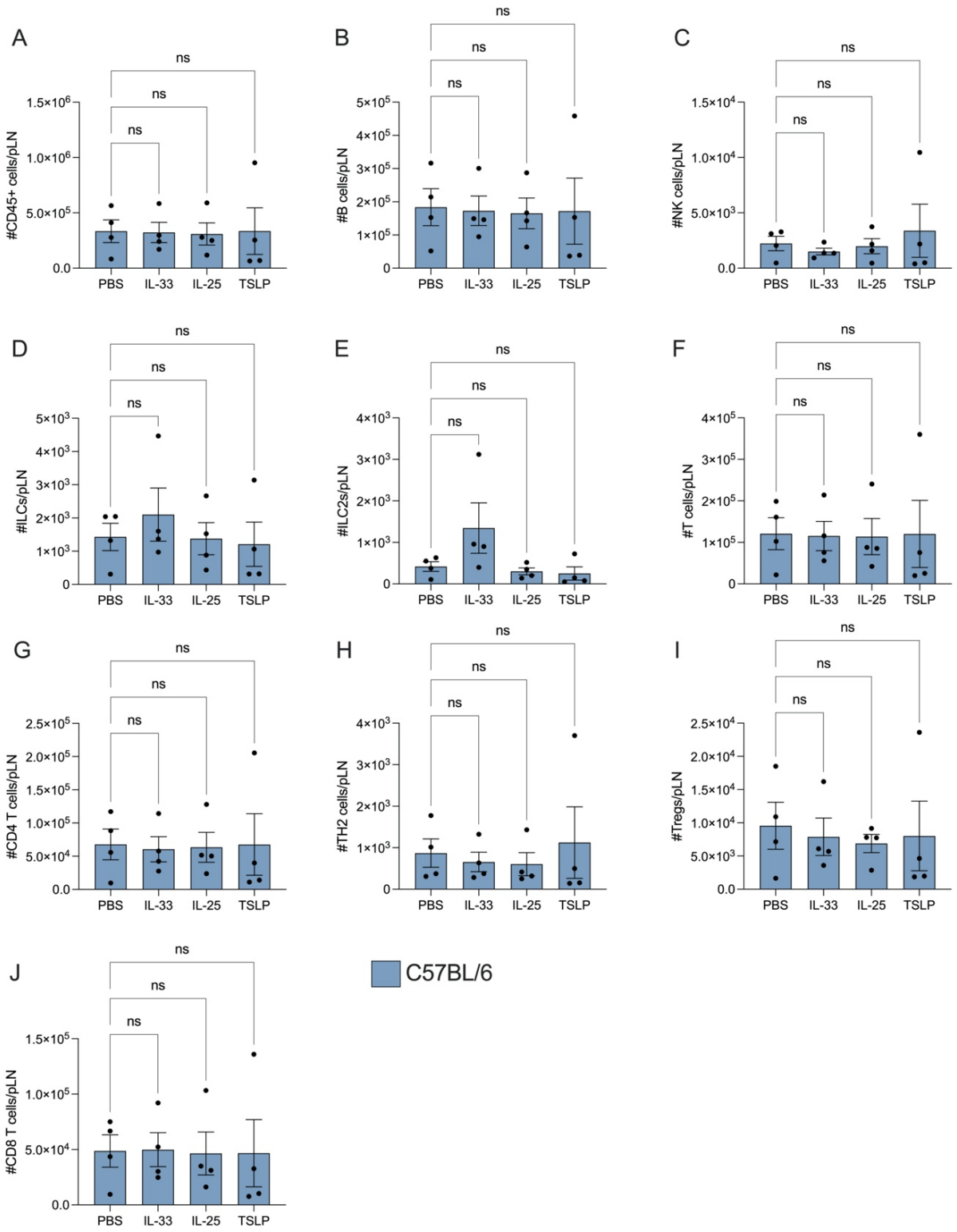

Figure S2 - IL-33 does not induce Type II inflammatory changes in the lymphoid compartment in pancreatic lymph nodes (pLN). A-J C57BL/6 mice were treated with 200ng recombinant IL-33, IL-25 or TSLP intraperitoneally on days 0 and 1 and were sacrificed on day 3 using flow cytometery (n=5). A-H, Quantification of number if CD45+ cells, B cells, NK cells, ILCs, ILC2s, T cells, CD4 T cells, TH2 cells, Tregs and CD8 T cells in the pancreas. A-H, Bar graphs indicate the mean (± s.e.m.) and show results from one experiment. A-H, Statistical significance was calculated using one-way ANOVA. ns=non significant.

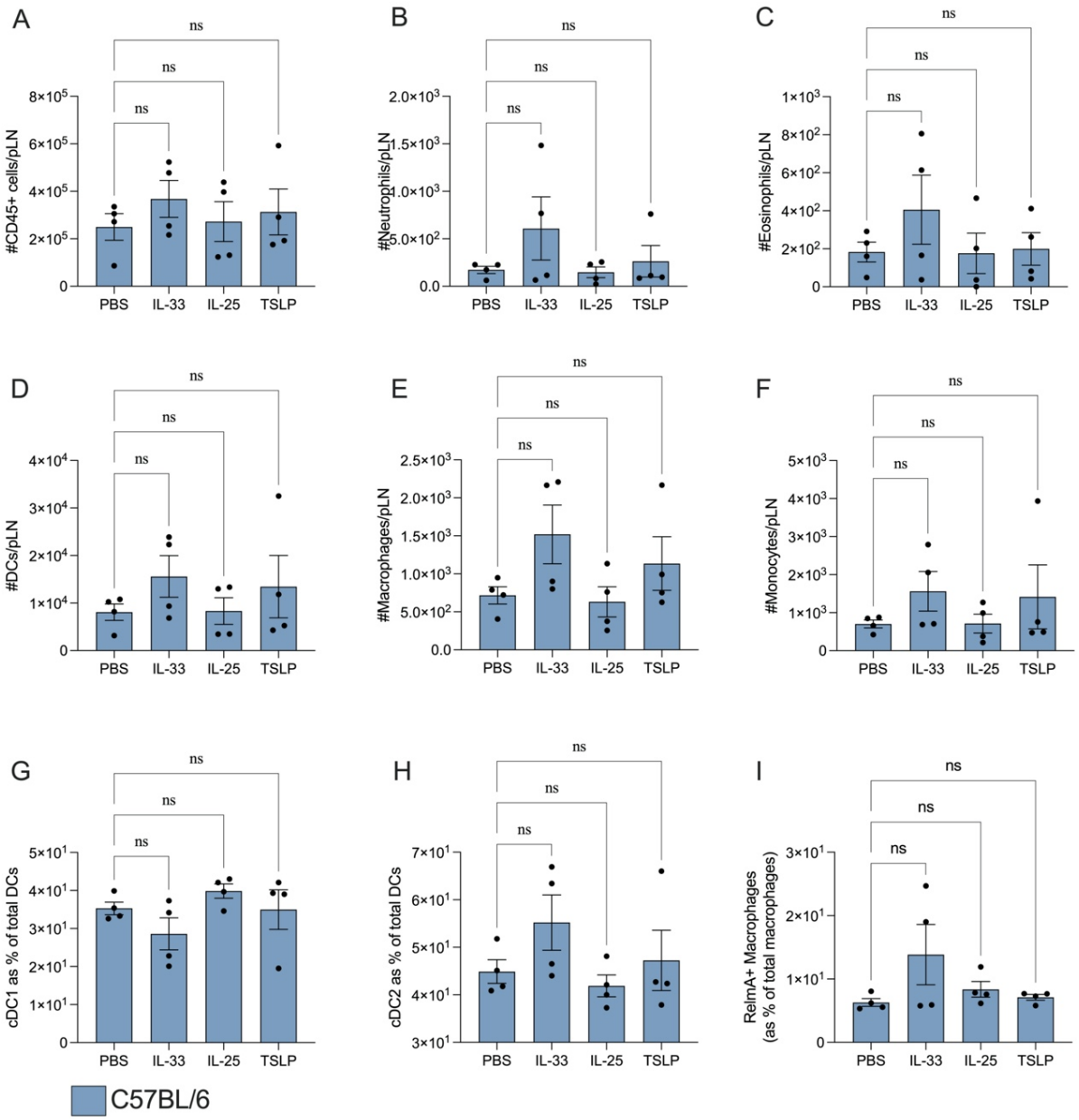

Figure S3 - IL-33 does not induce Type II inflammatory changes in the myeloid compartment in the pancreatic lymph nodes (pLN). C57BL/6 mice were treated with 200ng recombinant IL-33, IL-25 or TSLP intraperitoneally on days 0 and 1 and were sacrificed on day 3 followed by quantification of myeloid cell numbers from pLN bt flow cytometery (n=5). A-H, Quantification of CD45+ cells, neutrophils, eosinophils, DCs, macrophages, monocytes, cDC1s and cDC2s (% of total DCs) and relmA+ macrophages (% of total macrophages). A-H, Bar graphs indicate the mean (± s.e.m.) and the results are from one experiment. A-H, Statistical significance was calculated using one-way ANOVA. ns=non significant.

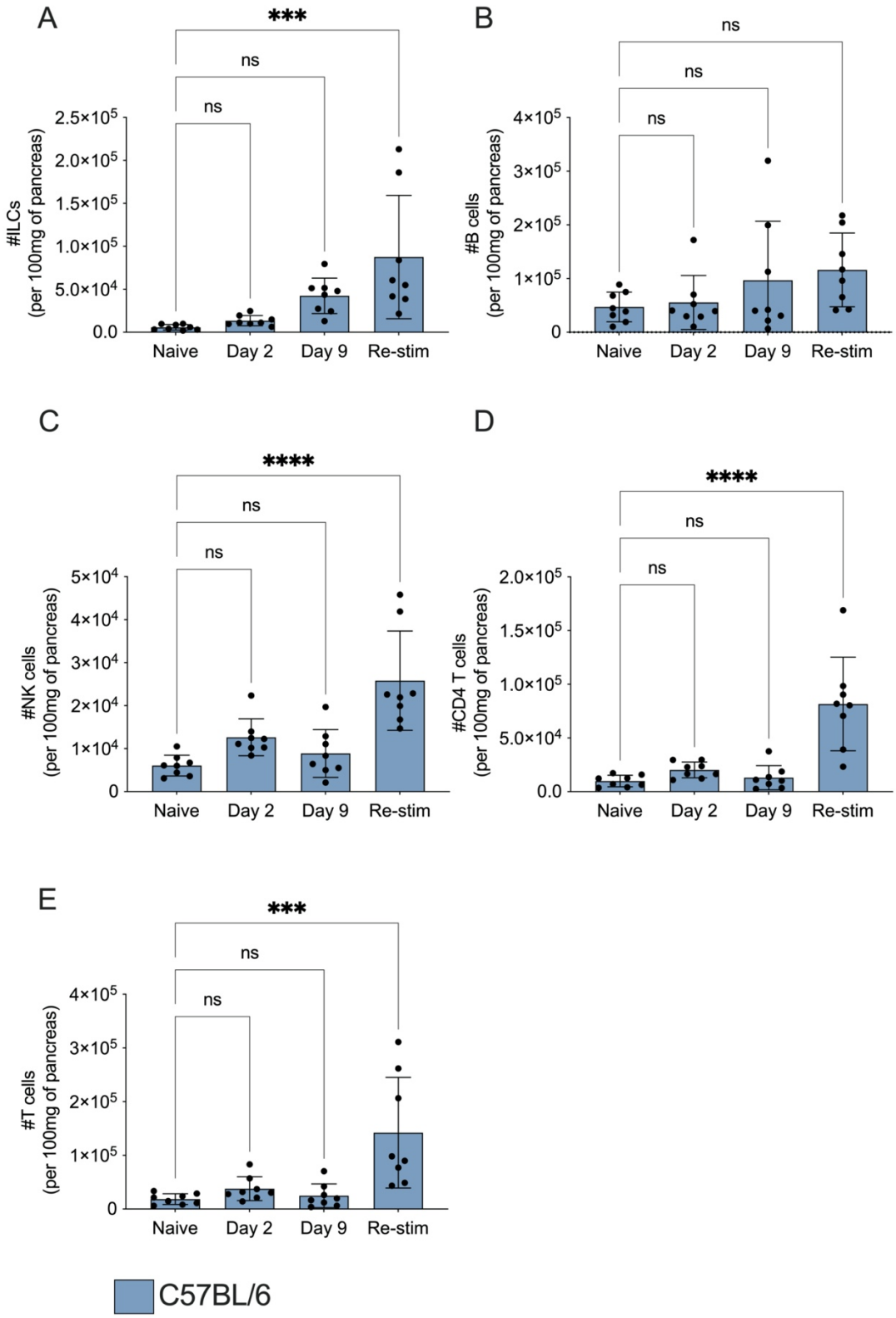

Figure S4 – Re-stimulation with IL-33 leads to expansion of lymphoid cells C57BL/6 mice were treated with 200ng recombinant IL-33 intraperitoneally either on 0 and 1 and sacrificed on day 2 and day 9, or on day 0,1,7 and 8 and were killed on day 9 (re-stim). This was followed by quantification of lymphoid cells in the pancreas by flow cytometery (n=7,8,8,8). A-E – Quantification of number of ILCs, B cells, NK cells, CD4 T cells and T cells respectively in the pancreas. Bar graphs indicate the mean (± s.e.m.) and show combined results from two experiments. Statistical significance was calculated using one-way ANOVA. ns=non significant. *= P≤0.05, **= P≤0.01, ***= P≤0.001, ****=P≤0.0001.

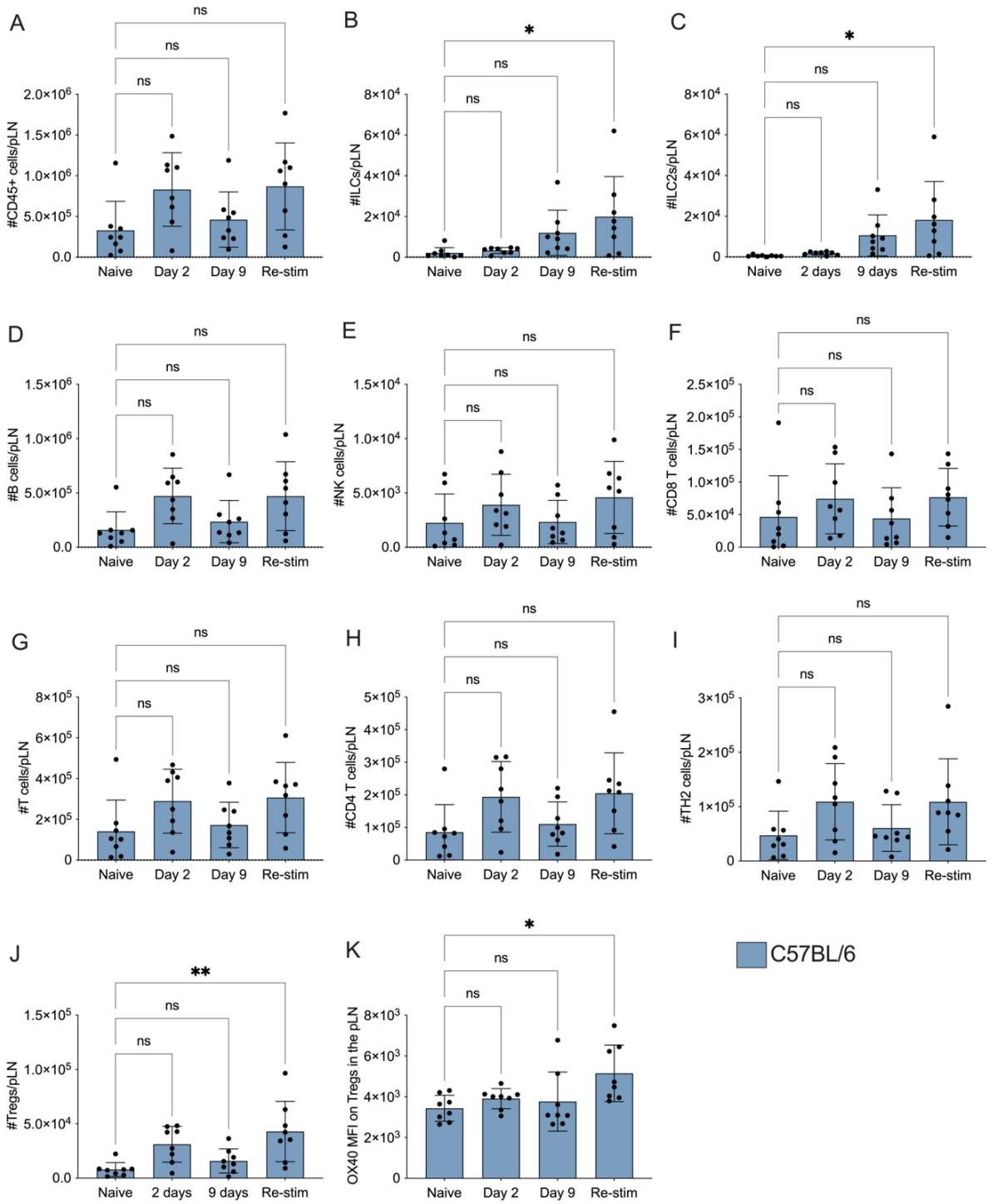

Figure S5 – Re-stimulation with IL-33 leads to expansion of Tregs in the pancreatic lymph node. C57BL/6 mice were treated with 200ng recombinant IL-33 intraperitoneally either on 0 and 1 and sacrificed on day 2 and day 9, or on day 0,1,7 and 8 and were killed on day 9 (re-stim). This was followed by quantification of lymphoid cells and OX40 MFI on Tregs in the pLN by flow cytometery (n=7,8,8,8). A-J – Quantification of number of CD45+ immune cells, ILCs, ILC2s, B cells, NK cells, CD8 T cells, T cells, CD4 T cells, TH2 cells and Tregs respectively in the pancreas. K, MFI of OX40-BV786 on Tregs in the pLN. Bar graphs indicate the mean (± s.e.m.) and show combined results from two experiments. Statistical significance was calculated using one-way ANOVA. ns=non significant. *= P≤0.05, **= P≤0.01, ***= P≤0.001, ****=P≤0.0001.

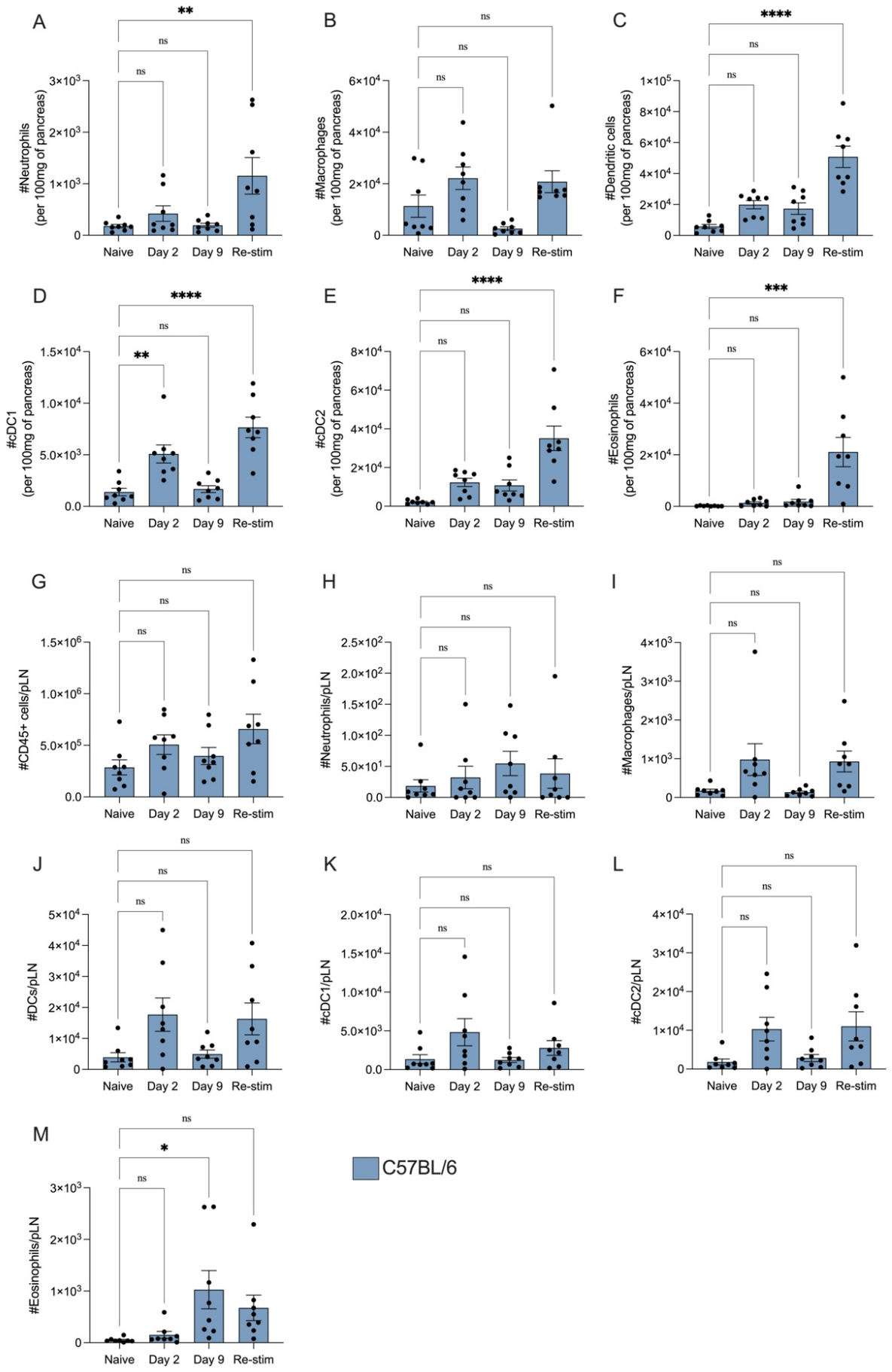
A
#Neutrophils (per 100mg of pancreas)
B
#Macrophages (per 100mg of pancreas)
C
#Dendritic cells (per 100mg of pancreas)
D
#cDC1 (per 100mg of pancreas)
E
#cDC2 (per 100mg of pancreas)
F
#Eosinophils (per 100mg of pancreas)
G
#CD45+ cells/pLN
H
#Neutrophils/pLN
I
#Macrophages/pLN
J
#DCs/pLN
K
#cDC1/pLN
L
#cDC2/pLN
M
#Eosinophils/pLN
Naive
Day 2
Day 9
Re-stim
ns
C57BL/6

Figure S6 – Re-stimulation with IL-33 leads to expansion of myeloid cells in the pancreas. . C57BL/6 mice were treated with 200ng recombinant IL-33 intraperitoneally either on 0 and 1 and sacrificed on day 2 and day 9, or on day 0,1,7 and 8 and were killed on day 9 (re-stim). This was followed by quantification of myeloid cells and in the pancreas by flow cytometery (n=7,8,8,8). A-F – Quantification of number of neutrophils, macrophages, DCs, cDC1s, cDC2s and eosinophils respectively in the pancreas. J-M, Quantification of DCs, cDC1s, cDC2s and eosinophils in the pLN. Bar graphs indicate the mean (± s.e.m.) and show combined results from two experiments. Statistical significance was calculated using one-way ANOVA. ns=non significant. *= P≤0.05, **= P≤0.01, ***= P≤0.001, ****=P≤0.0001.

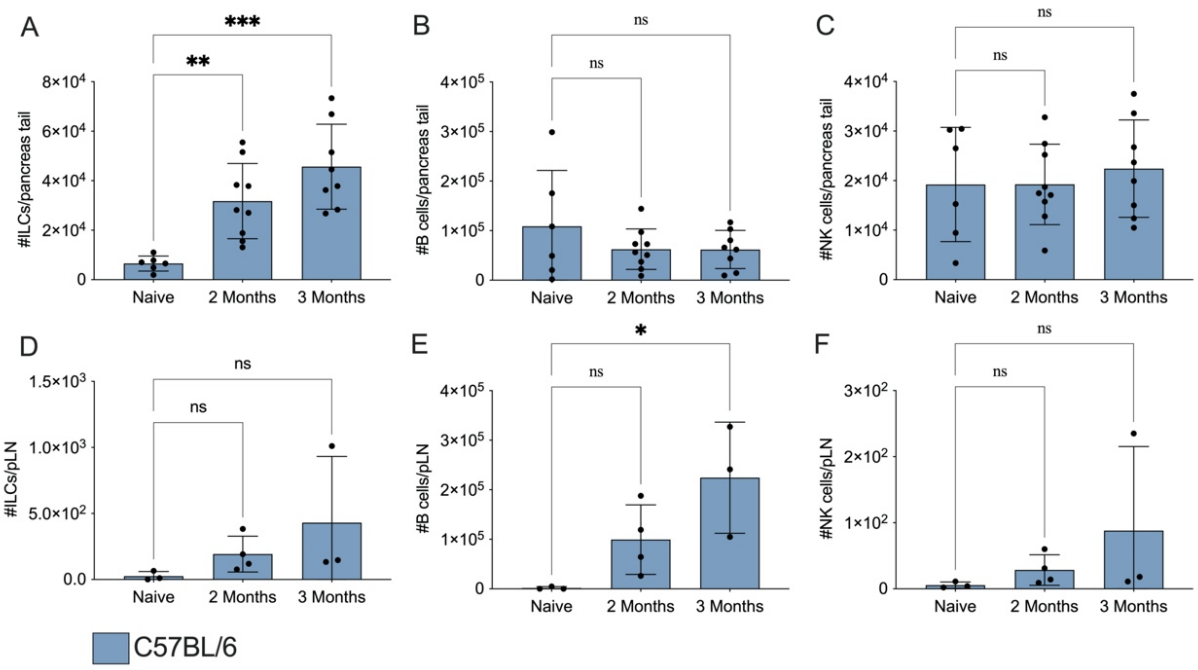

Figure S7 - IL-33 induced ILC expansion in the pancreas is sustained long term. C57BL/6 mice were treated with 200ng recombinant IL-33 intraperitoneally on day 0 and 1 and sacrificed 2 or 3 months after administration. This was followed by quantification of lymphoid cells in the pancreas (n=6) and pLN (n=3) by flow cytometery. A,B,C– Quantification of number of ILCs, B cells and NK cells respectively in the pancreas. D,E,G Quantification of ILCs, B cells and NK cells in the pLN. A,B,C, Bar graphs indicate the mean (± s.e.m.) and show combined results from two experiments. D,E,F, Bar graphs indicate the mean (± s.e.m.) and is representative of one experiment. Statistical significance was calculated using one-way ANOVA. ns=non significant. *= P≤0.05, **= P≤0.01, ***= P≤0.001, ****=P≤0.0001.

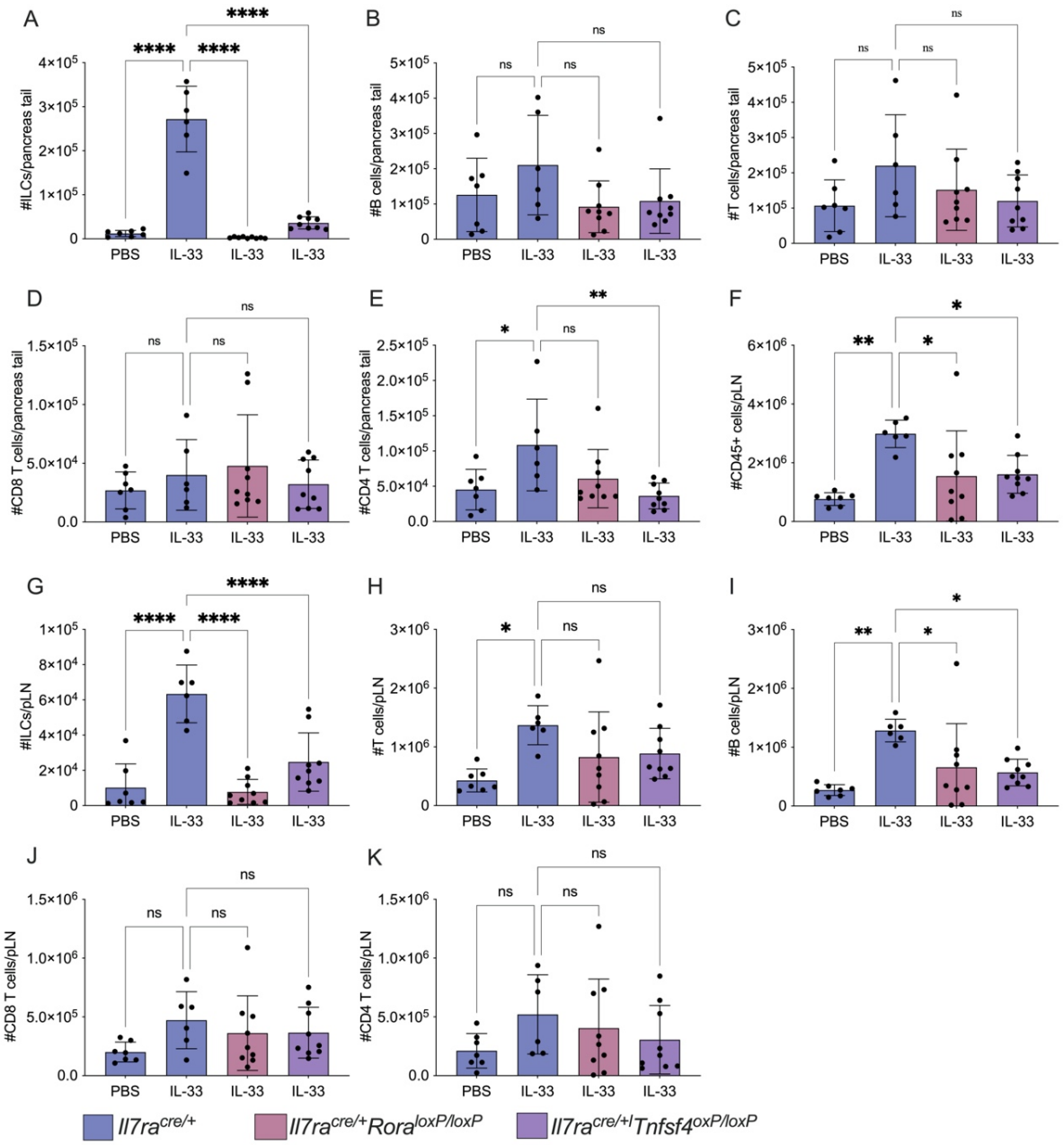

Figure S8 – IL-33 induced expansion of B cells in the pancreatic lymph node is ILC2 and OX40L dependent. *IL7Ra$^{cre/+}$, IL7ra$^{cre/+}$Rora$^{loxP/loxP}$ and IL7Ra$^{cre/+}$ Tnfsf4$^{loxP/loxP}$* mice were treated with 200ng recombinant IL-33 on days 0 and 1 and sacrificed on day 5. This was followed by quantification of lymphoid cell numbers in the pancreas and pancreas lymph node (n=6,6,9,8) by flow cytometery. A-E, Quantification of the number ILCs, B cells, T cells, CD8 T cells and CD4 T cells in the pancreas respectively. F-K, Quantification of the number of CD45+ immune cells, ILCs, T cells, B cells, CD8 T cells and CD4 T cells in the pancreatic lymph nodes respectively. A-K, Bar graphs indicate the mean (± s.e.m.) and show combined results from two experiments. Statistical significance was calculated using one-way ANOVA. ns=non significant. *= P≤0.05, **= P≤0.01, ***= P≤0.001, ****=P≤0.0001.

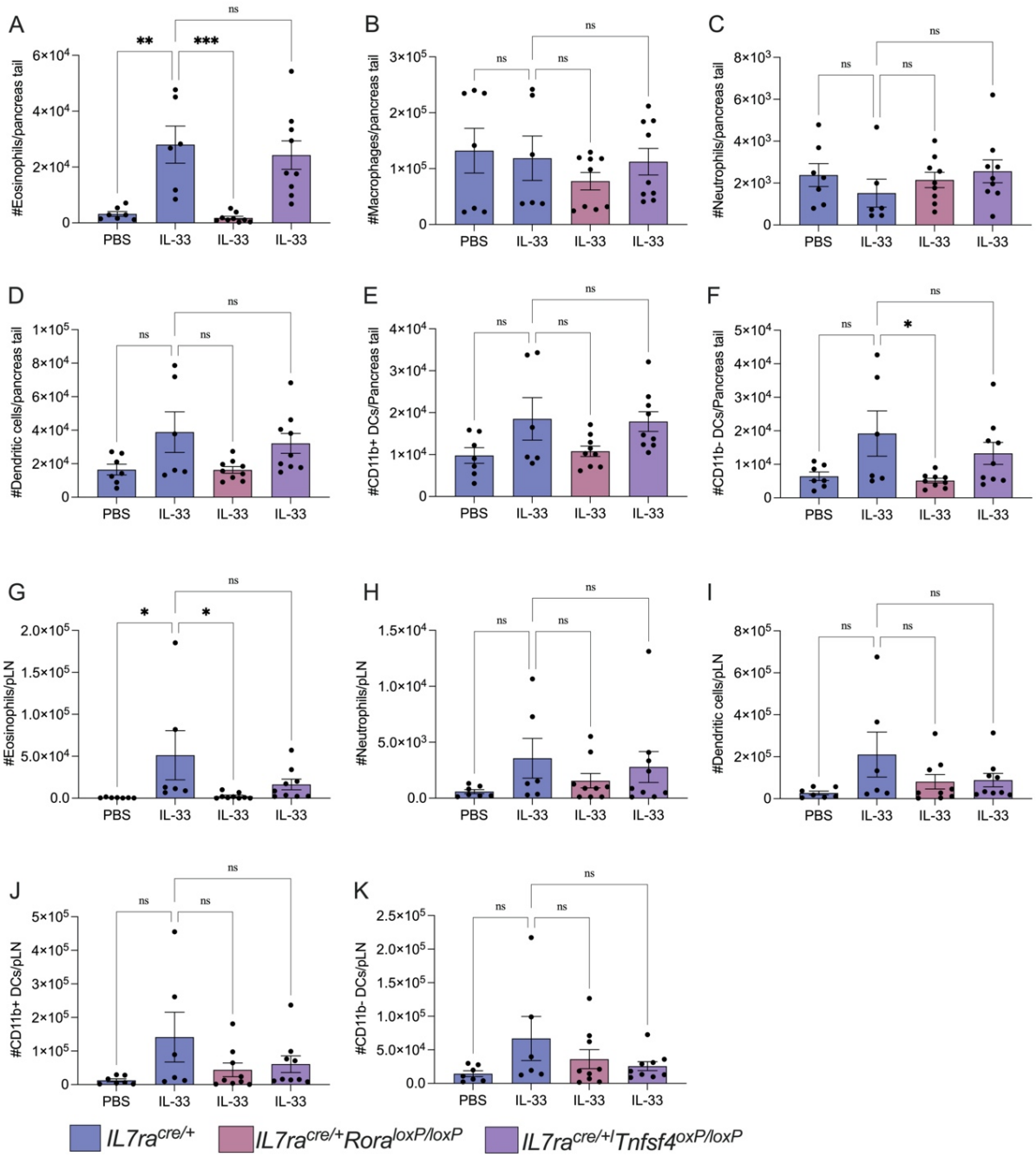

Figure S9 – IL-33 induced eosinophilia in the pancreas and pLN are ILC2 dependent. *IL7Ra$^{cre/+}$, IL7ra$^{cre/+}$Rora$^{loxP/loxP}$ and IL7Ra$^{cre/+}$ Tnfsf4$^{loxP/loxP}$* mice were treated with 200ng recombinant IL-33 on days 0 and 1 and were sacrificed on day 5. This was followed by quantification of myeloid cell numbers in the pancreas and pancreas lymph node (n=6,6,9,8) by flow cytometery. A-F, Quantification of the number Eosinophils, Macrophages, Neutrophils, Dendritic cells (DCs), CD11b+ DCs cells and CD11b0- DCs in the pancreas respectively. G-K, Quantification of the number of eosinophils, neutrophils, DCs, CD11b+ DCs and CD11b- DCs in the pancreatic lymph nodes respectively. A-K, Bar graphs indicate the mean (± s.e.m.) show combined results from two experiments. Statistical significance was calculated using one-way ANOVA. ns=non significant. *= P≤0.05, **= P≤0.01, ***= P≤0.001, ****=P≤0.0001.

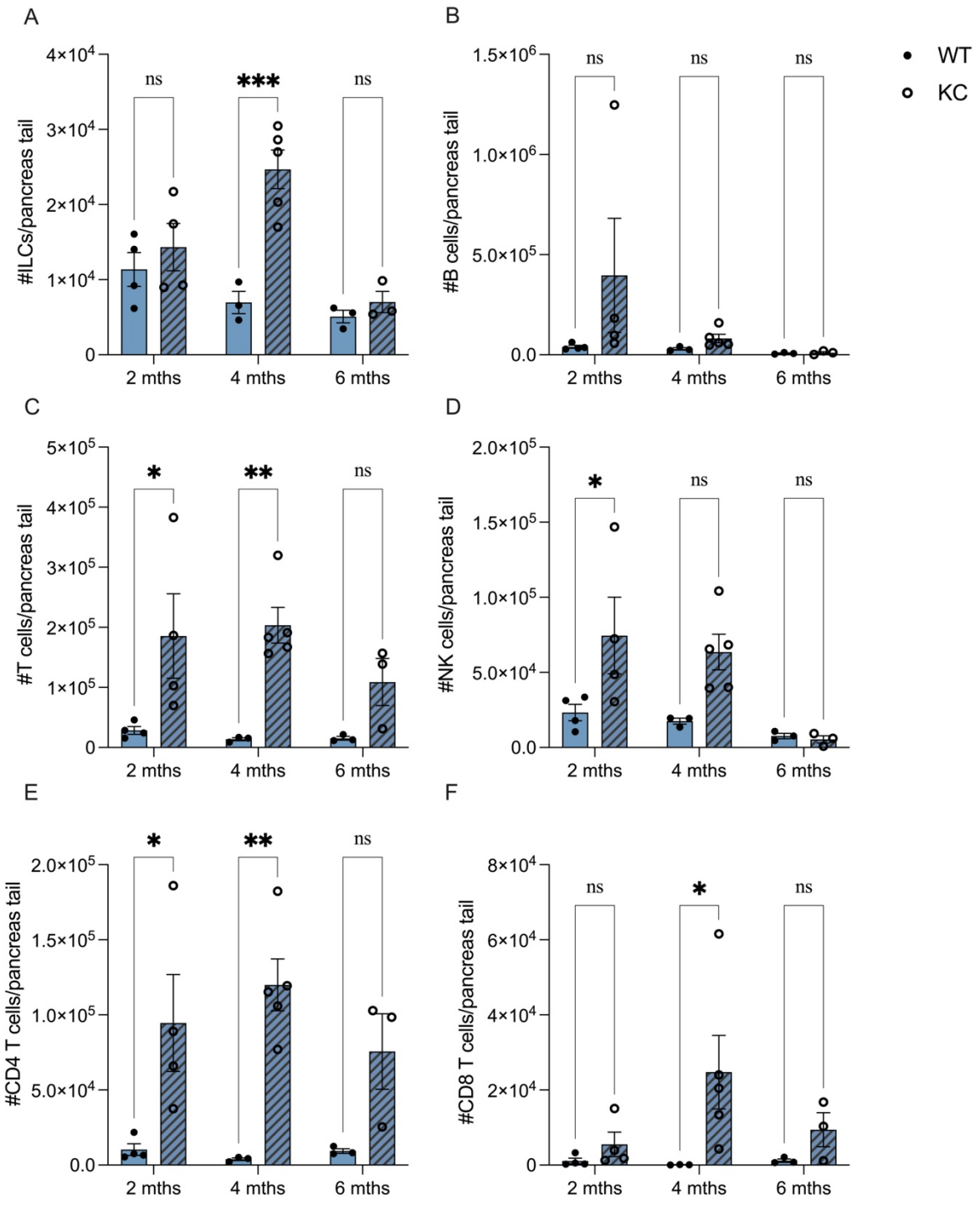

Figure S10 – ILC and CD4 T cell numbers are increased in panINs. Pancreas from KC mice were collected at 2, 4 and 6 months of age and lymphoid immune cells were quantified (n=4,4,3,5,3,3) by flow cytometery. A-F, Quantification of ILCs, B cells, T cells, NK cells, CD4 T cells and CD8 T cells in the pancreas. A-F, Bar graphs indicate the mean (± s.e.m.) and show results 3 individual experiments. Statistical significance was calculated using two-way ANOVA. ns=non significant. *= P≤0.05, **= P≤0.01, ***= P≤0.001, ****=P≤0.0001.

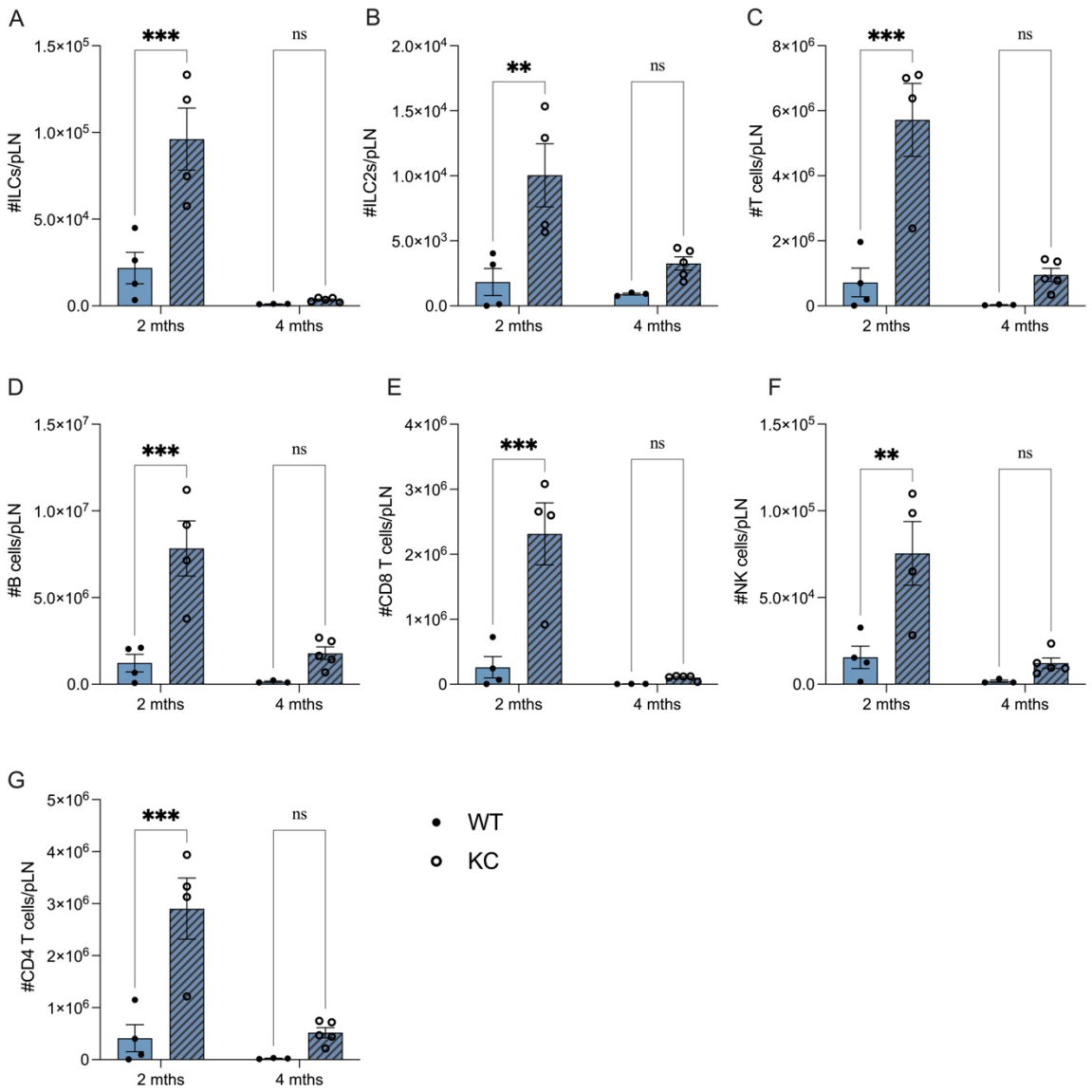

Figure S11 – Lymphoid immune cell numbers are increased in pLN of mice with panINs. pLN from KC mice were collected at 2 and 4 months of age and lymphoid immune cells were quantified (n=4,4,3,5) by flow cytometery. A-G, Quantification of ILCs, ILC2s, T cells, B cells, CD8 T cells, NK cells and CD4 T cells in the pLN. A-G, Bar graphs indicate the mean (± s.e.m.) and show results 2 individual experiments. Statistical significance was calculated using two-way ANOVA. ns=non significant. *= P≤0.05, **= P≤0.01, ***= P≤0.001, ****=P≤0.0001.

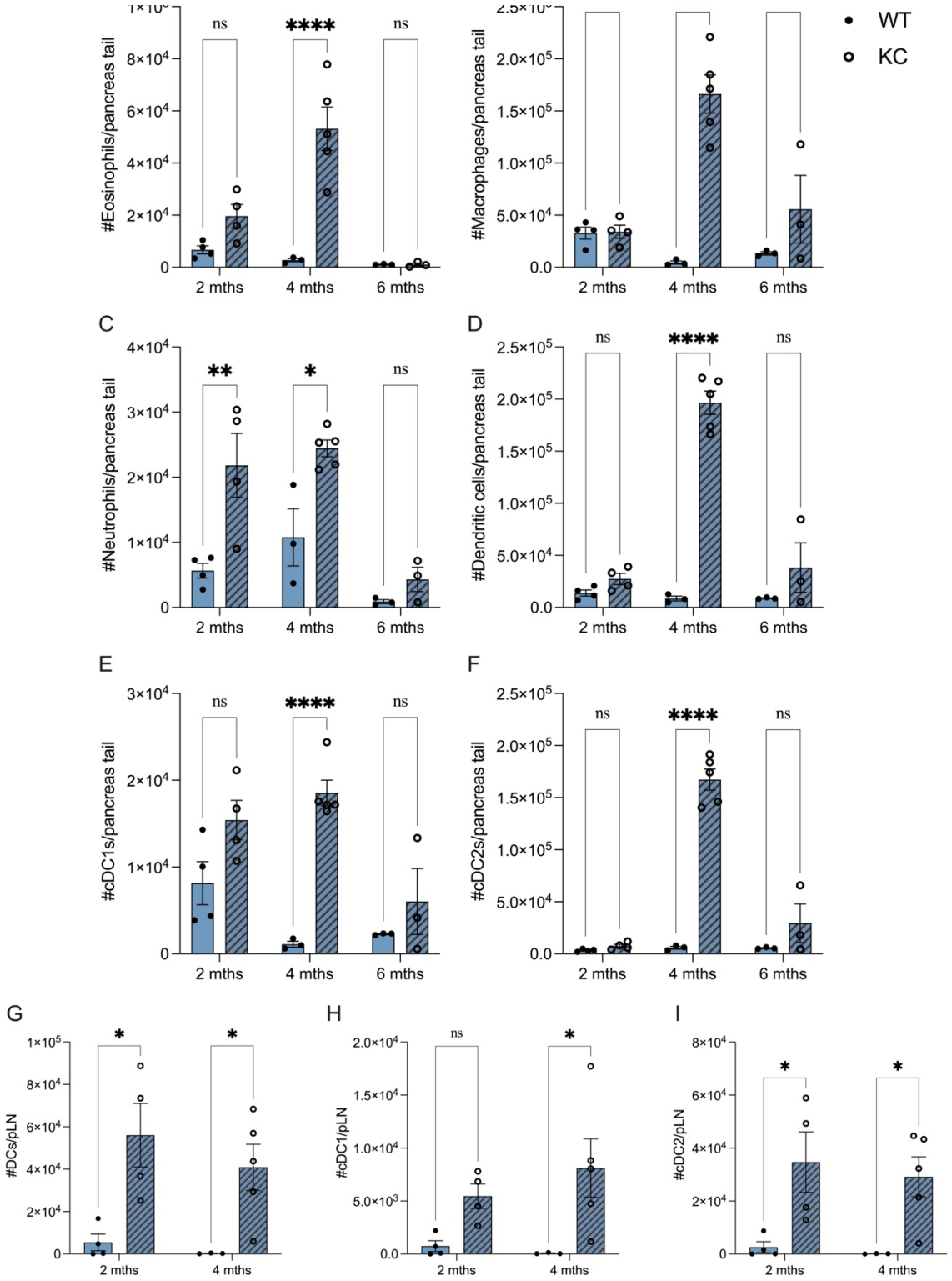

Figure S12 - Myeloid immune cell numbers are increased in panINs and pLN of mice with panINs. Pancreas and pLN from KC mice were collected at 2 and 4 months of age and myeloid immune cells were quantified (n=4,4,3,5) by flow cytometery. A-F, Quantification of eosinophils, macrophages, neutrophils, DCs, cDC1s and cDC2s in the pancreas. G-I, Quantification of DCs, cDC1s and cDC2s in the pLN. A-I, Bar graphs indicate the mean (± s.e.m.) and show results 2 individual experiments. Statistical significance was calculated using two-way ANOVA. ns=non significant. *= P≤0.05, **= P≤0.01, ***= P≤0.001, ****=P≤0.0001.

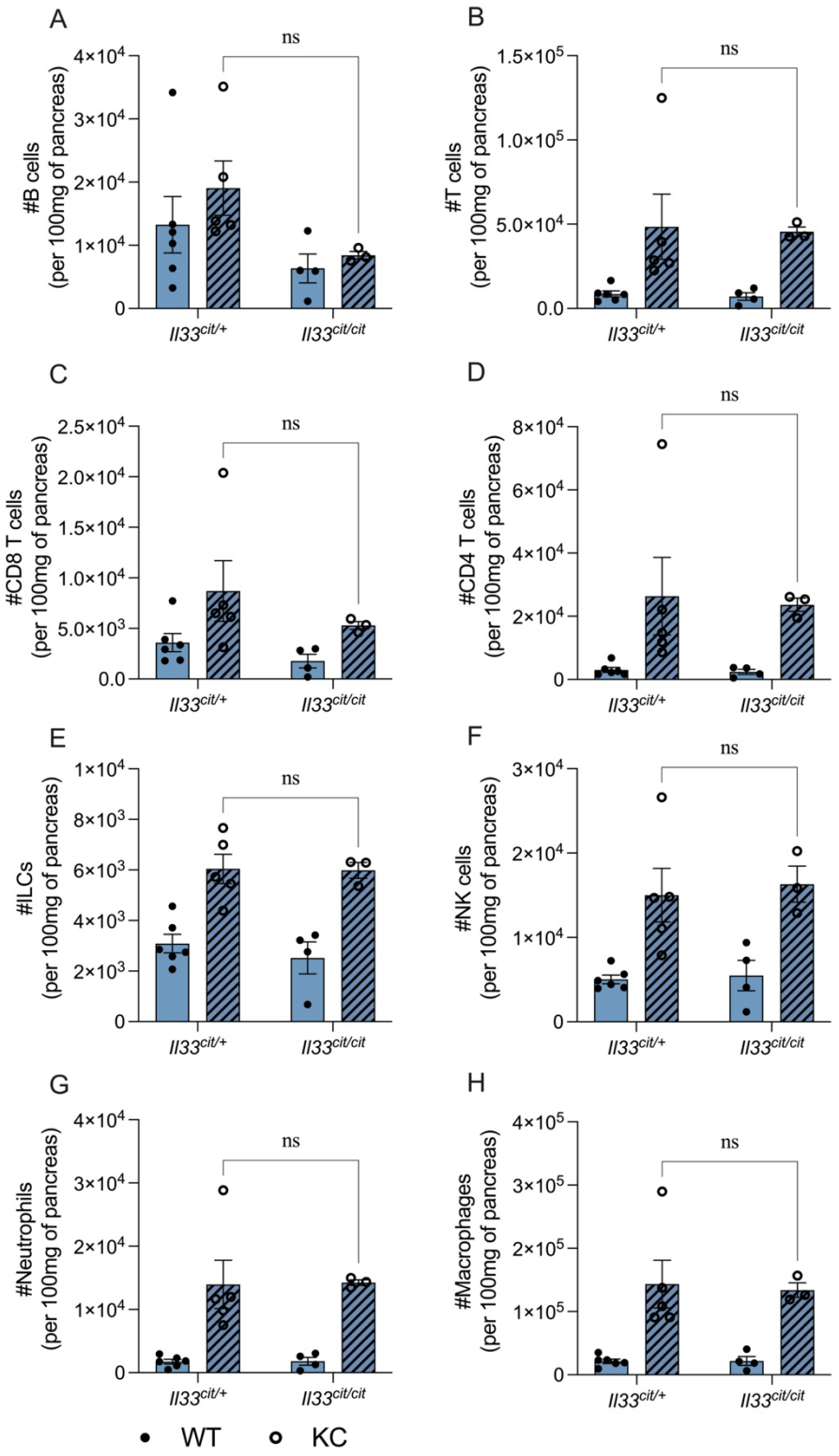

Figure S13 – Immune cell influx in panINs is not IL-33 dependent. Pancreas from KC mice with or without IL-33 expression (IL-33$^{cit/+}$ or IL-33$^{cit/cit}$) were collected at 3 months of age and immune cells were quantified (n=4,3,6,5) by flow cytometery. A-H, Quantification of B cells, T cells, CD8 T cells, NK cells, ILCs, Neutrophils, CD4 T cells and Macrophages in the pancreas. A-H, Bar graphs indicate the mean (± s.e.m.) and show results of 1 experiment. Statistical significance was calculated using two-way ANOVA. ns=non significant. *= P≤0.05, **= P≤0.01, ***= P≤0.001, ****=P≤0.0001.

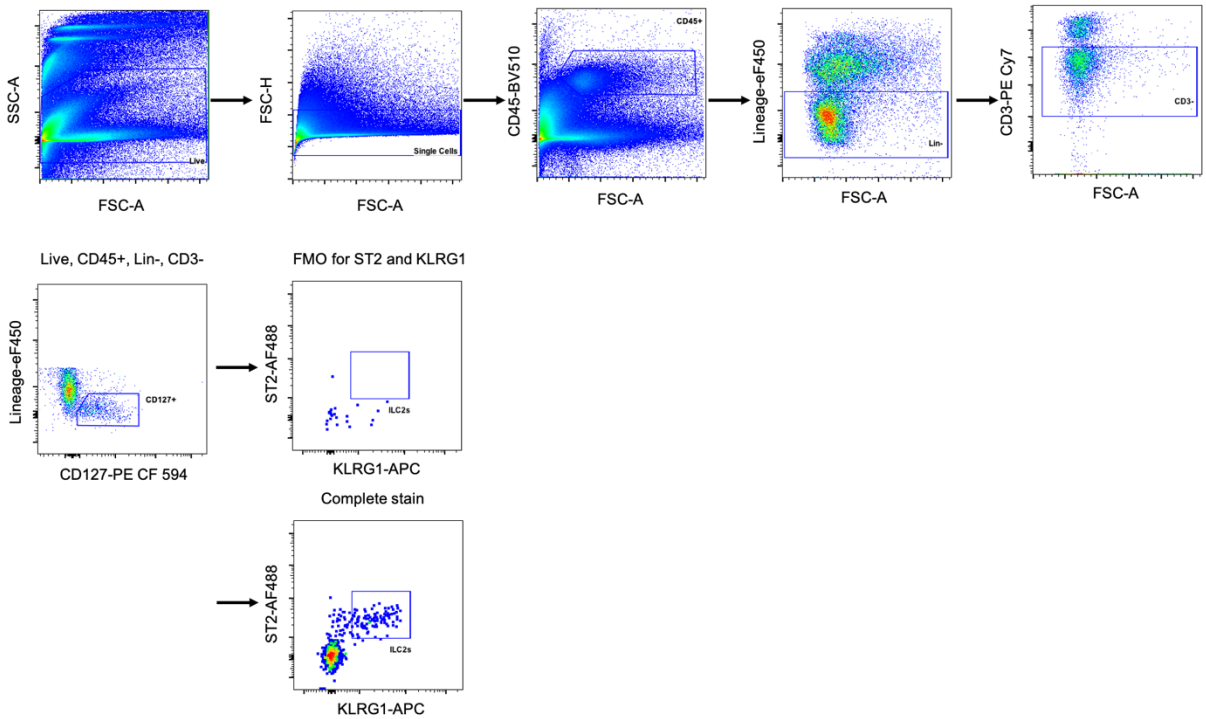

Figure S14 – Representative gating strategy for sorting of ILC2s from the pancreas. C57BL/6 mice were treated with 200ng recombinant IL-33 intraperitoneally on days 0 and 1 and were sacrificed on day 3 followed sorting of ILC2s. ILC2s were identified as Live, single cells, CD45+, Lineage – (lineage = CD5, CD11b, CD11c, Gr-1, Ter119, CD19, F4/80, FcERa, NK1.1, B220), CD3-, CD127+, ST2+ and KLRG1+.

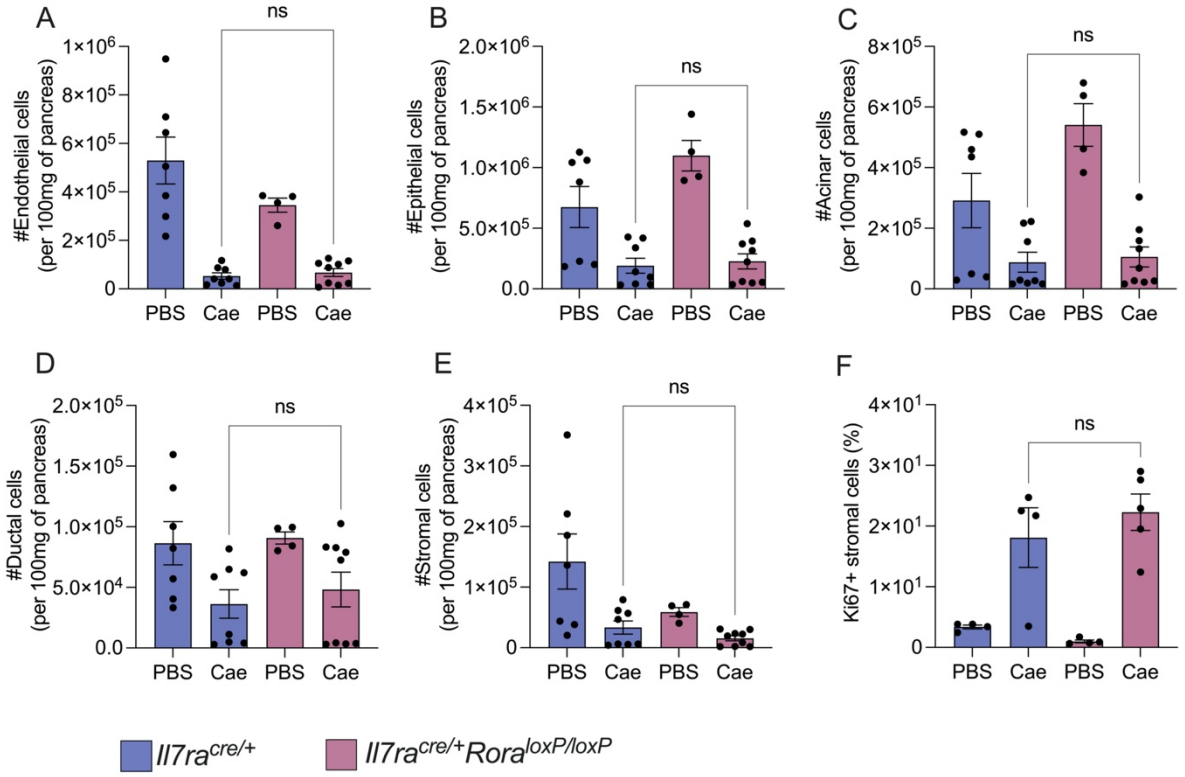

Figure S15 – ILC2 deficient mice do not show any changes in the stromal/epithelial compartment. *Il7ra*$^{cre/+}$ (control) or *Il7ra*$^{cre/+}$ *Rora*$^{loxP/loxP}$ (ILC2 deficient) mice were injected with 50ug/Kg of caerulein sacrificed at 24 hours after first caerulein injection. This was followed by quantification of non-immune in the pancreas using flow cytometry. Bar graphs indicate the mean (± s.e.m.) and show data from two independent experiments. Statistical significance was calculated using one-way ANOVA. ns=non significant. *= P≤0.05, **= P≤0.01, ***= P≤0.001, ****=P≤0.0001.

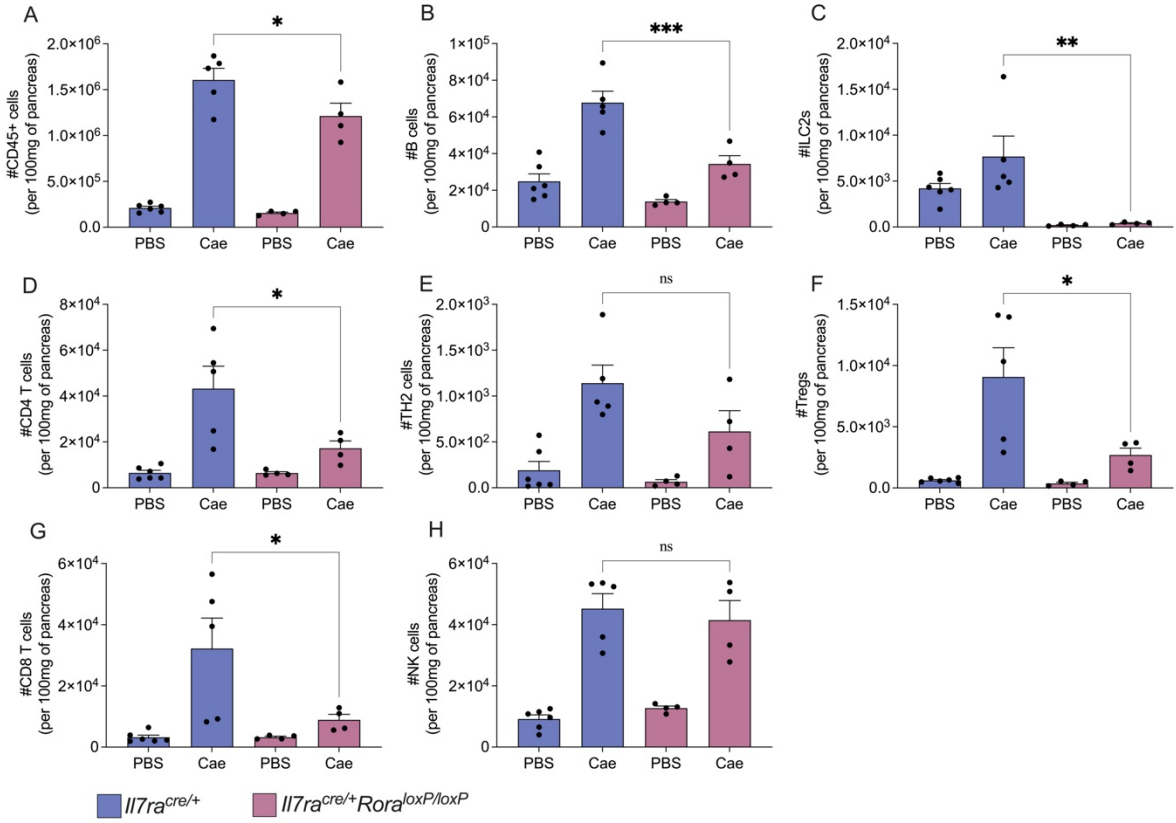

Figure S16 – ILC2 deficient mice show reduction in Tregs, CD8 T cells and B cells during pancreatitis recovery. *Il7ra*$^{cre/+}$ (control) or *Il7ra*$^{cre/+}$ *Rora*$^{loxP/loxP}$ (ILC2 deficient) mice were injected with 75ug/Kg of caerulein on day 0 and day 1 and sacrificed 3 days after induction of pancreatitis. This was followed by quantification of immune cells in the pancreas using flow cytometry. Bar graphs indicate the mean (± s.e.m.) and show data from one experiment. Statistical significance was calculated using one-way ANOVA. ns=non significant. *= P≤0.05, **= P≤0.01, ***= P≤0.001, ****=P≤0.0001.

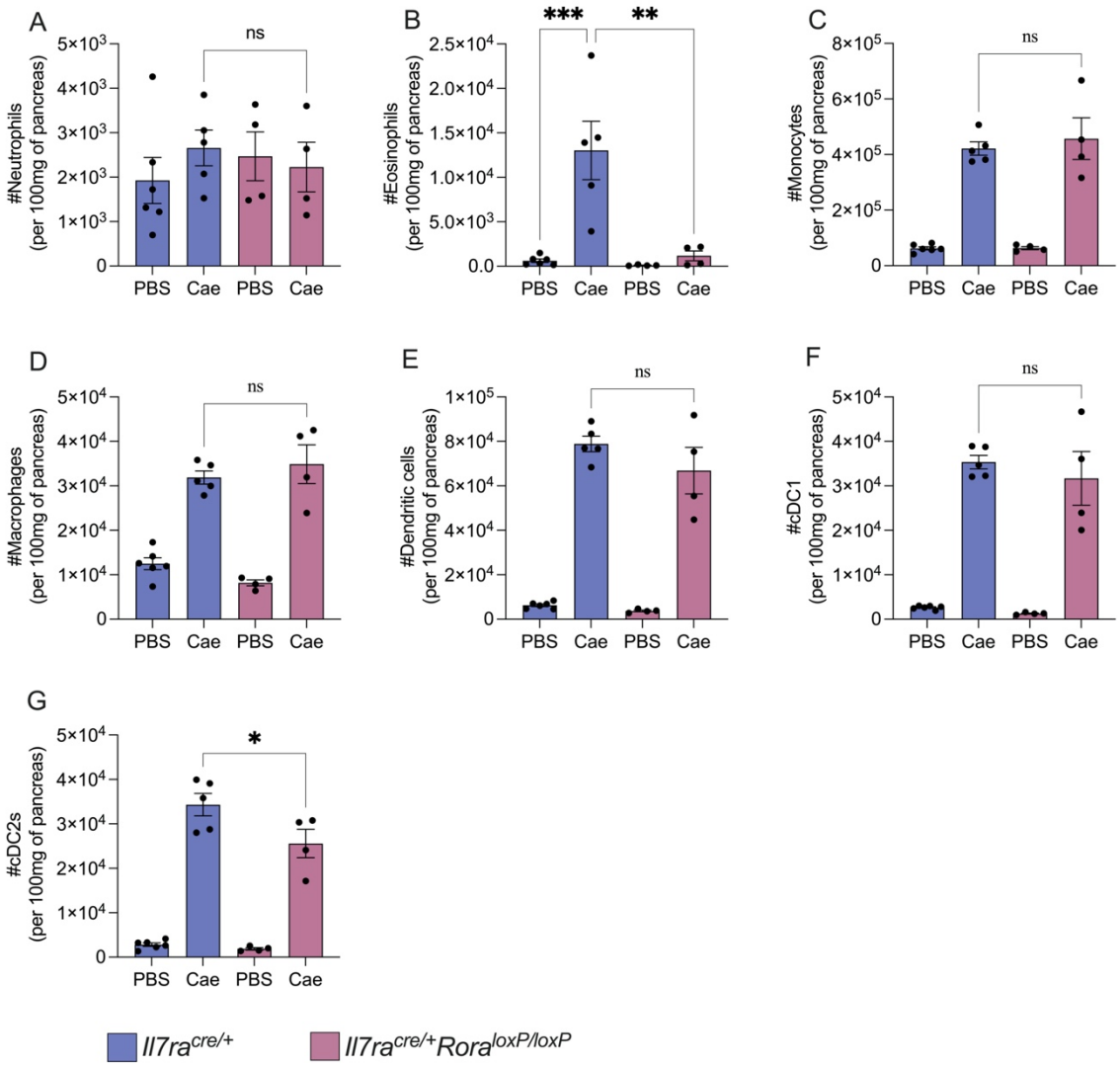

Figure S17 – ILC2 deficient mice show reduction in eosinophil and cDC2 numbers during pancreatitis recovery. *Il7ra*$^{cre/+}$ (control) or *Il7ra*$^{cre/+}$ *Rora*$^{loxP/loxP}$ (ILC2 deficient) mice were injected with 75ug/Kg of caerulein on day 0 and day 1 and sacrificed on 3 days after induction of pancreatitis. This was followed by quantification of immune cells in the pancreas using flow cytometry. Bar graphs indicate the mean (± s.e.m.) and show data from one experiment. Statistical significance was calculated using one-way ANOVA. ns=non significant. *= P≤0.05, **= P≤0.01, ***= P≤0.001, ****=P≤0.0001.

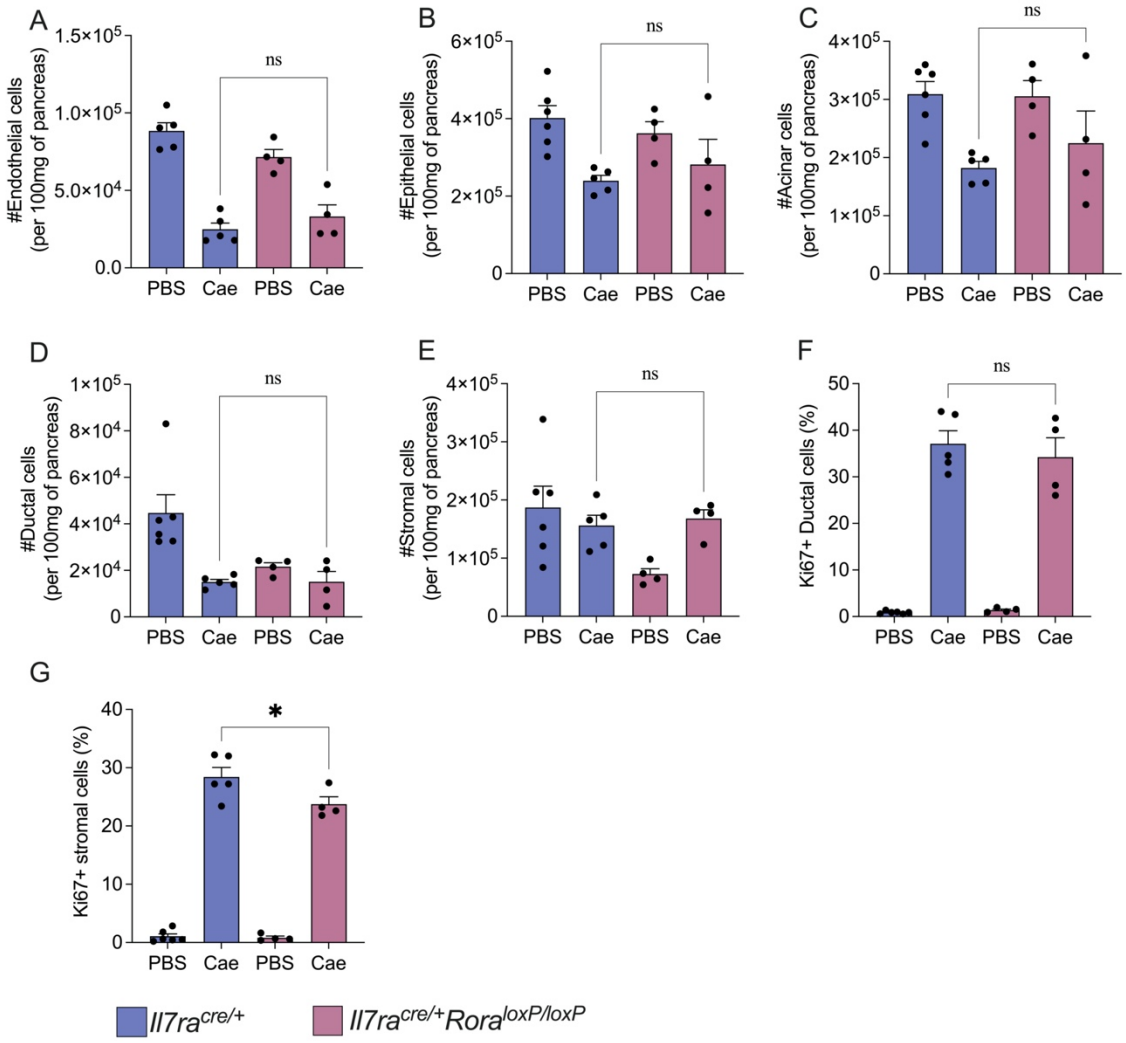

Figure S18 – ILC2 deficient mice show a reduction in cycling stromal cells during pancreatitis recovery. *Il7ra*$^{cre/+}$ (control) or *Il7ra*$^{cre/+}$ *Rora*$^{loxP/loxP}$ (ILC2 deficient) mice were injected with 75ug/Kg of caerulein on day 0 and day 1 and sacrificed on 3 days after induction of pancreatitis. This was followed by quantification of non-immune cells using flow cytometry. Bar graphs indicate the mean (± s.e.m.) and show data from one experiment. Statistical significance was calculated using one-way ANOVA. ns=non significant. *= P≤0.05, **= P≤0.01, ***= P≤0.001, ****=P≤0.0001.

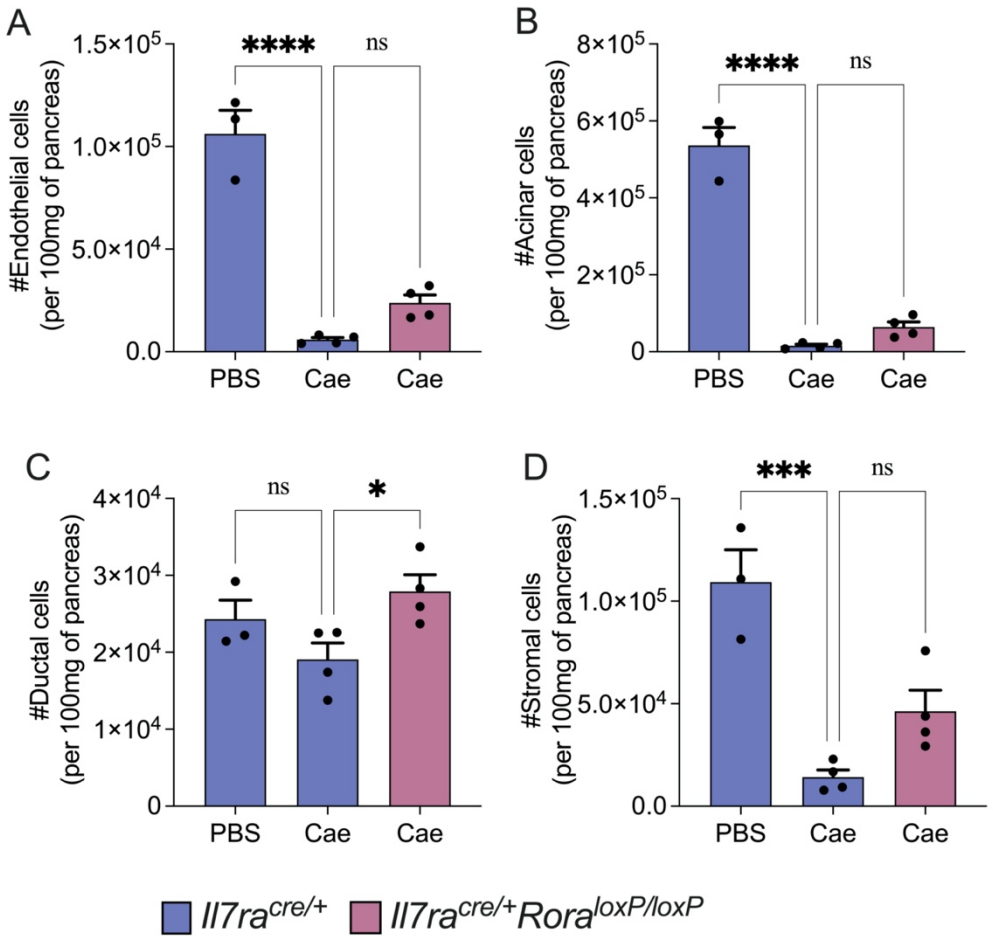

Figure S19 – ILC2 deficient mice do not show any changes in the stromal/epithelial compartment at the 6h timepoint in acute pancreatitis. *Il7ra*$^{cre/+}$ (control) or *Il7ra*$^{cre/+}$ *Rora*$^{loxP/loxP}$ (ILC2 deficient) mice were injected with 75ug/Kg of caerulein and sacrificed 6 hours after the first caerulein injection. Bar graphs indicate the mean (± s.e.m.) and show data from one experiment. Statistical significance was calculated using one-way ANOVA. ns=non significant. *= P≤0.05, **= P≤0.01, ***= P≤0.001, ****=P≤0.0001.

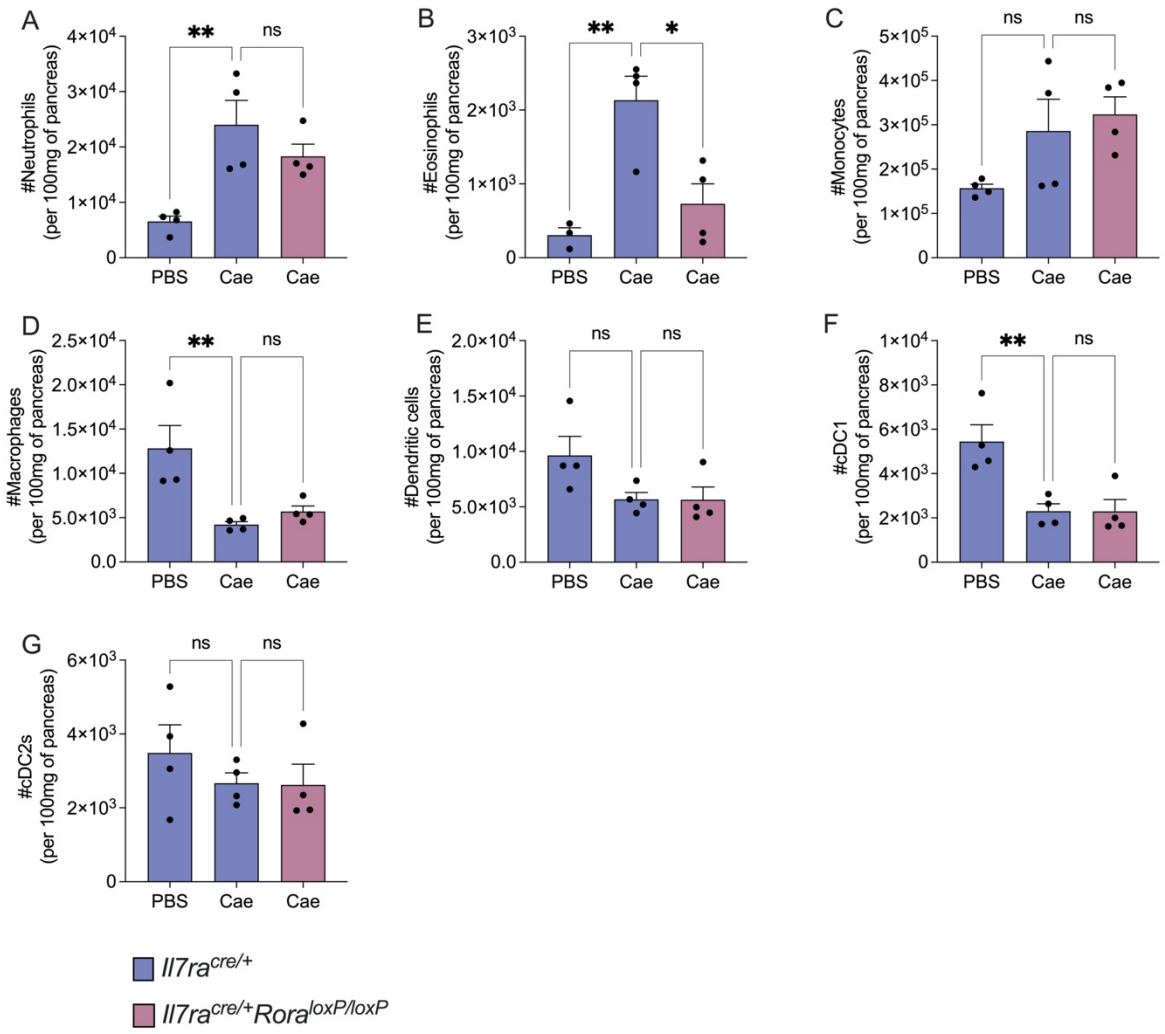

Figure S20 – ILC2 deificient mice show a reduction in eosinophil numbers at the 6h timepoint in acute pancreatitis. *Il7ra*$^{cre/+}$ (control) or *Il7ra*$^{cre/+}$ *Rora*$^{loxP/loxP}$ (ILC2 deficient) mice were injected with 75ug/Kg of caerulein and sacrificed 6 hours after the first caerulein injection. This was followed by quantification of immune cells in the pancreas using flow cytometry. Bar graphs indicate the mean (± s.e.m.) and show data from one experiment. Statistical significance was calculated using one-way ANOVA. ns=non significant. *= P≤0.05, **= P≤0.01, ***= P≤0.001, ****=P≤0.0001.

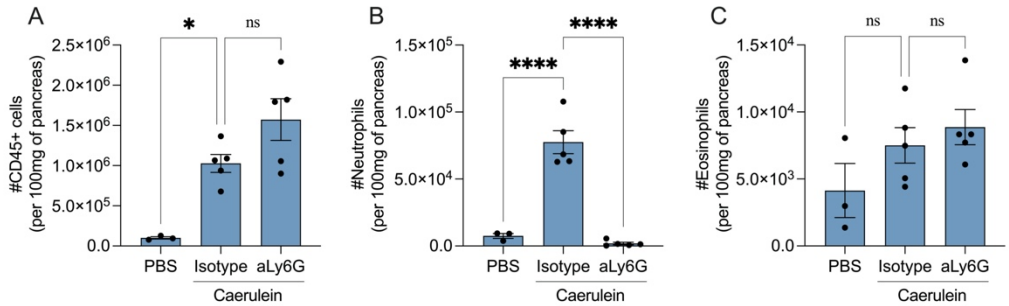

Figure S21 – aLy6G treatment leads to neutrophil depletion in the pancreas. C57BL/6 mice were treated with aLy6G (200ug) on day -1 and day 0 followed by 75ug/Kg Caerulein on day 0 and sacrificed 24h after the first caerulein injection. This was followed by quantification of immune cell numbers using flow cytometry. Bar graphs indicate the mean (± s.e.m.) and shows data from one experiment. Statistical significance was calculated using one-way ANOVA. ns=non significant. *= P≤0.05, **= P≤0.01, ***= P≤0.001, ****=P≤0.0001.

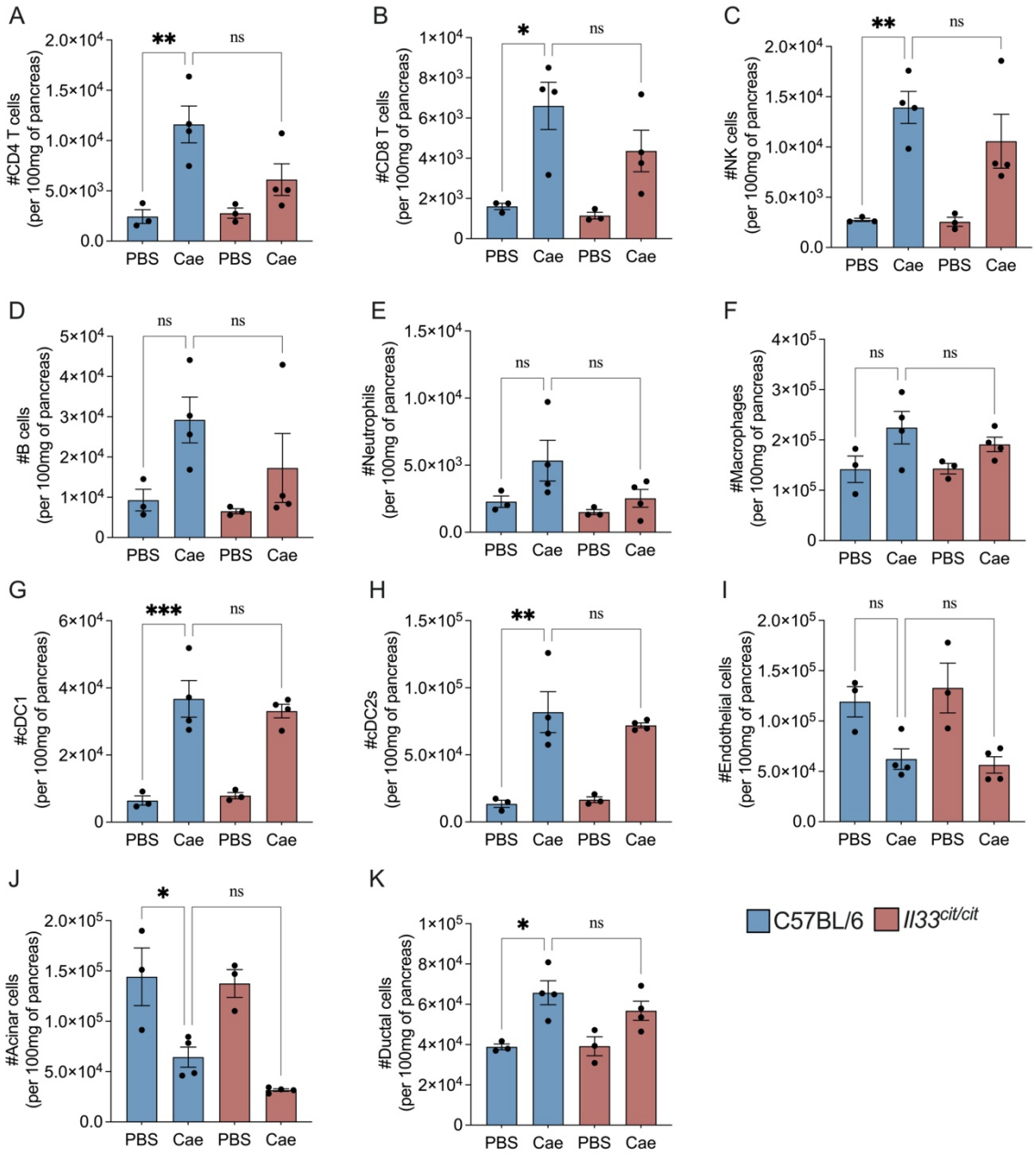

Figure S22 – IL-33 deficient mice with pancreatitis do not show any changes in other immune and non-immune cell numbers. *Il33$^{cit/cit}$* mice were injected with 50ug/Kg of caerulein on day 0 and day 1 and sacrificed 3 days after induction of pancreatitis. This was followed by quantification of immune cell numbers by flow cytometry. Bar graphs indicate the mean (± s.e.m.) and show data from one experiment. Statistical significance was calculated using one-way ANOVA. ns=non significant. *= P≤0.05, **= P≤0.01, ***= P≤0.001, ****=P≤0.0001.

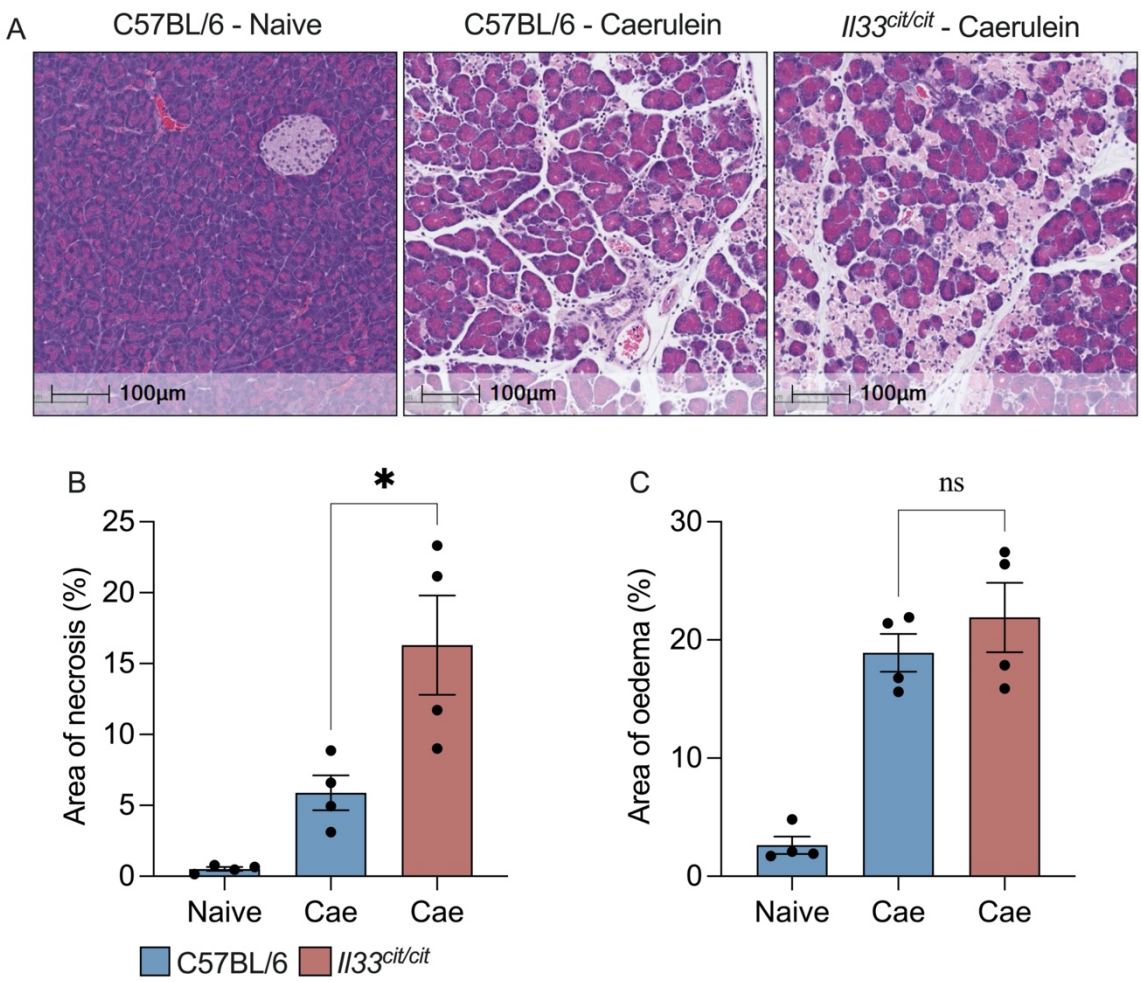

Figure S23 – IL-33KO mice show increased necrosis in acute pancreatitis. *Il33$^{cit/cit}$* mice were injected with 75ug/Kg of caerulein and sacrificed at 24h after the first caerulein injection. A, Pancreas was fixed, embedded, sectioned and stained with H&E and scanned images at 10X magnification are shown. B,C, Quantification of area of necrosis (B) and oedema (C) from images of H&E stained histological sections using the classifier function on the image analysis software Halo. Bar graphs indicate the mean (± s.e.m.) and show data from one experiment. Statistical significance was calculated using one-way ANOVA. ns=non significant. *= P≤0.05, **= P≤0.01, ***= P≤0.001, ****=P≤0.0001.

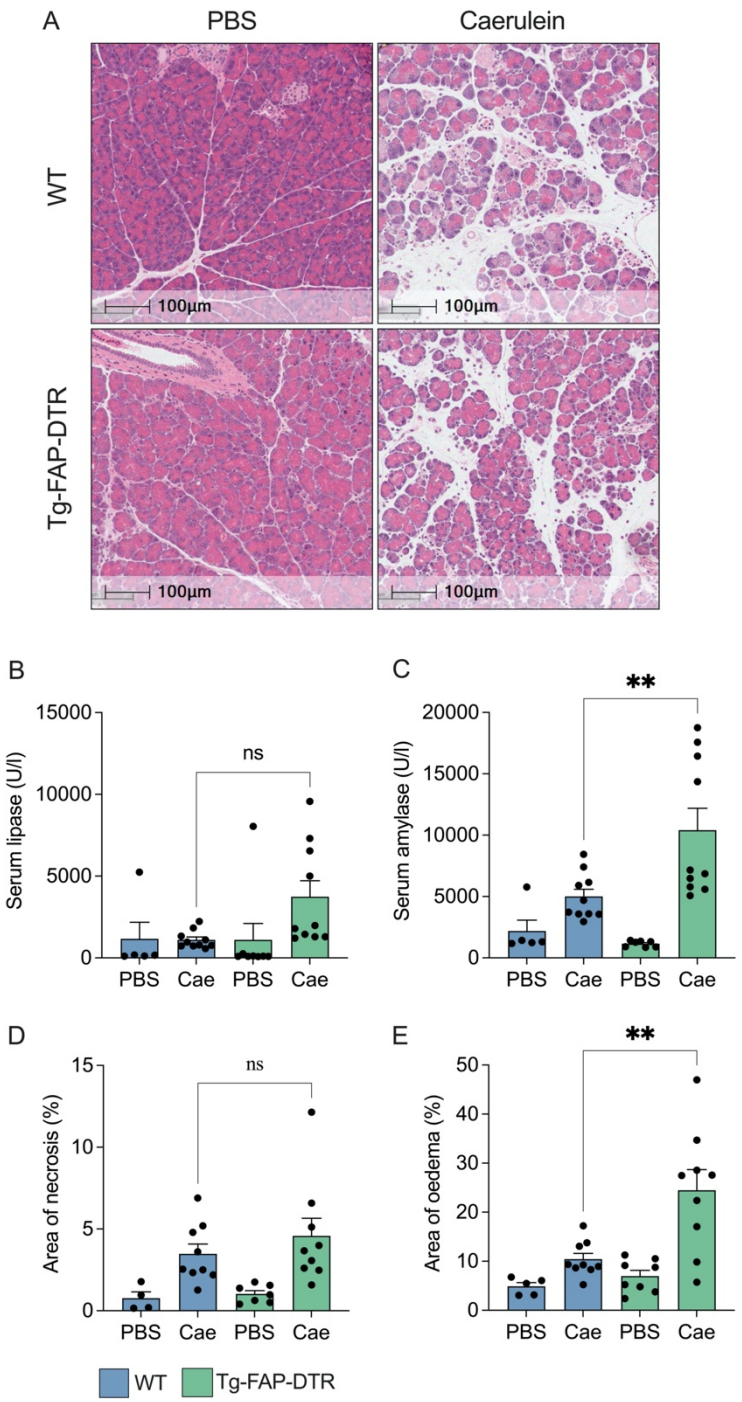

Figure S24 – Stromal cell KO mice show increased oedema in acute pancreatitis. Tg-FAP-DTR mice were injected with 50ug/Kg caerulein and sacrificed at 24h after first caerulein injection. A, Pancreas was fixed, embedded, sectioned and stained with H&E and scanned images at 10X magnification are shown. B,C, Quantification of serum amylase (B) and lipase (C) levels. D,E, Quantification of area of necrosis (D) and oedema (E) from images of H&E stained histological sections using the classifier function on the image analysis software Halo. Bar graphs indicate the mean (± s.e.m.) and show pooled data from two independent experiments. Statistical significance was calculated using one-way ANOVA. ns=non significant. *= P≤0.05, **= P≤0.01, ***= P≤0.001, ****=P≤0.0001.

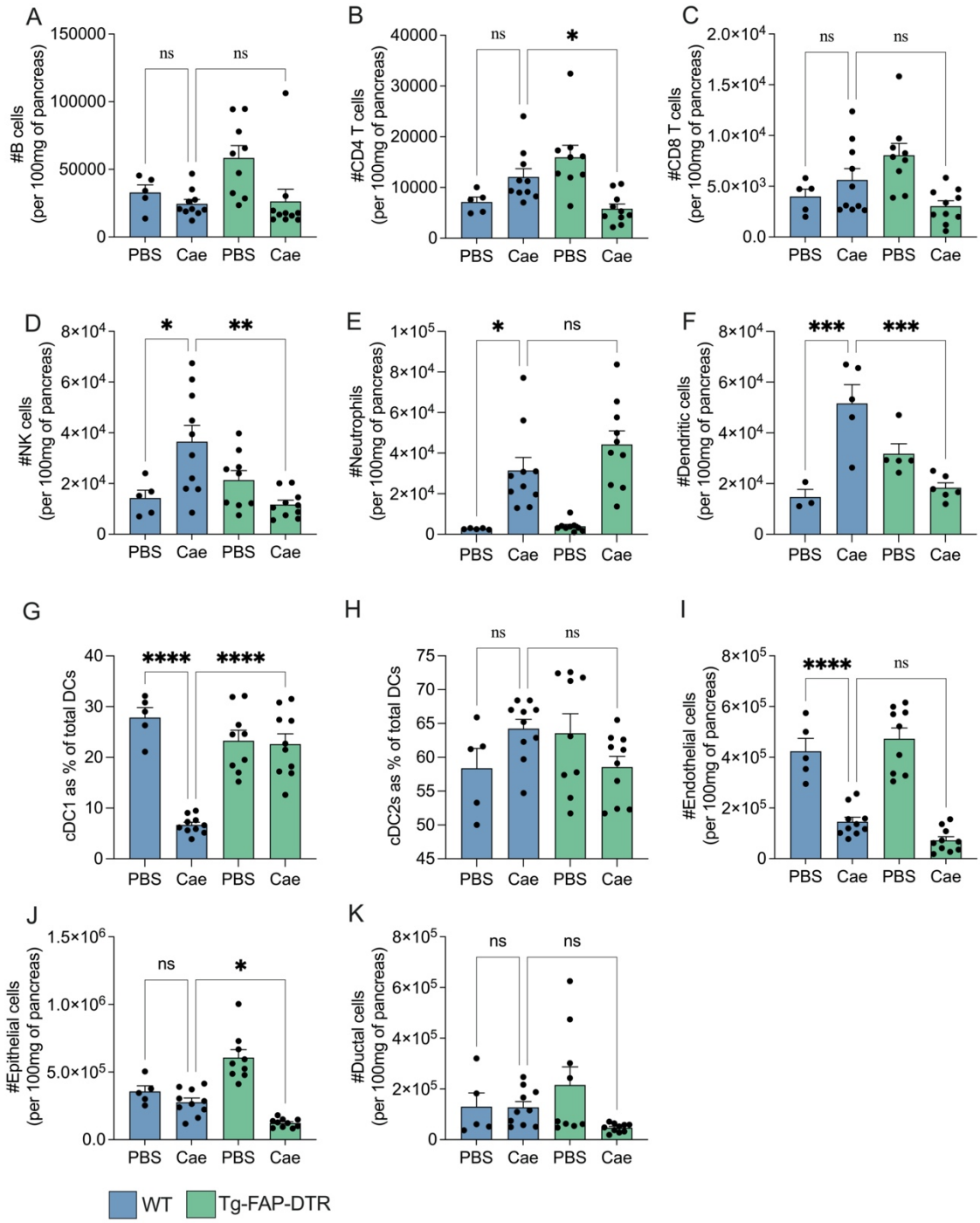

Figure S25 – Stromal cell KO mice with acute pancreatitis show various inflammatory changes. Tg-FAP-DTR mice were 50ug/Kg of caerulein sacrificed 24h after first caerulein injection. This was followed by quantification of immune and non-immune cells in the pancreas by flow cytometry. Bar graphs indicate the mean (± s.e.m.) and show pooled data from two experiments. Statistical significance was calculated using one-way ANOVA. ns=non significant. *= P≤0.05, **= P≤0.01, ***= P≤0.001, ****=P≤0.0001.

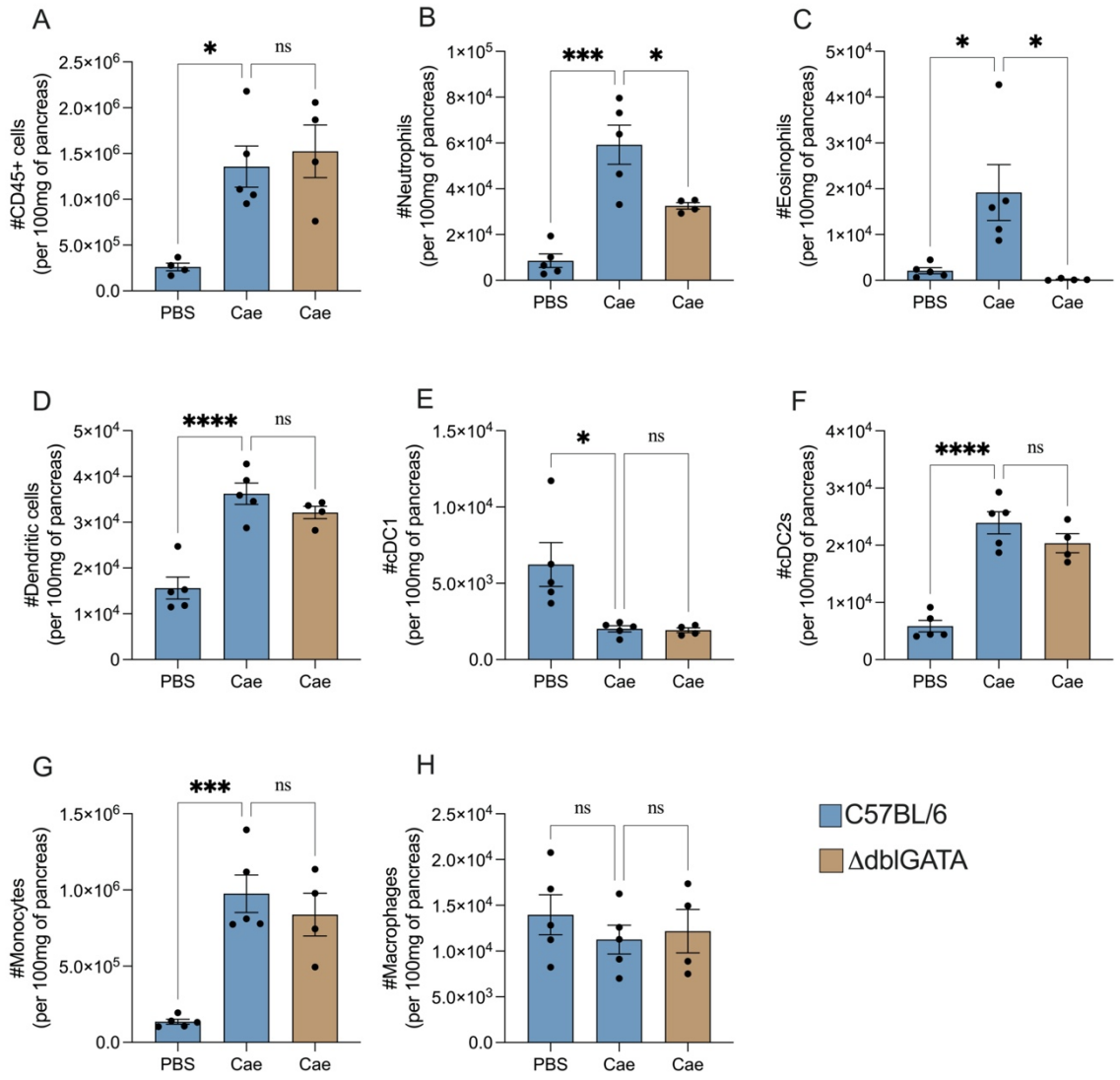

Figure S26 – Total immune influx (CD45+ cells) not affected in ΔdblGATA mice with acute pancreatitis. ΔdblGATA mice were injected with 75ug/Kg Caerulein sacrificed 24 hours after the first caerulein injection. This was followed by quantification of immune cells in the pancreas by flow cytometry. Bar graphs indicate the mean (± s.e.m.) and show data from one experiment. Statistical significance was calculated using one-way ANOVA. ns=non significant. *= P≤0.05, **= P≤0.01, ***= P≤0.001, ****=P≤0.0001.

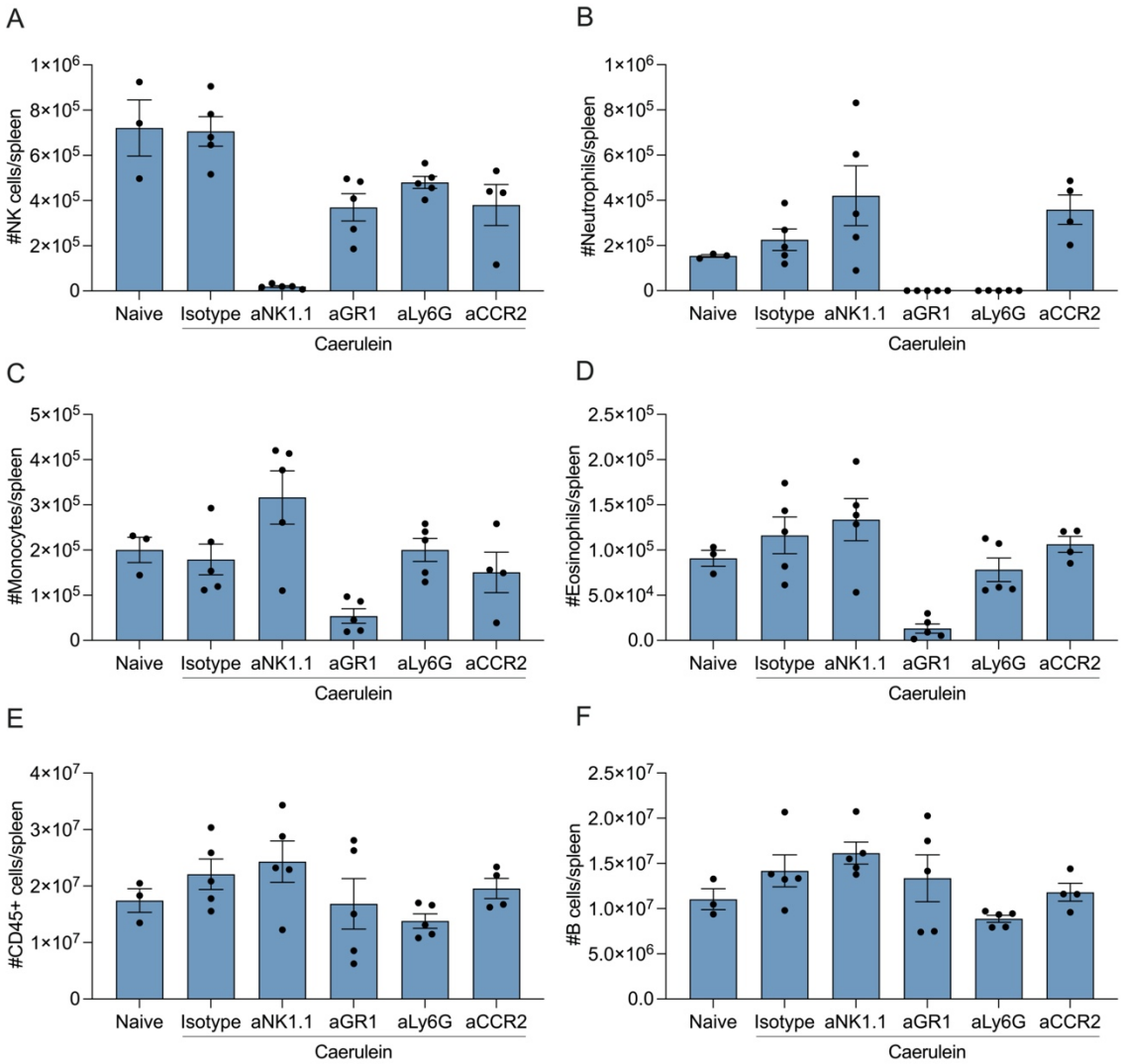

Figure S27 – Effect of depleting antibody confirmed using flow cytometry. C57BL/6 mice were treated with aNK1.1 (50ug), aCCR2 (20ug), aGR1 (200ug) or aLy6G (200ug) on day -1 and day 0, followed by 75ug/Kg Caerulein on day 0 and sacrificed 24h after the first caerulein injection. This was followed by quantification of immune cell numbers by flow cytometry. Bar graphs indicate the mean (± s.e.m.) and show data from one experiment.

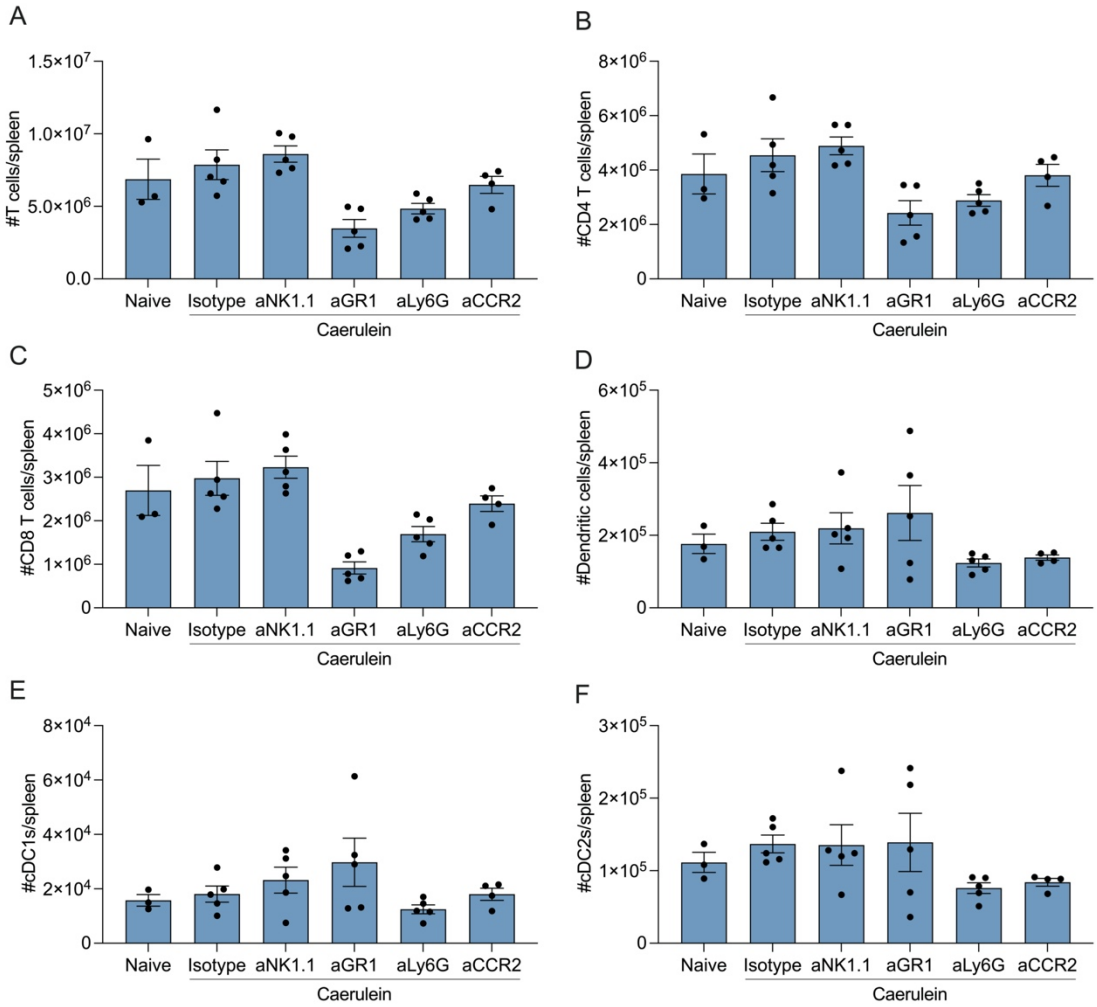

Figure S28 - Effect of depleting antibody confirmed using flow cytometry. C57BL/6 mice were treated with aNK1.1 (50ug), aCCR2 (20ug), aGR1 (200ug) or aLy6G (200ug) on day -1 and day 0, followed by 75ug/Kg Caerulein on day 0 and sacrificed 24h after the first caerulein injection. This was followed by quantification of immune cell numbers by flow cytometry. Bar graphs indicate the mean (± s.e.m.) and show data from one experiment.

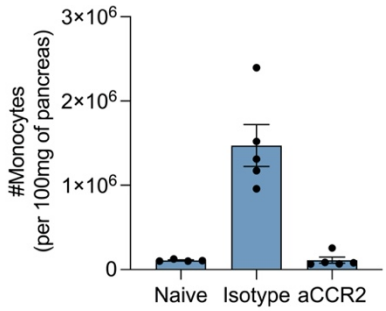

Figure S29 – aCCR2 treatment leads to monocyte depletion in the pancreas. C57BL/6 mice were treated with aCCR2 (20ug) on day -1 and day 0, followed by 75ug/Kg Caerulein on day 0 and sacrificed 24h after the first caerulein injection. This was followed by quantification of immune cell numbers by flow cytometry. Bar graphs indicate the mean (± s.e.m.) and show data from one experiment.

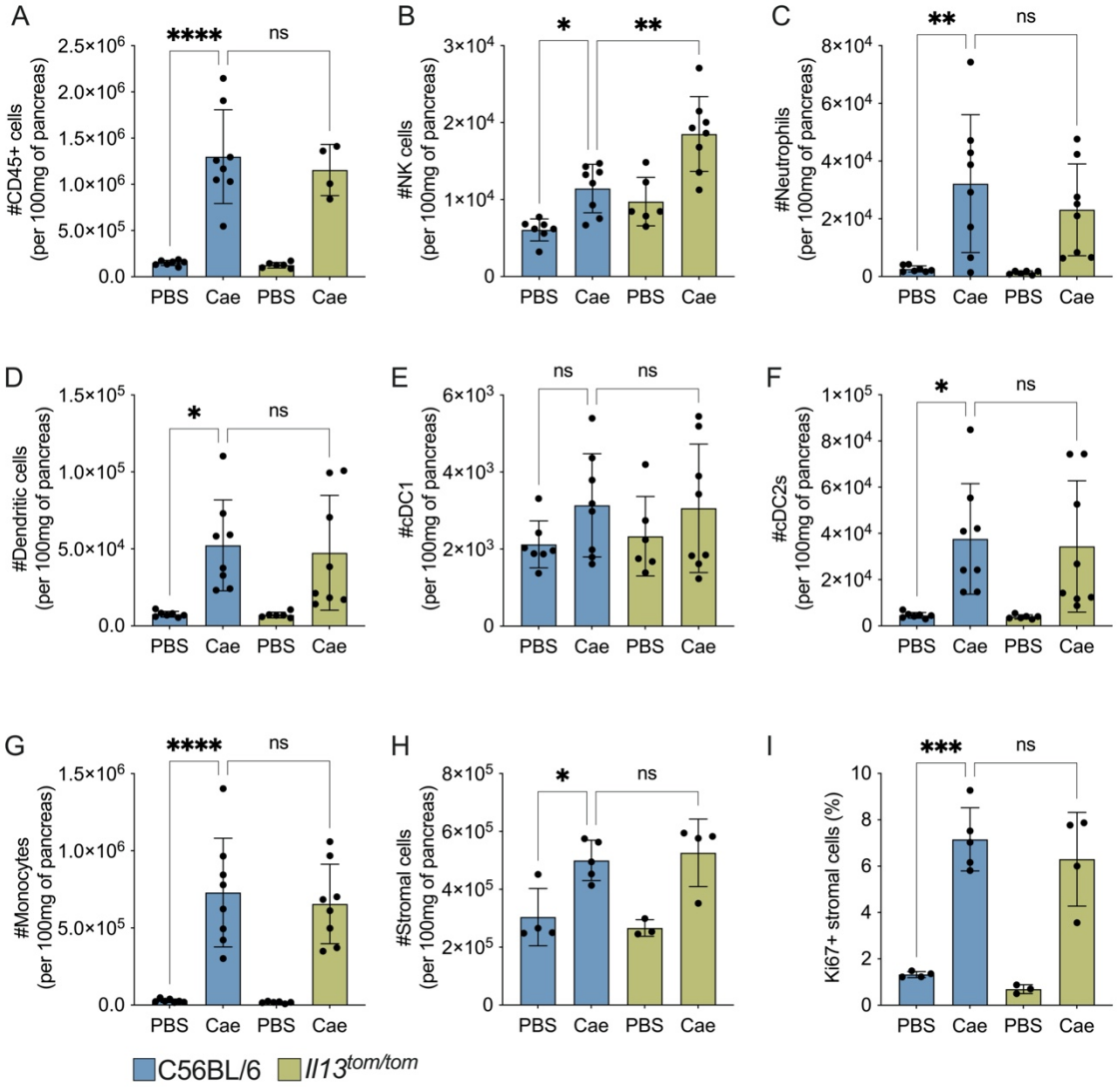

Figure S30 – IL-13 influences NK cell numbers in acute pancreatitis. *Il13$^{tom/tom}$* were injected with 50ug/Kg caerulein sacrificed 24 hours after the first caerulein injection. This was followed by quantification of immune cells by flow cytometry. Bar graphs indicate the mean (± s.e.m.) and show pooled data from 1-2 independent experiments. Statistical significance was calculated using one-way ANOVA. ns=non significant. *= P≤0.05, **= P≤0.01, ***= P≤0.001, ****=P≤0.0001.

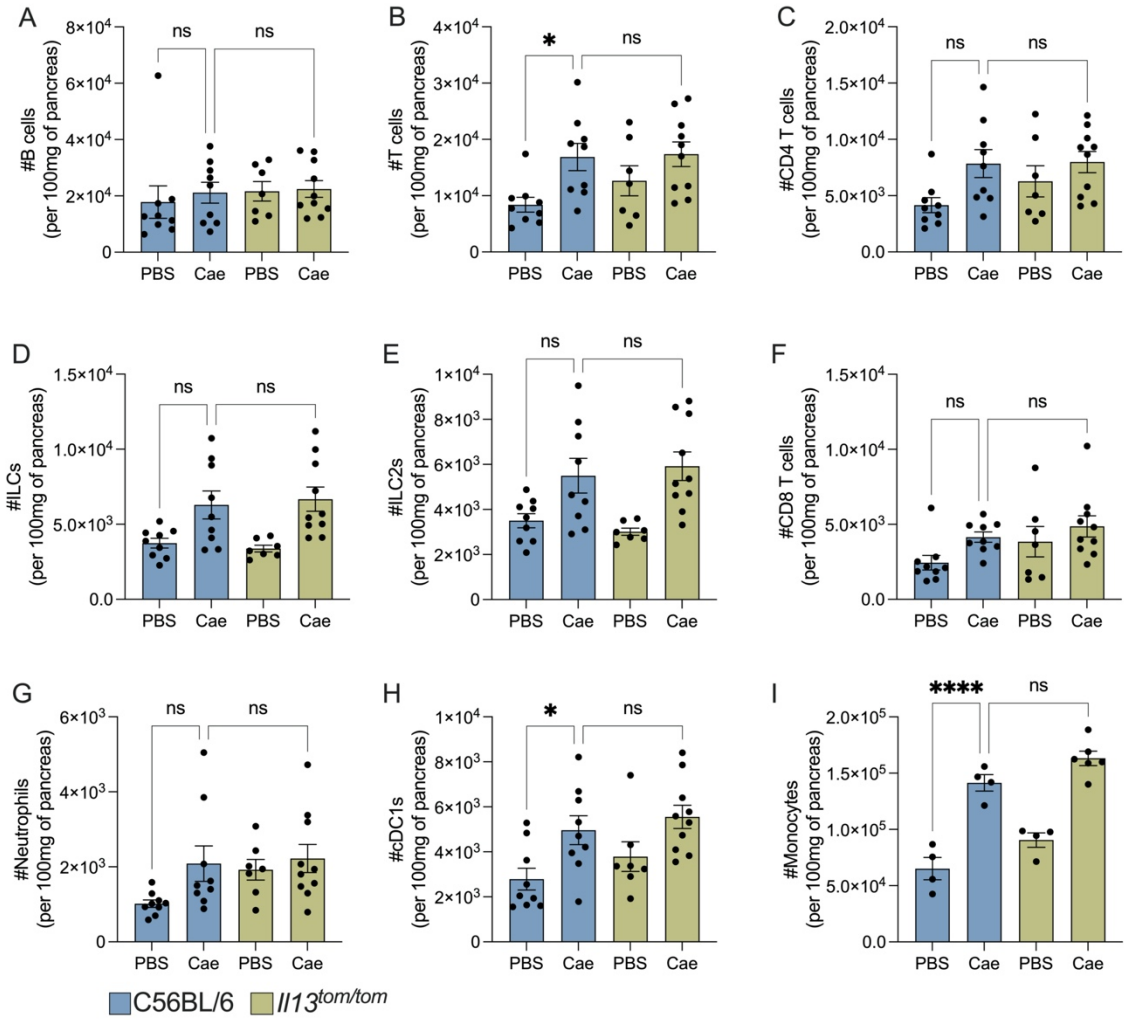

Figure S31 – IL-13KO mice with acute pancreatitis do not show changes in the adaptive immune compartment. *Il13$^{tom/tom}$* were injected with 75ug/Kg caerulein and sacrificed 24 hours after the first caerulein injection. This was followed by quantification of immune cell numbers by flow cytometry. Bar graphs indicate the mean (± s.e.m.) and show pooled data from two independent experiments. Statistical significance was calculated using one-way ANOVA. ns=non significant. *= P≤0.05, **= P≤0.01, ***= P≤0.001, ****=P≤0.0001.

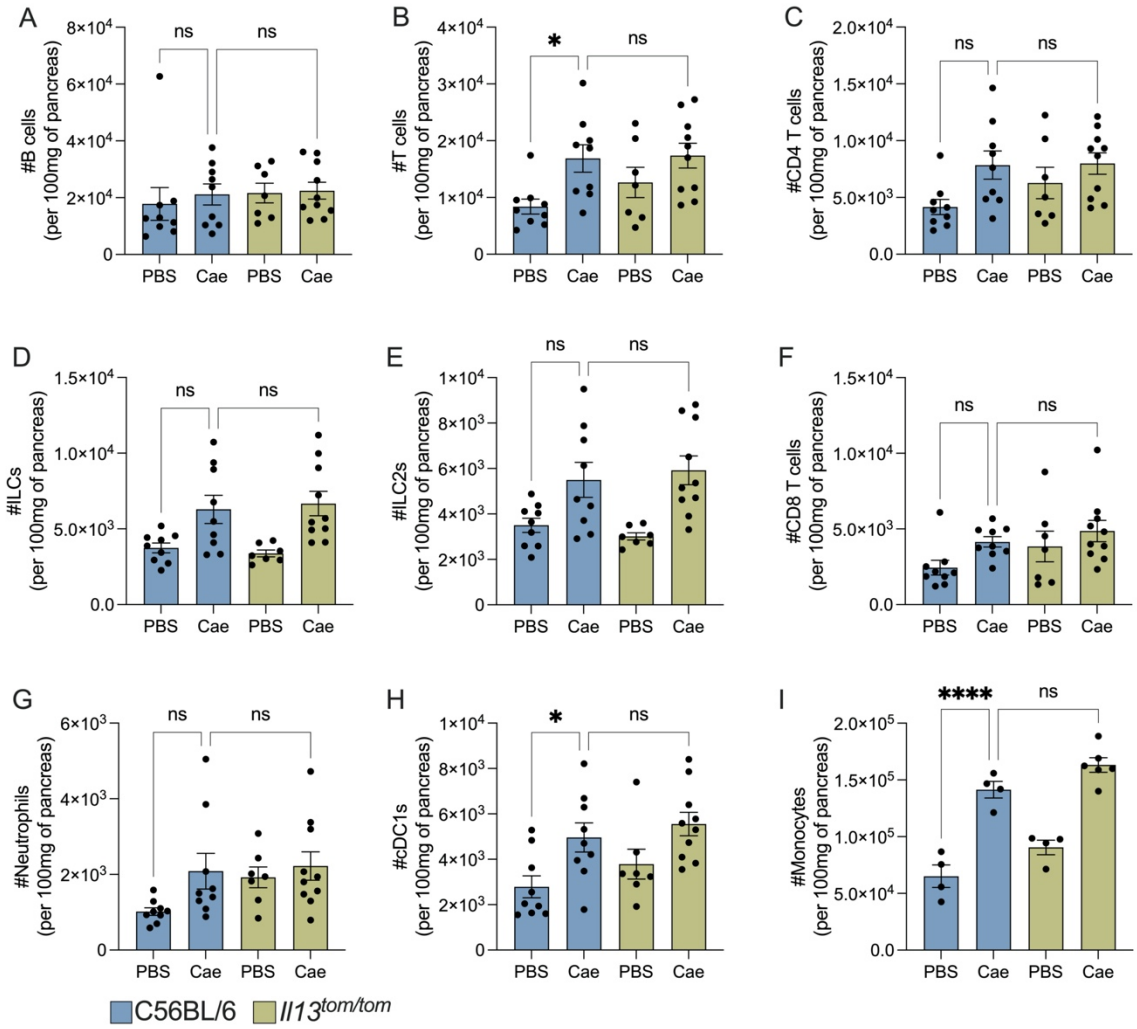

Figure S32 – IL-13 does not influence the adaptive immune compartment during pancreatitis recovery. *Il13$^{tom/tom}$* were injected with 50ug/Kg caerulein and mice on day 0 and day 1 and sacrificed 7 days post induction of pancreatitis This was followed by quantification of immune cells numbers using flow cytometry. Bar graphs indicate the mean (± s.e.m.) and shows data pooled from 1-2 independent experiments. Statistical significance was calculated using one-way ANOVA. ns=non significant. *= P≤0.05, **= P≤0.01, ***= P≤0.001, ****=P≤0.0001.

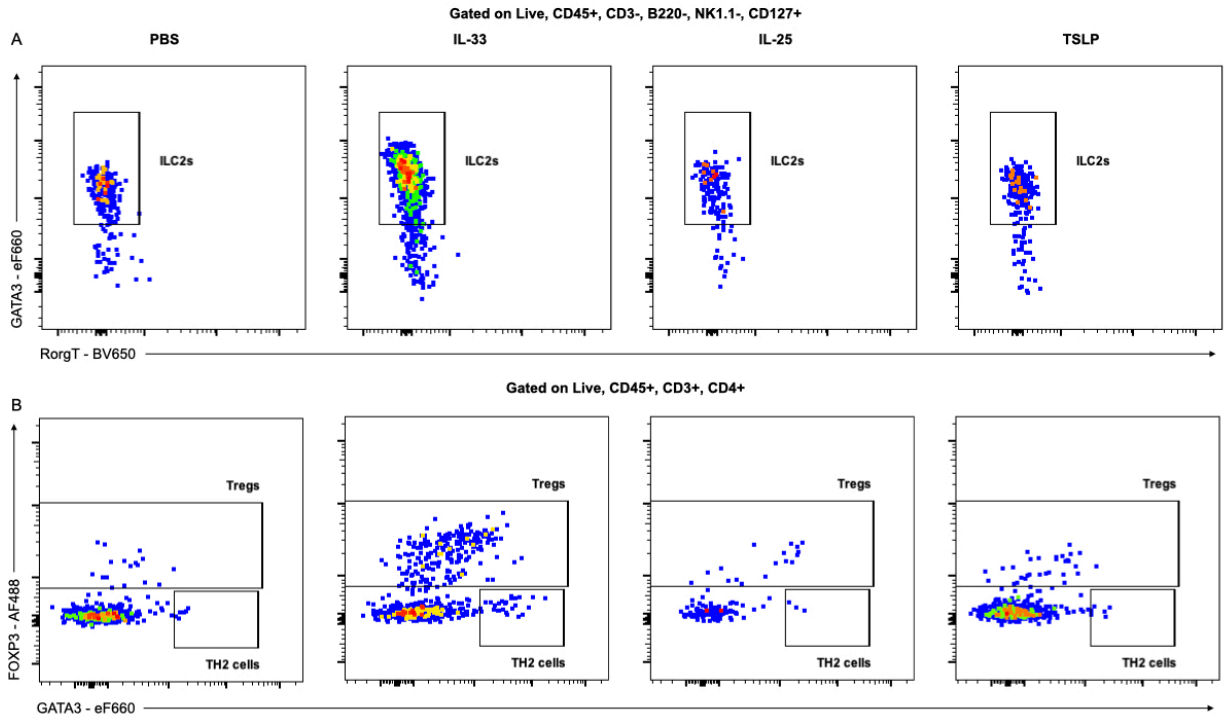

Figure S33 – **IL-33 induces ILC2 and Treg expansion in the pancreas.** C57BL/6 mice were treated with 200ng recombinant IL-33, IL-25 or TSLP intraperitoneally on days 0 and 1 and were sacrificed on day 3 followed by cytokine quantification using flow cytometry. A, Representative gating for ILC2s. B, Representative gating for Tregs and TH2 cells.

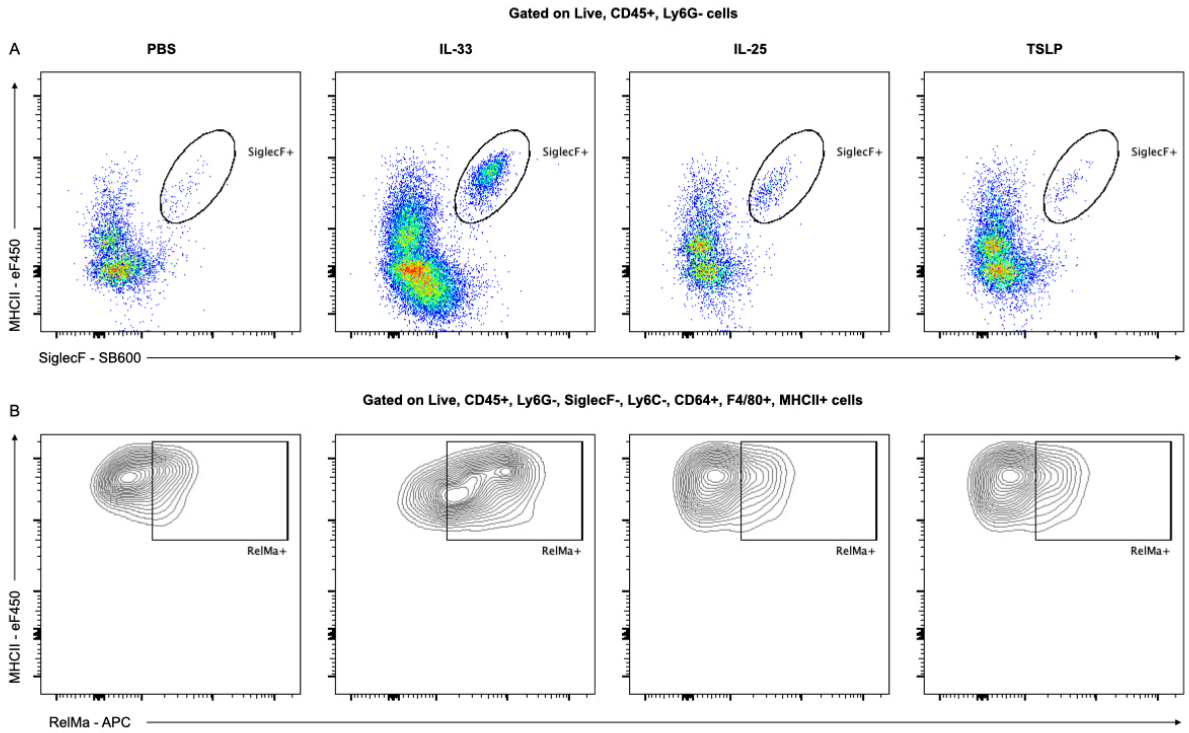

Figure S34 – **IL-33 induces myeloid cell expansion in the pancreas.** C57BL/6 mice were treated with 200ng recombinant IL-33, IL-25 or TSLP intraperitoneally on days 0 and 1 and were sacrificed on day 3 followed by cytokine quantification using flow cytometry. A, Representative gating for eosinophils. B, Representative gating for M2 macrophages

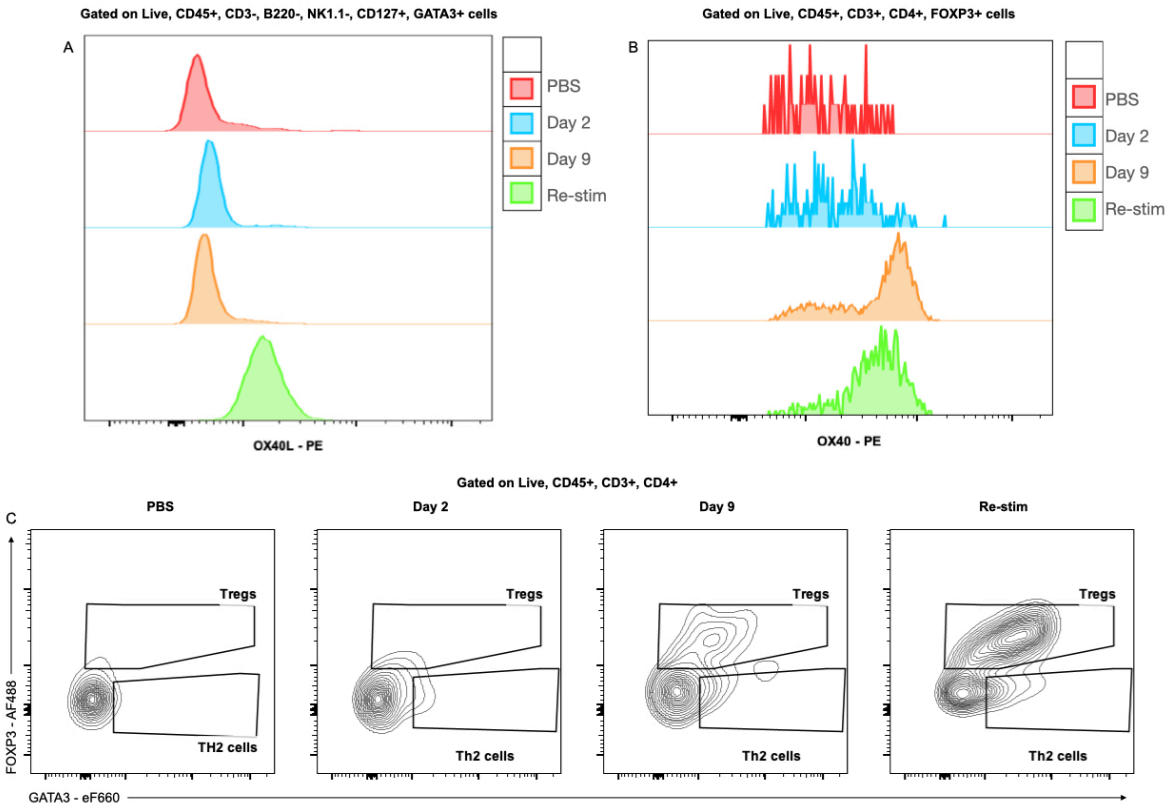

Figure S35 – **Re-stimulation with IL-33 leads to enhanced ILC2 and Treg expansion.** C57BL/6 mice were treated with 200ng recombinant IL-33 intraperitoneally either on 0 and 1 and sacrificed on day 2 and day 9, or on day 0,1,7 and 8 and were killed on day 9 (re-stim). This was followed by quantification of lymphoid cells, OX40L MFI on ILC2s and OX40 MFI on Tregs in the pancreas by flow cytometry (n=7,8,8,8). A, Representative histogram of OX40L-PE expression on ILC2s. B, Representative histogram of OX40-PE expression on Tregs C, Representative gating for Tregs and TH2 cells.

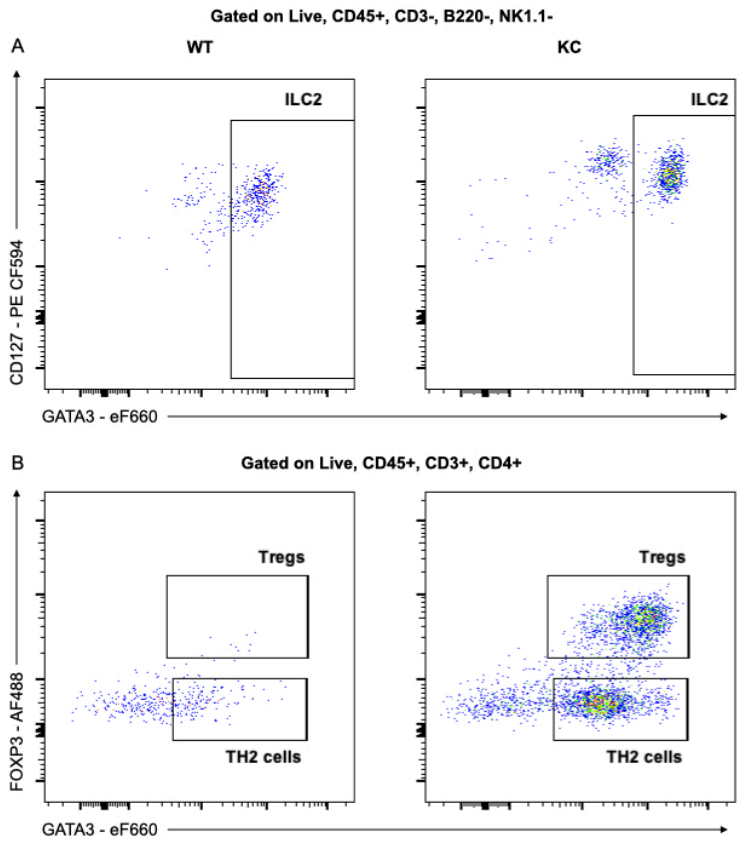

Figure S36 – ILC2 and Treg numbers are increased in pancreatic intraepithelial neoplasia (panIN). Pancreas from KC mice were collected at 2, 4 and 6 months of age and lymphoid immune cells were quantified by flow cytometry (n=4,4,3,5,3,3). A, Representative gating of ILC2s B, Representative gating of Tregs and TH2 cells.

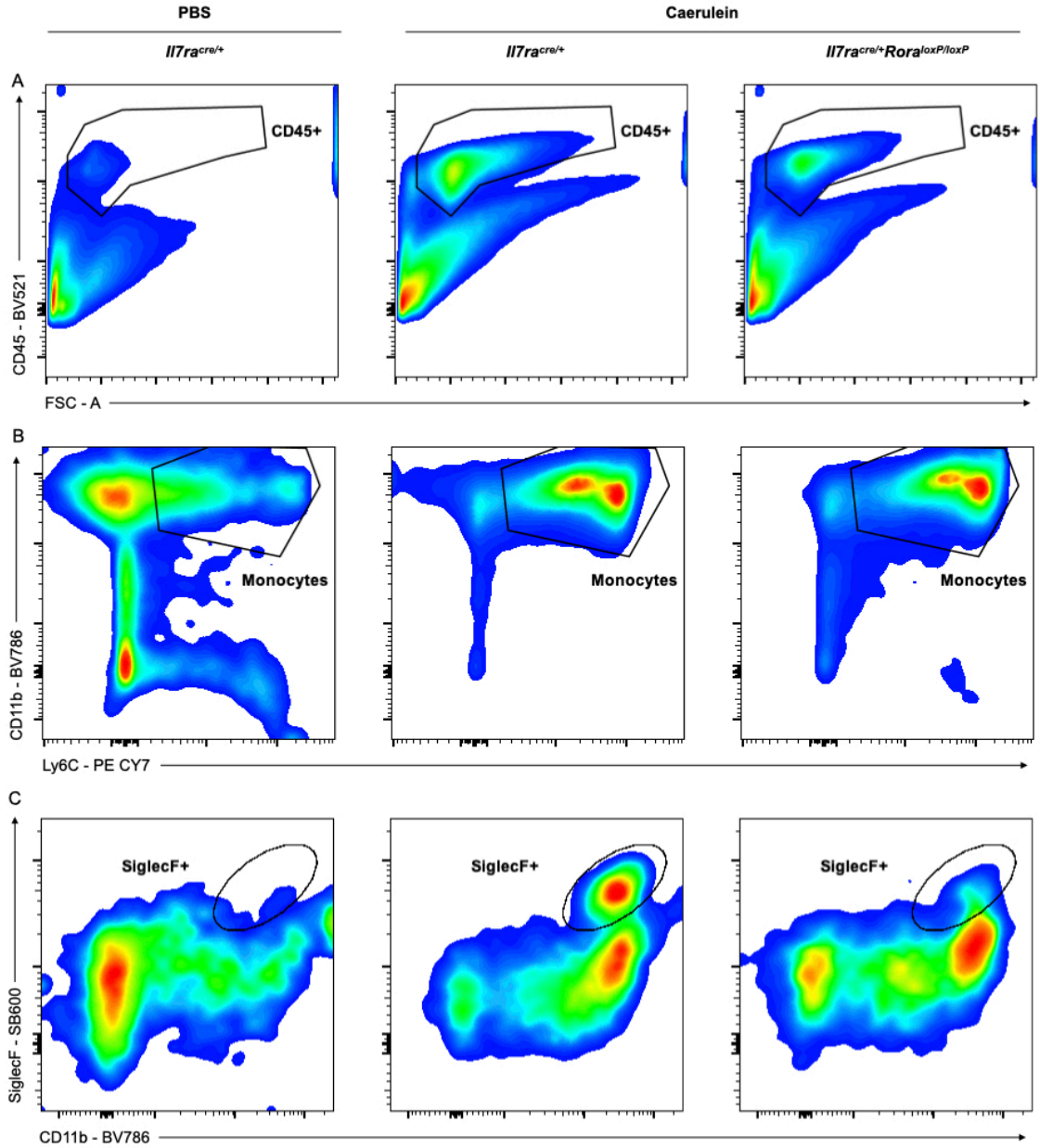

Figure S37 – ILC2 deficient mice show reduced inflammation during acute pancreatitis. *Il7ra*$^{cre/+}$ or *Il7ra*$^{cre/+}$ *Rora*$^{loxP/loxP}$ mice were injected with PBS or 50ug/Kg of caerulein and the mice were sacrificed at 24 hours after the first caerulein injection. This was followed by quantification of lymphoid immune cells in the pancreas by flow cytometry. A, B, C, Representative gating for CD45+ cells, monocytes and eosinophils.

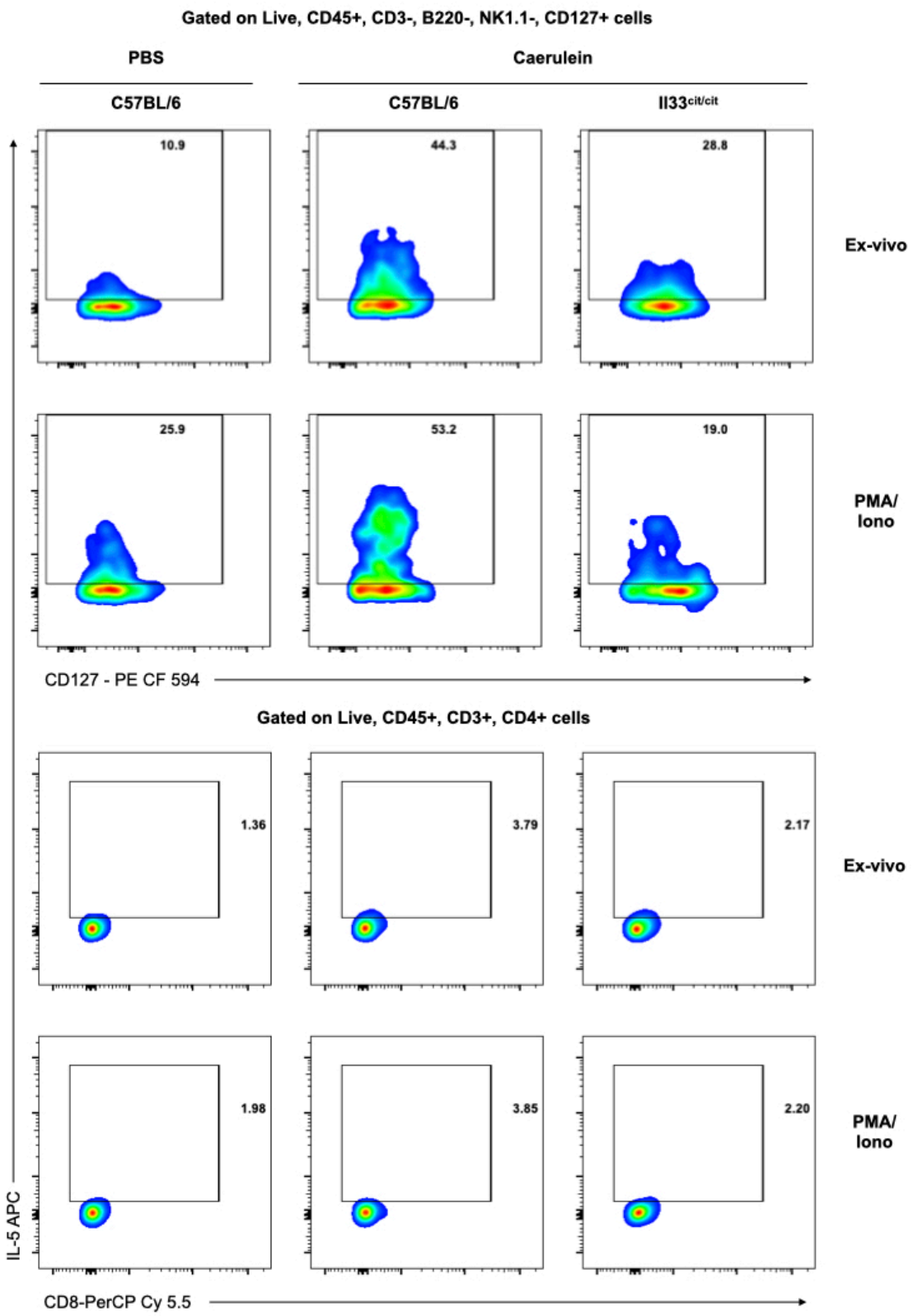

Figure S38 – ILC2s are activated in acute pancreatitis. C57BL/6 mice, Il33$^{cit/+}$ or Il33$^{cit/cit}$ were injected with 50ug/Kg of caerulein and sacrificed 6 hours after the first caerulein injection. Single cell suspension prepared from the pancreas were analysed using flow cytometry. Representative gating for IL-5-APC on ILCs and CD4 T cells with and without PMA/Ionomycin treatment has been shown here.

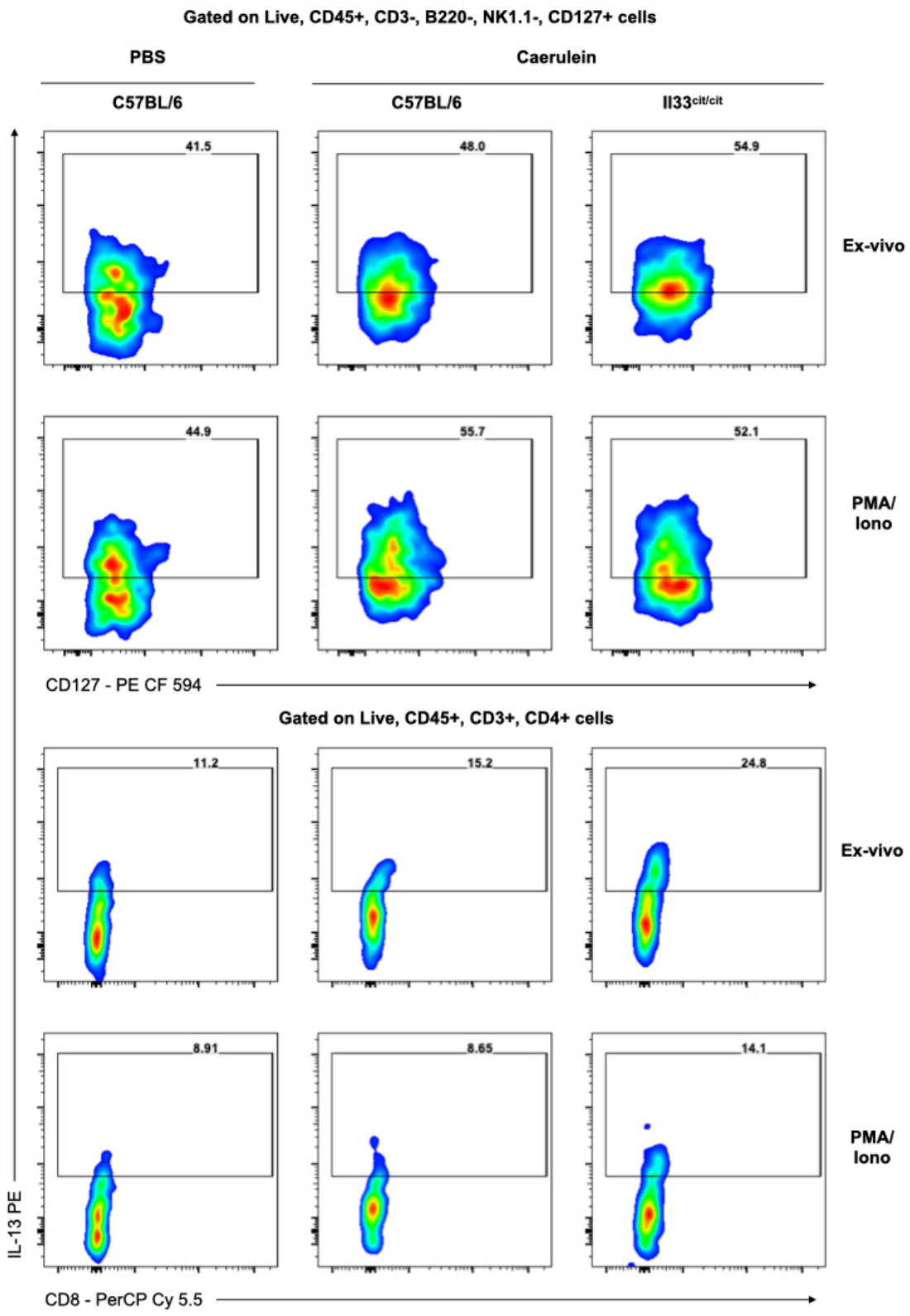

Figure S39 – ILC2s are activated in acute pancreatitis. C57BL/6 mice, Il33$^{cit/+}$ or Il33$^{cit/cit}$ were injected with 50ug/Kg of caerulein and sacrificed 6 hours after the first caerulein injection. Single cell suspension prepared from the pancreas were analysed using flow cytometry. Representative gating for IL-13-PE on ILCs and CD4 T cells with and without PMA/Ionomycin treatment has been shown here.

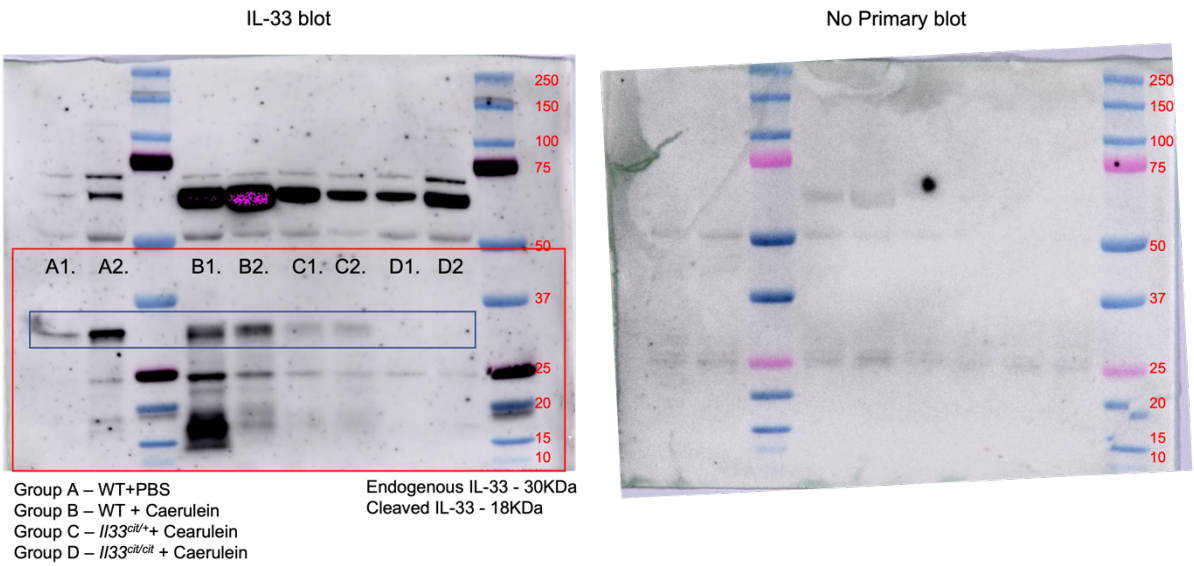

Figure S38 – ILC2s are activated in acute pancreatitis. C57BL/6 mice, Il33$^{cit/+}$ or Il33$^{cit/cit}$ were injected with 50ug/Kg of caerulein and sacrificed 6 hours after the first caerulein injection. Pancreas tissue was frozen immediately and later lysed and run on a 12% SDS-PAGE. Western blotting on nitrocellulose membrane was performed using semi-dry transfer. The blot was stained with primary antibody for IL-33 and associated secondary antibody. Detection was done using chemiluminescence. Specificity of antibody was confirmed using a no-primary antibody blot and recombinant IL-33 as positive control. Endogenous IL-33 was identified at around 30KDa.

References

Aho, H. J., Koskensalo, S. M., & Nevalainen, T. J. (1980). Experimental pancreatitis in the rat. Sodium taurocholate-induced acute haemorrhagic pancreatitis. *Scandinavian Journal of Gastroenterology*, *15*(4), 411–416.

Apte, M. V., Haber, P. S., Darby, S. J., Rodgers, S. C., McCaughan, G. W., Korsten, M. A., Pirola, R. C., & Wilson, J. S. (1999). Pancreatic stellate cells are activated by proinflammatory cytokines: implications for pancreatic fibrogenesis. *Gut*, *44*(4), 534–541.

Bachem, M. G., Schünemann, M., Ramadani, M., Siech, M., Beger, H., Buck, A., Zhou, S., Schmid-Kotsas, A., & Adler, G. (2005). Pancreatic carcinoma cells induce fibrosis by stimulating proliferation and matrix synthesis of stellate cells. *Gastroenterology*, *128*(4), 907–921.

Barbu, E. A., Dominical, V. M., Mendelsohn, L., & Thein, S. L. (2021). An Imaging Flow Cytometry Method to Measure Citrullination of H4 Histone as a Read-out for Neutrophil Extracellular Traps Formation. *Bio-Protocol*, *11*(4), e3927.

Barlow, J. L., Bellosi, A., Hardman, C. S., Drynan, L. F., Wong, S. H., Cruickshank, J. P., & McKenzie, A. N. J. (2012). Innate IL-13-producing nuocytes arise during allergic lung inflammation and contribute to airways hyperreactivity. *The Journal of Allergy and Clinical Immunology*, *129*(1), 191-8.e1-4.

Baumgarth, N. (2011). The double life of a B-1 cell: self-reactivity selects for protective effector functions. *Nature Reviews. Immunology*, *11*(1), 34–46.

Bedrosian, A. S., Nguyen, A. H., Hackman, M., Connolly, M. K., Malhotra, A., Ibrahim, J., Cieza-Rubio, N. E., Henning, J. R., Barilla, R., Rehman, A., Pachter, H. L., Medina-Zea, M. V., Cohen, S. M., Frey, A. B., Acehan, D., & Miller, G. (2011). Dendritic cells promote pancreatic viability in mice with acute pancreatitis. *Gastroenterology*, *141*(5), 1915-26.e1-14.

Bending, D., De La Peña, H., Veldhoen, M., Phillips, J. M., Uyttenhove, C., Stockinger, B., & Cooke, A. (2009). Highly purified Th17 cells from BDC2.5NOD mice convert into Th1-like cells in NOD/SCID recipient mice. In *Journal of Clinical Investigation* (Vol. 119, Issue 3, pp. 565–572). https://doi.org/10.1172/jci37865

Bernink, J. H., Peters, C. P., Munneke, M., te Velde, A. A., Meijer, S. L., Weijer, K., Hreggvidsdottir, H. S., Heinsbroek, S. E., Legrand, N., Buskens, C. J., Bemelman, W. A., Mjösberg, J. M., & Spits, H. (2013). Human type 1 innate lymphoid cells accumulate in inflamed mucosal tissues. *Nature Immunology*, *14*(3), 221–229.

Borthwick, L. A., Barron, L., Hart, K. M., Vannella, K. M., Thompson, R. W., Oland, S., Cheever, A., Sciurba, J., Ramalingam, T. R., Fisher, A. J., & Wynn, T. A. (2016). Macrophages are critical to the maintenance of IL-13-dependent lung inflammation and fibrosis. *Mucosal Immunology*, *9*(1), 38–55.

Boxhoorn, L., Voermans, R. P., Bouwense, S. A., Bruno, M. J., Verdonk, R. C., Boermeester, M. A., van Santvoort, H. C., & Besselink, M. G. (2020). Acute pancreatitis. *The Lancet*, *396*(10252), 726–734.

Brock, C., Nielsen, L. M., Lelic, D., & Drewes, A. M. (2013). Pathophysiology of chronic pancreatitis. *World Journal of Gastroenterology: WJG*, *19*(42), 7231–7240.

Bruce, D. W., Stefanski, H. E., Vincent, B. G., Dant, T. A., Reisdorf, S., Bommiasamy, H., Serody, D. A., Wilson, J. E., McKinnon, K. P., Shlomchik, W. D., Armistead, P. M., Ting, J. P. Y., Woosley, J. T., Blazar, B. R., Zaiss, D. M. W., McKenzie, A. N. J., Coghill, J. M., & Serody, J. S. (2017). Type 2 innate lymphoid cells treat and prevent acute

gastrointestinal graft-versus-host disease. *The Journal of Clinical Investigation*, *127*(5), 1813–1825.

Bruchard, M., & Ghiringhelli, F. (2019). Deciphering the Roles of Innate Lymphoid Cells in Cancer. *Frontiers in Immunology*, *10*, 656.

Buonocore, S., Ahern, P. P., Uhlig, H. H., Ivanov, I. I., Littman, D. R., Maloy, K. J., & Powrie, F. (2010). Innate lymphoid cells drive interleukin-23-dependent innate intestinal pathology. *Nature*, *464*(7293), 1371–1375.

Califano, D., Furuya, Y., Roberts, S., Avram, D., McKenzie, A. N. J., & Metzger, D. W. (2018). IFN-γ increases susceptibility to influenza A infection through suppression of group II innate lymphoid cells. *Mucosal Immunology*, *11*(1), 209–219.

Carrière, C., Young, A. L., Gunn, J. R., Longnecker, D. S., & Korc, M. (2009). Acute pancreatitis markedly accelerates pancreatic cancer progression in mice expressing oncogenic Kras. *Biochemical and Biophysical Research Communications*, *382*(3), 561–565.

Cella, M., Fuchs, A., Vermi, W., Facchetti, F., Otero, K., Lennerz, J. K. M., Doherty, J. M., Mills, J. C., & Colonna, M. (2009). A human natural killer cell subset provides an innate source of IL-22 for mucosal immunity. *Nature*, *457*(7230), 722–725.

Chang, W.-J., Du, Y., Zhao, X., Ma, L.-Y., & Cao, G.-W. (2014). Inflammation-related factors predicting prognosis of gastric cancer. *World Journal of Gastroenterology: WJG*, *20*(16), 4586–4596.

Chang, Y.-J., Kim, H. Y., Albacker, L. A., Baumgarth, N., McKenzie, A. N. J., Smith, D. E., Dekruyff, R. H., & Umetsu, D. T. (2011). Innate lymphoid cells mediate influenza-induced airway hyper-reactivity independently of adaptive immunity. *Nature Immunology*, *12*(7), 631–638.

Cheng, E., Souza, R. F., & Spechler, S. J. (2012). Tissue remodeling in eosinophilic esophagitis. *American Journal of Physiology. Gastrointestinal and Liver Physiology*, *303*(11), G1175-87.

Chuvin, N., Vincent, D. F., Pommier, R. M., Alcaraz, L. B., Gout, J., Caligaris, C., Yacoub, K., Cardot, V., Roger, E., Kaniewski, B., Martel, S., Cintas, C., Goddard-Léon, S., Colombe, A., Valantin, J., Gadot, N., Servoz, E., Morton, J., Goddard, I., … Bartholin, L. (2017). Acinar-to-Ductal Metaplasia Induced by Transforming Growth Factor Beta Facilitates KRASG12D-driven Pancreatic Tumorigenesis. *Cellular and Molecular Gastroenterology and Hepatology*, *4*(2), 263–282.

Cohn, L., Elias, J. A., & Chupp, G. L. (2004). Asthma: mechanisms of disease persistence and progression. *Annual Review of Immunology*, *22*, 789–815.

Context | Pancreatitis | Guidance | NICE. (n.d.). Retrieved August 6, 2021, from https://www.nice.org.uk/guidance/ng104/chapter/Context

Crellin, N. K., Trifari, S., Kaplan, C. D., Cupedo, T., & Spits, H. (2010). Human NKp44+IL-22+ cells and LTi-like cells constitute a stable RORC+ lineage distinct from conventional natural killer cells. *The Journal of Experimental Medicine*, *207*(2), 281–290.

Cupedo, T., Crellin, N. K., Papazian, N., Rombouts, E. J., Weijer, K., Grogan, J. L., Fibbe, W. E., Cornelissen, J. J., & Spits, H. (2009). Human fetal lymphoid tissue-inducer cells are interleukin 17-producing precursors to RORC+ CD127+ natural killer-like cells. *Nature Immunology*, *10*(1), 66–74.

Dadi, S., Chhangawala, S., Whitlock, B. M., Franklin, R. A., Luo, C. T., Oh, S. A., Toure, A., Pritykin, Y., Huse, M., Leslie, C. S., & Li, M. O. (2016). Cancer Immunosurveillance by Tissue-Resident Innate Lymphoid Cells and Innate-like T Cells. *Cell*, *164*(3), 365–377.

Dahlgren, M. W., Jones, S. W., Cautivo, K. M., Dubinin, A., Ortiz-Carpena, J. F., Farhat, S., Yu, K. S., Lee, K., Wang, C., Molofsky, A. V., Tward, A. D., Krummel, M. F., Peng, T., & Molofsky, A. B. (2019). Adventitial Stromal Cells Define Group 2 Innate Lymphoid Cell Tissue Niches. *Immunity*. https://doi.org/10.1016/j.immuni.2019.02.002

Dalmas, E., Lehmann, F. M., Dror, E., Wueest, S., Thienel, C., Borsigova, M., Stawiski, M., Traunecker, E., Lucchini, F. C., Dapito, D. H., Kallert, S. M., Guigas, B., Pattou, F., Kerr-Conte, J., Maechler, P., Girard, J.-P., Konrad, D., Wolfrum, C., Böni-Schnetzler, M., … Donath, M. Y. (2017). Interleukin-33-Activated Islet-Resident Innate Lymphoid Cells Promote Insulin Secretion through Myeloid Cell Retinoic Acid Production. *Immunity*, *47*(5), 928-942.e7.

Demols, A., Le Moine, O., Desalle, F., Quertinmont, E., Van Laethem, J. L., & Devière, J. (2000). CD4(+)T cells play an important role in acute experimental pancreatitis in mice. *Gastroenterology*, *118*(3), 582–590.

Drake, L. Y., Iijima, K., & Kita, H. (2014). Group 2 innate lymphoid cells and CD4+ T cells cooperate to mediate type 2 immune response in mice. *Allergy*, *69*(10), 1300–1307.

Drake, Li Yin, & Kita, H. (2017). IL-33: biological properties, functions, and roles in airway disease. *Immunological Reviews*, *278*(1), 173–184.

Ebbo, M., Crinier, A., Vély, F., & Vivier, E. (2017). Innate lymphoid cells: major players in inflammatory diseases. *Nature Reviews. Immunology*, *17*(11), 665–678.

Eckert, C., Kim, Y. O., Julich, H., Heier, E.-C., Klein, N., Krause, E., Tschernig, T., Kornek, M., Lammert, F., Schuppan, D., & Lukacs-Kornek, V. (2016). Podoplanin discriminates distinct stromal cell populations and a novel progenitor subset in the liver. *American Journal of Physiology. Gastrointestinal and Liver Physiology*, *310*(1), G1-12.

Elyada, E., Bolisetty, M., Laise, P., Flynn, W. F., Courtois, E. T., Burkhart, R. A., Teinor, J. A., Belleau, P., Biffi, G., Lucito, M. S., Sivajothi, S., Armstrong, T. D., Engle, D. D., Yu, K. H., Hao, Y., Wolfgang, C. L., Park, Y., Preall, J., Jaffee, E. M., … Tuveson, D. A. (2019). Cross-Species Single-Cell Analysis of Pancreatic Ductal Adenocarcinoma Reveals Antigen-Presenting Cancer-Associated Fibroblasts. *Cancer Discovery*, *9*(8), 1102–1123.

Fallon, P. G., Ballantyne, S. J., Mangan, N. E., Barlow, J. L., Dasvarma, A., Hewett, D. R., McIlgorm, A., Jolin, H. E., & McKenzie, A. N. J. (2006). Identification of an interleukin (IL)-25--dependent cell population that provides IL-4, IL-5, and IL-13 at the onset of helminth expulsion. *The Journal of Experimental Medicine*, *203*(4), 1105–1116.

Feig, C., Jones, J. O., Kraman, M., Wells, R. J. B., Deonarine, A., Chan, D. S., Connell, C. M., Roberts, E. W., Zhao, Q., Caballero, O. L., Teichmann, S. A., Janowitz, T., Jodrell, D. I., Tuveson, D. A., & Fearon, D. T. (2013). Targeting CXCL12 from FAP-expressing carcinoma-associated fibroblasts synergizes with anti-PD-L1 immunotherapy in pancreatic cancer. *Proceedings of the National Academy of Sciences of the United States of America*, *110*(50), 20212–20217.

Flood-Page, P., Menzies-Gow, A., Phipps, S., Ying, S., Wangoo, A., Ludwig, M. S., Barnes, N., Robinson, D., & Kay, A. B. (2003). Anti-IL-5 treatment reduces deposition of ECM proteins in the bronchial subepithelial basement membrane of mild atopic asthmatics. *The Journal of Clinical Investigation*, *112*(7), 1029–1036.

Folias, A. E., Penaranda, C., Su, A. L., Bluestone, J. A., & Hebrok, M. (2014). Aberrant innate immune activation following tissue injury impairs pancreatic regeneration. *PloS One*, *9*(7), e102125.

Forsmark, C. E., Vege, S. S., & Wilcox, C. M. (2016). Acute Pancreatitis. *The New England Journal of Medicine*, *375*(20), 1972–1981.

Goc, J., Hepworth, M. R., & Sonnenberg, G. F. (2016). Group 3 innate lymphoid cells: regulating host-commensal bacteria interactions in inflammation and cancer. *International Immunology*, *28*(1), 43–52.

Goc, J., Lv, M., Bessman, N. J., Flamar, A.-L., Sahota, S., Suzuki, H., Teng, F., Putzel, G. G., JRI Live Cell Bank, Eberl, G., Withers, D. R., Arthur, J. C., Shah, M. A., & Sonnenberg, G. F. (2021). Dysregulation of ILC3s unleashes progression and immunotherapy resistance in colon cancer. *Cell*, *184*(19), 5015-5030.e16.

Goh, Y. P. S., Henderson, N. C., Heredia, J. E., Red Eagle, A., Odegaard, J. I., Lehwald, N., Nguyen, K. D., Sheppard, D., Mukundan, L., Locksley, R. M., & Chawla, A. (2013). Eosinophils secrete IL-4 to facilitate liver regeneration. *Proceedings of the National Academy of Sciences of the United States of America*, *110*(24), 9914–9919.

Goodchild, G., Chouhan, M., & Johnson, G. J. (2019). Practical guide to the management of acute pancreatitis. *Frontline Gastroenterology*, *10*(3), 292–299.

Guerra, C., Collado, M., Navas, C., Schuhmacher, A. J., Hernández-Porras, I., Cañamero, M., Rodriguez-Justo, M., Serrano, M., & Barbacid, M. (2011). Pancreatitis-induced inflammation contributes to pancreatic cancer by inhibiting oncogene-induced senescence. *Cancer Cell*, *19*(6), 728–739.

Guerra, C., Schuhmacher, A. J., Cañamero, M., Grippo, P. J., Verdaguer, L., Pérez-Gallego, L., Dubus, P., Sandgren, E. P., & Barbacid, M. (2007). Chronic pancreatitis is essential for induction of pancreatic ductal adenocarcinoma by K-Ras oncogenes in adult mice. *Cancer Cell*, *11*(3), 291–302.

Halim, T. Y. F., Hwang, Y. Y., Scanlon, S. T., Zaghouani, H., Garbi, N., Fallon, P. G., & McKenzie, A. N. J. (2016). Group 2 innate lymphoid cells license dendritic cells to potentiate memory TH2 cell responses. *Nature Immunology*, *17*(1), 57–64.

Halim, T. Y. F., Krauss, R. H., Sun, A. C., & Takei, F. (2012). Lung natural helper cells are a critical source of Th2 cell-type cytokines in protease allergen-induced airway inflammation. *Immunity*, *36*(3), 451–463.

Halim, T. Y. F., MacLaren, A., Romanish, M. T., Gold, M. J., McNagny, K. M., & Takei, F. (2012). Retinoic-acid-receptor-related orphan nuclear receptor alpha is required for natural helper cell development and allergic inflammation. *Immunity*, *37*(3), 463–474.

Halim, T. Y. F., Rana, B. M. J., Walker, J. A., Kerscher, B., Knolle, M. D., Jolin, H. E., Serrao, E. M., Haim-Vilmovsky, L., Teichmann, S. A., Rodewald, H.-R., Botto, M., Vyse, T. J., Fallon, P. G., Li, Z., Withers, D. R., & McKenzie, A. N. J. (2018). Tissue-Restricted Adaptive Type 2 Immunity Is Orchestrated by Expression of the Costimulatory Molecule OX40L on Group 2 Innate Lymphoid Cells. *Immunity*, *48*(6), 1195-1207.e6.

Halim, T. Y. F., Steer, C. A., Mathä, L., Gold, M. J., Martinez-Gonzalez, I., McNagny, K. M., McKenzie, A. N. J., & Takei, F. (2014). Group 2 innate lymphoid cells are critical for the initiation of adaptive T helper 2 cell-mediated allergic lung inflammation. *Immunity*, *40*(3), 425–435.

Hams, E., Armstrong, M. E., Barlow, J. L., Saunders, S. P., Schwartz, C., Cooke, G., Fahy, R. J., Crotty, T. B., Hirani, N., Flynn, R. J., Voehringer, D., McKenzie, A. N. J., Donnelly, S. C., & Fallon, P. G. (2014). IL-25 and type 2 innate lymphoid cells induce pulmonary fibrosis. *Proceedings of the National Academy of Sciences of the United States of America*, *111*(1), 367–372.

Hanahan, D., & Weinberg, R. A. (2011). Hallmarks of cancer: the next generation. *Cell*, *144*(5), 646–674.

Hardman, C. S., Panova, V., & McKenzie, A. N. J. (2013). IL-33 citrine reporter mice reveal the temporal and spatial expression of IL-33 during allergic lung inflammation. *European Journal of Immunology*, *43*(2), 488–498.

Heredia, J. E., Mukundan, L., Chen, F. M., Mueller, A. A., Deo, R. C., Locksley, R. M., Rando, T. A., & Chawla, A. (2013). Type 2 innate signals stimulate fibro/adipogenic progenitors to facilitate muscle regeneration. *Cell*, *153*(2), 376–388.

Hezel, A. F., Kimmelman, A. C., Stanger, B. Z., Bardeesy, N., & Depinho, R. A. (2006). Genetics and biology of pancreatic ductal adenocarcinoma. *Genes & Development*, *20*(10), 1218–1249.

Hines, O. J., & Pandol, S. J. (2019). Management of severe acute pancreatitis. *BMJ* , *367*, l6227.

Hingorani, S. R., Petricoin, E. F., Maitra, A., Rajapakse, V., King, C., Jacobetz, M. A., Ross, S., Conrads, T. P., Veenstra, T. D., Hitt, B. A., Kawaguchi, Y., Johann, D., Liotta, L. A., Crawford, H. C., Putt, M. E., Jacks, T., Wright, C. V. E., Hruban, R. H., Lowy, A. M., & Tuveson, D. A. (2003). Preinvasive and invasive ductal pancreatic cancer and its early detection in the mouse. *Cancer Cell*, *4*(6), 437–450.

Hodzic, Z., Schill, E. M., Bolock, A. M., & Good, M. (2017). IL-33 and the intestine: The good, the bad, and the inflammatory. *Cytokine*, *100*, 1–10.

Hogan, S. P., Koskinen, A., Matthaei, K. I., Young, I. G., & Foster, P. S. (1998). Interleukin-5-producing CD4+ T cells play a pivotal role in aeroallergen-induced eosinophilia, bronchial hyperreactivity, and lung damage in mice. *American Journal of Respiratory and Critical Care Medicine*, *157*(1), 210–218.

Hoque, R., Sohail, M., Malik, A., Sarwar, S., Luo, Y., Shah, A., Barrat, F., Flavell, R., Gorelick, F., Husain, S., & Mehal, W. (2011). TLR9 and the NLRP3 inflammasome link acinar cell death with inflammation in acute pancreatitis. *Gastroenterology*, *141*(1), 358–369.

Hosein, A. N., Brekken, R. A., & Maitra, A. (2020). Pancreatic cancer stroma: an update on therapeutic targeting strategies. *Nature Reviews. Gastroenterology & Hepatology*, *17*(8), 487–505.

Hoyler, T., Klose, C. S. N., Souabni, A., Turqueti-Neves, A., Pfeifer, D., Rawlins, E. L., Voehringer, D., Busslinger, M., & Diefenbach, A. (2012). The transcription factor GATA-3 controls cell fate and maintenance of type 2 innate lymphoid cells. *Immunity*, *37*(4), 634–648.

Hurst, S. D., Muchamuel, T., Gorman, D. M., Gilbert, J. M., Clifford, T., Kwan, S., Menon, S., Seymour, B., Jackson, C., Kung, T. T., Brieland, J. K., Zurawski, S. M., Chapman, R. W., Zurawski, G., & Coffman, R. L. (2002). New IL-17 family members promote Th1 or Th2 responses in the lung: in vivo function of the novel cytokine IL-25. *Journal of Immunology* , *169*(1), 443–453.

Hyun, J. J., & Lee, H. S. (2014). Experimental models of pancreatitis. *Clinical Endoscopy*, *47*(3), 212–216.

Ikutani, M., Yanagibashi, T., Ogasawara, M., Tsuneyama, K., Yamamoto, S., Hattori, Y., Kouro, T., Itakura, A., Nagai, Y., Takaki, S., & Takatsu, K. (2012). Identification of innate IL-5-producing cells and their role in lung eosinophil regulation and antitumor immunity. *Journal of Immunology* , *188*(2), 703–713.

Jang, J.-E., Hajdu, C. H., Liot, C., Miller, G., Dustin, M. L., & Bar-Sagi, D. (2017). Crosstalk between Regulatory T Cells and Tumor-Associated Dendritic Cells Negates Anti-tumor Immunity in Pancreatic Cancer. *Cell Reports*, *20*(3), 558–571.

Jin, L., Gao, D., Feng, T., Tremblay, J. R., Ghazalli, N., Luo, A., Rawson, J., Quijano, J. C., Chai, J., Wedeken, L., Hsu, J., LeBon, J., Walker, S., Shih, H.-P., Mahdavi, A., Tirrell,

D. A., Riggs, A. D., & Ku, H. T. (2016). Cells with surface expression of CD133highCD71low are enriched for tripotent colony-forming progenitor cells in the adult murine pancreas. *Stem Cell Research*, *16*(1), 40–53.

Jovanovic, I. P., Pejnovic, N. N., Radosavljevic, G. D., Pantic, J. M., Milovanovic, M. Z., Arsenijevic, N. N., & Lukic, M. L. (2014). Interleukin-33/ST2 axis promotes breast cancer growth and metastases by facilitating intratumoral accumulation of immunosuppressive and innate lymphoid cells. *International Journal of Cancer. Journal International Du Cancer*, *134*(7), 1669–1682.

Kang, R., Zhang, Q., Hou, W., Yan, Z., Chen, R., Bonaroti, J., Bansal, P., Billiar, T. R., Tsung, A., Wang, Q., Bartlett, D. L., Whitcomb, D. C., Chang, E. B., Zhu, X., Wang, H., Lu, B., Tracey, K. J., Cao, L., Fan, X.-G., … Tang, D. (2014). Intracellular Hmgb1 inhibits inflammatory nucleosome release and limits acute pancreatitis in mice. *Gastroenterology*, *146*(4), 1097–1107.

Karamitopoulou, E. (2019). Tumour microenvironment of pancreatic cancer: immune landscape is dictated by molecular and histopathological features. *British Journal of Cancer*, *121*(1), 5–14.

Kirchberger, S., Royston, D. J., Boulard, O., Thornton, E., Franchini, F., Szabady, R. L., Harrison, O., & Powrie, F. (2013). Innate lymphoid cells sustain colon cancer through production of interleukin-22 in a mouse model. *The Journal of Experimental Medicine*, *210*(5), 917–931.

Kleeff, J., Korc, M., Apte, M., La Vecchia, C., Johnson, C. D., Biankin, A. V., Neale, R. E., Tempero, M., Tuveson, D. A., Hruban, R. H., & Neoptolemos, J. P. (2016). Pancreatic cancer. *Nature Reviews. Disease Primers*, *2*, 16022.

Kleeff, J., Whitcomb, D. C., Shimosegawa, T., Esposito, I., Lerch, M. M., Gress, T., Mayerle, J., Drewes, A. M., Rebours, V., Akisik, F., Muñoz, J. E. D., & Neoptolemos, J. P. (2017). Chronic pancreatitis. *Nature Reviews. Disease Primers*, *3*, 17060.

Klochkov, A., Kudaravalli, P., Lim, Y., & Sun, Y. (2021). Alcoholic Pancreatitis. In *StatPearls*. StatPearls Publishing.

Laurent, P., Allard, B., Manicki, P., Jolivel, V., Levionnois, E., Jeljeli, M., Henrot, P., Izotte, J., Leleu, D., Groppi, A., Seneschal, J., Constans, J., Chizzolini, C., Richez, C., Duffau, P., Lazaro, E., Forcade, E., Schaeverbeke, T., Pradeu, T., … Truchetet, M.-E. (2021). TGFβ promotes low IL10-producing ILC2 with profibrotic ability involved in skin fibrosis in systemic sclerosis. *Annals of the Rheumatic Diseases*. https://doi.org/10.1136/annrheumdis-2020-219748

Lefrançais, E., Roga, S., Gautier, V., Gonzalez-de-Peredo, A., Monsarrat, B., Girard, J.-P., & Cayrol, C. (2012). IL-33 is processed into mature bioactive forms by neutrophil elastase and cathepsin G. *Proceedings of the National Academy of Sciences of the United States of America*, *109*(5), 1673–1678.

Lerch, M. M., & Aghdassi, A. A. (2010). The role of bile acids in gallstone-induced pancreatitis [Review of *The role of bile acids in gallstone-induced pancreatitis*]. *Gastroenterology*, *138*(2), 429–433.

Lerch, M. M., & Gorelick, F. S. (2013). Models of acute and chronic pancreatitis. *Gastroenterology*, *144*(6), 1180–1193.

Leyva-Castillo, J. M., Das, M., Artru, E., Yoon, J., Galand, C., & Geha, R. S. (2021). Mast cell-derived IL-13 downregulates IL-12 production by skin dendritic cells to inhibit the TH1 cell response to cutaneous antigen exposure. *The Journal of Allergy and Clinical Immunology*, *147*(6), 2305-2315.e3.

Leyva-Castillo, J. M., Galand, C., Mashiko, S., Bissonnette, R., McGurk, A., Ziegler, S. F., Dong, C., McKenzie, A. N. J., Sarfati, M., & Geha, R. S. (2020). ILC2 activation by keratinocyte-derived IL-25 drives IL-13 production at sites of allergic skin inflammation. *The Journal of Allergy and Clinical Immunology*. https://doi.org/10.1016/j.jaci.2020.02.026

Li, J., Razumilava, N., Gores, G. J., Walters, S., Mizuochi, T., Mourya, R., Bessho, K., Wang, Y.-H., Glaser, S. S., Shivakumar, P., & Bezerra, J. A. (2014). Biliary repair and carcinogenesis are mediated by IL-33–dependent cholangiocyte proliferation. *The Journal of Clinical Investigation*, *124*(7), 3241–3251.

Liew, F. Y., Girard, J.-P., & Turnquist, H. R. (2016). Interleukin-33 in health and disease. *Nature Reviews. Immunology*, *16*(11), 676–689.

Liou, G.-Y., Bastea, L., Fleming, A., Döppler, H., Edenfield, B. H., Dawson, D. W., Zhang, L., Bardeesy, N., & Storz, P. (2017). The Presence of Interleukin-13 at Pancreatic ADM/PanIN Lesions Alters Macrophage Populations and Mediates Pancreatic Tumorigenesis. *Cell Reports*, *19*(7), 1322–1333.

Liou, G.-Y., Döppler, H., Necela, B., Krishna, M., Crawford, H. C., Raimondo, M., & Storz, P. (2013). Macrophage-secreted cytokines drive pancreatic acinar-to-ductal metaplasia through NF-κB and MMPs. *The Journal of Cell Biology*, *202*(3), 563–577.

Liu, J., Akanuma, N., Liu, C., Naji, A., Halff, G. A., Washburn, W. K., Sun, L., & Wang, P. (2016). TGF-β1 promotes acinar to ductal metaplasia of human pancreatic acinar cells. *Scientific Reports*, *6*, 30904.

Liu, L., & Shi, G.-P. (2012). CD31: beyond a marker for endothelial cells [Review of *CD31: beyond a marker for endothelial cells*]. *Cardiovascular Research*, *94*(1), 3–5.

Lowenfels, A. B., Maisonneuve, P., Cavallini, G., Ammann, R. W., Lankisch, P. G., Andersen, J. R., Dimagno, E. P., Andrén-Sandberg, A., & Domellöf, L. (1993). Pancreatitis and the risk of pancreatic cancer. International Pancreatitis Study Group. *The New England Journal of Medicine*, *328*(20), 1433–1437.

Mack, M., Cihak, J., Simonis, C., Luckow, B., Proudfoot, A. E., Plachý, J., Brühl, H., Frink, M., Anders, H. J., Vielhauer, V., Pfirstinger, J., Stangassinger, M., & Schlöndorff, D. (2001). Expression and characterization of the chemokine receptors CCR2 and CCR5 in mice. *Journal of Immunology* , *166*(7), 4697–4704.

Manohar, M., Verma, A. K., Venkateshaiah, S. U., & Mishra, A. (2017). Significance of Eosinophils in Promoting Pancreatic malignancy. *Journal of Gastroenterology, Pancreatology & Liver Disorders*, *5*(1). https://doi.org/10.15226/2374-815X/5/1/001109

Manohar, M., Verma, A. K., Venkateshaiah, S. U., & Mishra, A. (2018). Role of eosinophils in the initiation and progression of pancreatitis pathogenesis. *American Journal of Physiology. Gastrointestinal and Liver Physiology*, *314*(2), G211–G222.

Manohar, M., Verma, A. K., Venkateshaiah, S. U., Sanders, N. L., & Mishra, A. (2017). Pathogenic mechanisms of pancreatitis. *World Journal of Gastrointestinal Pharmacology and Therapeutics*, *8*(1), 10–25.

McBrien, C. N., & Menzies-Gow, A. (2017). The Biology of Eosinophils and Their Role in Asthma. *Frontiers of Medicine*, *4*, 93.

McHedlidze, T., Waldner, M., Zopf, S., Walker, J., Rankin, A. L., Schuchmann, M., Voehringer, D., McKenzie, A. N. J., Neurath, M. F., Pflanz, S., & Wirtz, S. (2013). Interleukin-33-dependent innate lymphoid cells mediate hepatic fibrosis. *Immunity*, *39*(2), 357–371.

Mebius, R. E., Rennert, P., & Weissman, I. L. (1997). Developing lymph nodes collect CD4+CD3- LTbeta+ cells that can differentiate to APC, NK cells, and follicular cells but not T or B cells. *Immunity*, *7*(4), 493–504.

Meng, X.-M., Nikolic-Paterson, D. J., & Lan, H. Y. (2016). TGF-β: the master regulator of fibrosis. *Nature Reviews. Nephrology*, *12*(6), 325–338.

Merza, M., Hartman, H., Rahman, M., Hwaiz, R., Zhang, E., Renström, E., Luo, L., Mörgelin, M., Regner, S., & Thorlacius, H. (2015). Neutrophil Extracellular Traps Induce Trypsin Activation, Inflammation, and Tissue Damage in Mice With Severe Acute Pancreatitis. *Gastroenterology*, *149*(7), 1920-1931.e8.

Mjösberg, J. M., Trifari, S., Crellin, N. K., Peters, C. P., van Drunen, C. M., Piet, B., Fokkens, W. J., Cupedo, T., & Spits, H. (2011). Human IL-25- and IL-33-responsive type 2 innate lymphoid cells are defined by expression of CRTH2 and CD161. *Nature Immunology*, *12*(11), 1055–1062.

Moffitt, R. A., Marayati, R., Flate, E. L., Volmar, K. E., Loeza, S. G. H., Hoadley, K. A., Rashid, N. U., Williams, L. A., Eaton, S. C., Chung, A. H., Smyla, J. K., Anderson, J. M., Kim, H. J., Bentrem, D. J., Talamonti, M. S., Iacobuzio-Donahue, C. A., Hollingsworth, M. A., & Yeh, J. J. (2015). Virtual microdissection identifies distinct tumor- and stroma-specific subtypes of pancreatic ductal adenocarcinoma. *Nature Genetics*, *47*(10), 1168–1178.

Molofsky, A. B., Nussbaum, J. C., Liang, H.-E., Van Dyken, S. J., Cheng, L. E., Mohapatra, A., Chawla, A., & Locksley, R. M. (2013). Innate lymphoid type 2 cells sustain visceral adipose tissue eosinophils and alternatively activated macrophages. *The Journal of Experimental Medicine*, *210*(3), 535–549.

Monticelli, L. A., Osborne, L. C., Noti, M., Tran, S. V., Zaiss, D. M. W., & Artis, D. (2015). IL-33 promotes an innate immune pathway of intestinal tissue protection dependent on amphiregulin-EGFR interactions. *Proceedings of the National Academy of Sciences of the United States of America*, *112*(34), 10762–10767.

Monticelli, L. A., Sonnenberg, G. F., Abt, M. C., Alenghat, T., Ziegler, C. G. K., Doering, T. A., Angelosanto, J. M., Laidlaw, B. J., Yang, C. Y., Sathaliyawala, T., Kubota, M., Turner, D., Diamond, J. M., Goldrath, A. W., Farber, D. L., Collman, R. G., Wherry, E. J., & Artis, D. (2011). Innate lymphoid cells promote lung-tissue homeostasis after infection with influenza virus. *Nature Immunology*, *12*(11), 1045–1054.

Moral, J. A., Leung, J., Rojas, L. A., Ruan, J., Zhao, J., Sethna, Z., Ramnarain, A., Gasmi, B., Gururajan, M., Redmond, D., Askan, G., Bhanot, U., Elyada, E., Park, Y., Tuveson, D. A., Gönen, M., Leach, S. D., Wolchok, J. D., DeMatteo, R. P., … Balachandran, V. P. (2020). ILC2s amplify PD-1 blockade by activating tissue-specific cancer immunity. *Nature*, *579*(7797), 130–135.

Moro, K., Yamada, T., Tanabe, M., Takeuchi, T., Ikawa, T., Kawamoto, H., Furusawa, J.-I., Ohtani, M., Fujii, H., & Koyasu, S. (2010). Innate production of T(H)2 cytokines by adipose tissue-associated c-Kit(+)Sca-1(+) lymphoid cells. *Nature*, *463*(7280), 540–544.

Mosmann, T. R., Cherwinski, H., Bond, M. W., Giedlin, M. A., & Coffman, R. L. (1986). Two types of murine helper T cell clone. I. Definition according to profiles of lymphokine activities and secreted proteins. *Journal of Immunology* , *136*(7), 2348–2357.

Murthy, P., Singhi, A. D., Ross, M. A., Loughran, P., Paragomi, P., Papachristou, G. I., Whitcomb, D. C., Zureikat, A. H., Lotze, M. T., Zeh, H. J., Iii, & Boone, B. A. (2019). Enhanced Neutrophil Extracellular Trap Formation in Acute Pancreatitis Contributes to Disease Severity and Is Reduced by Chloroquine. *Frontiers in Immunology*, *10*, 28.

Nagashio, Y., Ueno, H., Imamura, M., Asaumi, H., Watanabe, S., Yamaguchi, T., Taguchi, M., Tashiro, M., & Otsuki, M. (2004). Inhibition of transforming growth factor beta decreases pancreatic fibrosis and protects the pancreas against chronic injury in mice. *Laboratory Investigation; a Journal of Technical Methods and Pathology*, *84*(12), 1610–1618.

Nakamura, K., & Smyth, M. J. (2020). Immunoediting of cancer metastasis by NK cells. *Nature Cancer*, *1*(7), 670–671.

Neill, D. R., Wong, S. H., Bellosi, A., Flynn, R. J., Daly, M., Langford, T. K. A., Bucks, C., Kane, C. M., Fallon, P. G., Pannell, R., Jolin, H. E., & McKenzie, A. N. J. (2010). Nuocytes represent a new innate effector leukocyte that mediates type-2 immunity. *Nature*, *464*(7293), 1367–1370.

Newland, S. A., Mohanta, S., Clément, M., Taleb, S., Walker, J. A., Nus, M., Sage, A. P., Yin, C., Hu, D., Kitt, L. L., Finigan, A. J., Rodewald, H.-R., Binder, C. J., McKenzie, A. N. J., Habenicht, A. J., & Mallat, Z. (2017). Type-2 innate lymphoid cells control the development of atherosclerosis in mice. *Nature Communications*, *8*, 15781.

Nile, C. J., Barksby, E., Jitprasertwong, P., Preshaw, P. M., & Taylor, J. J. (2010). Expression and regulation of interleukin-33 in human monocytes. *Immunology*, *130*(2), 172–180.

Nussbaum, J. C., Van Dyken, S. J., von Moltke, J., Cheng, L. E., Mohapatra, A., Molofsky, A. B., Thornton, E. E., Krummel, M. F., Chawla, A., Liang, H.-E., & Locksley, R. M. (2013). Type 2 innate lymphoid cells control eosinophil homeostasis. *Nature*, *502*(7470), 245–248.

Öhlund, D., Handly-Santana, A., Biffi, G., Elyada, E., Almeida, A. S., Ponz-Sarvise, M., Corbo, V., Oni, T. E., Hearn, S. A., Lee, E. J., Chio, I. I. C., Hwang, C.-I., Tiriac, H., Baker, L. A., Engle, D. D., Feig, C., Kultti, A., Egeblad, M., Fearon, D. T., … Tuveson, D. A. (2017). Distinct populations of inflammatory fibroblasts and myofibroblasts in pancreatic cancer. *The Journal of Experimental Medicine*, *214*(3), 579–596.

Oliphant, C. J., Hwang, Y. Y., Walker, J. A., Salimi, M., Wong, S. H., Brewer, J. M., Englezakis, A., Barlow, J. L., Hams, E., Scanlon, S. T., Ogg, G. S., Fallon, P. G., & McKenzie, A. N. J. (2014). MHCII-mediated dialog between group 2 innate lymphoid cells and CD4(+) T cells potentiates type 2 immunity and promotes parasitic helminth expulsion. *Immunity*, *41*(2), 283–295.

Owyang, A. M., Zaph, C., Wilson, E. H., Guild, K. J., McClanahan, T., Miller, H. R. P., Cua, D. J., Goldschmidt, M., Hunter, C. A., Kastelein, R. A., & Artis, D. (2006). Interleukin 25 regulates type 2 cytokine-dependent immunity and limits chronic inflammation in the gastrointestinal tract. *The Journal of Experimental Medicine*, *203*(4), 843–849.

Pancreatic cancer statistics. (2015, May 14). https://www.cancerresearchuk.org/health-professional/cancer-statistics/statistics-by-cancer-type/pancreatic-cancer

Papayannopoulos, V. (2018). Neutrophil extracellular traps in immunity and disease. *Nature Reviews. Immunology*, *18*(2), 134–147.

Price, A. E., Liang, H.-E., Sullivan, B. M., Reinhardt, R. L., Eisley, C. J., Erle, D. J., & Locksley, R. M. (2010). Systemically dispersed innate IL-13-expressing cells in type 2 immunity. *Proceedings of the National Academy of Sciences of the United States of America*, *107*(25), 11489–11494.

Rafei-Shamsabadi, D. A., van de Poel, S., Dorn, B., Kunz, S., Martin, S. F., Klose, C. S. N., Arnold, S. J., Tanriver, Y., Ebert, K., Diefenbach, A., Halim, T. Y. F., McKenzie, A. N. J., & Jakob, T. (2018). Lack of Type 2 Innate Lymphoid Cells Promotes a Type I-Driven Enhanced Immune Response in Contact Hypersensitivity. *The Journal of Investigative Dermatology*, *138*(9), 1962–1972.

Rak, G. D., Osborne, L. C., Siracusa, M. C., Kim, B. S., Wang, K., Bayat, A., Artis, D., & Volk, S. W. (2016). IL-33-Dependent Group 2 Innate Lymphoid Cells Promote Cutaneous Wound Healing. *The Journal of Investigative Dermatology*, *136*(2), 487–496.

Rana, B. M. J., Jou, E., Barlow, J. L., Rodriguez-Rodriguez, N., Walker, J. A., Knox, C., Jolin, H. E., Hardman, C. S., Sivasubramaniam, M., Szeto, A., Cohen, E. S., Scott, I. C., Sleeman, M. A., Chidomere, C. I., Cruz Migoni, S., Caamano, J., Jorgensen, H. F., Carobbio, S., Vidal-Puig, A., & McKenzie, A. N. J. (2019). A stromal cell niche sustains ILC2-mediated type-2 conditioning in adipose tissue. *The Journal of Experimental Medicine*, *216*(9), 1999–2009.

Rauber, S., Luber, M., Weber, S., Maul, L., Soare, A., Wohlfahrt, T., Lin, N.-Y., Dietel, K., Bozec, A., Herrmann, M., Kaplan, M. H., Weigmann, B., Zaiss, M. M., Fearon, U., Veale, D. J., Cañete, J. D., Distler, O., Rivellese, F., Pitzalis, C., … Ramming, A. (2017). Resolution of inflammation by interleukin-9-producing type 2 innate lymphoid cells. *Nature Medicine*, *23*(8), 938–944.

Renninger, M. L., Seymour, R. E., Whiteley, L. O., Sundberg, J. P., & Hogenesch, H. (2010). Anti-IL5 decreases the number of eosinophils but not the severity of dermatitis in Sharpin-deficient mice. *Experimental Dermatology*, *19*(3), 252–258.

Ricardo-Gonzalez, R. R., Van Dyken, S. J., Schneider, C., Lee, J., Nussbaum, J. C., Liang, H.-E., Vaka, D., Eckalbar, W. L., Molofsky, A. B., Erle, D. J., & Locksley, R. M. (2018). Tissue signals imprint ILC2 identity with anticipatory function. *Nature Immunology*, *19*(10), 1093–1099.

Roberts, E. W., Deonarine, A., Jones, J. O., Denton, A. E., Feig, C., Lyons, S. K., Espeli, M., Kraman, M., McKenna, B., Wells, R. J. B., Zhao, Q., Caballero, O. L., Larder, R., Coll, A. P., O'Rahilly, S., Brindle, K. M., Teichmann, S. A., Tuveson, D. A., & Fearon, D. T. (2013). Depletion of stromal cells expressing fibroblast activation protein-α from skeletal muscle and bone marrow results in cachexia and anemia. *The Journal of Experimental Medicine*, *210*(6), 1137–1151.

Roediger, B., Kyle, R., Yip, K. H., Sumaria, N., Guy, T. V., Kim, B. S., Mitchell, A. J., Tay, S. S., Jain, R., Forbes-Blom, E., Chen, X., Tong, P. L., Bolton, H. A., Artis, D., Paul, W. E., Fazekas de St Groth, B., Grimbaldeston, M. A., Le Gros, G., & Weninger, W. (2013). Cutaneous immunosurveillance and regulation of inflammation by group 2 innate lymphoid cells. *Nature Immunology*, *14*(6), 564–573.

Saeki, K., Kanai, T., Nakano, M., Nakamura, Y., Miyata, N., Sujino, T., Yamagishi, Y., Ebinuma, H., Takaishi, H., Ono, Y., Takeda, K., Hozawa, S., Yoshimura, A., & Hibi, T. (2012). CCL2-induced migration and SOCS3-mediated activation of macrophages are involved in cerulein-induced pancreatitis in mice. *Gastroenterology*, *142*(4), 1010-1020.e9.

Saluja, A. K., Lerch, M. M., Phillips, P. A., & Dudeja, V. (2007). Why does pancreatic overstimulation cause pancreatitis? *Annual Review of Physiology*, *69*, 249–269.

Saluzzo, S., Gorki, A.-D., Rana, B. M. J., Martins, R., Scanlon, S., Starkl, P., Lakovits, K., Hladik, A., Korosec, A., Sharif, O., Warszawska, J. M., Jolin, H., Mesteri, I., McKenzie, A. N. J., & Knapp, S. (2017). First-Breath-Induced Type 2 Pathways Shape the Lung Immune Environment. *Cell Reports*, *18*(8), 1893–1905.

Satoh-Takayama, N., Kato, T., Motomura, Y., Kageyama, T., Taguchi-Atarashi, N., Kinoshita-Daitoku, R., Kuroda, E., Di Santo, J. P., Mimuro, H., Moro, K., & Ohno, H. (2020). Bacteria-Induced Group 2 Innate Lymphoid Cells in the Stomach Provide Immune Protection through Induction of IgA. *Immunity*. https://doi.org/10.1016/j.immuni.2020.03.002

Satoh-Takayama, N., Vosshenrich, C. A. J., Lesjean-Pottier, S., Sawa, S., Lochner, M., Rattis, F., Mention, J.-J., Thiam, K., Cerf-Bensussan, N., Mandelboim, O., Eberl, G., & Di Santo, J. P. (2008). Microbial flora drives interleukin 22 production in intestinal NKp46+ cells that provide innate mucosal immune defense. *Immunity*, *29*(6), 958–970.

Saunders, S. P., Moran, T., Floudas, A., Wurlod, F., Kaszlikowska, A., Salimi, M., Quinn, E. M., Oliphant, C. J., Núñez, G., McManus, R., Hams, E., Irvine, A. D., McKenzie, A. N. J., Ogg, G. S., & Fallon, P. G. (2016). Spontaneous atopic dermatitis is mediated by innate immunity, with the secondary lung inflammation of the atopic march requiring adaptive immunity. *The Journal of Allergy and Clinical Immunology*, *137*(2), 482–491.

Sawa, S., Cherrier, M., Lochner, M., Satoh-Takayama, N., Fehling, H. J., Langa, F., Di Santo, J. P., & Eberl, G. (2010). Lineage relationship analysis of RORgammat+ innate lymphoid cells. *Science*, *330*(6004), 665–669.

Schneider, C., O'Leary, C. E., von Moltke, J., Liang, H.-E., Ang, Q. Y., Turnbaugh, P. J., Radhakrishnan, S., Pellizzon, M., Ma, A., & Locksley, R. M. (2018). A Metabolite-Triggered Tuft Cell-ILC2 Circuit Drives Small Intestinal Remodeling. *Cell*, *174*(2), 271-284.e14.

Schuijs, M. J., & Halim, T. Y. F. (2018). Group 2 innate lymphocytes at the interface between innate and adaptive immunity. *Annals of the New York Academy of Sciences*, *1417*(1), 87–103.

Schuijs, M. J., Png, S., Richard, A. C., Tsyben, A., Hamm, G., Stockis, J., Garcia, C., Pinaud, S., Nicholls, A., Ros, X. R., Su, J., Eldridge, M. D., Riedel, A., Serrao, E. M., Rodewald, H.-R., Mack, M., Shields, J. D., Cohen, E. S., McKenzie, A. N. J., … Halim, T. Y. F. (2020). ILC2-driven innate immune checkpoint mechanism antagonizes NK cell antimetastatic function in the lung. *Nature Immunology*. https://doi.org/10.1038/s41590-020-0745-y

Schwartz, C., Moran, T., Saunders, S. P., Kaszlikowska, A., Floudas, A., Bom, J., Nunez, G., Iwakura, Y., O'Neill, L., Irvine, A. D., McKenzie, A. N. J., Ogg, G., Walsh, P. T., Demengeot, J., & Fallon, P. G. (2019). Spontaneous atopic dermatitis in mice with a defective skin barrier is independent of ILC2 and mediated by IL-1β. *Allergy*, *74*(10), 1920–1933.

Scott, I. C., Majithiya, J. B., Sanden, C., Thornton, P., Sanders, P. N., Moore, T., Guscott, M., Corkill, D. J., Erjefält, J. S., & Cohen, E. S. (2018). Interleukin-33 is activated by allergen- and necrosis-associated proteolytic activities to regulate its alarmin activity during epithelial damage. *Scientific Reports*, *8*(1), 3363.

Serra, M. B., Koike, M. K., Barbeiro, D. F., Machado, M. C. C., & de Souza, H. P. (2021). Sodium Taurocholate Induced Severe Acute Pancreatitis in C57BL/6 Mice. *Journal of Visualized Experiments: JoVE*, *172*. https://doi.org/10.3791/61547

Shek, F. W.-T., Benyon, R. C., Walker, F. M., McCrudden, P. R., Pender, S. L. F., Williams, E. J., Johnson, P. A., Johnson, C. D., Bateman, A. C., Fine, D. R., & Iredale, J. P. (2002). Expression of transforming growth factor-beta 1 by pancreatic stellate cells and its implications for matrix secretion and turnover in chronic pancreatitis. *The American Journal of Pathology*, *160*(5), 1787–1798.

Shi, G., DiRenzo, D., Qu, C., Barney, D., Miley, D., & Konieczny, S. F. (2013). Maintenance of acinar cell organization is critical to preventing Kras-induced acinar-ductal metaplasia. *Oncogene*, *32*(15), 1950–1958.

Shinozaki, S., Mashima, H., Ohnishi, H., & Sugano, K. (2010). IL-13 promotes the proliferation of rat pancreatic stellate cells through the suppression of NF-kappaB/TGF-beta1 pathway. *Biochemical and Biophysical Research Communications*, *393*(1), 61–65.

Siret, C., Collignon, A., Silvy, F., Robert, S., Cheyrol, T., André, P., Rigot, V., Iovanna, J., van de Pavert, S., Lombardo, D., Mas, E., & Martirosyan, A. (2019). Deciphering the Crosstalk Between Myeloid-Derived Suppressor Cells and Regulatory T Cells in Pancreatic Ductal Adenocarcinoma. *Frontiers in Immunology*, *10*, 3070.

Spits, H., Artis, D., Colonna, M., Diefenbach, A., Di Santo, J. P., Eberl, G., Koyasu, S., Locksley, R. M., McKenzie, A. N. J., Mebius, R. E., Powrie, F., & Vivier, E. (2013). Innate lymphoid cells--a proposal for uniform nomenclature. *Nature Reviews. Immunology*, *13*(2), 145–149.

Storz, P. (2017). Acinar cell plasticity and development of pancreatic ductal adenocarcinoma. *Nature Reviews. Gastroenterology & Hepatology*, *14*(5), 296–304.

Trabanelli, S., Chevalier, M. F., Martinez-Usatorre, A., Gomez-Cadena, A., Salomé, B., Lecciso, M., Salvestrini, V., Verdeil, G., Racle, J., Papayannidis, C., Morita, H., Pizzitola, I., Grandclément, C., Bohner, P., Bruni, E., Girotra, M., Pallavi, R., Falvo, P., Leibundgut, E. O., … Jandus, C. (2017). Tumour-derived PGD2 and NKp30-B7H6 engagement drives an immunosuppressive ILC2-MDSC axis. *Nature Communications*, *8*(1), 593.

Trabanelli, S., Curti, A., Lecciso, M., Salomé, B., Riether, C., Ochsenbein, A., Romero, P., & Jandus, C. (2015). CD127+ innate lymphoid cells are dysregulated in treatment naïve acute myeloid leukemia patients at diagnosis. *Haematologica*, *100*(7), e257.

Trzpis, M., McLaughlin, P. M. J., de Leij, L. M. F. H., & Harmsen, M. C. (2007). Epithelial cell adhesion molecule: more than a carcinoma marker and adhesion molecule. *The American Journal of Pathology*, *171*(2), 386–395.

Tsuji, Y., Watanabe, T., Kudo, M., Arai, H., Strober, W., & Chiba, T. (2012). Sensing of commensal organisms by the intracellular sensor NOD1 mediates experimental pancreatitis. *Immunity*, *37*(2), 326–338.

Vieira, A. T., Fagundes, C. T., Alessandri, A. L., Castor, M. G. M., Guabiraba, R., Borges, V. O., Silveira, K. D., Vieira, E. L. M., Gonçalves, J. L., Silva, T. A., Deruaz, M., Proudfoot, A. E. I., Sousa, L. P., & Teixeira, M. M. (2009). Treatment with a novel chemokine-binding protein or eosinophil lineage-ablation protects mice from experimental colitis. *The American Journal of Pathology*, *175*(6), 2382–2391.

Vivier, E., Artis, D., Colonna, M., Diefenbach, A., Di Santo, J. P., Eberl, G., Koyasu, S., Locksley, R. M., McKenzie, A. N. J., Mebius, R. E., Powrie, F., & Spits, H. (2018). Innate Lymphoid Cells: 10 Years On. *Cell*, *174*(5), 1054–1066.

Vivier, E., Raulet, D. H., Moretta, A., Caligiuri, M. A., Zitvogel, L., Lanier, L. L., Yokoyama, W. M., & Ugolini, S. (2011). Innate or adaptive immunity? The example of natural killer cells. *Science*, *331*(6013), 44–49.

Vivier, E., Ugolini, S., Blaise, D., Chabannon, C., & Brossay, L. (2012). Targeting natural killer cells and natural killer T cells in cancer. *Nature Reviews. Immunology*, *12*(4), 239–252.

Vonarbourg, C., Mortha, A., Bui, V. L., Hernandez, P. P., Kiss, E. A., Hoyler, T., Flach, M., Bengsch, B., Thimme, R., Hölscher, C., Hönig, M., Pannicke, U., Schwarz, K., Ware, C. F., Finke, D., & Diefenbach, A. (2010). Regulated expression of nuclear receptor RORγt confers distinct functional fates to NK cell receptor-expressing RORγt(+) innate lymphocytes. *Immunity*, *33*(5), 736–751.

Wang, X., Li, X., Wei, X., Jiang, H., Lan, C., Yang, S., Wang, H., Yang, Y., Tian, C., Xu, Z., Zhang, J., Hao, J., & Ren, H. (2020). PD-L1 is a direct target of cancer-FOXP3 in pancreatic ductal adenocarcinoma (PDAC), and combined immunotherapy with antibodies against PD-L1 and CCL5 is effective in the treatment of PDAC. *Signal Transduction and Targeted Therapy*, *5*(1), 38.

Watanabe, T., Kudo, M., & Strober, W. (2017). Immunopathogenesis of pancreatitis. *Mucosal Immunology*, *10*(2), 283–298.

Watanabe, T., Sadakane, Y., Yagama, N., Sakurai, T., Ezoe, H., Kudo, M., Chiba, T., & Strober, W. (2016). Nucleotide-binding oligomerization domain 1 acts in concert with the cholecystokinin receptor agonist, cerulein, to induce IL-33-dependent chronic pancreatitis. *Mucosal Immunology*, *9*(5), 1234–1249.

Whelan, D. S., Caplice, N. M., & Clover, A. J. P. (2020). Mesenchymal stromal cell derived CCL2 is required for accelerated wound healing. *Scientific Reports*, *10*(1), 2642.

Wong, S. H., Walker, J. A., Jolin, H. E., Drynan, L. F., Hams, E., Camelo, A., Barlow, J. L., Neill, D. R., Panova, V., Koch, U., Radtke, F., Hardman, C. S., Hwang, Y. Y., Fallon, P. G., & McKenzie, A. N. J. (2012). Transcription factor RORα is critical for nuocyte development. *Nature Immunology*, *13*(3), 229–236.

Wu, J., Zhang, L., Shi, J., He, R., Yang, W., Habtezion, A., Niu, N., Lu, P., & Xue, J. (2020). Macrophage phenotypic switch orchestrates the inflammation and repair/regeneration following acute pancreatitis injury. *EBioMedicine*, *58*, 102920.

Xiao, X., Fischbach, S., Fusco, J., Zimmerman, R., Song, Z., Nebres, P., Ricks, D. M., Prasadan, K., Shiota, C., Husain, S. Z., & Gittes, G. K. (2016). PNA lectin for purifying mouse acinar cells from the inflamed pancreas. *Scientific Reports*, *6*, 21127.

Xue, J., Sharma, V., Hsieh, M. H., Chawla, A., Murali, R., Pandol, S. J., & Habtezion, A. (2015). Alternatively activated macrophages promote pancreatic fibrosis in chronic pancreatitis. *Nature Communications*, *6*, 7158.

Yadav, D., & Lowenfels, A. B. (2013). The epidemiology of pancreatitis and pancreatic cancer. *Gastroenterology*, *144*(6), 1252–1261.

Yang, X., Yao, L., Fu, X., Mukherjee, R., Xia, Q., Jakubowska, M. A., Ferdek, P. E., & Huang, W. (2020). Experimental Acute Pancreatitis Models: History, Current Status, and Role in Translational Research. *Frontiers in Physiology*, *11*, 614591.

Yasuda, T., Ueda, T., Takeyama, Y., Shinzeki, M., Sawa, H., Nakajima, T., Ajiki, T., Fujino, Y., Suzuki, Y., & Kuroda, Y. (2006). Significant increase of serum high-mobility group box chromosomal protein 1 levels in patients with severe acute pancreatitis. *Pancreas*, *33*(4), 359–363.

Yu, C., Cantor, A. B., Yang, H., Browne, C., Wells, R. A., Fujiwara, Y., & Orkin, S. H. (2002). Targeted deletion of a high-affinity GATA-binding site in the GATA-1 promoter leads to selective loss of the eosinophil lineage in vivo. *The Journal of Experimental Medicine*, *195*(11), 1387–1395.

Yu, Y., Tsang, J. C. H., Wang, C., Clare, S., Wang, J., Chen, X., Brandt, C., Kane, L., Campos, L. S., Lu, L., Belz, G. T., McKenzie, A. N. J., Teichmann, S. A., Dougan, G., & Liu, P. (2016). Single-cell RNA-seq identifies a PD-1hi ILC progenitor and defines its development pathway. *Nature*, *539*(7627), 102–106.

Zhang, H., & Verkman, A. S. (2013). Eosinophil pathogenicity mechanisms and therapeutics in neuromyelitis optica. *The Journal of Clinical Investigation*, *123*(5), 2306–2316.

Zhang, M., Alicot, E. M., Chiu, I., Li, J., Verna, N., Vorup-Jensen, T., Kessler, B., Shimaoka, M., Chan, R., Friend, D., Mahmood, U., Weissleder, R., Moore, F. D., & Carroll, M. C. (2006). Identification of the target self-antigens in reperfusion injury. *The Journal of Experimental Medicine*, *203*(1), 141–152.

Zhao, W., Fogg, D. K., & Kaplan, M. J. (2015). A novel image-based quantitative method for the characterization of NETosis. *Journal of Immunological Methods*, *423*, 104–110.

Zheng, L. (2017). PD-L1 Expression in Pancreatic Cancer. *Journal of the National Cancer Institute*, *109*(6). https://doi.org/10.1093/jnci/djw304

Zook, E. C., & Kee, B. L. (2016). Development of innate lymphoid cells. *Nature Immunology*, *17*(7), 775–782.